Pulsed Biosparging of the E10 Gasoline Source in the Borden Aquifer

By

Jennifer Marie Lambert

A thesis

presented to the University of Waterloo

in fulfillment of the

thesis requirement for the degree of

Master of Science

in

Earth Sciences

Waterloo, Ontario, Canada, 2008

I hereby declare that I am the sole author of this thesis. This is a true copy of this thesis, including any required final revisions, as accepted by my examiners.

I understand that my thesis may be made electronically available to the public.

Abstract

Air sparging is a technique used to remediate gasoline contamination. In sparging, air is injected below the target zone and removes contamination via two separate mechanisms; volatilization and biodegradation. In volatilization, the air contacts the contamination as it moves upward. The contaminant will partition to the vapor phase based on its volatility and will be removed as the air reaches the atmosphere. For biodegradation, the oxygen in the airstream is used for microbial activity. Pulsed air sparging, otherwise known as pulsed biosparging, has been found to be more effective than continuous air sparging. Pulsed biosparging enhances treatment because it induces groundwater movement and mixing.

The general mechanisms for treatment of gasoline sources using air sparging are relatively well characterized. However, air flow through the subsurface and the total hydrocarbon mass lost are difficult to predict and quantify. This project was intended to quantify the mass lost through volatilization and through biodegradation at the E10 gasoline source using pulsed biosparging, and to determine the effect of the source zone removal on downgradient dissolved BTEX concentrations.

The remedial system consisted of two major components: the air sparging system, with three injection points; and a soil gas collection system. The soil gas collection system was comprised of an airtight box that covered the source area and the monitoring wells upgradient and downgradient of the source. Off-gas from the soil gas collection system was monitored continuously using a PID. The off-gas was also sampled frequently for BTEX, pentane, and hexane to determine the hydrocarbon mass removed; and for O_2 and CO_2 to determine biodegradation rates.

The remedial system ran for approximately 280 hours over 33 days. Of the estimated 22.3 kg of gasoline residual in the source zone, 4.6 kg or 21% of the residual was removed via volatilization and 4.9 kg or 22% of the residual was removed via biodegradation. Leakage outside the system was estimated at less than 0.1% of the total mass. Groundwater samples were collected when the last sparged air was calculated to arrive at the row 2 downgradient fence. The average BTEX groundwater concentration after sparging was 40% of the pre-sparging concentration. The benzene mass discharge decreased 27%, the ethylbenzene mass discharge decreased 65%, the p/m-xylene mass discharge decreased 6%, and the o-xylene mass discharge decreased 5%. The mass discharge for naphthalene and TMB isomers increased 19%. However, these values fit in with long-term groundwater concentration trends. Additional sampling is recommended to determine if the sparging made a significant impact on mass discharge leaving the source.

Acknowledgements

I would like to thank Jim Barker, my advisor, for his invaluable advice and flexibility when I was unable to get timely approval for the field component of this project. Neil Thomson was a great help in working out many of the technical details and was patient with my many questions that had to be answered right away (or so I thought at the time). I'd also like to thank Neil Thomson and Barb Butler for reviewing this work and providing constructive criticism.

Construction of the treatment system was a large undertaking, and much of the credit goes to Paul Johnson and Bob Ingleton for ordering materials (and figuring out what we needed, exactly) and for taking the lead on constructing the system. They also constructed, installed, and developed piezometers, open-screen monitoring wells, and the injection wells. They were also patient when our original conception had to be ripped up and replaced.

Shirley Chatten and Marianne VanderGriendt analyzed a multitude of groundwater and off-gas samples. They were both patient and accommodating, especially when I needed Shirley to come in on the weekends to run Friday samples. Claudia Naas gave me a complete introduction to Borden and shepherded my approval and university paperwork through various hoops. She was also a great help in the field.

Daniel Gardner and Colin McCarter were the coop students who helped out both summers in both the field and the lab. Their assistance in all aspects of the project is greatly appreciated. Construction and sampling required the help of a veritable army of graduate students, some of whom were induced into doing hours of manual labor. Grad students who helped out with treatment system construction/removal and sampling included Adria Bells, Neelmoy Biswas, Juliana Freitas, Dale Holtze, Bobby Katanchi, Jason Peasgood, Amir Rouzrokh, Matt Shumacher, and Andrew Stevenson. Gillian Roos and Tianxiao Yang deserve special mention for helping with the January sparging round, in frigid weather. Juliana Freitas and Gillian Roos were also great for sharing ideas and equipment while they were working on their own projects at Borden.

Finally, I'd like to thank my parents, Kathleen and Wayne, for their support and encouragement. Peter Whittlesey also deserves thanks for his support and patience when project completion was later than expected.

Table of Contents

List of Figures

List of Tables

Chapter 1: Introduction

1.1 Overview

Gasoline is near ubiquitous in North America and is an extremely common pollutant. The most common route for gasoline pollution is leaking underground storage tanks (USTs). In 1993, the US Environmental Protection Agency (EPA) estimated that approximately 10% or 295,000 of the USTs in the US are leaking. In addition to USTs, gasoline may be released into the environment via surface spills, pipeline leaks, and industrial releases from pits, ponds, or lagoons (ACOE 2002).

The most direct way to remove gasoline NAPL (non-aqueous phase liquid) is to simply dig it up. However, this is difficult to do with sources below the water table, impractical for large-scale spills, and presents disposal issues with the contaminated soil. Each time the soil is moved or processed, the costs and potential liability increase. For groundwater plumes, traditional remediation methods, such as pump and treat, need to run near indefinitely and the effluent (treated water, spent filters, etc) often has its own disposal problems. In-situ methods were developed in part to minimize these disposal problems.

Gasoline is a convenient carbon source for microbial systems, which break down the complex carbons molecules into carbon dioxide (CO_2) as well as incorporating the carbon in their cell walls, as reviewed by Brassington et al. (2007). In a gasoline source zone and the core of the plume leaving the source, oxygen (O_2) is the limiting factor for microbial activity. For this reason O_2 addition is a common method to assist with the breakdown of many organic contaminants, including gasoline.

O_2 can be added to the subsurface using oxidizers, supersaturated water, and air sparging (NRC, 2004). Oxidizers, such as peroxide, persulfate, or Fenton's reagent, tend to be hazardous and dangerous to handle, and since they are injected as a liquid, they tend to displace the contaminated water they are supposed to treat. O_2 can also be added via supersaturated water containing microbubbles, but when injected at relatively low flow rates to preserve the structure of the bubbles, they tend to produce "pencils" of oxygenated water. In order to increase treatment area, multiple wells can be combined to pull the groundwater through different areas and increase coverage. Another option is recirculating wells, which are expensive but also increase the area affected (Spargo, 1999). Sparging is the injection of air or other gases below the target zone and is discussed in detail in the following sections.

1.2 Pulsed Biosparging

Air sparging can be used to remediate source zones as well as the plumes emanating from them. The air is injected below the target zone and removes contamination via two separate mechanisms, volatilization and biodegradation (Johnson et al., 1998). See Figure 1.1 for a conceptual model for air sparging. In volatilization the air contacts the contamination as it moves upward. The contaminant will partition to the vapor phase based on its volatility (vapor pressure for NAPL and Henry's law constant for the dissolved phase) and will be released to the atmosphere or off-gas collection system. In biodegradation the oxygen in the airstream is used for microbial activity. In pulsed biosparging, the sparging system is operated intermittently to maximize biodegradation.

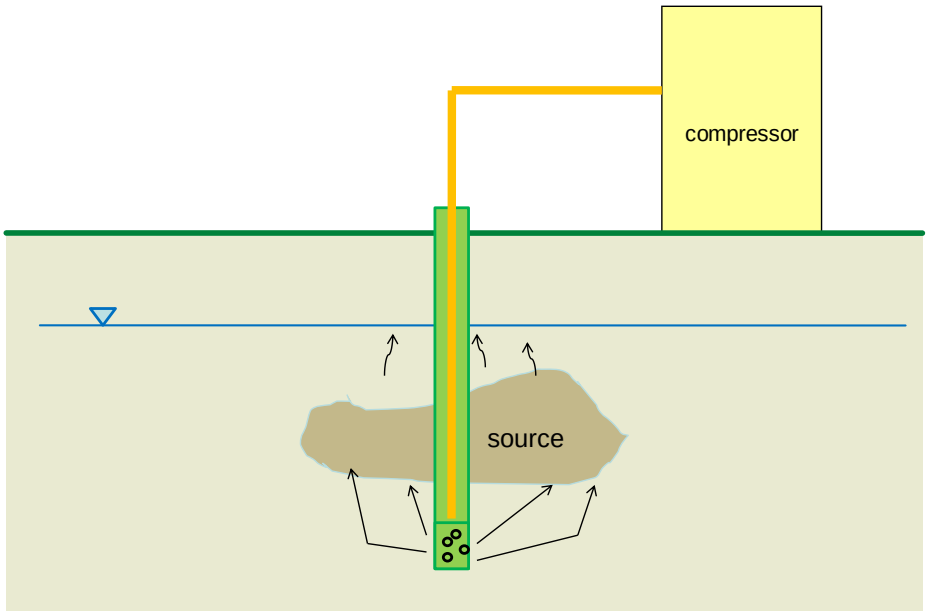

Figure 1.1 Air sparging conceptual model

In-situ air sparging is a relatively simple remedial method that was first used as a remediation technology in the mid-1980s (Bass et al., 2000). Between 2002 and 2005, the most recent dates available, air sparging represented one of the most common remedial systems in national priority list (NPL) sites in the United States, with almost 30% of NPL sites using air sparging as part of treatment. Bioremediation was used at 27% of the sites, and this trend had been accelerating over the previous six years (EPA, 2007).

Brown et al. (1994) suggest that air sparging is generally the most cost-effective oxygen delivery method per mass of oxygen delivered, with costs orders of magnitude lower than injection of hydrogen peroxide, sparging with pure oxygen, and slow-release solid peroxide (e.g. ORC, or oxygen release compound). Drawbacks include the low solubility of oxygen in water, which limits oxygen availability for

biodegradation in contaminated zones; lowered hydraulic conductivity, especially for "curtains" of air bubbles designed to intersect plumes; and limited areal coverage per sparge point.

Bass et al. (2000) reviewed a database of 49 sites remediated with air sparging. The database indicated that 36% of the systems had permanent contaminant reductions of more than 95% and 47% had permanent reductions of more than 90%. The study found that the most successful systems had a higher sparge well density and were designed for dissolved plumes rather than residual contamination. In-well sparging (using a sparge pipe inserted down an existing monitoring well) was not found to be effective. Rebound can occur months later and is often associated with a water level rise when groundwater encounters a smear zone.

According to Brown et al. (1994), air sparging works best when the contaminant has a vapor pressure greater than 1 mm Hg, solubility less than 20 g/L, biological oxygen demand (BOD) greater than 0.01 mg/L, and a Henry's law constant greater than 10^{-5} atm m^3/mol. These values for BTEX (benzene, toluene, ethylbenzene, and xylene) compounds, provided in Table 1.1 below, show that a gasoline source should be amenable to air sparging.

compound	vapor pressure (mm Hg)	solubility (mg/L)	BOD (g/g)	H law constant (atm*m^3/mol)
benzene	95	1740 - 1850	2.18	0.00377 - 0.00588
toluene	27.8 - 28.4	500 - 547	2.15	0.00549 - 0.00651
ethylbenzene	9.6 - 9.9	187 - 208	--	0.00662 - 0.00784
o-xylene	6.6	167 - 176	1.64	0.00424 - 0.00499
m-xylene	8.3	157 - 196	2.53	0.00608 - 0.00744
p-xylene	8.8	163 - 200	1.40	0.00568 - 0.00744

Data from Montgomery, 2000.

Table 1.1 Physical properties of BTEX compounds

Johnson (1998) suggests that when evaluating the potential effectiveness of air sparging, several assumptions are made:

1. Contamination is uniformly distributed. [This is not the case for this field site, as discussed in Section 2.3.]

2. Air flows at a high enough rate that the dissolved oxygen concentration at the water-air interface is constant and uniform. [This should be an acceptable assumption.]

3. Air channels have radial symmetry and their boundaries are stationary. [Tomlinson et al., (2003) showed that air channels from sparging at Borden were not radially symmetrical and field observations during this project showed that they did not have stationary boundaries.]

4. Bulk water movement is perpendicular to channel boundaries (radial flow). [This is not likely to cause significant variance at Borden.]

5. Reactions with dissolved oxygen are instantaneous. [These reactions are often rapid in regard to surface water flow but slow relative to buoyant gas phase rise in the subsurface.]

6. If contaminants do not degrade, the dissolved concentration in the channel is much less than the dissolved concentration in equilibrium with residual NAPL. [This is generally true for active airflow channels.]

7. Conditions are steady-state. [The treatment system used pulsed sparging, so transition periods and sparge-off periods may not be reflective of steady-state conditions.]

These assumptions are biased toward a perfect system; field systems will be much less uniform and efficient. Ahlfeld et al. (1994) also suggest that Henry's law, which is used to determine the mass of a chemical that can transition into the vapor phase, is only valid if the chemical has time to equilibrate with the surrounding air. However, this should not be a significant factor for this project.

Pulsed air sparging has been found to be more effective than continuous air sparging in several laboratory studies (Johnson et al., 1999 and Ahlfeld et al., 1994) and field studies (Kirtland and Aelion, 2000, Kirtland et al., 2001, and Yang et al., 2005). Yang et al. found that pulsed air sparging increased the hydrocarbon removal rate by 66%. Pulsed-air sparging enhances treatment because it induces groundwater flow and mixing. Air that is added to the aquifer displaces groundwater in larger pores and increases groundwater flow around the sparging well(s). Once the air flow reaches steady state, preferential pathways for air are formed, minimizing induced groundwater movement. The contaminant removal and oxygen dissolution rates, which are based on diffusion, are limited to the edges of these preferential pathways. If the air flow is pulsed, groundwater circulates as the air channels collapse and re-form for each sparging cycle. Therefore, the "off" cycle of pulsed sparging allows the less treated groundwater to flow into the air channels and mix with the oxygenated water, increasing contaminant removal (Yang et al., 2005).

1.3 Soil Vapor Assessment

The off-gas from an air sparging system is used to determine contaminant removal rates. The off-gas can be measured several ways and there is little scientific consensus as to the best way to capture and measure it. However, the methods to measure soil off-gas can generally be divided into passive vs. active systems.

Passive systems collect the off-gas emanating from the subsurface without creating significant pressure gradients. For example, Kirtland et al. (2001) used multi-level soil vapor probes and Cho et al. (1997) used soil vapor probes installed within the same borehole as the piezometers used. These probes were constructed of 6.3 mm outer diameter (OD) copper tubing that was attached to a section of slotted schedule 40 PVC pipe at the bottom (the intake) and a quick-connect fitting at the top. Passive systems can be as simple as a metal tube with a screen at the end and hand driven to the desired depth, such as the system used by Flynn (1994).

More complex systems have been used to collect a more representative off-gas sample from a larger area. Jellali et al. (2003) used a vapor discharge meter consisting of a 0.3 m^3 chamber made of high-density polyethylene (HDPE) installed to a depth of 0.1 m below ground surface (bgs). The free air volume of the chamber was about 18L. Vapor was pumped through 3 outlets at a rate of approximately 1 L/min. They were connected to 2 activated carbon traps, a flowmeter, and a peristaltic pump. To minimize soil air aspiration in excess of standard (non-pumped) flow rates, the cleaned air was returned to the chamber. The discharge per unit surface is:

$$(Ø) = \frac{m_{res} + m_{ads}}{A\Delta t} \qquad (1.1)$$

where m_{res} is residual vapor mass in the chamber, m_{ads} is the mass adsorbed on the trap, A is the surface area covered, and Δt is the monitoring interval (Jellali et al., 2003). Similar discharge chambers were also used by Tillman et al. (2003).

Active off-gas collection systems often use a soil vapor extraction (SVE) system. SVE has been in use since the 1970s and can be used alone or to complement air sparging systems. SVE and other gas collection systems work by using a pressure gradient to create airflow above the water table. SVE systems can be designed to blow air into the soil or to remove air, but generally air removal is preferred in order to measure and treat off-gas (ACOE, 2002). Active gas collection can use either SVE, which is intended to use a flow rate high enough to enhance volatilization, or bioventing, which adds air at a rate sufficient to assist biodegradation and minimize off-gas.

1.4 Subsurface Air Distribution

Air is significantly more mobile than groundwater and its movement through the subsurface is difficult to predict. Ji et al. (1993) found that for most geological deposits other than gravel, air tends to move through channels rather than as discrete bubbles. Ahlfeld et al. (1994) noted that these channels constrain air movement, making it more likely that residual contamination will be missed. With heterogeneous soils, lower-permeability pockets are likely to be missed altogether. Therefore, other methods have been developed to determine presence and movement. For example, geophysics, especially ground-penetrating radar (GPR), have been used successfully at Borden to determine soil air saturation (Nelson, 2007 and Tomlinson et al., 2003). Tracer tests can also be used to determine the extent of gas migration from the sparge points and the amount of gas added that can be recovered using a gas collection system.

In a tracer test, a tracer gas is added or measured prior to sparging and the concentrations in soil gas and/or groundwater are measured. Tracers can be added to the air sparging airstream, or the components already in the air being sparged can be tracked to examine transport and fate of the injected gas. Common tracers for air sparging include helium and sulfur hexafluoride (SF_6) (Johnson, 2001A). Isotopes, specifically ^{14}C, and dissolved oxygen have also been used to study biodegradation and air sparging efficiency (Aelion et al., 1997), but were not used for this study.

Dissolved O_2 in groundwater is a popular parameter to determine the distribution of air that has been added to the subsurface. However, several factors complicate the behavior of oxygen. Reduced species such as Fe^{2+} and aerobic microbial activity may consume the O_2. The process of collecting groundwater samples may also introduce oxygen or allow it to be lost through cavitation (Johnson et al., 2001A).

SF_6 is slightly more soluble than oxygen in groundwater (40 g/L from Bullister et al., 2002) and can be used as a groundwater tracer instead of dissolved oxygen (Johnson et al., 2001A) to determine how much sparged air has dissolved into groundwater and where it reaches the surface. It has several advantages over dissolved oxygen as a groundwater tracer. It does not occur naturally, so background concentrations are negligible; it can be detected at less than 1 µg/L in air and water, so it can be measured more accurately than O_2; and it is not biodegradable (acts as a conservative tracer). Therefore, SF_6 was planned to be used as a groundwater tracer instead of dissolved O_2.

For an SF_6 tracer test, Johnson et al. (2001A) suggest that the SF_6 should be mixed into the injection gas stream at a known concentration and injected for 12 to 24 hours. This allows SF_6 to dissolve into groundwater in a short enough time that it should not be significantly affected by groundwater movement. If SF_6 in groundwater is greater than 40% of the theoretical solubility (based on the injected gas composition), the sample is within the "zone of aeration". If the SF_6 is less than 10% of the theoretical

solubility, the sample may be within the "zone of treatment". Samples that contain no SF_6 are presumed to be outside the treatment area. The data collected from the downgradient monitoring wells is compared to a sample created by bubbling the same concentration of air and SF_6 into a sample of the same groundwater. Bruce et al. (2001) provide a more detailed discussion of this process.

Helium is a common tracer for air sparging because it is relatively inexpensive, readily available, and can be detected using easy-to-use field instruments. Johnson et al. (2001C) make the following suggestions to conduct a helium tracer test: Helium should be added to the air stream of the sparging system at a set concentration between 2% and 10%. When injection begins, all of the vadose zone monitoring points and any groundwater monitoring wells screened above the water table should be monitored for helium. Sampling should be repeated at monitoring points and wells until 20 minutes after helium injection begins. After this time, the helium should be well mixed. The SVE off-gas should be monitored until the helium concentrations stabilize. If the helium and air injection rates are known, as well as the rate of air leaving the subsurface, then the fraction of helium leaving the system can be calculated using a ratio: observed helium concentration / helium injection rate / air removal rate, as long as the extraction rate is higher than the injection rate (Johnson et al., 2001).

^{14}C has also been used to determine CO_2 production from contaminant biodegradation, although this particular tracer was not planned for this work. Aelion et al. (1997) examined ^{14}C ratios and found that radiocarbon measurements were more sensitive than soil gas composition or stable carbon isotopes for indicating aerobic petroleum degradation. However, carbonate aquifer materials would give an older ^{14}C age in the soil gas CO_2, masking the effect of biodegradation. The authors suggested that comparison of soil gas in a nearby, uncontaminated area would allow for a correction factor.

1.5 Project Objective

The general mechanisms for treatment of gasoline sources using air sparging are relatively well characterized. Pulsed sparging has been identified as having potential advantages over continuous air sparging. However, air flow through the subsurface and the total hydrocarbon mass lost are difficult to predict and quantify. This project is intended to quantify the mass lost through volatilization and through biodegradation in a relatively well-known source using pulsed air sparging and to determine the effect of the source zone removal on downgradient dissolved BTEX concentrations.

This project was developed to build on the results and used techniques developed from several studies of the Borden aquifer. Tomlinson et al. (2003) studied the air distribution caused by air sparging; Nelson (2007) injected CO_2-saturated water into 3-component system in a closed cell at Borden; Fraser (2007)

developed a Raoult's law program for determining source dissolution and plume characteristics using up to 19 components; Mocanu (2007) injected the E10 source, determined the source area size, and monitored the resulting plume; and Yang (2008) examined the relationship between hydraulic conductivity and hydrocarbon concentrations at the E10 source and residual hydrocarbon concentrations.

The extensive studies previously performed at Borden allowed for a detailed understanding of the site hydrogeology and air sparging system performance. This project was intended to take advantage of this institutional knowledge to determine the mass removal of the source zone and its impacts on groundwater concentrations downgradient with an accuracy that is difficult to replicate in field studies, which generally have an unknown source mass and composition and more complex hydrogeology. This project is larger-scale than most laboratory studies and can be considered a bridge between standard laboratory and field studies.

Chapter 2: Site Description

2.1 Project Location

The field site is located at Canadian Forces Base Borden, which is approximately 130 km northeast of Waterloo and close to Alliston in Ontario, Canada. The Borden facility has been used for groundwater research by the University of Waterloo since 1978. The test cell area (Figure 2.1) is located in the sand pit experiment area.

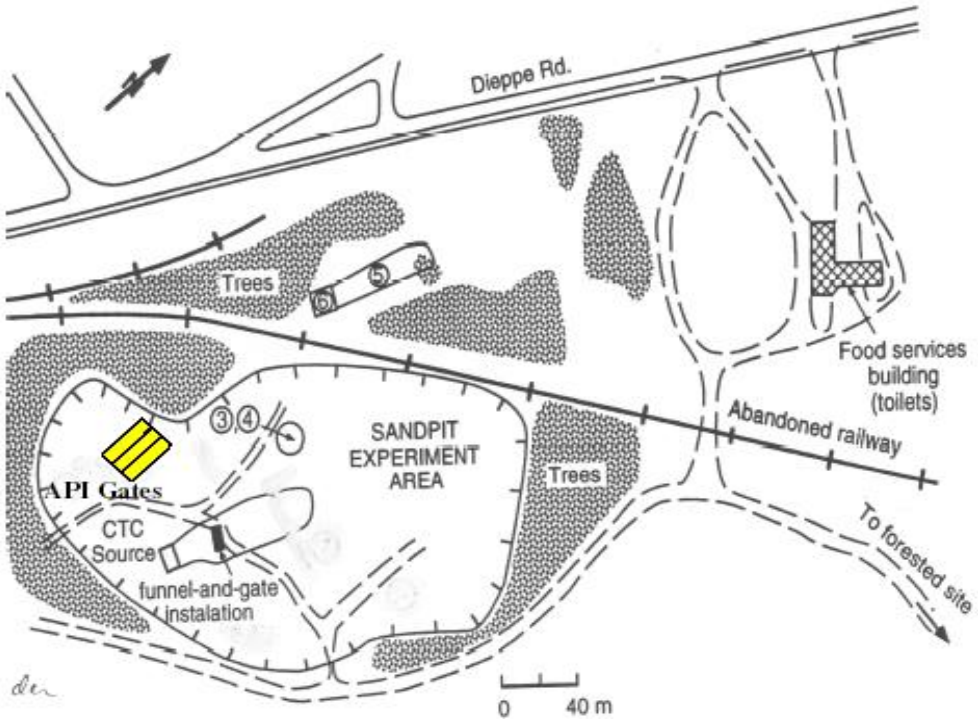

Figure 2.1 Sand pit area with test cells highlighted.

2.2 Test Cell Setup

The treatment area contains three test cells with different gasoline sources. This remedial system was located in the E10 cell, which is the western-most cell in the three API gates. See Figure 2.2 for cell layout.

The cell walls consist of two rows of sheet piling driven to a depth of 7 m. The sheet piling acts as a seal to prevent contamination from the other cell. The sheet piling was supposed to be oriented parallel to flow. Subsequent groundwater sampling showed that the plume is angled slightly to the right facing downgradient and that the plume position in the test cell did not vary seasonally. The test cell contains four rows of six multilevel monitoring wells 1.2 m apart. Each multilevel well has 14 monitoring points

spaced 0.18 m apart, starting at 1.5 m below ground surface (bgs). The last point is the center stalk, which has an open-screened interval from 4.84 to 5.45 m bgs (Mocanu 2007). Open-screened wells were also installed between all multilevel wells. Two open-screened wells were also installed directly downgradient of well 3, which is located in the center of the plume. All open-screened wells are screened from 1 to 5 m bgs.

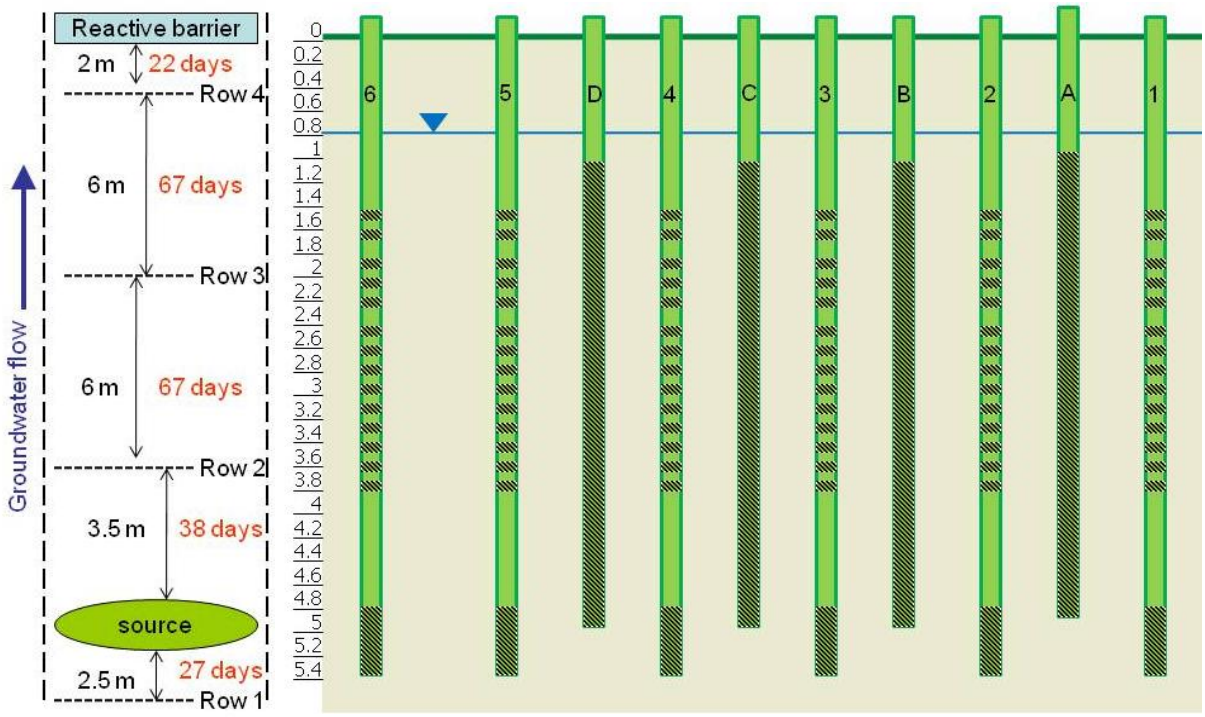

Figure 2.2 Test cell schematic and Row 2 cross section

Figure 2.2 shows the test cell schematic on the left and a cross-section of the row 2 monitoring wells facing downgradient on the right. The groundwater travel time is shown in red; screened well sections are cross-hatched (darker) in the cross sections. The distances between wells are approximated.

2.3 Site Hydrogeology

Site hydrogeology is an important consideration for air sparging systems. Brown et al. (1994) suggest that the aquifer should have no impervious layers above the sparge interval; the permeability should be greater than 10-5 if the horizontal:vertical ratio is less than 2:1, or greater than 10^{-4} if the ratio is greater than 3:1; the saturated aquifer thickness should be between 2 and 10 m; and the depth to water should be greater than 2 m. For the Borden aquifer all of these conditions except for the last are met, as described below.

The aquifer is a relatively homogeneous, clean, well sorted fine to medium sand. Tomlinson et al. (2003) found distinct lower permeability layers at approximately 2.2, 3.0, and 3.9 m bgs in the Borden aquifer near the source layer. Yang (2008) studied the cores collected from the center of and upgradient of the E10 source zone and found differences between the cores even though they were only 50 cm apart. Both cores had a relatively low-conductivity zone from 3.2 to 3.6 m bgs and relatively high conductivity zones at about 2.5 and 4.5 m. These low-conductivity layers tend to impede upward migration of air, causing additional lateral movement. The radius of influence was found to be approximately 2.5 m with a sparge rate of 200 m^3/day, or approximately 5 ft^3/min. The aquifer extends to a thick clayey aquitard beginning approximately 7 to 8 m bgs. Just above the aquitard is a relatively anoxic leachate zone with contaminated groundwater; however, the leachate zone is considered to be relatively thin in this area.

2.4 Hydrogeology and Groundwater Flow

The hydrogeological properties of the Borden sand aquifer have been studied extensively. Mackay et al. (1986) found the porosity to be 0.33 and the average groundwater velocity to be 0.09 m/day. Sudicky et al. (1983) found the following apparent dispersivities: $\alpha_L = 0.36$, $\alpha_{TH} = 0.03$, $\alpha_{TV} = 0.0$. Frind et al. (1999) found the median grain size (d_{50}) to be 0.15 mm, the specific storage to be 0.001 m^{-1}, and the average residual water saturation to be 0.07%. Estimates of hydraulic conductivity in the Borden aquifer vary from $4x10^{-5}$ to $1.04x10^{-4}$ m/s according to several authors (Mackay et al., 1986; Sudicky, 1986; and Schirmer et al., 1998).

In the summer of 2007 additional fieldwork was carried out to determine the hydraulic conductivity of the aquifer within the E10 test cell. Hydraulic conductivity was measured at the layer scale in approximately 20-cm sections with permeameter testing and at the well scale with slug testing. Yang (2008) performed permeameter tests on cores from the source area, just upgradient of the source area, and downgradient of the Row 2 fence (well E) at both gates. Permeameter testing found the average hydraulic conductivity to be about $7.85x10^{-5}$ m/s, which is within the range determined by other authors.

High BTEX concentrations in the source zone were found in area with both high and low conductivity (Yang, 2008). Yang proposed that the high residual concentrations in the low conductivity areas were trapped due to the relatively low-permeability material and that those in the high conductivity areas were from preferential flow of the gasoline into these areas.

Slug tests were also performed in the E10 cell as part of this project using the open-screened monitoring wells in Row 2. Slug test results are discussed in Chapter 6.

2.5 Geochemistry and Biodegradation

The test site aquifer was originally aerobic. However, within the source zone, the aquifer is anticipated to be anaerobic. As oxygen is used by microbes for respiration and removed from the system (oxygen levels below 0.5 – 1 mg/L), aerobic activity stops and anaerobic organisms are able to function. The addition of organic carbon in the form of gasoline allows the existing microbial community to grow because organic carbon is no longer a limiting factor in the aquifer. As the system becomes anaerobic, nitrate provides the next-highest energy potential and is therefore preferentially used once the oxygen is depleted. After nitrate is used, manganese (IV), iron (III), sulfate, and finally CO_2 are used (methanogenesis). However, the electron acceptors utilized are expected to vary depending on distance from the source, with more anaerobic conditions closest to the source and more aerobic conditions at the fringes of the plume (Aronson and Howard, 1997).

Several studies in other aquifers have found that benzene biodegrades aerobically. However, Aronson and Howard's review of field studies (1997) speculated that the field studies indicated aerobic degradation along the flow path, rather than pure anaerobic conditions. More controlled studies in the review found anaerobic biodegradation of benzene, but only in the presence of other nutrients and over long periods. Environmental conditions, such as redox and temperature, did not significantly affect benzene degradation rates.

Aronson and Howard found that toluene does appear to have been biodegraded at all field sites reviewed; however the degradation rate varies with redox condition. It degrades fastest under nitrate-reducing conditions, and degradation rates slow with increasingly reducing conditions. Ethylbenzene and xylenes degrade at similar rates, both slower than toluene. However, they all appear to biodegrade under reducing conditions. However, in some sites, xylenes did not biodegrade unless nitrate was added to the aquifer (Aronson and Howard 1997).

Chen et al. (2008) noted that the only anaerobic redox conditions that the aquifer appears to support are sulfate and nitrate reducing; previous experiments did not find evidence of iron-reducing and methanogenic conditions even with an excess of hydrocarbons. Only toluene has been degraded under sulfate-reducing conditions, but nitrate-reducing conditions are more favorable for biodegradation. Under denitrification, toluene was the most readily degraded (0.170/day), followed by ethylbenzene (0.030/day), then o-xylene (0.013/day). M/p-xylene had a long lag period of minimal degradation, but eventually had a rate constant of 0.018 over 118 days. Benzene did not degrade significantly relative to abiotic controls, indicating that at least under denitrifying conditions, benzene would not be expected to degrade in the Borden aquifer.

2.6 Source Composition

The E10 source, which is a gasoline mix with 10% ethanol, was emplaced below the water table between October 8 and 13, 2004 (Mocanu, 2007). American Petroleum Institute gasoline (API 91-01) was used. 1.13 L of the E10 gasoline was injected in each of fifteen wells at three depths, with water injected above and below the gasoline in an effort to minimize its movement up or down. The fifteen wells were arranged in two rows, for a total row width of 3 m. See Figure 2.3 for the injection well configuration.

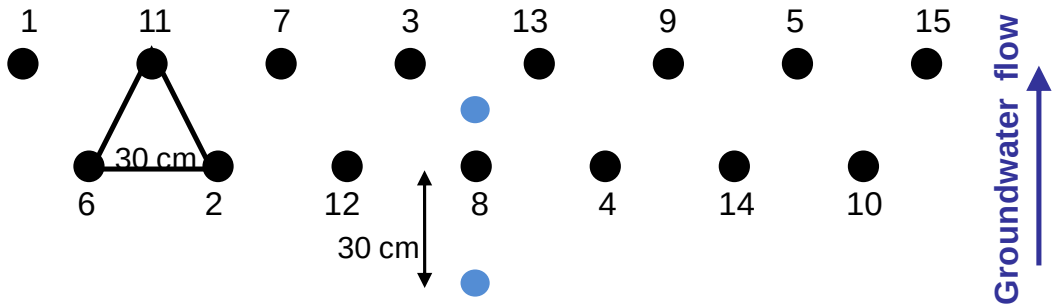

Figure 2.3 Injection well configuration (black dots) and 2008 soil core locations (blue dots)

Approximately 2260 L of water was added during the injection process. A total of approximately 51 L of gasoline mixture was emplaced below the water table. After injection 10.86 L of free product was removed from the injection wells, leaving an initial residual volume of 40.1 L and mass of 29.6 kg.

Mocanu (2007) used the BIONAPL model calibration and detected plume concentrations to determine the source zone dimensions to be approximately 1 m in the direction of groundwater flow, 3.2 m transverse to groundwater flow, and 1.7 m deep.

2.6.1 Estimated composition

Source zone remediation began on April 28, 2008. The source zone is expected to have been depleted by the effects of dissolution and biodegradation in the four years since source emplacement. The gasoline composition remaining in the source zone was determined using a program developed by Fraser (2007) based on Raoult's law. Program details and solubility results are presented in Appendix D.1. Note that the program does not account for degradation effects.

Mocanu (2007) determined concentrations of benzene, toluene, o-xylene, 1,2,3-trimethylbenzene (TMB), and ethanol in the gasoline using gas chromatograph (GC) analysis. Yang (2008) identified potential interference problems with Mocanu's analysis of the pure-phase gasoline: in this phase, other hydrocarbons tended to co-elute with benzene, giving artificially high values. For this reason,

concentrations given by API were used for all compounds except for ethanol, which was added to the gasoline separately. Since Fraser's program has been set up to estimate the mass for 19 chemicals, only contaminants with available water solubilities at environmental temperatures and a weight percent above 1% in the original formulation were used. The other hydrocarbons were assumed to have a solubility of 0.1 mg/L (i.e. essentially insoluble compared to the other compounds) in the absence of additional solubility data.

Based on the program, 22.9 kg or 31.1 L of NAPL would remain in the source area on April 28, approximately 1260 days after emplacement. In addition, approximately 267 g ethylbenzene, 246 g toluene, and 829 g total xylenes, and negligible benzene ($9.2x10^{-7}$ g) would remain in the source zone. Ethanol is completely miscible and would have left within a few months.

2.6.2 Coring results

Yang (2008) took soil cores from within, slightly upgradient of, and downgradient of the E10 source zone in June 2007. All three cores were along the central axis of the source zone, with the central core located as close to the center of the injection area as possible. The downgradient core was located 4.5 m from the source zone and no residual NAPL was found. As such this core is not discussed further. Soil samples were taken at 10 cm intervals, with 25 taken from the central core and 24 taken from the upgradient core. Figure 2.3 shows these core locations.

The upgradient core was collected 30 cm from the center of the source zone and 15 cm from the upgradient injection wells. Soil in the upgradient core had a maximum concentration that was roughly half of the value considered to be indicative of the presence of NAPL based on Feenstra et al. (1991), so concentrations were not high enough to be considered a NAPL source zone.

The core from the center of the source injection zone had concentrations approximately 20 times greater than the NAPL indicator concentration. The NAPL zone was located from 2.9 to 4.1 m bgs, approximately the same depth as the original source emplacement of 3 to 4 m bgs. Therefore, the source zone appears to have remained in the same general vicinity of where it was emplaced.

The high residual concentration in the soil caused similar co-eluting problems as the Mocanu (2007) original NAPL source GC analysis described previously. Therefore, the GC analysis cannot be relied upon for a definitive contaminant concentration within the source zone. For example, the benzene mass derived from the soil core data may be up to 2.5 times greater than the actual concentration (Yang, 2008).

Table 2.1 compares the initial mass to the residual mass determined by Yang (2008) using the Feenstra method and the residual mass expected from Raoult's law. With the exception of benzene discussed

previously, concentrations are lower than projected from Raoult's law, indicating potential biodegradation. The program assumes that the residual hydrocarbons are able to dissolve up to the solubility limit in the groundwater (i.e. reach equilibrium). However, if the residual was not in equilibrium, this would cause a higher residual mass than expected. The contaminant residual masses in Table 2.1 were lower than anticipated, with the exception of benzene, so this possibility is not likely. Another possibility is that the balance of the gasoline mass is not as insoluble as assumed. In this case, more of the mass would have left the source than anticipated.

Component	initial mass (g)	Residual mass from soil lab analysis (Feenstra)	Residual mass from Raoult's law
benzene	326	21	0.00005
Naphthalene	140	15	57
Toluene	2061	41	807
Ethylbenzene	905	60	313
P,M-xylene	1991	107	735
O-xylene	709	47	231
1,3,5-TMB	292	28	197
1,2,4-TMB	905	76	606
1,2,3-TMB	184	13	123

Table 2.1 Residual source zone mass from Yang (2008)

For calculations in this work, the residual mass from Raoult's law was considered to be the source material, for two reasons. First, the soil cores used in the Feenstra analysis were taken a year before remediation. Second, the residual mass from Raoult's law was a more conservative estimate. If the residual mass from Raoult's law was considered, the percentage of mass removed would be lower. However, the soil data were used in the final comparison of masses removed.

Chapter 3: Treatment and Sampling Design

The treatment system was comprised of several components, including the air sparging system and collection and analysis of off-gas and downgradient groundwater samples. For planning purposes, the anticipated length of treatment was calculated first.

3.1 Expected Treatment Length

The theoretical effectiveness of the treatment system was used to estimate the estimated treatment time required to remove the aromatics. As there are two ways that air sparging removes contaminants (volatilization and biodegradation), as discussed in Section 1.2, the treatment time depends on the interaction of these two different processes. In both cases, the following calculations are based on the NAPL source area described in Section 2.6.

The source zone was assumed to have the Borden aquifer porosity of 0.33 (Mackay et al, 1986) and a volume of 5.4 m^3 as discussed in Section 2.6, so the total pore volume would be 1.8 m^3. If air is sparged into the system to increase the air-filled pore volume to 10% of the available pore space, the volume of air would be 0.18 m^3. This air-filled pore volume was selected as a conservative value because Tomlinson et al. (2003) found air saturations of up to 60% in the immediate vicinity of the sparging point with GPR.

Gasoline is composed of a large number of compounds. In order to determine the volume of air required for volatilization and the mass of oxygen required for biodegradation, the residual mass was assumed to be one hydrocarbon. In this case, the BTEX compound with the highest vapor pressure (benzene) and the hydrocarbon with the highest vapor pressure that was analyzed (pentane) were used as analogues for the total mass. Cho et al. (1997) and Kirtland et al. (2001) used hexane, which has a vapor pressure between that of pentane and benzene, as an analogue for the gasoline mass for their calculations.

Assuming the source consisted of benzene, the aerobic reaction to break down the contamination is

$$C_6H_6 + 7.5O_2 \rightarrow 3CO_2 + 1.5H_2O \qquad (3.1)$$

If the source consisted entirely of pentane, the aerobic reaction would be

$$C_5H_{12} + 11.5O_2 \rightarrow 5CO_2 + 6H_2O \qquad (3.2)$$

based on Rogers et al. (2007). The source zone mass is 22,300 g, which would be 285.5 mol benzene or 308.9 mol pentane. The amount of O_2 required to completely mineralize a benzene source area according to Equation 1.1 is 2142 mol O_2 (285.5 mol x 7.5) or 68,540 g O_2. The amount of O_2 required to

completely mineralize a pentane source area according to Equation 1.2 is 3552 mol O_2 (308.9 mol x 11.5) or 113,700 g O_2. O_2 has a solubility of approximately 0.01 g/L. In the best-case scenario, 6.9 million L of oxygenated water would be required to treat the source area. This shows that dissolving oxygen in groundwater is not enough to stimulate biodegradation in the source zone within a reasonable time frame; therefore, air sparging is required to remove contaminants more efficiently.

First, the gas constant is used to determine the molar concentration of the contaminant (benzene or pentane) in the pore space, as provided below.

$$n = \frac{Pi}{(RT)} \qquad (1.3)$$

In Equation 1.3, n is the molar concentration (mol/L), R is the gas constant (0.08206 atm-L/mol-K), T is the temperature (283.15 K), and P_i is the ideal vapor pressure (0.125 atm for benzene and 0.6776 atm for pentane from Montgomery, 2000). Therefore, the molar concentrations would be 0.00538 mol/L and 0.0292 mol/L for benzene and pentane, respectively. These are multiplied by the volume of air in the pores (180L) and result in 0.968 mol benzene or 5.26 mol pentane in the air fraction of the source zone pore volume.

If the air sparging simply physically removed the source zone vapor (e.g. volatilization) then 276 pore volumes would be required to remove a benzene source and 59 pore volumes to remove a pentane source. Soil air conductivity can be difficult to measure, but is generally lower in saturated soils such as those at Borden. Benner et al. (2002) found a water-saturated horizontal soil air conductivity of 130 m/day for a site with similar stratigraphy to Borden (fine to medium sand with some fines). Using the standard rule that the vertical conductivity is 1/10 of the horizontal conductivity (Freeze and Cherry, 1979), this would give a vertical air conductivity of 13 m/day. With a source zone area of 3.2 m^2, this gives an overall flow rate of 42 m^3/day (1.73 m^3/hr). The air-filled pore volume is assumed to be 0.18 m^3, so it would take 0.104 hr to remove a pore volume. Therefore, it would take 28 hours to remove a benzene source and 6 hours to remove a pentane source through volatilization. This assumes a best case scenario: the air injected would contact all of the residual source material, have time to equilibrate and reach full air saturation, and then be able to freely move upward and release into the atmosphere.

Biodegradation depends on O_2 rather than simply air availability and O_2 is the limiting factor for hydrocarbon biodegradation. Air is 20% oxygen by volume, so the amount of O_2 in this pore volume would be 0.036 m^3 or 36 L. If the entire source were to react with the O_2, the molar concentration of O_2 required at atmospheric pressure can be determined using Equation 1.3. In this case, the same value for R

and T described above and an air pressure of 1 atm are used. This value is then multiplied by the 36 L O_2 in the pore volume to get 0.3099 mol oxygen. As discussed above, 2142 mol O_2 are required to mineralize the benzene source and 3552 mol O_2 for the pentane source. Therefore, it would require 6900 pore volumes (30 days) to biodegrade the benzene source and 11,500 pore volumes (50 days) to biodegrade the pentane source.

It is important to note that the treatment times discussed are for ideal conditions. Even with perfectly homogenous material, the air channels will bypass at least some of the NAPL. So, a total active sparging time of 30 hours was planned to remove the hydrocarbons by volatilization, with the expectation that some of O_2 added would assist in biodegradation.

3.2 Analytical Methods

Analytical methods for each media are described in the following subsections.

3.2.1 Hydrocarbon (off-gas)

Off-gas samples were analyzed using GC for hydrocarbon analysis. The gas samples were originally planned to be analyzed for BTEX, TMB, and naphthalene, the standard suite for groundwater, but initial analyses found much higher concentrations of lighter hydrocarbons. Therefore, the samples were analyzed for BTEX, pentane, and hexane instead. Pentane and hexane were chosen for consistency with the analyses performed as part of Nelson's (2007) work. Also, pentane and hexane were two of the four compounds with the highest concentration anticipated in the source zone after 1260 days of emplacement. They were also two of the top five compounds with the highest vapor pressure from the hydrocarbons used in the Raoult's law program discussed in Section 2.6.1. Since BTEX, pentane, and hexane did not make up the bulk of the compounds detected, the data was analyzed to produce C_5-C_{10} total petroleum hydrocarbon (TPH) data.

The samples were run using a Hewlett Packard 5890 gas chromatograph equipped with a split injection port, capillary column, photo-ionization detector (PID), and a Varian Genesis headspace autosampler (Chatten, 2008). Samples were held upside-down in water to minimize sample loss, then added directly to the autosampler carousel. Calibration standards were prepared by spiking the vials with methanolic stocks, sealing, and then analyzing using the same method as the field samples. Peak areas were measured using a HP 3392A integrator. The Fraction 1 TPH (C5-C10) was determined by adding the peak areas from RT 1.9 to 15.05 and dividing by the average response factor of hexane and toluene. The method detection limit (MDL) ranged from 2 to 5 ppb.

Quality control samples for the off-gas included duplicates, blanks of the injected air ("tracer" samples), equipment blanks, and trip blanks. Duplicates were collected immediately after the original sample and sent to the lab blind, with the identifier and the sample it was connected with written on the field log sheets. Equipment blanks were collected to ensure that the sampling equipment was properly cleaned out by flushing through ambient air. They were collected by filling the sample syringe with clean air and filling the vials the same way as a regular field samples. Trip blanks were vials of clean air that were capped underwater. Duplicates and tracer samples were collected daily, and trip blanks were collected periodically. In addition, samples were collected of the isobutylene calibration gas and sent for analysis the same way.

3.2.2 Hydrocarbon (groundwater)

Aqueous samples for hydrocarbon analysis and standards were equilibrated to room temperature prior to extraction (VanderGriendt, 2008). To extract a sample or standard, the Teflon® screw cap of the vial was quickly removed and 5.0 mL of sample was discarded with a glass/stainless syringe. This was followed immediately by the addition of 2.0 mL of methylene chloride containing the internal standards m-fluorotoluene and fluorobiphenyl (25 mg/L). The vial was quickly resealed and agitated on its side at 350 rpm on a platform shaker for 20 min. After shaking, the vial was inverted and the phases were allowed to separate for 30 min. Approximately 1.0 mL of the methylene chloride phase was removed from the inverted vial with a gas tight glass syringe, through the Teflon septum. The solvent was added to a Teflon sealed autosampler vial for injection into the GC. Samples were analyzed with a HP 5890 capillary gas chromatograph, a HP7673A autosampler, and a flame ionization detector. Three µL of methylene chloride was injected in splitless mode (purge on 0.5 min, purge off 10.0 min) onto a 0.25 mm x 30 m long DB5 capillary column with a stationary phase film thickness of 0.25µm. Helium column flow rate was 2 mL/min with a make-up gas flow rate of 30 mL/min. Injection temperature was 275˚C, detector temperature was 325˚C and initial column oven temperature was 35˚C. This was held for 0.5 min, then ramped at 15˚C/min to a final temperature of 300˚C and held for 2 min. Chromatographic run time was 10 minutes. Data integration was completed with a HP 3396A integrator.

Calibrations were made in internal standard mode and standards were run in triplicate at five (or more) different concentrations covering the expected sample range. Standards were prepared by spiking water with concentrated methanolic stock standards (purchased and certified from Ultra Scientific Analytical Solutions). Standards were extracted and analyzed by gas chromatography in the same way as samples. A multiple point linear regression was performed to determine the linearity and slope of the calibration curve. Quality control information on calibration curves (percent relative standard deviation and percent error) and blank information were included with reported data. Extraction duplicates were performed on

samples and results were acceptable when they agreed within 10%. Matrix spikes were performed when necessary by spiking a known amount of midrange standard into a duplicate field sample and then calculating the amount recovered after extraction. Method Detection Limits (MDLs) were 1.9 µg/L for benzene, 1.8 µg/L for toluene, 1.7 µg/L for ethylbenzene, 3.7 µg/L for p/m-xylene, 1.5 µg/L for o-xylene, 1.5 µg/L for 1,3,5-trimethylbenzene (TMB), 1.3 µg/L for 1,2,4-TMB and 1,2,3 TMB, and 1.7 µg/L for naphthalene.

A number of field quality control samples were collected, including field duplicates, equipment blanks, and trip blanks. Field duplicates consisted of an entire field sample set collected after the original sample was completed. Duplicates were taken approximately every 20 field samples or at a minimum once per field event. Duplicates were sent "blind" to the laboratory and will therefore only had the duplicate number, along with the date and time, on the sample bottles. After analysis is complete, the duplicate was checked against the sample concentration. Lab duplicates were taken from the same aliquot or another bottle and compared to the original, and were taken approximately every 10 samples.

Equipment blanks were collected every 20 field samples, alternating with field duplicates. Therefore, some sort of QC sample was taken every 10 field samples. Equipment blanks were taken the same way as field samples, except that the pump/sampling apparatus was attached to a tube in a container of de-ionized water instead of a field sampling tube. The field sample collected before and after the rinsate blank was recorded. The rinsate blank is used to determine the degree, if any, of cross-contamination between samples.

Trip blanks were used to ensure that the sampling bottleware and rinsate blank water (as applicable) are free of contaminants. Examples of possible contamination are bottle/water storage near gasoline tanks or gas stations as well as bottle contamination from inadequate cleaning. Trip blanks were collected by pouring de-ionized water into bottles from the same sample tray/lot as the field samples and were to travel with the other samples at all times.

3.2.3 O_2 and CO_2 (off-gas)

A Fisher/Hamilton Model 29 Gas Partitioner was used for CO_2 and O_2 analysis. The instrument has two chromatographic columns in series with a detector at the end of each column. This arrangement permits analysis of widely different types of gases in a single sample. Gas was collected in the field in disposable 30mL Becton Dickinson Luer Lok™ Tip syringes. The syringes were sealed with single use Becton Dickinson 22 gauge precision glide needle tips and a black butyl rubber stopper.

The samples were equilibrated to room temperature prior to analysis. A 1 mL sample loop was used to introduce gas samples into the carrier gas stream with a precision of 0.3%. With this setup, CO_2 was eluted from column 1 and detected at the first detector while O_2 and nitrogen separated in column 2 and were measured individually at the second detector. CO_2 was permanently absorbed as it entered column 2 and never reached the second detector.

The external standard method was used for calibration with commercially obtained, certified gas mixtures (three concentrations in triplicate) in the expected range of the collected samples. When the chromatogram of the standard mixture was obtained, the peak height of each component was measured from the actual baseline of the peak. The obtained calibration data are subjected to linear regression analysis and the resultant equation is used to determine unknown sample concentrations. At least 3 samples of a calibration mixture were run prior to the analysis of unknown samples and also after every 10 unknown samples to ensure the gas partitioner was operating in a consistent manner. Sample peak heights are measured, and the concentration of the unknown components determined using linear regression.

The method detection limit for this procedure has not yet been determined according to EPA protocol. However, CO_2 can be detected with an accuracy of 0.589 mg/L and O_2 with an accuracy of 7.14 mg/L in a 1 mL gas sample under normal operating conditions.

The Fisher/Hamilton Partitioner malfunctioned in the second month of treatment and samples were run on a GOW-MAC (series 350 GP) GC equipped with a thermal conductivity detector instead. Peak areas were measured by a HP3380A integrator. This method could not determine O_2 data, so for this period only CO_2 data was recorded. Gas samples were injected into a 2 mL sample loop (overfilled) and a valve switch introduced the sample into the carrier gas stream.

The GC was calibrated using an external standard method with commercially obtained, certified gaseous standards in the expected range of the collected samples. CO_2 standards consisted of 0.5%,10.0%, 25%, 50% and 100% CO_2 purchased from Praxair, and air at 0.03% CO_2. When the chromatogram of the standard gas mixture was obtained, the peak area was subjected to linear regression analysis and the resultant equation was used to determine unknown gas sample concentrations. At least 3 samples of CO_2 (at 5 concentrations) were run prior to the analysis of unknown samples and also after every 10 unknown samples, to ensure the gas chromatogram was operating consistently. Sample peak areas were measured and the gaseous CO_2 concentration was determined using the linear regression equation.

Quality control samples for the O_2/CO_2 samples included field duplicates and "tracer" samples, containing samples of the injected air. Duplicates were collected daily, and tracer samples about every 2 days.

The O_2 data appears to include instrument error. For example, in Figure 5.11, from 25 to 50 hours, the O_2 data seems to "rest" at the same concentration. Lab blanks recorded concentrations that were approximately 0.05 % too low, which are much smaller concentrations than the differences seen in the field data. Therefore, the observed concentrations would appear to reflect field conditions rather than instrument error.

3.2.4 SF_6 (groundwater and off-gas)

The SF_6 analysis procedure is the same for both aqueous and gas samples (Chatten 2008). Samples of both media were collected in 40 mL screw cap glass vials. The vials were fitted with Teflon-lined septa and stored at 4˚C for less than one week prior to analysis. For each sample, a 10-mL aliquot was withdrawn from the sample bottle into a 30-mL glass syringe followed by 10 mL of air. If sample dilution was required, a 2mL aliquot was withdrawn into a 10-mL glass syringe and 8 mL of air added. The syringe was shaken and allowed to equilibrate for 1 hour. A 4 µL aliquot of the gas phase from the syringe (for liquid samples) or sample vial (for vapor samples) was injected for chromatographic analysis.

The gas samples were analyzed with a Shimadzu GC-9A GC equipped with an electron capture detector. The GC was calibrated in an external standard mode using several concentrations, which were prepared by spiking small volumes (100-2 µL) of SF_6 into 1 L bottles. The dissolved SF_6 concentrations in the original water samples were calculated based on 100% partitioning into the headspace. The MDL for SF_6 is < 1.0 µg/L.

Quality control samples were collected for SF_6 at the same rate as those discussed in Section 3.2.1 (for off-gas) and Section 3.2.2 (for groundwater).

3.3 Treatment System Design

The air sparging system was coupled with a collection system to capture the off-gas. The off-gas was continually monitored using a PID and sampled for BTEX, pentane, hexane, oxygen, and carbon dioxide at regular intervals. Helium and SF_6 samples were collected during tracer tests. The treatment system consists of several components: the off-gas collection system, the air sparging points, tracer injection points, and piezometers for water level and temperature measurements. See Figure 3.1 for a plan view of the treatment system and Figure 3.2 for a close-up plan view of the downgradient monitoring wells.

The treatment system design was modified from an earlier iteration of the treatment system that ran in January 2008. The original system and the changes made in response to this first treatment round are discussed in Appendix A.

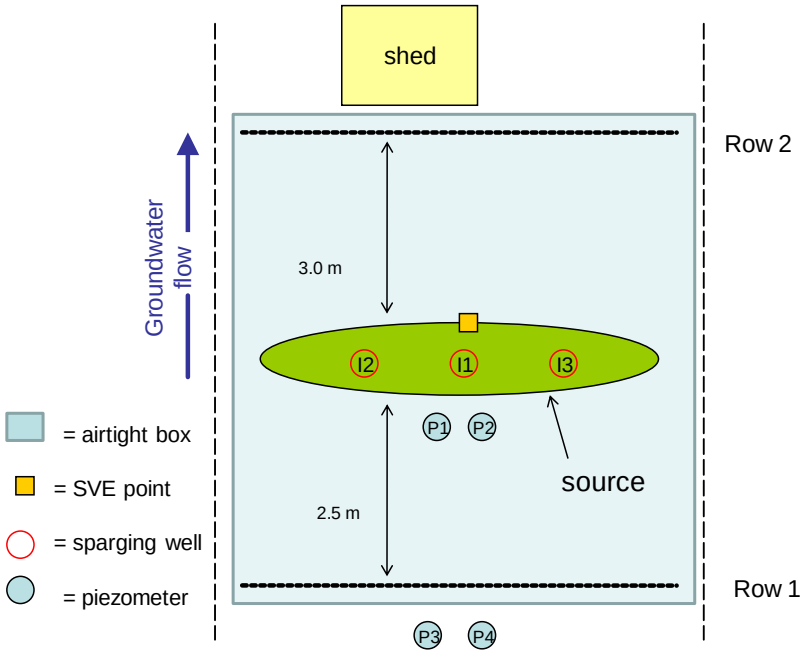

Figure 3.1 Treatment system schematic

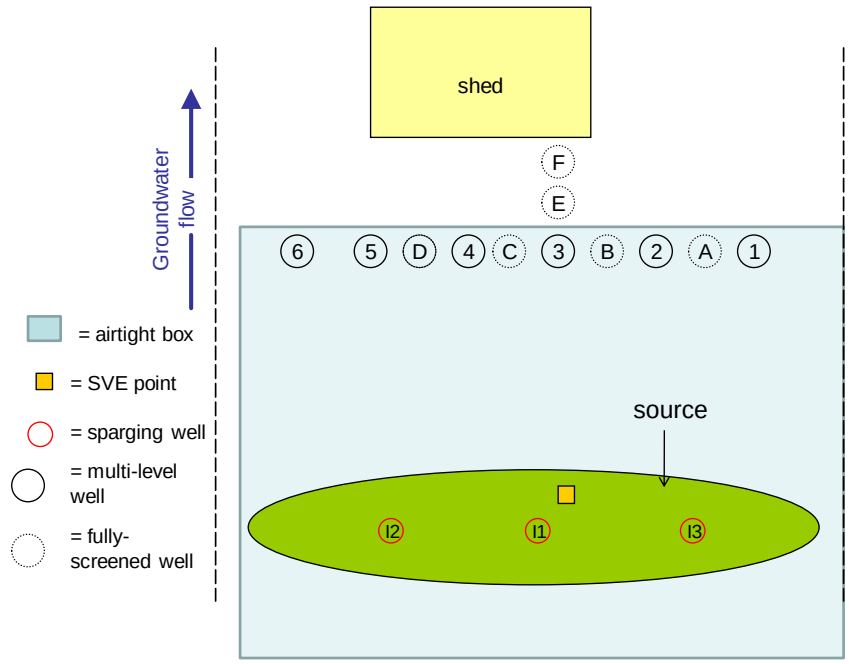

Figure 3.2 Monitoring wells with treatment system

3.3.1 Air sparging well configuration

The number and configuration of air sparging wells depends on the wells' "radius of influence", which is the radial distance from the sparge well where air saturation is sufficient for treatment. Tomlinson et al. (2003) found the air-saturated zone to be approximately 2.5 m in diameter in the Borden aquifer.

The source zone width is approximately 4.5 m, so one sparge point should have been sufficient based on the work by Tomlinson et al. However, for this work the sparge point was set above the leachate zone (Section 2.3) to avoid altering its redox conditions. This left minimal room below the contaminant zone (maximum depth of approximately 4 m) for the sparged air to spread laterally before reaching the source zone. Therefore, the radius of influence of a single sparge well within the source zone may be smaller than described by Tomlinson et al. Consequently, two additional injection wells were added, one on either side of the main sparge point.

Ahlfeld et al. (1994) suggest that sparging point construction is not critical, as the dominant factor in air movement in the subsurface is the formation material itself once the air is further than a few cm from the initial sparge point. The injection point construction in this study was similar to that used by Tomlinson et al. The injection points were threaded to 1.8 cm ID/2.7 cm OD drill rods and driven using a jackhammer to minimize soil disturbance around each point. Each sparge point was 20 cm long and 3 cm in diameter, and had rings of 4 8-mm holes covered with stainless steel mesh located every 2.5 cm along the length of

the housing. The sparge point was connected to the compressor by 1 cm ID teflon tubing. The top of the screen was set at 5 m bgs. Air was sparged using a compressor instead of a tank because the largest portable tank available only contains 12.6 m^3 (445 ft^3) of gas, or enough for approximately 1.5 hours of sparging.

Injection point I-3 was constructed differently from the others because the Teflon tubing was shaken off the barbed fitting at the top of the screen during installation. As the fitting was located below the top of the casing 5m bgs, it could not be attached securely to the barbed fitting. Rather than re-drill and possibly provide a conduit to the atmosphere via the backfilled hole, the injection point was left in place. The Teflon tubing was connected to the top of the casing, which was threaded and wrapped with Teflon tape to avoid air leaks.

The air sparging configuration is provided in Figure 3.3. Note that for the first sparging round, both tracer gases were added to the main line with a single t-connector, rather than having separate inlets. Also, the flowmeter on the main line was added after the first sparging round.

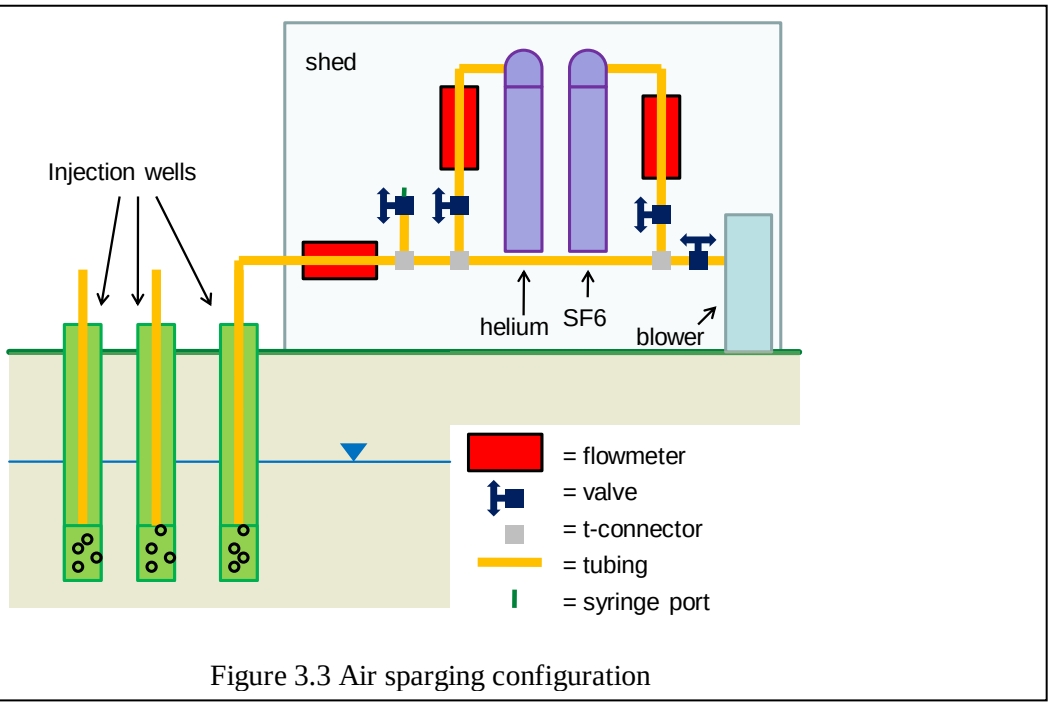

Figure 3.3 Air sparging configuration

3.3.2 Off-gas collection

The air collection system used an air-tight box to collect vapors above ground surface. The box was designed to have a wall height of 45 cm, with a perimeter dug to a depth of 15 cm bgs to help seal in the air. The sides of the box were covered with pool liner material and the top was covered with a single piece of slightly thicker pond liner that extended down over the sides. All seams were sealed with

Tauck™ tape. Box supports were designed using frames which rested on blocks to allow for free air circulation. The box heights were checked with a laser level; from this, it was found that the ground surface was relatively uneven, so that box height ranged from 8” to 18” high. Some of the walls were cut short to minimize extra digging.

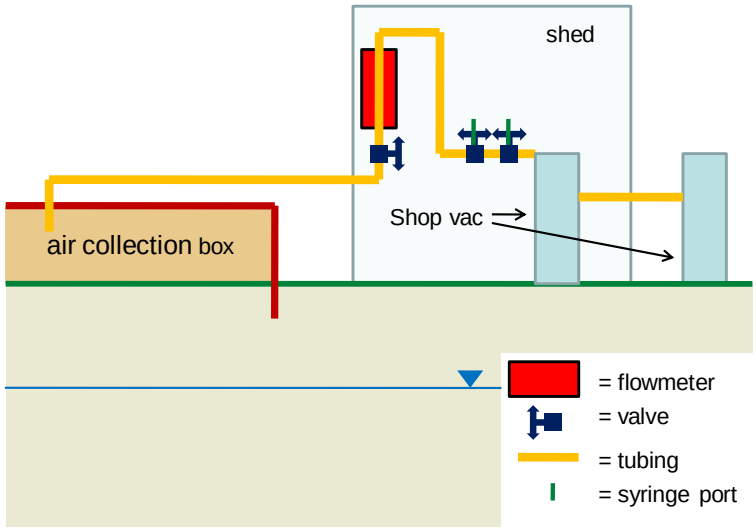

Figure 3.4 Air collection system

The soil gas collection line started at the center of the box slightly downgradient of injection point 2 and connected inside the shed to the sample ports and first in-line vacuum pump. The flow diagram (Figure 3.4) shows the connections, flowmeters, and ports for the system. Note that the dosimeter well F shown in Figure 3.2 was used for another study and not discussed here.

Figure 3.5. Box construction (left) and setup during high water table (right)

Extensions were added to piezometers 1 and 2 so that they could be accessed from the top of the box. Construction photos for the revised treatment system are shown in Figure 3.5. Note that for all photos of the box, the uneven ground and sheet piling heights create the illusion that the box is tilted. However, laser-level checks indicated that the sides had absolute height differences of less than 3 cm.

A test of the off-gas collection system showed that with longer tubing (the shed was placed near the edge of the box instead of its orginal position next to the treatment system), the system had significant pressure loss. An additional vacuum pump was added.

The January test showed that groundwater response peaked at approximately 45 minutes after sparging, so the sparging time was adjusted to 1.5 hours on and 1.5 hours off instead of the 4 hours originally planned for the first test. After the first 30 hours of sparging, this was shortened to 1 hour on and 1 hour off.

3.3.3 Off-gas hydrocarbon monitoring – GC

GC analysis was the primary method used to determine contaminant concentrations in the system off-gas. Samples were collected every 10 minutes for the first two sparging rounds, after which the sampling rate was decreased to once every 20 minutes during the course of treatment.

The samples were collected using gas-tight syringes inserted into the sample port. The syringe needle made an airtight seal with the sample port tubing. This was indicated by an inability to draw air into the syringe prior to opening the sample port valve. The sample vials used for GC analysis were previously checked to ensure that they were free of chips in the neck. They were subsequently filled with clean (de-

ionized) water and placed upside-down in a basin of water. The sample syringe was then emptied into the sample vial, displacing the water. Once the vial was filled with air, it was capped with a crimp seal. This method has been developed from previous work at Borden (Nelson, 2007). The syringes were cleaned by filling and evacuating the syringe with clean air prior to sampling.

The samples were kept as airtight as possible. A lockable syringe was used to pull air from the system. The sample ports were kept closed until the syringe was inserted into the port, opened for sampling, and closed immediately thereafter. The BTEX sampling syringes were placed in a tub of water immediately upon sample collection, then used to fill the vials as described. The vials were then stored upside-down inside a cooler with their seals under water. O_2 and CO_2 samples were taken using disposable syringes from the same sample ports as the hydrocarbon lab samples. Tracer samples confirmed that the air added via the air sparging system had similar O_2 and CO_2 ratios to clean air at standard temperature and pressure. See Section 3.2.2 for analytical methods.

The vacuum pumps used leaked because they were designed to draw air into the chambers to cool the motor. This did not impact the sample ports, which were "upstream" of the pumps (see Figure 3.4). The only impact of air leaks into the vacuum pumps was a decreased flow as measured by the off-gas flowmeters, which were also upstream of the pumps. The off-gas flowmeters therefore measured the "true" flow of air leaving the box, but the air flow through the pumps and to the PID/helium sample ports was much higher, causing dilution.

3.3.4 Off-gas hydrocarbon monitoring – PID

The off-gas was monitored continuously for total VOCs using a PID, which recorded the concentration every 10 s. The PID is a sensitive but non-selective instrument that uses UV light to ionize chemicals for detection. PIDs do not burn or permanently alter samples (Rae Systems, 2008B). The PID was calibrated each morning with fresh air (0 ppm hydrocarbons) and 100 ppm isobutylene. The calibration was checked several times per day as well as at the end of each day. The PID has response correction factors with a range of 0.35 to 67 (unitless) for the 10.6 eV lamp used, so it was intended to supplement the GC sampling data and not to make quantitative hydrocarbon measurements. See Table 3.1 for a list of PID response factors for source hydrocarbons with at least 1% weight percent in the initial emplaced source. Compounds without listed correction factors are not included.

	correction factors		ionization energy (eV)	% total pre-treatment source
	10.6 eV	11.7 eV		
n-hexane	4.3	0.54	10.13	2.56
n-pentane	8.4	0.7	10.35	2.31
n-butane	67	1.2	10.53	2.29
toluene	0.50	0.51	8.82	1.93
m-xylene	0.44	0.40	8.56	1.85
n-heptane	2.8	0.6	9.92	1.38
ethylbenzene	0.52	0.51	8.77	1.09
p-xylene	0.39	0.38	8.44	0.74
o-xylene	0.46	0.43	8.56	0.52
1,2,3-trimethylbenzene	0.53	0.6	9.25	0.26
benzene	0.35	0.3	8.41	<.01

Table 3.1 PID response factors of selected hydrocarbons (Rae Systems, 2008B)

Nelson (2007) also used a PID to calibrate the GC data from treatment system off-gas; however, he used a simplified system with only pentane, hexane, and soltrol. The pentane and hexane were the volatile components and the soltrol was used as an analogue for the bulk of the contaminant, which was relatively inert. The first phase of work used a correction factor to determine hexane and pentane concentrations, while the second phase used two PIDs calibrated to pentane and hexane. Nelson found the actual response factor for the isobutylene and hexane (using commercial gas mixtures) to be different from published values, even before taking into account temperature and moisture changes in a field environment. Therefore, the PID accuracy is relatively low compared to the GC analysis even for single-compound gases.

This gasoline source, however, is a mixture of a large number of hydrocarbons, as discussed in Section 2.6. Therefore, the PID was used only qualitatively to ensure that the 20-minute GC sampling interval did not miss any changes in off-gas concentrations.

One of the concerns prior to starting treatment was that the concentrations of the off-gas would be higher than the PID could read. The PID has a maximum concentration reading of 10,000 ppm isobutylene or 5,300 ppm benzene. In order to ensure that the PID did not “max out” on readings, a calculation was performed to determine the concentration of benzene-saturated air. The vapor pressure of benzene is 75 mm Hg or 0.0987 atm at 20°C (Montgomery 2000). The vapor pressure was converted to a concentration using Equation 1.3. With a molar weight of 78.1 g/mol, this gives a concentration of 0.315 g/L. Since

benzene has a density of 88 g/cm, this translates to a concentration of approximately 358 ppm and therefore would not "max out" the PID.

3.3.5 Tracer injection and monitoring

Helium was the primary tracer used during the treatment. SF_6 was injected only for the last day of sparging in order to determine how much of the sparged O_2 would dissolve in groundwater and persist in the plume.

The tracer sample port was attached to the air injection line approximately 30 cm downstream of the tracer injection port. This was approximately 3 times more than the minimum length of 10 pipe diameters suggested by Bruce et al. (2001) for complete mixing of the tracer and injected gases. During the tracer test, the tracer gas pressure was kept at least 10 psi above the airline. See Figure 3.1 for a diagram including tracer gas injection configuration.

The helium tracer tests were initially planned to be run as suggested by Johnson et al. (2001C) and described in Section 1.4. However, the helium tanks that were small enough to be brought to the site held less than 20 minutes' worth of helium at the recommended concentration of at least 1% for a tracer test. Therefore, tests were run for a shorter length of time. This change also provided additional data concerning the length of time it took for the injected helium to re-appear in the off-gas outlet.

3.3.6 Transducers

Water level pressure transducers can be used to determine the time required to reach near steady-state air distribution in the aquifer, volume of air channels, and to assess the general distribution of potential lower-permeability zones, which may trap air (Johnson et al., 2001B). Johnson et al. (2001A) suggest that piezometers with transducers do not need to be evenly distributed around the sparge well because groundwater pressure propagates much more evenly than air. For this field test, transducers were added to nested piezometers screened at depths of 3 to 3.5 m and 3.5 to 4 m bgs, with each pair of wells located 1 and 3 m away from the sparging well. See Figure 3.1 for piezometer locations. Previously, Tomlinson et al. (2003) used transducers in piezometers located 0.2 m, 3 m, and 6 m from the sparge well at Borden, with the best responses closer to the sparge wells. Therefore, the closer well cluster was installed in order to determine timing of the sparging cycle and the further well cluster was installed to evaluate effects at the edge of the source area.

When the well was to be sparged, the spike in hydraulic pressure and subsequent decline were measured. Once the pressure recorded (water level) returned to the pre-sparging pressure, sparging was stopped.

This cessation of air flow would cause the pressure to drop and then slowly return to the original level. After this point, sparging could be started again.

Reelogger™ transducers with 50,000 memory points were used to record pressures in each of the piezometers. Readings were initially taken every 5 s, but pressure changes were slow enough to justify changing the rate to every 10 s.

The transducers also recorded ambient and groundwater temperatures at the same time the water levels were recorded. The transducers were set at the bottom of the wells so the groundwater temperature would be minimally affected by surface temperature fluctuations. Ambient temperatures were expected to be higher for transducers installed at piezometers 1 and 2 because the temperature probes were located about 10 cm above the black box liner material, which heated up significantly in the sun.

3.4 Plume Testing and Sampling

The monitoring well fence located directly downgradient of the source area (row 2) was used for plume analysis. It is described in Section 2.2. Figure 3.2 shows the row 2 well configuration. Groundwater samples were collected using several methods to determine mass discharge through the fence. Hydraulic conductivity (slug) tests were conducted to refine mass discharge estimates.

3.4.1 Groundwater sampling

Groundwater samples were collected from the multilevel wells using a peristaltic pump, with the sample collected before going through the pump head to reduce cavitation. Samples were collected in 40 mL vials and capped with Teflon-lined septa. Vials were filled completely to minimize headspace and preserved in the field with 0.4 mL of 10% sodium azide solution (v/v). This method is consistent with previous work performed at this site (Mocanu 2007).

In addition to the existing multilevel wells, open-screened wells were installed in 2007 as described in Section 2.2. The open-screened wells were sampled using a variety of methods to determine the overall concentration in the well at a given time. The samples were collected from well E, located 0.5 m downgradient of well 3 and in line with the center of the plume.

Method 1 involved purging a well volume by raising and lowering the tubing intake (connected to a peristaltic pump) and then filling the standard sample volume (three 40 mL vials) by turning the pump down and pulling up the tubing quickly to try and get a representative sample. Method 2 involved mass evacuation with a trash pump. The hose was raised and lowered the length of the well, agitating and removing a significant volume of water from the entire screened interval. After the hose was raised and

lowered, the outlet was attached to a 20 L plastic carboy and the hose moved up the well as the carboy was filled. Method 3 was the EPA low-flow sampling method (EPA 1992). A peristaltic pump was used (sampling before the pump head) with a flow rate of 100 mL/min. DO, conductivity, turbidity, and temperature were monitored, and sampling commenced once all of the indicators were stable (within 3%). Method 4 was essentially the same as method 1, except that the sample collection bottle was 1L in order to produce more even mixing of groundwater while minimizing headspace during sample collection.

Ceramic dosimeters were planned to be used in the open-screen wells to determine the discharge over time. However, results from a field test at the nearby GMT cell from October to December 2007 were inconclusive, as dosimeter mass discharge estimates were up to 2 orders of magnitude lower than expected for peak concentrations. Lower concentrations in the nearby multilevel wells were consistent with dosimeter results. Therefore, dosimeters were not installed in the E10 gate as part of this project.

3.4.2 Hydraulic conductivity tests

Hydraulic conductivity (slug) tests were conducted in August 2007 at all of the row 2 wells. The slug tests were conducted by dropping a solid PVC slug (3.8 cm in diameter, 100 cm long) into the well and measuring rebound using transducers.

Chapter 4: System Performance

The off-gas collection system ran for approximately 280 hours over the 33 days of active sparging. It was shut down at night because the vacuum pumps tended to produce erratic flow rates if not adjusted manually. Also, the system initially overloaded the circuits and shut down. The off-gas collection system was operated for a half hour prior to initiating sparging each day and at least 2 hours after ending sparging for the day. As a result, the sparging run time was 98 hours, less than half of the total off-gas removal run time.

In general, air injection rates were lower than anticipated, so the airflow rates out through the off-gas collection system were lowered to reduce dilution. Injection points did not perform equally, as two were clogged to varying degrees. A high water table during treatment allowed easier observation of leaks, but caused problems with sealing tape degradation toward the end of treatment.

4.1 Sparging Effects on Groundwater

Air sparging impacts on the subsurface could only be measured indirectly, as the box used for gas collection covered most of the affected area and had only one outlet. However, the impact of sparging could be seen in water level changes in piezometers located inside and outside of the box, groundwater temperature changes inside the box, and in the physical rise of the water table around the box.

4.1.1 Water level changes

Johnson et al. (2001A) noted that the length of time required for a pressure pulse to return to the original level is a general indicator of aquifer permeability. If the pressure returns to the original value within a few minutes it may indicate a highly permeable formation, with a narrow treatment zone and possibly short-circuiting to the surface. On the other hand, if the pressure does not return to the original level in a few hours, it is an indication of one or more impermeable zones that may block air flow to target areas.

The transducers measured the height of the water column. Each piezometer had a slightly different total depth, so to compare the relative piezometric surface elevation, the ground surface was given an arbitrary elevation of 10 m. This kept all values positive for simplicity. The conversion factors for the raw data and a diagram showing the relative elevations are provided in Figure 4.1.

	total depth (m bgs)	elev. Bottom (m)
P-1	3.56	6.44
P-2	3.14	6.86
P-3	3.57	6.43
P-4	3.12	6.88

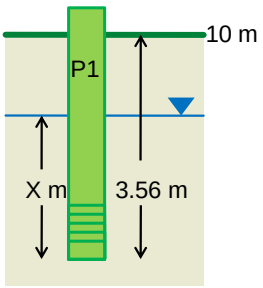

Figure 4.1 Piezometer elevations and sample diagram

See Figure 3.3 for piezometer locations, Appendix B for daily water level graphs, and Appendix E.3 for groundwater data. Note that the curves for P1 often appear to be broken up, even after replacement of the original transducer. Since P1 is the closest piezometer to the injection points and was sealed to the box to prevent air leakage, the erratic readings are likely due to bubbling within the well and a higher air pressure.

The transducers within P-1 and P-2 were located inside the box and sealed in place, but the transducers in P-3 and P-4 were removed at night. This caused some scatter in the mornings when the transducers were started relatively quickly after emplacement. Figure 4.2 below is an example of typical water level changes in the beginning of the experiment at injection point 1-1, with a sparging on/off period of 1.25 hours. Two rounds of sparging were conducted.

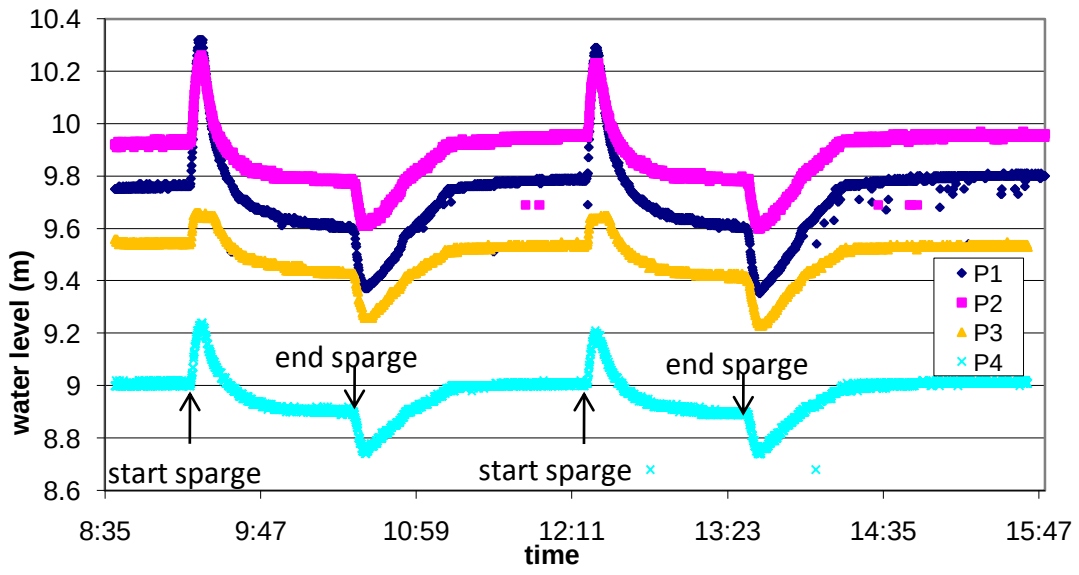

Figure 4.2 April 30 water levels relative to 10 m datum

The water levels indicate that pressure changes spiked in approximately 5 minutes and dropped off quickly, with the water levels equilibrating below the initial water level. The pressure drop after air sparging shutoff had a similar shape, although the trough had a smaller magnitude than the peak. It also took slightly longer to reach the minimum after shutoff, most likely because the injection point remained connected to the blower used for air injection and pressure did not drop as quickly.

The piezometers inside the box had the highest initial water levels, with a piezometric surface above the ground surface. It should also be noted that the curve for P-3 appears to be cut off at 9.66 m, which is below the ground surface. This held true throughout the treatment period, and once the water table dropped, the curve for P-3 had a similar peak to the other piezometers. It is likely that P-3 was cracked or otherwise damaged below ground surface at this elevation, allowing water to escape.

The water levels would be expected to increase after injection and the initial spike in water level because the groundwater had been initially displaced by the injected air and it is likely that some of the air remained entrapped in the subsurface. In this case, the likely explanation is that the air bubbles entering the piezometers move upward and become trapped within the box, keeping the water level in the well down. This happened in the piezometers outside the box as well, indicating some degree of short-circuiting to the outside. Air bubbles may have also caused some of the scatter in the data from the inside piezometers.

The amount of air that could be injected via different sparging points help determine how much of the source zone was affected by sparging, and can been seen in the water level data. Injection point I-2 allowed only a minimum amount of air into the subsurface. The blower was set to shut down once the pressure reached 50 psi and only ran for 10 minutes before shutting down. Therefore, the pressure was maintained without additional airflow after 10 minutes. It should be noted that if left alone in this situation, the blower would restart 10 min after initial shutdown, indicating some degree of air flow to the aquifer. However, the blower was shut off after this in order to retain a clear record of water levels. Some degree of airflow in this situation is confirmed by the water level data, an example of which is provided as Figure 4.3.

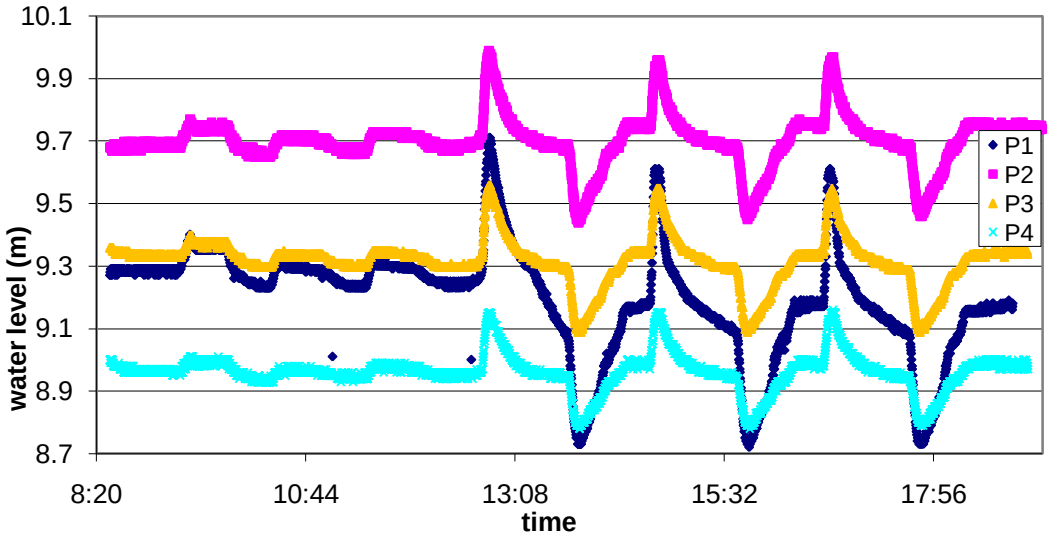

Figure 4.3 June 18 water levels relative to 10 m datum with injection at I-2, then I-1

On June 18, I-2 was sparged for 10 minutes starting at 8:45, 10:20, and 11:25. Sparging started at I-1at 12:45. The difference between the sets of three peaks is clear. The poor performance of I-2 could be the result of either a less-permeable formation in the vicinity of the injection point or a problem with the injection point itself. As discussed in Section 3.3, I-3 ended up being constructed slightly differently from the other injectors in that the tubing did not lead directly to the screen. While this may have affected the efficiency with which air could be pushed out of the screen, it should not be material because of the pressure buildup and the absence of leaks (at 50 psi, any leaks were loud enough to notice over ambient noise).

The injection point was flushed out with clean water using a stainless-steel rod to support tubing through which the smaller peristaltic tubing could be run through the barbed fitting and into the injection port's screened portion. Water was pumped into the well and removed several times; however, it appeared that only the water initially added was removed and that the screen was clogged.

Injection point I-3 was used initially with no problems. However, it became clogged with use, as indicated by the blower stopping short of the full hour of sparging. Flushing the screen with water allowed air to flow in for the full hour of sparging, but this process had to be repeated after every sparge. Figure 4.43 below is an example of I-3's effect on water levels in the earlier part of treatment.

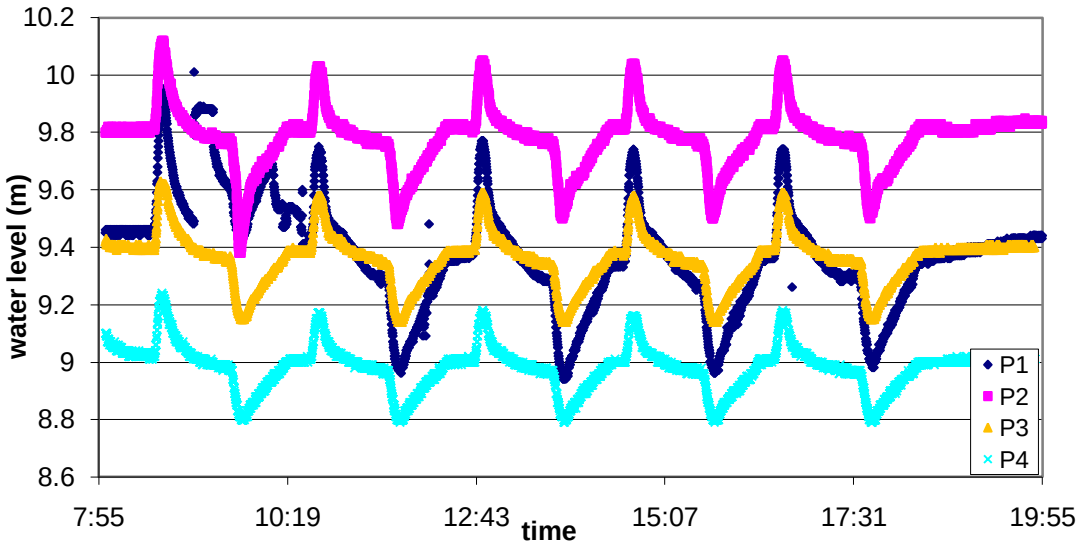

Figure 4.4 June 5 water levels relative to 10 m datum (I-3)

Figure 4.3 shows the clear impact of sparging on water levels. Note that the P-1 transducer data is somewhat erratic from approximately 9:00 to 10:30. The peak magnitudes are slightly smaller than those for I-1, indicating potentially less-effective sparging. For example, the magnitude of the first peak on April 30 (see Figure 4.1) is approximately 0.56 m, the same value as the first peak on June 2, over a month later. The magnitude of the first peak on June 5, after sparging was switched to I-3, was 0.49 m. When sparging was re-started at I-1 on June 11, the magnitude of the first peak was 0.52 m.

On June 10, sparging was re-started at I-3, four days after the last time it was sparged. The blower shut off 10 minutes after starting the first sparging attempt, and 20 minutes after starting the second sparging round. See Figure 4.5 for water level data for this day.

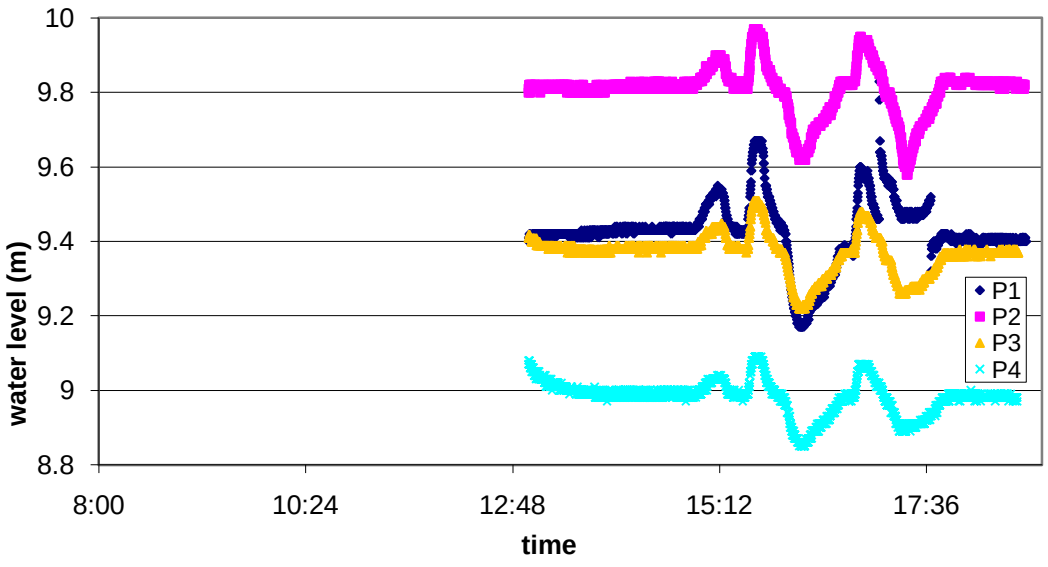

Figure 4.5 June 10 water levels relative to 10 m datum

Note that Figure 4.5 has been expanded so that it can be more easily compared to other figures in this section. The first peak on the figure reflects the airline switch from I-2, which was under pressure, to I-3. The second P-1 peak has a magnitude of only 0.23 m, or approximately half that of the peak from the week before, while the third peak is smaller still. Also, the water levels rebounded much more slowly (a wider trough) after sparging shut off.

A comparison between Figure 4.4 and Figure 4.5 show that I-3 had started to lose efficiency over the course of treatment. The problem is that the hydrocarbon concentration in the off-gas is expected to decrease over time as the amount of NAPL in immediate contact with air channels (the easiest to treat) decreases. Decreases in off-gas concentrations are usually attributed to decrease in source concentrations. If the injection points start to lose efficiency, an investigator may conclude that the available NAPL has been remediated, when the lower concentrations are due solely to equipment concerns.

4.1.2 Groundwater temperature changes

The sparged air is warmer than ambient (approximately 40˚C) because of compression and the air compressor running temperature, which heated up enough to shut down the blower if the housing was not open to vent air. The ambient air temperature ranged from 0 to 27˚C, with an average temperature of about 15˚C in the first month of sparging (May) and from 9-30˚C, with an average temperature of about 20˚C in the last month of sparging (June). See Appendix B.3 for ambient temperature data. Both average temperatures were much warmer than the groundwater, which was approximately 7˚C. It could be that the warmer sparged air which was forced into the formation may aid in biodegradation.

Water temperatures within the piezometers inside the box were affected by the sparging. See Figure 4.5 for an example of daily temperature fluctuations. Note that Figure 4.6 is showing data for the same day as Figure 4.4. The additional water level data (P1, P3, and P4) show the same water level trends, but were removed for clarity.

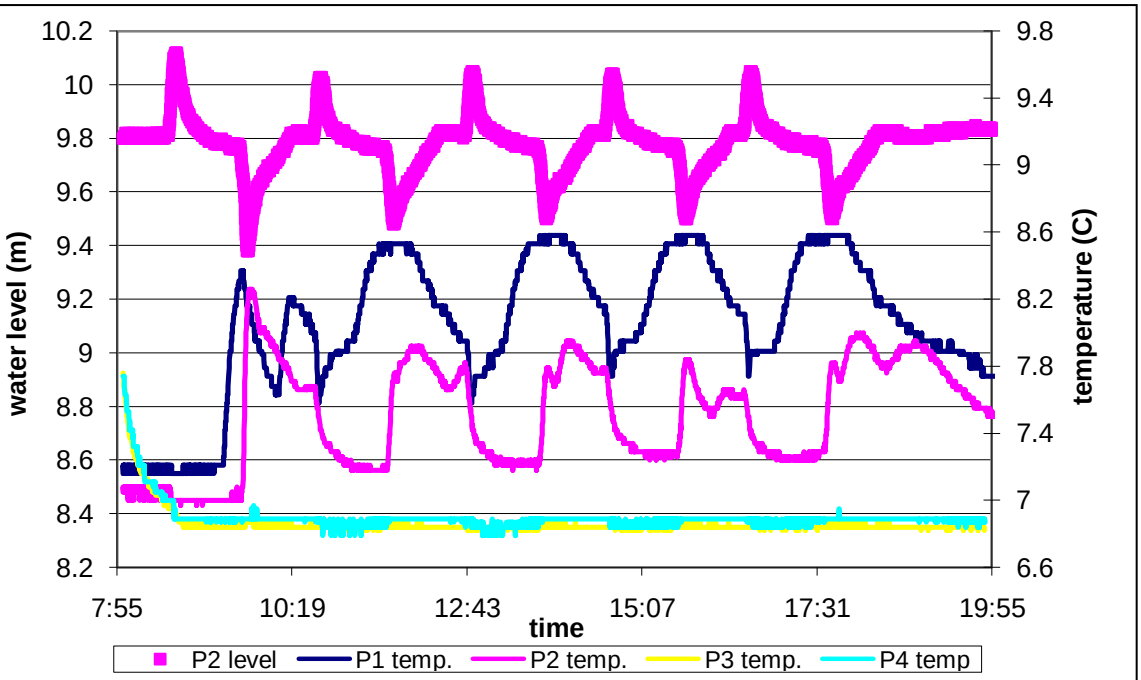

Figure 4.6 June 5 water temperatures and water levels

The transducers were located at the bottom of the wells (more than 3 m below ground surface) and did not appear to be affected by the ambient air temperature. The ambient air temperature was 16˚C when the transducers started recording on June 5, increased steadily to a maximum temperature of 24˚C at 15:30, and dropped to 19˚C by the time the transducers were turned off.

Pre-sparging groundwater temperatures within the box started slightly higher than those outside the box, which were not significantly affected by sparging. Temperatures at the deepest piezometer inside the box (P1) immediately spiked when the airflow was turned off, while P2 appeared to have a slightly delayed reaction and lower temperatures. In theory, the temperature would be expected to increase when warmer air is injected, not when the sparging stops. One possible explanation is that the much warmer air within the box is affecting the piezometers' water column. If this were true, P2, which is shallower and is closer to the warm air between the box and the ground, should have a larger temperature increase. However, after the initial increase in temperature, P2 remains consistently cooler than P1, which is deeper and

therefore closer to the source. Other possible mechanisms for the spike in temperatures at this time are unknown.

The starting temperature for the piezometers inside the box was only 0.4˚C higher than the temperature outside the box, except for the first 15 minutes of readings for P3 and P4, which reflected the transducer equilibrating with the surrounding groundwater temperature after installation. On June 5, the treatment system had been operated the previous 4 days, so any longer-term warming of groundwater would have taken place already if it was going to. Therefore, warmer air sparged into the subsurface has a minimal effect on subsurface temperatures and biodegradation other than a short-lived effect in the immediate vicinity of the sparged well.

Johnson et al. (2001D) alluded to other work involving examining temperatures in wells to determine air distribution, but no other work was cited or found discussing this issue.

4.1.3 Visible water level changes

The water table remained several cm above ground surface for the first month of treatment, but dropped steadily. By May 26, only puddles remained. Once sparging began, the groundwater was pushed above ground surface and remained above ground surface up to two hours after air injection was stopped for the day. Ahlfeld et al. (1994) suggest that groundwater mounding is caused by activation of a SVE system in conjunction with air sparging. However, in this case water level measurements were started before the off-gas collection system and several times were left until after system shutoff. This demonstrates that the off-gas collection system operation did not have an impact on water pressures. For example, on April 30 (Figure 4.2), the off-gas collection system was started 5 minutes after transducer start, and the transducers were left on up to 20 minutes after system shutoff with no apparent change in pressure.

Figure 4.7 shows the progression of rising water level slightly more than halfway through treatment. The ground surface was dry when the off-gas collection system was turned on, but started filling with water almost immediately after air sparging began. At least part of the puddle volume was because of a small water leak out of the box a few cm above ground surface.

The water mounding outside (and inside, as shown by the leak above ground surface) the box indicates that some of the air was entrapped and displaced groundwater during and up to two hours after sparging, suggesting that the lower water levels recorded by the transducers may have been due to air trapped above the water column, as discussed in Section 4.1.1.

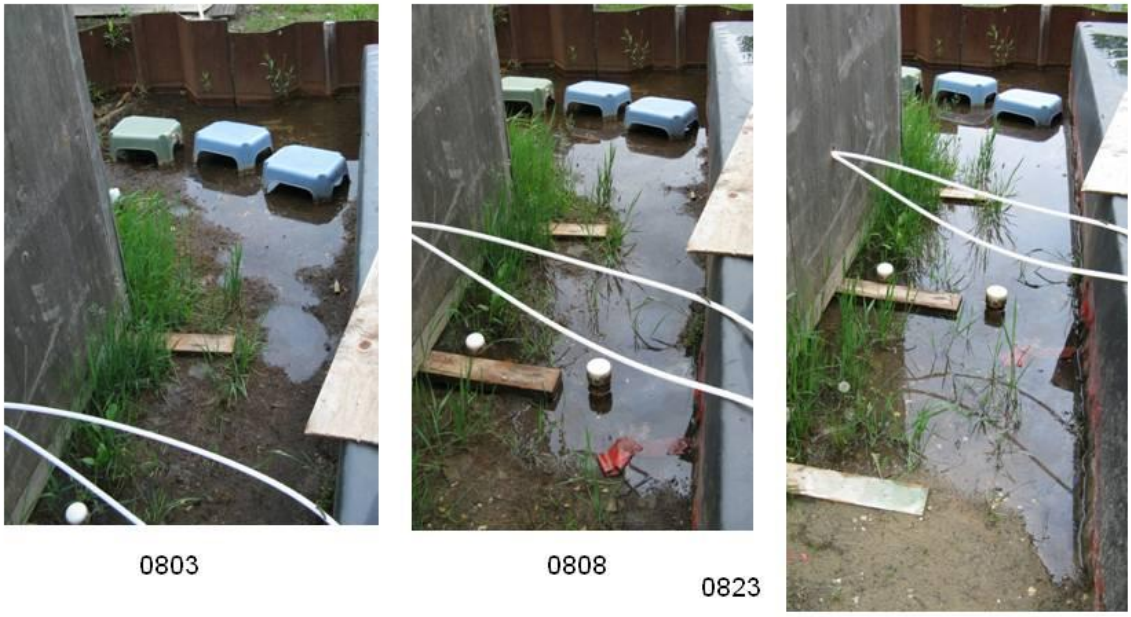

Figure 4.7 Water mounding after air sparging start (June 12)

4.2 System Efficiency

Tracer tests were the primary means of determining system efficiency, or how much of the sparged air was captured using the off-gas collection system. In addition, the unexpectedly high water table (static level above ground surface for the first half of the treatment) acted as a simple way to detect air leaks. Samples of these leaks provide some insight into how much of the hydrocarbon mass may be lost. The other aspect of system performance with a significant impact on the treatment was the sparging well efficiency, or the degree to which sparged air reached the targeted zone and was captured by the off-gas collection system.

4.2.1 Helium tracer tests

Helium tracer tests were intended to see how much of the sparged air was captured in the off-gas collection system. Also, the timing of helium appearance in the off-gas showed how fast the injected air moved through the subsurface.

Helium tracer tests were performed as discussed in Section 3.4.3. There was not sufficient helium available, so instead of measuring the concentration of the helium removed and comparing it to the concentration added, as suggested by Johnson (2001C), the total mass of helium removed was compared to the mass of helium added. The helium detector readings were in ppmv (µL/L), so they were multiplied

by the helium density (163.6 mg/L at atmospheric pressure and 25˚C, Lide, 2008). The equation to determine the helium mass from the concentration in ppm is as follows:

$$M = C\rho xt \qquad (4.1)$$

C is the helium concentration from the detector (ppm or mg/kg), ρ is the helium density (0.1636 g/L according to Lide, 2008), x is the off-gas flow rate (converted to L/min), and t is the sampling interval (min).

The mass of helium entering the system was determined first from the input concentration and air sparging flow rate, using Equation 4.1. In addition, the mass was also calculated from the pressure of helium inside the tank before and after sparging, where this information was available. The pressures were recorded consistently for the last half of treatment.

The concentrations and pressures in a tank can be described using the ideal gas law below.

$$PV = nRT \qquad (4.2)$$

For the ideal gas law, P is the gas pressure, n is the number of moles, V is the gas volume, R is the ideal gas constant, and T is the absolute temperature. This can be rearranged as shown below.

$$\frac{PV}{nRT} = 1 \qquad (4.3)$$

To determine the amount of helium available in a compressed tank at a specific temperature and pressure, the empty tank can be compared to the full tank. When the gas in the tank is compared to the same mass of the gas at atmospheric pressure, the equation can be rearranged. Assuming that if the gas inside the tank is gas_1 and the same amount of gas at atmospheric pressure is gas_2, then the equations can be set equal to each other.

$$g_1 = \frac{P_1V_1}{1nR_1T_1} = \frac{P_2V_2}{1nR_2T_2} = g_2 \qquad (4.4)$$

Since the equation is comparing the same gas, just compressed versus not compressed, T, R, and n are the same on both sides of the equation and drop out. This leaves:

$$P_1V_1 = P_2V_2 \qquad (4.5)$$

where P_1 is the compressed gas pressure read from the gauge, V_1 is the internal cylinder volume, P_2 is atmospheric pressure (1 atm, or 14.7 psi), and V_2 is the volume of the same gas that would exist at atmospheric pressure. Equation 4.5 is necessary to determine the volume of gas present using only the pressure gauge on the tank. The tracer gas tanks were size "Q" from Praxair, which have a 16 L capacity. Equation 4.5 can then be rearranged.

$$\frac{P_1}{V_2} = \frac{P_2}{V_1} = \frac{16L}{14.7\,psi} = Y \qquad (4.6)$$

To determine the mass of tracer injected, the tank pressure is multiplied by the value in Equation 4.6 (1.088 psi/L) and the helium density as follows:

$$M = P_1 \cdot Y \cdot \rho \qquad (4.7)$$

For Equation 4.7, M is the mass of helium (g), P1 is the pressure of the air inside the tank (psi) as read by the pressure gauge, Y is the constant that converts pressure to volume for a 16L tank (1.088 L/psi) from Equation 4.6, and ρ is the gas density (0.1636 g/L for helium, Lide, 2008).

The helium detector was set downstream of the vacuum pumps because the helium detector's intake could not operate at negative pressure between the soil gas outlet and the pumps. Therefore, the helium detector concentrations were diluted by air leaking into the pumps.

For this reason hydrocarbon GC samples were taken from both the PID outlet (after the pump) and the syringe outlet (before the pump) at the same time to determine if a consistent dilution factor that could be used. When SF_6 was added to the system on the last day, additional PID outlet samples were also collected. The dilution varied over a 10% range, with the exception of the third day of sampling, which is discussed further below. These dilution samples were collected daily, so the dilution factor used for each helium test was selected based on the date. If multiple dilution samples were collected, the one closest to the helium test time was selected. See Table 4.1 for the % TPH retained between the sample ports upstream and downstream of the vacuum pumps.

% TPH retained			% TPH retained			% SF6 retained		
Round	% TPH	ET (hr)	Round	% TPH	ET (hr)	Round	% SF6	ET (hr)
6	6.151	15.0	39	2.796	106.3	117	1.524	276.3
7	58.192	16.6	40	3.712	110.1	118	2.252	279.7
8B	86.403	22.3	45	1.816	122.6			
11	7.492	31.1	50	1.084	133.2			
13	3.073	38.7	53	6.395	140.3			
16	2.738	46.1	60	1.572	158.3			
20	5.474	56.3	66	0.902	171.7			
22	2.454	60.9	71	1.477	182.7			
28	3.285	74.3	75	2.268	194.9			
29	1.972	78.8	78	0.300	199.2			
32	1.538	90.3	80	0.164	205.5			
33	3.443	93.4	87	0.561	220.3			
35	3.619	98.4	91	8.939	228.4			
37	4.263	102.3	102	0.553	250.5			

Table 4.1 Percent TPH and SF_6 in off-gas after passing through vacuum pump

The round number in Table 4.1 is the sparging round used for sample identification and ET is the elapsed time from the start of treatment. The % TPH retained was used to determine dilution factors in Table 4.2.

round	sparge point	mass OUT (g)	dilution factor	mass IN based on tank (g)	mass IN based on tracer samples (g)	Graph shape
16	I-1	22.1	36.5	382.7	0.8	2 peaks, fast drop
19	I-1	14.4	18.3	--	0.8	1 broad peak
33	I-1	6.2	29.0	--	0.3	1 broad peak, fast drop
36	I-1	4.5	23.5	80.1	3.7	2 sharp peaks, slow drop
54	I-1	4.8	15.6	71.2	0.3	1 large peak, slow drop
61	I-3	3.8	63.6	62.3	0.2	inconclusive
68	I-1	17.7	67.7	124.6	0.7	low conc., sharp peak at end
79	I-1	418.3	333.3	53.4	0.2	1 peak at start, scatter, fast drop
96	I-2	0.6	21.1	126.4	0.8	1 peak at start, immediate drop
102	I-1	273.3	180.8	87.2	2.1	1 peak at start, scatter, fast drop
109	I-3	63.0	96.3	80.1	3.6	inconclusive
112	I-2	3.0	96.3	--	0.4	1 peak at start, scatter, fast drop

Table 4.2 Helium mass recovery from tracer tests

The helium test data are inconclusive primarily because the estimates of helium added are off by up to two orders of magnitude. The mass of helium injected (mass IN in Table 4.2) based on tank volume could be erroneously high because of leaks in the delivery system. However, the mass of helium injected based on samples of the tracer port is erroneously low, as the mass calculated for each helium test is lower than the mass calculated to have been injected. The tracer sampling port was designed to be far enough downstream to enable complete mixing, as discussed in Section 3.3.5, so that shouldn't be a factor in the anomalously low readings. Most likely, the helium detector was not reading the correct value.

In the field, the helium detector required 2-3 minutes to equilibrate. This is a much longer time than test runs in the lab, but the higher humidity and temperatures in the field may have caused performance problems. With relatively short tracer injection times, the helium measurements of the gas entering the system may have taken too long and registered concentrations that were too low. When the off-gas was measured, it often took several minutes for the instrument to re-zero, with several attempts to tare the detector in clean air. Therefore, the instrument readings for the off-gas may have been erroneously high. The other problem was the detector's sensitivity. It had a detection limit of 25 ppm and operated in increments of 25 ppm. The instrument was re-zeroed in clear air approximately every 10 minutes.

Graphs of the helium test recovery are provided in Appendix D.3.1, but the general shape of each graph is provided in Table 4.2. They show that the off-gas did not have a clear pattern of return concentrations, even for the same injection point under similar conditions. Therefore, the helium tests are considered to be inconclusive and the helium test results were not used to determine the amount of air captured by the system as a percentage of the amount of air injected. Visual observations of leaks were used instead.

4.2.2 SF_6 tracer tests

SF_6 was added as a tracer only for the last day of treatment. The SF_6 was captured and measured in the off-gas collection system during the day it was injected, and later measured in groundwater at the time calculated for the sparged groundwater to reach the row 2 monitoring wells. SF_6 is not considered a conservative tracer because it dissolves into water. The SF_6 was initially added to determine how much of the sparged air would be incorporated into the groundwater and when the sparged groundwater would appear in downgradient monitoring wells. However, it was useful as an additional tracer gas for determining how much of the sparged air was captured by the off-gas collection system because the SF_6 samples were collected at the same port as the hydrocarbon analysis, before dilution from the vacuum pumps.

SF_6 tracer was injected into the subsurface as quickly as possible, using all three injection points, so that it would be added to the groundwater as essentially a single slug to move downgradient. The SF_6 mass

added was calculated by determining the volume of gas in the tank using Equation 4.7 and a SF_6 density of 5.9696 g/L (Lide, 2008).

Two tanks of SF_6 were used. The first had a starting pressure of 1700 psi and an ending pressure of 70 psi, so 1774 L (10.59 kg) were added. The second had a starting pressure of 800 psi and an ending pressure of 70 psi, so 4740 g of SF_6 were added.

The mass removed via volatilization and captured by the collection system is determined using the concentration, time interval, and flow rate as set forth in the following equation.

$$M = Cxt \qquad (4.8)$$

This is the same equation as 4.1, but in this case the concentration from GC analysis (C) is already in µg/L and a density conversion is not required. As with Equation 4.1, x is the off-gas flow rate (converted to L/min), and t is the sampling interval (min). Figure 4.8 shows the result of the SF_6 tracer test.

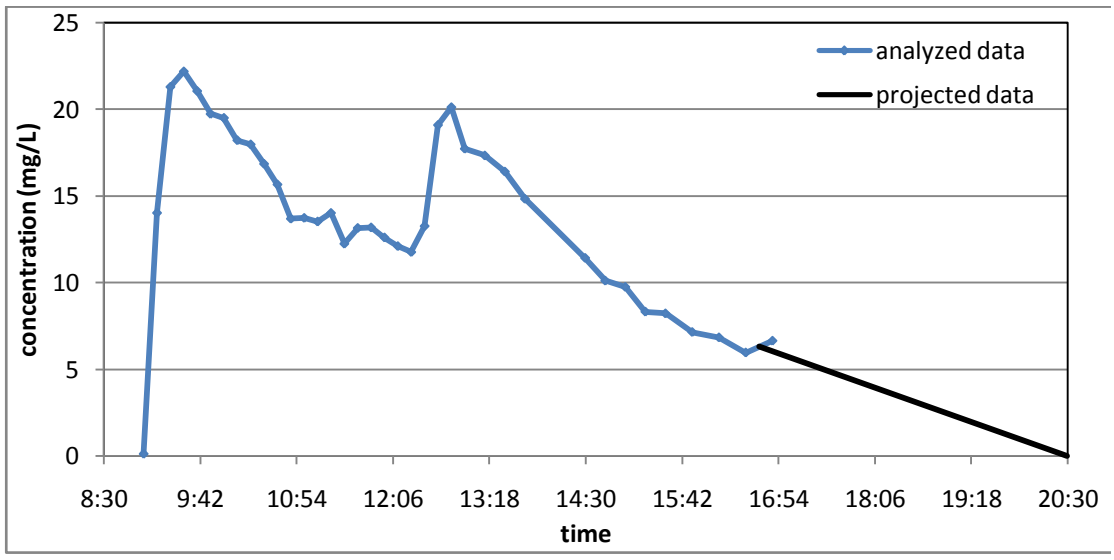

Figure 4.8 June 23 SF_6 tracer test results

During the helium tests, the concentrations went to zero within 4 hours of injection, so the SF_6 samples were collected until approximately 5 hours after initial injection. However, it is clear that injected air with significant SF_6 concentrations was still being collected and removed after the last sample was collected. The two peaks at 9:30 and 13:00 correspond to tracer injection; the slight uptick at the end of sampling is to be considered within the range of experimental error and not indicative of an upward trend.

The mass from the collected data shows that approximately 540 g of SF_6 were recovered. Using the values based on what was originally injected, 412 g would have been removed. This value is much closer than the helium values, so the 540 g are used as a relatively accurate representation of the mass removed. If the concentrations were to follow the projected line in Figure 4.8, approximately 590 g of SF_6 would have been removed. If 590 g of SF_6 were volatilized, then the rest (15.3 kg) can be assumed to have dissolved into groundwater or leaked.

Bullister et al. (2002) determined the freshwater SF_6 solubility to be approximately 0.2728 mol/L-atm. Assuming the pore space to be at atmospheric pressure, the solubility would then be 39.75 g/L. If 15.3 kg of SF6 were dissolved into water at the solubility limit, then the volume of water affected would be 0.385 m^3. With an available pore space of 0.33 as discussed in Section 3.1, the aquifer volume affected would be 1.2 m^3, 20% of the source area volume, in 40 minutes.

4.2.3 Visible leakage

As discussed in section 4.1.2, even at the end of the test (June 23) the ground surface was covered with water during active air sparging. The elevated water level was useful because it allowed monitoring of air and water leaks outside of the box. The maximum area of leakage was observed to be approximately 1 m wider than the box and the leaks represented a very small portion of the gas discharge from the box.

In the first few weeks of treatment, most of the air leakage was intercepted by the open-screened wells E and F, located slightly downgradient of row 2. See Figure 3.2 for monitoring well locations. Leakage was not surprising, as it was downgradient of and between the two wells that had shown significant short circuiting (highly aerated water pouring out of the wells) during the January sparging. However, this leakage consisted of bubbles moving up the outside of well E and occasionally water seeping out from beneath the cap of well F.

The air leaked was captured in the third day of treatment and measured using an inverted plastic container. Based on the volume of air displaced, the leakage rate was 0.07 L/min, compared to an off-gas collection flow rate of 127 L/min (4.5 ft^3/min) during sampling, or a 0.04% loss. The container was sampled by inserting a needle and syringe into the side, and then preparing it for GC analysis using the method discussed in Section 3.4.2. See Figure 4.9.

When air sparging was moved to I-3, bubbles started to appear closer to the right side of the cell downgradient of the injection point, as well as around well E. This was expected because the new bubbling area was located downgradient of I-3. These bubbles were more diffuse and sporadic, and

therefore difficult to sample. These were sampled by filling the sample vials with water and inverting them underwater so that the leaks bubbled directly into the vials. See Figure 4.10.

For these samples, each of the two 20-mL vials took approximately 10 minutes to fill. The sample locations for the vials varied, but the leaks with the highest air flow were selected for sampling each time. These locations were chosen for practical reasons: the airflow at a particular location would stop when the vials were set firmly into the sediment, and the vials tended to fall over when they filled more than 50% with air, so they had to be held above the intermittent air stream. Approximately 10 air bubble streams were seen at once, and so it was assumed that an additional 5 air bubble streams from other locations were missed, for a total of 15. Therefore, the flow rate from leakage was estimated at 60 mL/min or 0.0021 ft^3/min. This rate is similar to the earlier flow rate of 54 mL/min, and since the flow rate is an estimate, it was assumed to be 3.4 L/hr (0.002 ft^3/min) over the course of treatment. The observed bubbling time ranged from 40 minutes to 2 hours per round, with most observed bubbling times of about 1 hour. See appendix C for an observation timeline. Therefore, the length of active bubbling is assumed to be 118 hours.

Figure 4.9 April 30 sampling air leak around sides of well E

Figure 4.10 June 11 sampling of air leaks near well E

The other leakage concern was that the tape sealing the collection box started to degrade from exposure to the sun, warm temperatures, and on the downgradient side of the box, immersion in water for weeks. A few leaks were found around edges of the box, but they leaked water out because of increased water

levels inside the box. Airflow out of the box through the off-gas collection system was always kept higher than the airflow injected and continued after ending sparging, so the air leaks should have been into, not out of the box. This preserves contaminant mass at the expense of potential additional dilution.

4.3 Area of influence

The air sparging area of influence must be inferred, as the entire treatment area was captured by a box with a single central extraction point. However, the water level and temperature data, tracer test results, and visual observations can be combined to help determine how much of the source has been affected by the sparging. If a particular area was missed, then the plume may not have been affected. Note that discussion of plume impacts is located in Chapter 6.

The area that had some indication of air sparging impact (bubbles, water level changes) was quite large, with bubbles seen up to 3.5 m from the injection points. However, the actual area that was most affected by the sparging was much smaller. The transducer water level data provide some indirect evidence of the degree of influence. For example, Figure 4.2 shows that after sparging ended, the two piezometers outside of the box returned to their initial level, but the piezometers within the box had a slightly higher level. This likely indicates that some of the injected air was still trapped in the subsurface, physically displacing some of the groundwater in the immediate vicinity of the injection point but not 2.5 meters away. Temperature changes were similarly restricted primarily to the piezometers inside the box, suggesting an area of primary influence less than 2.5 m in diameter but at least 1 m in diameter.

SF_6 tracer data indicate that the volume affected by sparging would be about 20% of the treatment area for an active sparging period of 40 minutes using all three injection points, and that it would take about 5 hours for all of the injected air to reach the surface. This supports the groundwater data, which indicates an air pocket that is depleted very slowly after sparging stops.

Tomlinson et al. (2003) used geophysical data to determine a 2.5 m radius of influence around a sparging well in the same area, with indirect evidence (piezometric surface fluctuations, % dissolved O_2) indicating a larger zone of air saturation. Since the flow rate during treatment was approximately 0.1 m^3/min (3.7 ft^3/min) or 75% of the flow rate used by Tomlinson et al., the radius of influence during treatment is estimated to be approximately 1.9 m, which is in line with the other indirect data from the treatment.

Chapter 5: Source Area Mass Discharge

Volatilization rates were determined from off-gas hydrocarbon analysis and biodegradation rates from off-gas CO_2/O_2 analysis. These data were combined with the continuous PID monitoring and flow measurement of the extracted gas to determine mass removal from each process. Tracer tests and samples from bubbles rising up outside the off-gas containment were used to help quantify mass missed by the off-gas collection system.

5.1 Mass Removal via Off-Gas Collection System

Mass removal rates are described in greater detail in the following subsections.

5.1.1 Laboratory results

See Section 3.3.2 for a discussion of analytical methods and sampling rationale. The overall trend for lab results is provided on Figure 5.1. Note that benzene is not included because it was not detected in any of the analyses.

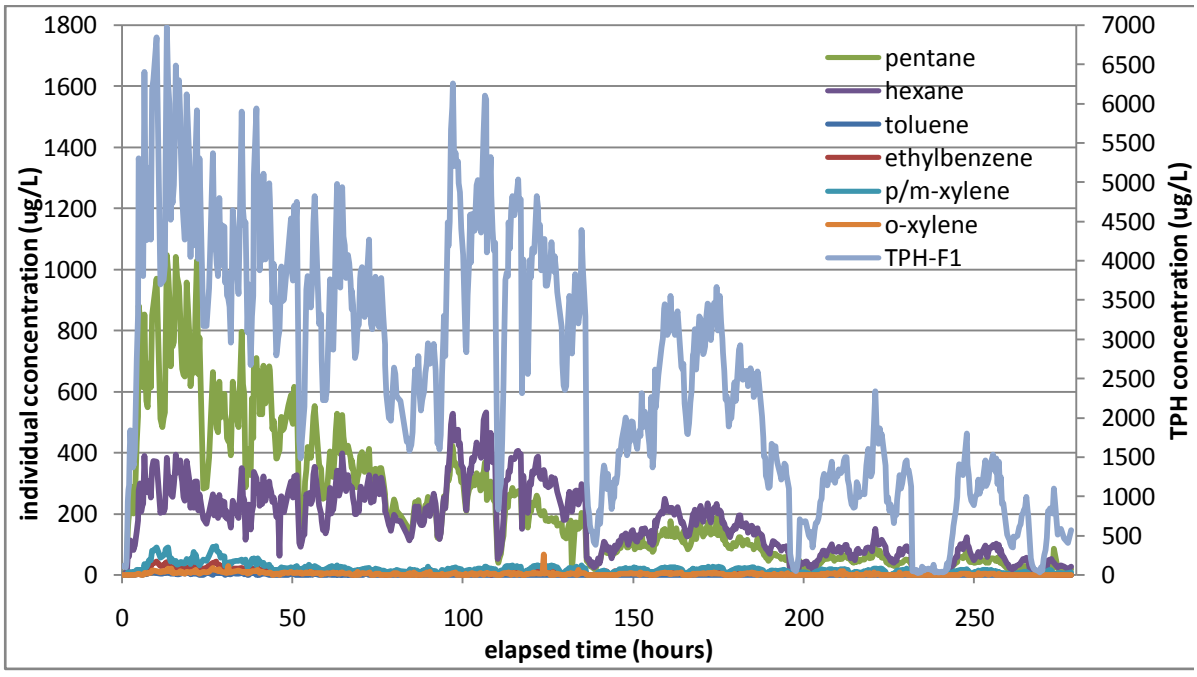

Figure 5.1 Laboratory results over the course of sparging (hours of operation shown only).

The gas concentrations peaked in the first 16 hours of vapor extraction from I-1 (maximum peak midday on April 29, the 13th hour of sparging) with a relatively steady drop-off. The second peak at

approximately 100 hours into the experiment corresponds to a switch to air injection at I-3. See Figure 3.2 for injection locations. The third injection point (I-2) turned out to be partially blocked, as discussed in Section 4.1, and allowed only a minimum of air flow, causing low off-gas concentrations. I-2 was used at approximately 140 hours into the experiment and from 230-240 hours. See Figure 5.2 for injection points used.

Several of the sharp low points on Figure 5.1 correspond to the low concentrations at system startup or restart days after the system had been last stopped, e.g. at 50 and 110 hours. The box covered an area of approximately 50 m^2 and was an average of 0.4 m high, so the total volume of air was 20 m^3, assuming the water table to be at about ground surface. With an average off-gas flow rate of 0.1 m^3 (3.7 ft^3) per minute, it would take approximately 37 minutes to remove the air that had been originally trapped in the box.

This air inside the box above ground surface is likely to have anomalously low hydrocarbon concentrations due to biodegradation over the relatively long periods of inactivity. The air temperature inside the box was significantly higher than the expected ground temperature because the liner was black vinyl and significantly warmer than the surrounding air temperature. The subsurface temperatures were not expected to be significantly higher due to the insulating properties of the saturated soil. Therefore, biodegradation rates for air trapped in the box above ground surface for several days may be anomalously high, causing "cleaner" air than is actually present in the subsurface soil gas. As a consequence, the first samples taken within 30 minutes after system startup after more than one day of inactivity were not considered to be representative of subsurface hydrocarbon gas concentrations.

sample date	gap (days)	Sample removed
4-May-2008	4	9A-SVE-1
8-May-2008	3	13A-SVE-1
12-May-2008	3	19A-SVE-1
18-May-2008	2	33A-SVE-1
25-May-2008	6	40A-SVE-1
1-Jun-2008	4	51A-SVE-1
10-Jun-2008	4	76A-SVE-1
17-Jun-2008	4	92A-SVE-1

Table 5.1 Samples removed from analysis

After removing these samples, as well as several samples that were anomalously low compared to the overall daily trend (see Section 5.1.4), the remaining data were averaged over hourly intervals to show trends more clearly. See Figure 5.2.

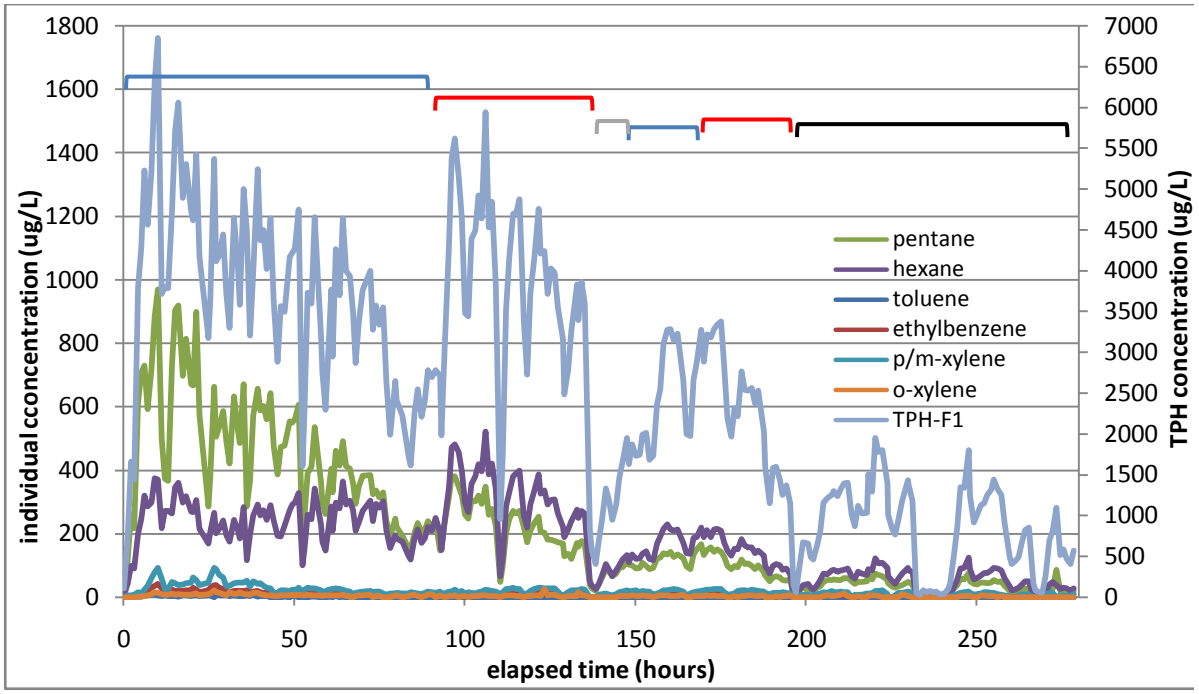

Figure 5.2 Adjusted petroleum hydrocarbon results over the course of sparging.

In Figure 5.2, the brackets at the top of the figure indicate which injection wells were sparged. Blue brackets indicate that I-1 was sparged, red indicates that I-3 was sparged, gray indicates that I-2 was sparged, and black indicates that the three injection points were alternated (about 3 hours between injection well changes).

The data also show that the more volatile compounds were removed preferentially. In order show this more clearly, the relative percent change in concentration was determined for TEX, pentane, and hexane using the following equation.

$$\%_H = \frac{C_H}{C_{TPH}} \cdot 100 \qquad (5.1)$$

In Equation 5.1, $\%_H$ is the percent change in concentration for the hydrocarbon in question, C_H is the hydrocarbon concentration (µg/L), and C_{TPH} is the TPH concentration (µg/L). TPH was used because it encompassed the total mass of hydrocarbons removed. See Figure 5.3.

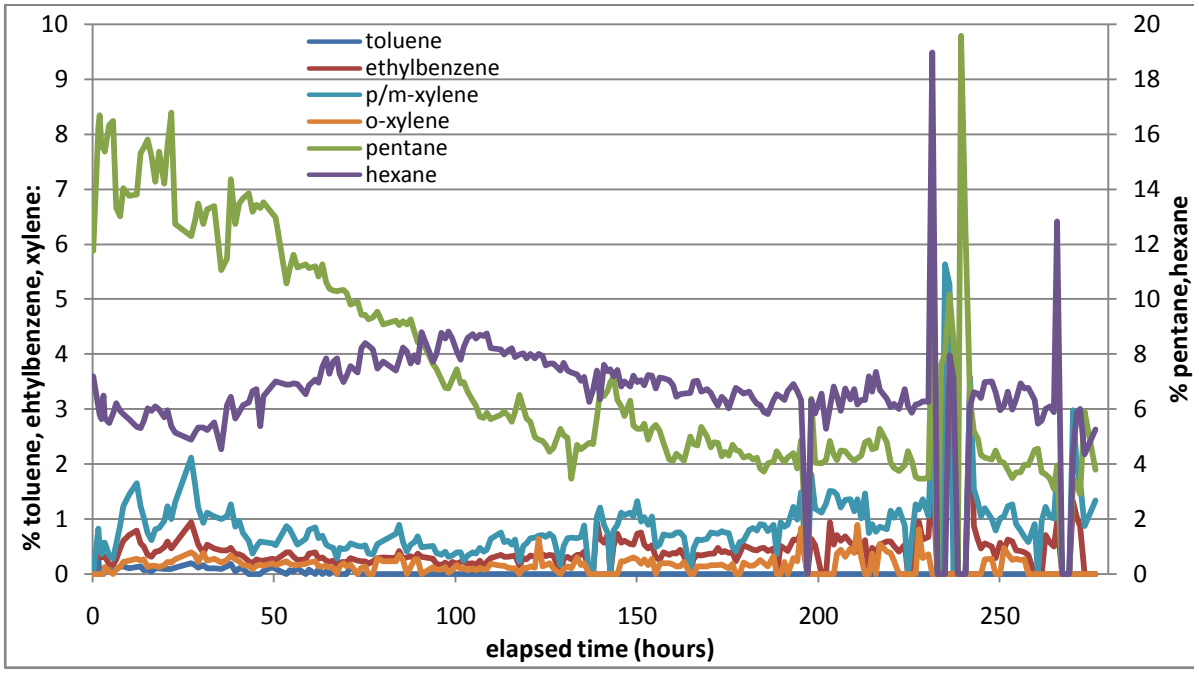

Figure 5.3 Concentrations shown as a percent of TPH

Pentane and hexane were put on the right axis in Figure 5.3 in order to show the lower-concentration hydrocarbon trends more clearly. The most volatile compound (i.e. the one with the highest vapor pressure) analyzed was pentane. For the first 70 hours, pentane concentrations were the highest of the individual compounds analyzed. The pentane concentration proceeded to drop off faster than the TPH concentration. Starting at about 100 hours into the experiment, hexane concentrations became slightly higher than the pentane concentrations. The increased relative hexane concentration coincides with the switch to I-3 from the initial central point (I-1) at 100 hours. The relative hexane concentrations started increasing and the relative pentane concentrations started decreasing approximately 30 hours into the treatment.

The BTEX concentrations remained low compared to the TPH concentration. The exception was a surge from 230 to 240 hours during I-2 operation, where the TPH concentration was extremely low and the relative concentrations of the compounds detected (pentane, hexane, ethylbenzene, and p/m xylene) were the highest seen during treatment. It is important to note that the concentrations did decrease in absolute terms; however, they did not decrease nearly as much as the total TPH decrease. This suggests that the residual in the vicinity of I-2 may either have a different composition, or that the other hydrocarbons otherwise present had been drawn off already by the central point.

Kirtland et al. (2001) suggest that BTEX compounds are among the first hydrocarbons removed during gasoline SVE; however, these results show higher pentane and hexane concentrations in the off-gas and relatively small amounts of BTEX removed throughout treatment.

5.1.2 Raoult's law and off-gas

The hydrocarbons should volatilize according to their vapor pressures, with the less-volatile compounds making up a greater proportion of the source mass as treatment continues. This can be seen in Figure 5.3, which shows that the lighter hydrocarbons were removed first. The field results can be compared to the theoretical relative removal rates. These can be determined using Raoult's law, which was used to determine the source zone composition in Section 2.6.1. For gases, the vapor pressures and not solubility are used to determine concentrations. Raoult's law was used for treatment off-gas by Nelson (2007), but in this case the number of compounds is much larger.

$$C = \frac{m_w PX}{RT} \qquad (5.2)$$

In Equation 5.2, C is the gas concentration (g/L) in equilibrium with the NAPL source, m_w is the molecular weight (g/mol), P is the vapor pressure (Pa), X is the mole fraction of the hydrocarbon in the NAPL, R is the gas constant (8314.4 L*Pa/K*mol) and T is the temperature (283 K). The Raoult's law program designed by Fraser (2007) was modified so that the concentrations were determined using Equation 5.2 above.

The source composition and vapor pressures used in this calculation are provided in Table 5.2. The pre-treatment source composition was determined using Raoult's law for aqueous solubility (1260 days after emplacement) as described in Section 2.6.1. This is only an approximation, as Section 2.6 discusses. It neglects potential biodegradation over 4 years, and the unspecified gasoline components make up more than ½ of the total. The vapor pressure for the source is considered to be the same as the original emplaced gasoline composition due to a lack of other evidence for the pre-treatment vapor pressure. API-91-1 gasoline has a Reid vapor pressure of 8.5, which was converted to a standard vapor pressure of 101.6 mm Hg using Blackmer's (1971) figure. Individual vapor pressures are from Montgomery (2000).

compound	mass at 1260 days (g)	% total mass	vapor pressure (Pa)
2-methylpentane	1340	5.99	29,038
1,2,4-trimethylbenzene	578	2.59	270.6
n-hexane	570	2.56	20,000
n-pentane	514	2.31	70,120
n-butane	510	2.29	242,700
toluene	431	1.93	3733
m-xylene	412	1.85	1107
3-methylhexane	410	1.84	8213
2,3-dimethylbutane	397	1.78	31,280
2-methylhexane	393	1.76	8786
2,3-dimethylpentane	308	1.38	9186
n-heptane	308	1.38	5999
ethylbenzene	242	1.09	1293
p-xylene	165	0.740	1173
o-xylene	117	0.523	879.9
1,2,3-trimethylbenzene	57.2	0.257	201.3
All Other Compounds	15,500	69.7	4903
total	22,300	100	13,550

Table 5.2 Values used for off-gas Raoult's law calculations

The use of air flow rates through the subsurface based on the actual rate of airflow injected into the aquifer is problematic because Raoult's law assumes the flow to be essentially the same for the portion of the aquifer in question. The air flow through the aquifer is difficult to predict because air is compressible, and as discussed in section 4.1.3, the air was trapped in the subsurface, causing mounding. Tomlinson et al. (2003) found that airflow in the aquifer continued for up to 5 hours after sparging ended. In addition, the system was operated in pulsed mode and air was injected less than half the total treatment time.

Taking into account the time when the sparging portion of the system was not operating, the average air flow rate into the aquifer over the sparging period was 14 L/min. The air collection system averaged 9 hours of operation per day, so if the flow out lasted 15 hours, then the overall flow rate would be 8.4 L/min or 0.504 m^3/hour. This is about 1/3 the rate calculated initially in Section 3.1. The pore volume was assumed to be 0.18 m^3, as discussed in Section 3.1, so each time step for the calculations was 21.4 min or 0.357 hr.

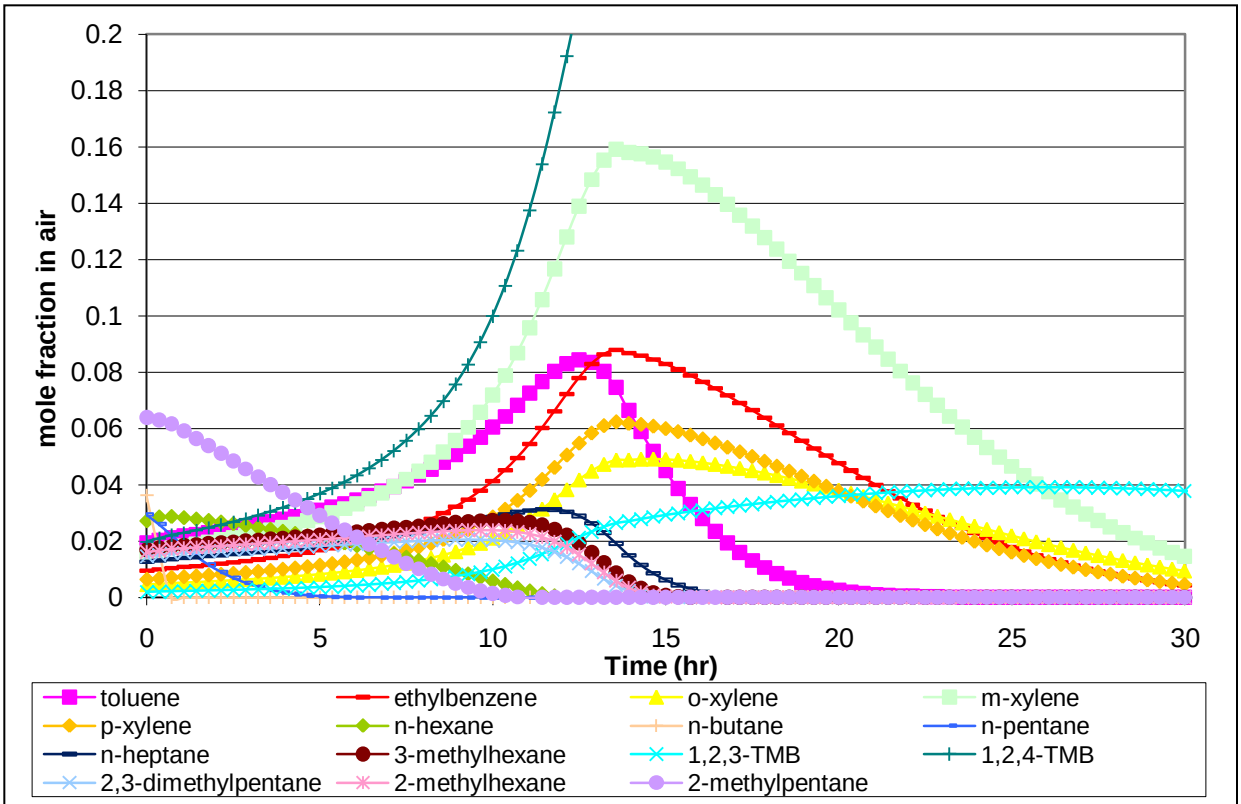

Figure 5.4 Mole fraction of hydrocarbons in off-gas according to Raoult's law

Note that the top of Figure 5.4 has been cut short to better show the trends for most of the hydrocarbons. 1,2,4-TMB has a peak of approximately 0.35 at approximately 25 hours. As expected, the least volatile compounds make up a larger proportion of the molar mass of the off-gas after the more volatile ones are removed. Figure 5.4 is somewhat cluttered because several of the lighter hydrocarbons (butane, pentane, 2-methylhexane, and heptanes) made up a smaller percentage of the overall mass. See Figure 5.5 for a graph of each compound's variability compared to the initial value over time.

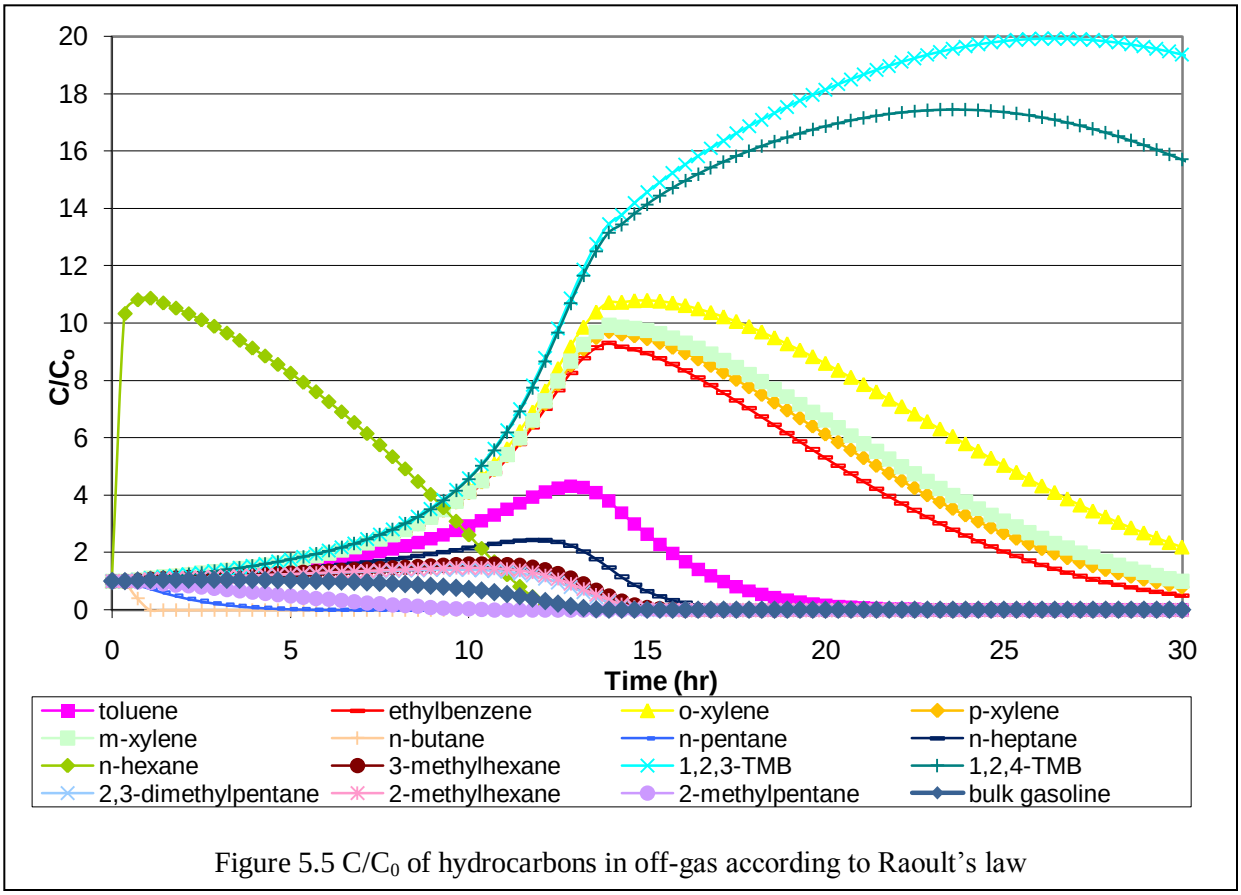

Figure 5.5 C/C_0 of hydrocarbons in off-gas according to Raoult's law

Figure 5.5 shows that of the compounds that were determined using GC, the hexane would have the first peak, followed almost immediately by pentane. Benzene was not included in this simulation, since it was expected to have such a low concentration in the source zone. Toluene would be expected to have an off-gas peak concentration slightly ahead of ethylbenzene and the xylenes, but as Figure 5.2 shows, the TEX concentrations remained low relative to hexane and pentane throughout treatment.

5.1.3 PID results

The PID data are problematic because the instrument was connected downstream of the vacuum pumps, which allowed dilution, as discussed in Section 4.2.1.See Table 4.1 for dilution factors. The concentrations recorded by the PID never went above 500 ppm, so concentrations were well within the operating range of the instrument.

Because of this uncertainty, PID results have only been used to establish the trends between GC samples. Duplicate TPH samples analyzed using the GC were within 3% on average, with a detection limit of less than 5µg/L, so the TPH samples are considered to be more precise than the PID data. The PID data do not show any short duration peaks that would have been missed by the sampling schedule adopted, so it confirms that the samples collected were representative of the overall trends of hydrocarbon removal.

Note that the PID data were collected every 10 seconds and have occasional peaks and dips when the PID was removed to check calibration or collect other samples from the PID inlet (e.g. for "PID" samples). The PID recorded data every 10 s, but this turned out to be unwieldy, so the data was averaged over 2 minute intervals. Data averaged over 2 minutes did not miss or minimize variation significantly, especially over longer periods.

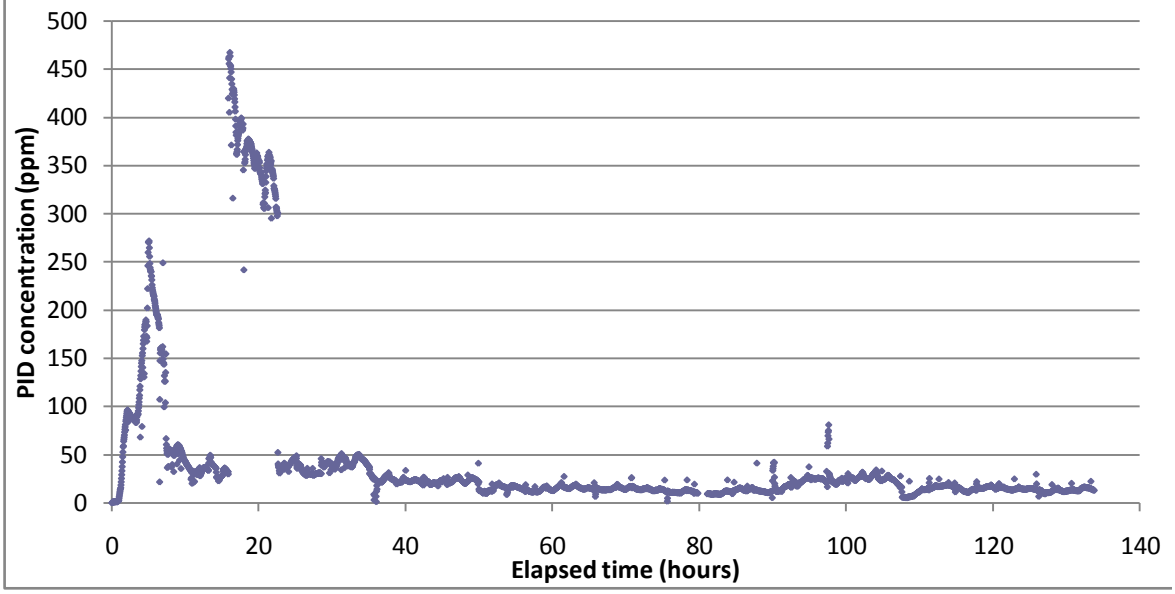

Figure 5.6 PID detections for the first half of treatment

Figure 5.6 shows that the PID response had an initial single peak at approximately 5 hours into the experiment. This corresponds to a similar elevated concentrations found in samples submitted for GC analysis. The slight peak at approximately 100 hours into the experiment corresponds to the change to injection point I-3 and again, an elevated concentration in the GC samples. The large peak from 16 to 22.5 hours appears to be disconnected to the rest of the curve. It is due to minimal dilution of sparged gas compared to the rest of the treatment period, as seen from the round 7 and 8 dilution data (Table 5.2 on the previous page). It does not correlate to the measured concentration in the GC samples. Also, the PID calibration was checked in the morning and afternoon and gave a response within 10% of the calibration gas, so the instrument calibration was not the reason for this anomaly. PID readings other than this were fairly consistent from one day to the next, as shown in Figure 5.7.

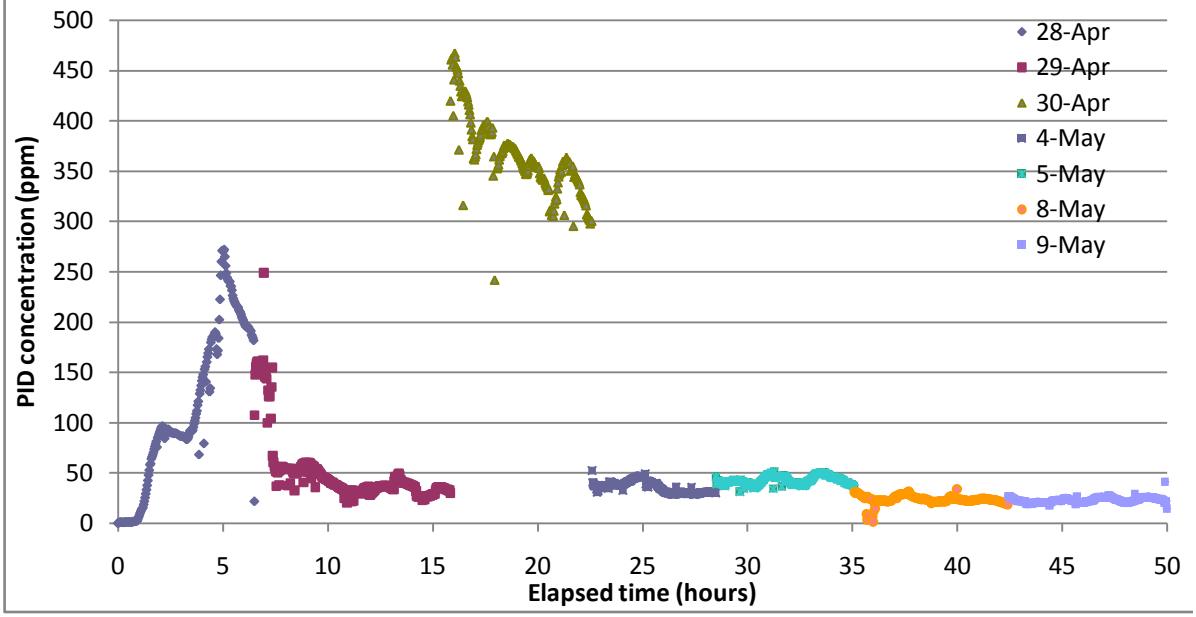

Figure 5.7 PID concentrations for the first 50 hours of treatment

Note that some of the individual PID readings do not fit with the general shape of the curve in Figure 5.6 and Figure 5.7, i.e. at hour 50. These points are from when the instrument was removed from the discharge line to check the calibration at 0 ppm and 100 ppm isobutylene, or when the instrument was turned off temporarily to clear an obstruction in the tubing or filter.

The PID values for Figure 5.6 were divided by the dilution factor. However, since the dilution factor varied significantly, an equation was determined for each line segment between dilution factors. This provided a curve to normalize the PID data. When this is done, the high concentrations from April 30 disappear and the PID data is more aligned with the curve of the GC hydrocarbon data. See Figure 5.9. This was done because the PID data points were only 2 minutes apart.

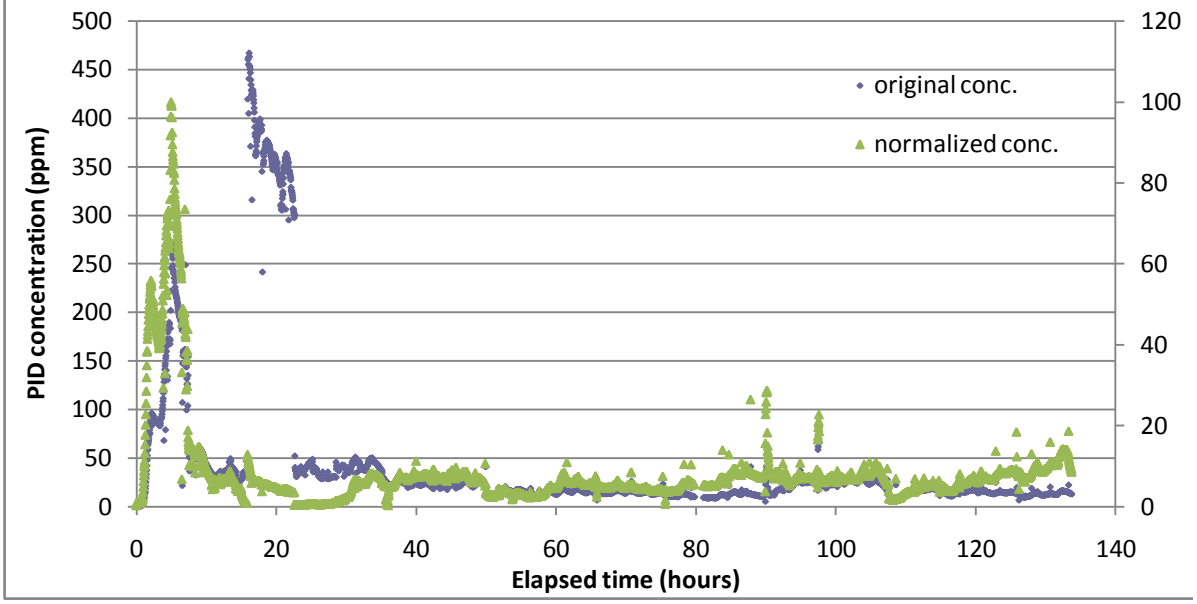

Figure 5.8 PID concentrations for the first half of treatment normalized to dilution rates

5.1.4 GC/PID comparison

The field plan originally specified the use of a PID in conjunction with sampling for GC analysis, with the assumption that the curve of the PID concentrations collected every 10 seconds could be used to calibrate the BTEX GC data. However, the changes in overall VOC off-gas were relatively small compared to the BTEX sampling rate and the resulting curves were generally well matched. The BTEX concentrations were relatively low compared to the complete hydrocarbon mass as measured by TPH, so TPH was used when comparing PID data to samples analyzed by GC. The curves matched better for later periods (after 50 hours into treatment), with a generally good fit with a 5:1 PID:TPH ratio. An example is Figure 5.9, from June 1. See Appendix B.1 for daily comparisons of PID and lab analysis concentrations.

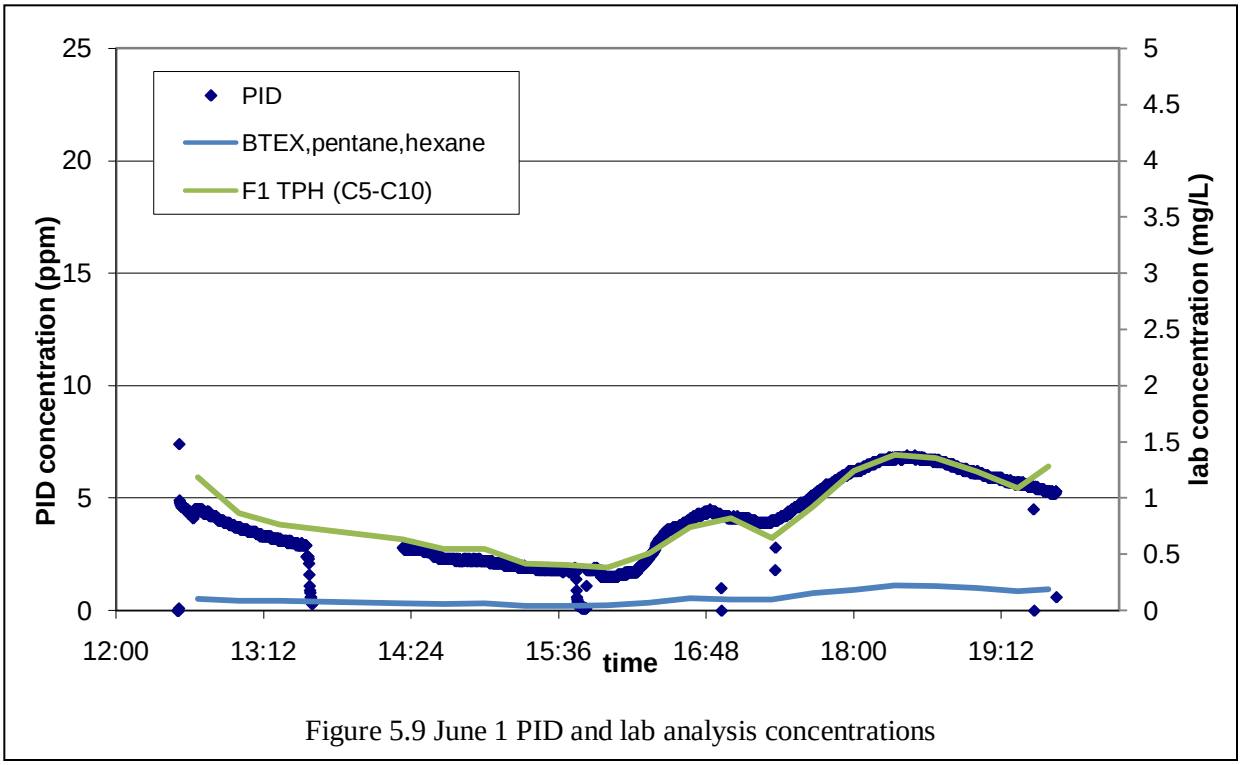

Figure 5.9 June 1 PID and lab analysis concentrations

The BTEX and TPH data were not generally adjusted to better fit the PID results. Three samples were anomalously low compared to their respective PID curves: 10B-SVE-4 from May 4, 13B-SVE-2 from May 8, and 26B-SVE-2 from May 14. These anomalies likely reflected the difficulty of keeping the samples air-tight during sampling, while filling vials, and during analysis, and so were removed. These samples are circled in the daily VOC graphs in appendix B.1.

5.1.5 Mass removal calculation

The mass lost through volatilization was calculated using Equation 4.8. The off-gas collection system removed gas at the rate of anywhere from 85 to 170 L/min (3 to 6 ft^3/min) over the treatment period. If the flow rate varied over a certain time period, that value was divided by the number of samples to get a flow rate for each shorter period. The resulting mass extracted is based on a 3-point average (hourly sampling points) and removal of the points discussed in sections 5.1.1 and 5.1.3. Calculation spreadsheets are provided in appendix D.4. See Table 5.3 for details.

The cumulative mass lost is provided in Figure 5.10. Cumulative mass was calculated using Equation 4.8. Note that the TPH mass is presented on the secondary axis, as it is significantly higher than the others.

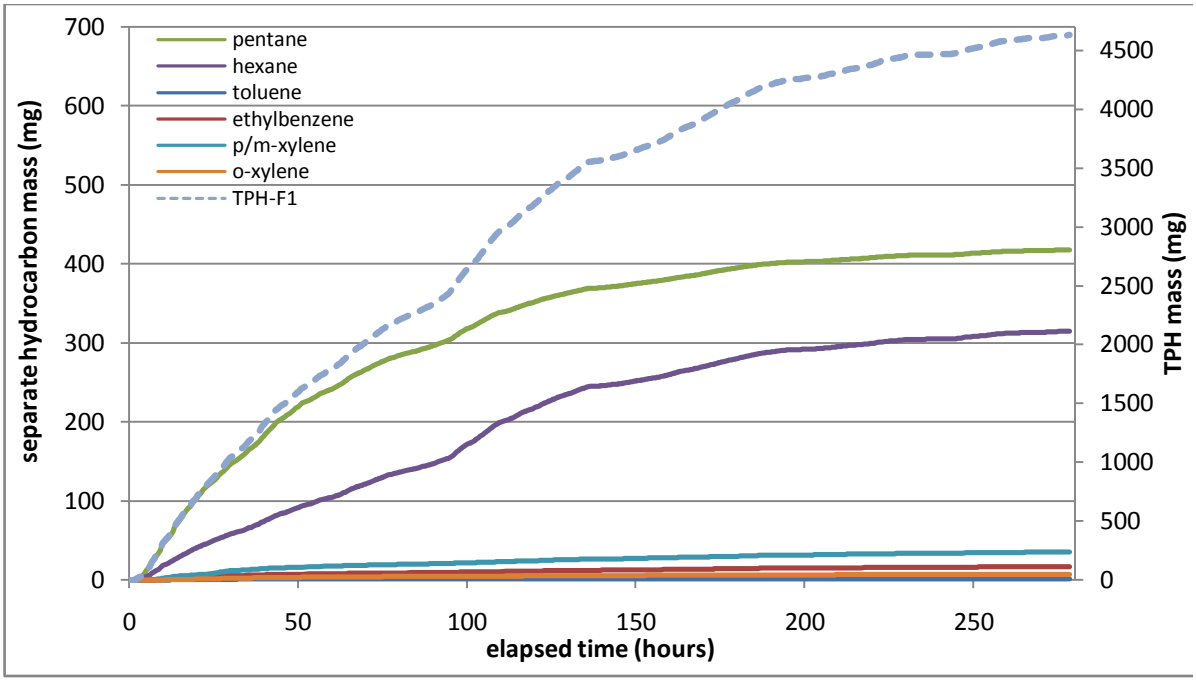

Figure 5.10 Cumulative mass removal over the course of sparging

The figure shows that the mass of pentane removed had started to plateau, while the hexane mass lost was still increasing at the end of the experiment. The curve of overall TPH mass removal showed the same increase when the second injector was started (at approximately 100 hours), but the curve had started to level off somewhat by the end of the experiment. The cumulative curve indicates that the mass removal rate was declining, but that mass was still being removed.

As discussed in Section 2.6.2, the percent mass removed was based on a source determined using Raoult's law. Calculations of the source zone mass based on soil cores and the Feenstra method were generally much lower. Table 5.3 also includes the estimated source zone mass based on the 2007 soil cores.

	Pentane	Hexane	Toluene	Ethylbenzene	P/M-xylene	O-xylene	Total P,H,TEX	TPH-F1
total mass extracted (g)	414	312	1.5	16.8	34.9	6.6	786	4590
est. source zone mass[1]	563	622	246	267	182	194	2070	22300
% extracted[1]	70	50	0.6	6	6	3	30	20
est. source zone mass[2]	--	--	41	60	107	47	--	--
% extracted[2]	--	--	4	30	30	10	--	--

Table 5.3 Contaminant mass removed via SVE system (1=Raoult's Law, 2=Feenstra)

Note that benzene was not included in Table 5.3 because it was not detected in any of the air samples. Benzene was not expected to be present in the source residual according to Raoult's law. The estimates are not for the same suite of analytes because the off-gas was not analyzed for the heavier hydrocarbons measured in the soil cores, and the soil cores were not analyzed for the lighter hydrocarbons. However, soil core data show that the relative percentage of BTEX compounds removed may be higher than calculated based on Raoult's law alone.

5.1.6 Potential additional mass removal

Hydrocarbons were still being removed when the system was shut down, as discussed in Section 5.1.3. Therefore, the curves in Figure 5.10 were extrapolated out to determine how much more mass would be removed if sparging had continued until 500 hours, approximately twice as long as actual treatment.

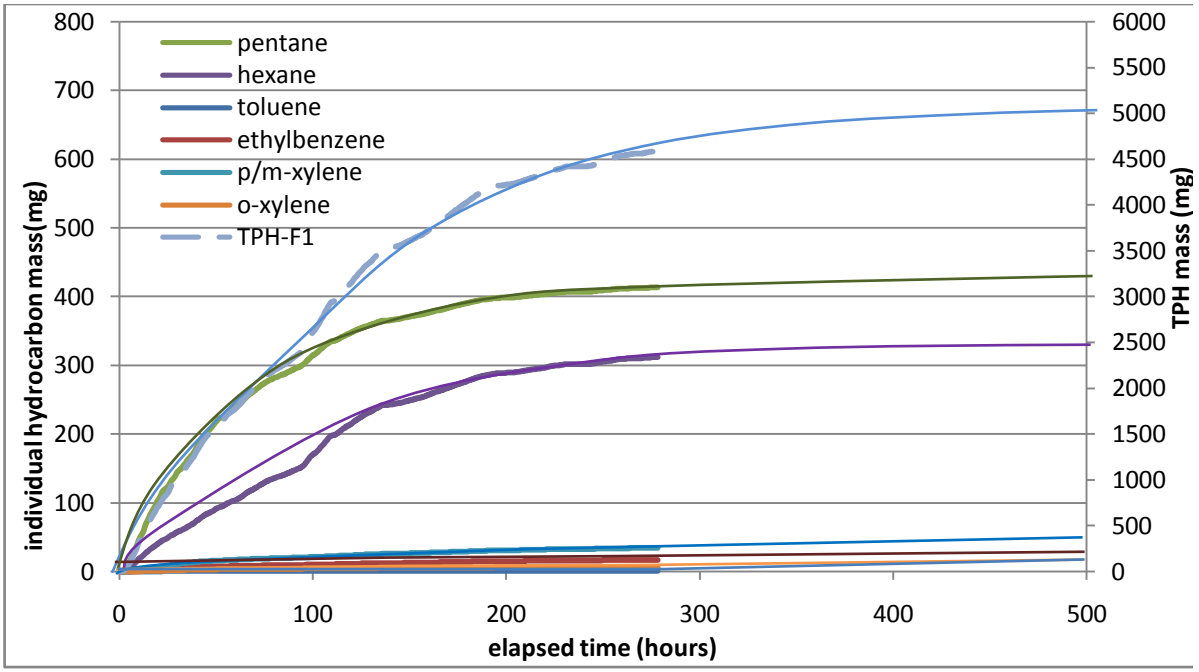

Figure 5.11 Extrapolated mass removal rates

Figure 5.11 shows that the cumulative mass removal rates had started to plateau. Table 5.4 shows the extrapolated mass removal rates if treatment had continued up to 500 hours under similar conditions. The Raoult's law estimate for the source zone is the only one considered here for simplicity.

	Pentane	Hexane	Toluene	Ethylbenzene	P/M-xylene	O-xylene	Total P,H,TEX	TPH-F1
% extracted (280 hr)	74	50	0.61	6.3	5.5	3.4	31	21
mass extracted, g (500 hr)	440	315	5	30	50	20	860	5000
est. source zone mass	563	622	246	267	182	194	2070	22300
% extracted (500 hr)	77	50	0.66	11	7.6	10	28	22

Table 5.4 Extrapolated contaminant mass removed via SVE system (at 500 hours)

Table 5.5 shows that if treatment were to continue, the total source mass removal (as measured by the F1 fraction of TPH) would be less than 10% higher than the mass removal at the actual end of the experiment.

As treatment continues, more effort (more air injected and extracted, and therefore longer equipment run times) is required to remove less mass.

5.2 Additional Mass Loss from Volatilization

The air flow rate outside of the box was estimated to be 3.4 L/hr, as discussed in Section 4.2.3. The samples taken from the air leaks outside the box do not have a simple relationship with the off-gas samples collected at the same time, as the off-gas collected by the treatment system is an average concentration of a much larger volume of air. For this reason, a weighted average of the air leak samples was used to determine the average hydrocarbon mass removed via leaks. Mass was determined using Equation 4.8. Table 5.5 shows that the leaked mass is insignificant compared to the mass removed through the SVE system. Even a leakage rate an order of magnitude above the rate calculated would not have a significant effect on the calculated mass removal.

	Pentane	Hexane	Toluene	Ethylbenzene	P/M-xylene	O-xylene	Total P,H,TEX	TPH-F1
total mass from system (g)	415	315	1.8	17.6	36.4	7.9	793	4598
total mass from leaks (g)	0.45	0.42	ND	0.0063	0.012	0.0024	0.88	7.7
% of total mass lost from leaks	0.1	0.1	--	0.04	0.03	0.03	0.1	0.2
est. mass in source zone (g)	573	624	758	277	658	202	3090	22,900

Table 5.5 Total contaminant mass volatilized

Again, only Raoult's law estimates of the source zone mass are used, with the understanding that these estimates may be higher than the actual source zone mass.

5.3 Biodegradation

Air samples were analyzed for O_2 and CO_2 to determine the effects of degradation, as discussed in Section 3.3.2.

5.3.1 O_2 and CO_2 trends

The O_2 and CO_2 concentrations over the treatment period are shown on Figure 5.12.

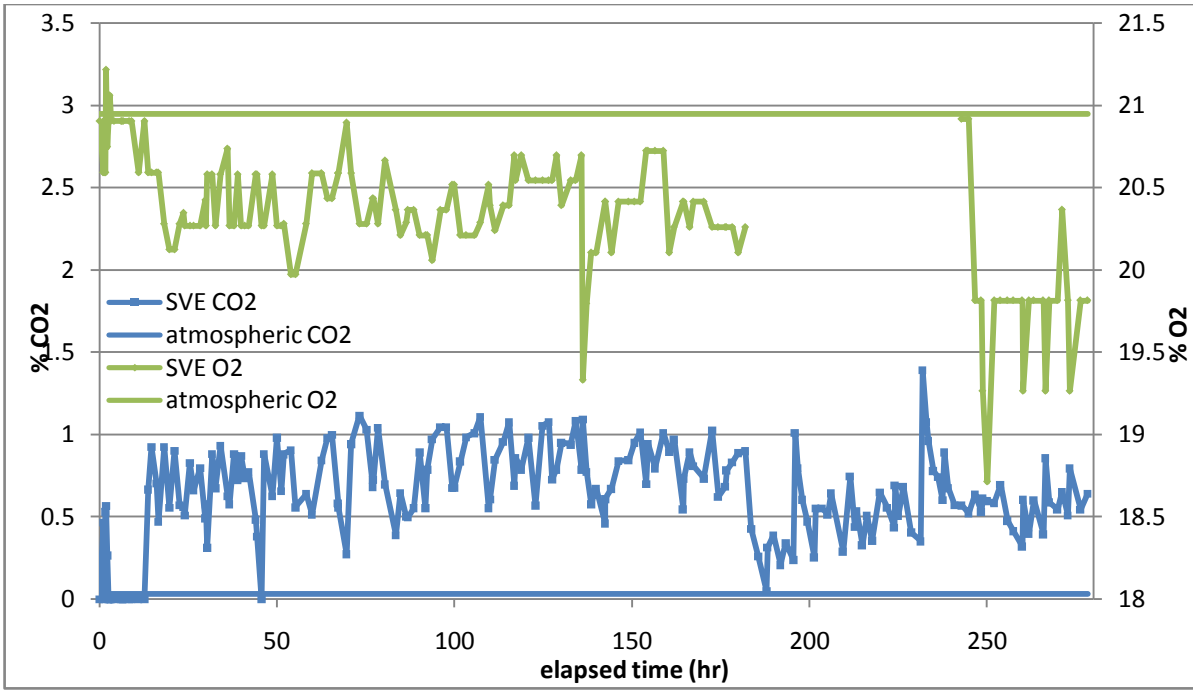

Figure 5.12 O_2 and CO_2 concentrations over treatment period

Analyses for CO_2 and O_2 were performed on a gas partitioner, as discussed in Section 3.2.2. The instrument stopped working partway through the test, and only CO_2 concentrations could be determined. On June 5-6, sample analyses were delayed and so these samples (184-195 hours into the test) were suspect and were removed from the analysis. The gas partitioner was repaired for the samples 243 hours into the test and beyond; CO_2 was then analyzed on both machines. The CO_2 values were within 10% for each machine and not consistently higher or lower for one machine, so the values were averaged.

The first few hours of the test shows some scatter, which can be attributed to the influence of the air originally within the box but not necessarily from soil gas. As discussed in Section 5.1.1, approximately 37 minutes of sparging was required to flush the box. From approximately 2 to 10 hours into the test, the air concentrations were consistently 0.0314 % and 0.0476 % lower than atmospheric CO_2 and O_2, respectively. These are not believed to be from instrument error for CO_2, as samples of the injected air generally had 0% CO_2. O_2 tracer samples were more erratic, with concentrations between 20.67 and 20.85; however, these were higher than the off-gas concentrations. These concentrations were taken as the background soil values.

CO_2 concentrations are expected to be inversely correlated with O_2 concentrations during aerobic biodegradation of petroleum hydrocarbons, as O_2 is used up and CO_2 produced. See Equation 3.1 and Equation 3.2. This correlation has been found in several field studies (Aelion and Kirtland, 2000; Yang et

al., 2005). This can be difficult to see in Figure 5.12, so it was assessed using the daily data. An example is given in Figure 5.13; curves for the other days are provided in Appendix B.2.

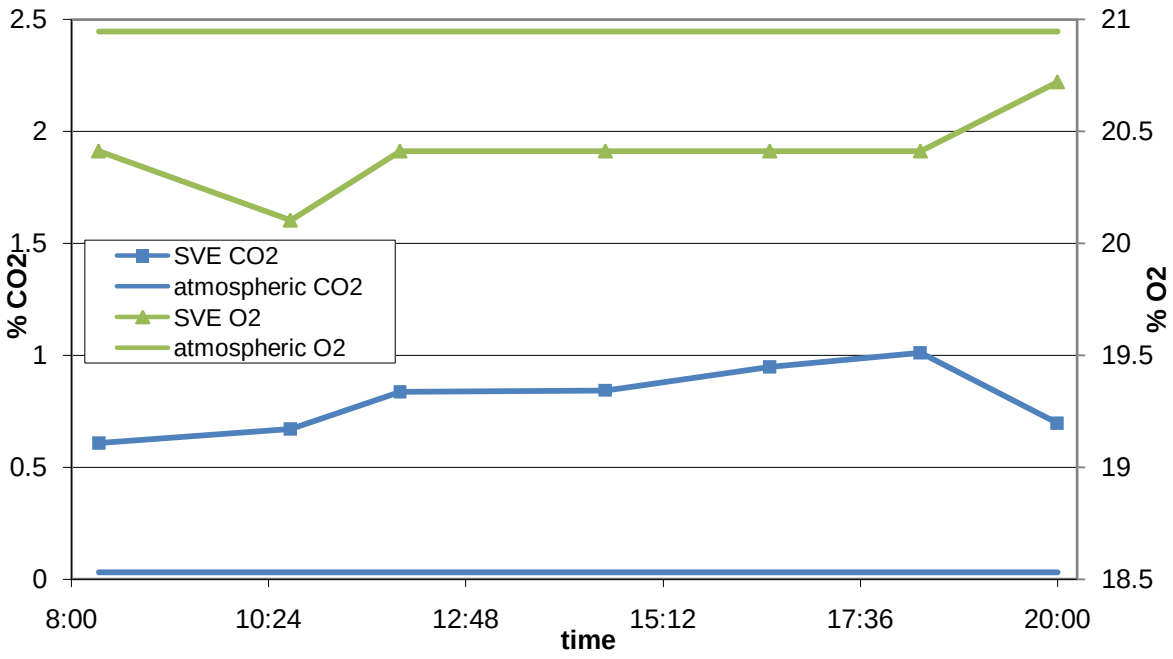

Figure 5.13 June 2 O_2 and CO_2 concentrations

The data do not show a clear inverse correlation. Rather, both sets are relatively close to the background value at system startup in the morning, diverge from background during the day, and trend toward background levels at the end of the day, when the air sparging system had been turned off for at least two hours.

After the results were adjusted as discussed in Section 5.1.1 and Section 5.1.3, they were plotted against the lab TPH curve to examine possible trends. See Figure 5.14. The data from only the first 180 hours of the experiment were graphed in order to show the correlation between O_2, CO_2, and TPH data more clearly, as well as to show as much of the O_2 data as possible before instrument breakdown.

Relative O_2 and CO_2 concentrations were determined by comparing them to background concentrations from the off-gas samples collected prior to starting sparging at the beginning of the test. The normalized O_2 concentration is the percent O_2 subtracted from the background concentration of 20.90%. The background CO_2 concentration was below the MDL, so the percent CO_2 did not need to be normalized.

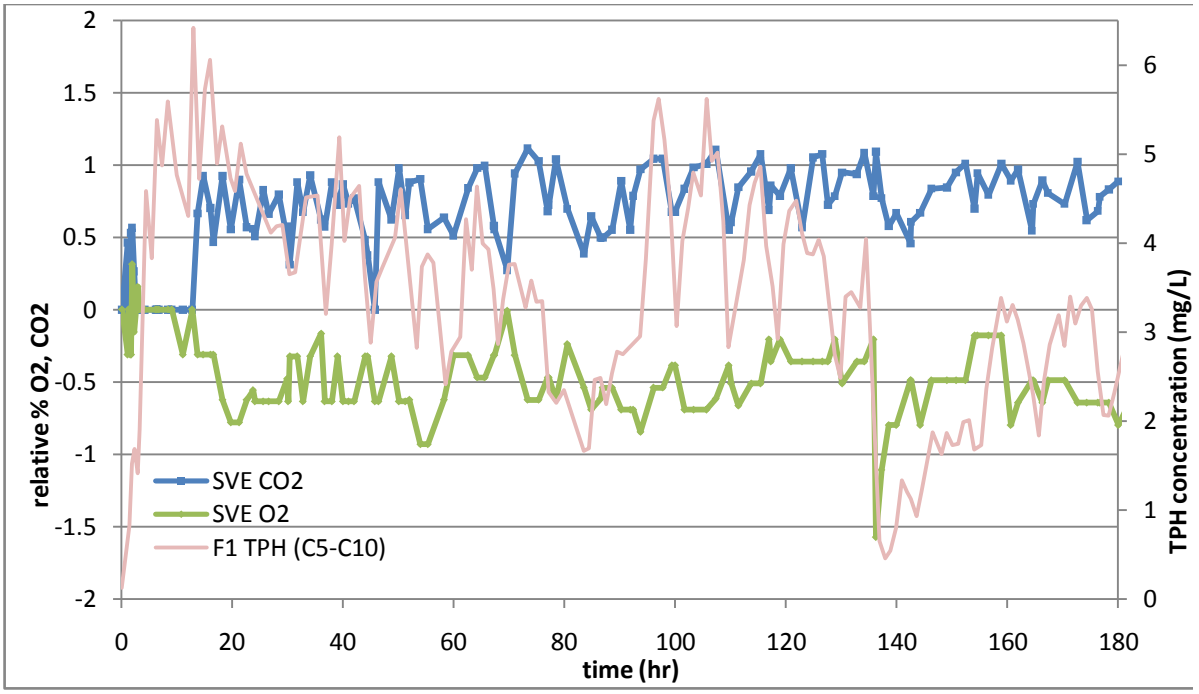

Figure 5.14 Relative O_2 and CO_2 concentrations plotted against F1 TPH

Figure 5.14 indicates that the off-gas collection system did not start removing CO_2 until approximately 13 hours into treatment, which was the same time as maximum TPH peak. The relative percent of CO_2 tends to drop significantly (e.g. CO_2 concentration returns to atmospheric concentrations) at the same time that the TPH concentration drops significantly. This was exemplified by the relatively steep CO_2 drops at 30 and 46 hours. Oxygen levels have similar spikes upward (toward atmospheric concentrations) at the same time. These indicate periods of dilution, usually from system startup. In general, the CO_2 data tends to follow the curve of TPH concentrations better while the O_2 data tends to return to similar concentrations. One exception occurred at approximately hour 140, when the TPH concentration and relative percentage of O_2 dropped significantly. This corresponds to the first time the air sparging was switched to the last injection port (I2), which was partially blocked by a tighter formation. One explanation is that the small amount of air that was pushed into the formation pushed out some extremely low-O_2 air that was otherwise trapped. This suggests that the biodegradation will depend on permeability as well as contaminant and O_2 loading. It suggests that low permeability sections may not be receiving sufficient O_2.

One concern with these trends is that the O_2 data may reflect instrument error to some degree. However, as discussed in Section 3.2.3, the concentrations seen appear to reflect field conditions rather than instrument error.

5.3.2 O_2 removal and CO_2 addition from baseline

The O_2 and CO_2 concentrations were reported as % by volume. These values were converted to a mass concentration by using the following equation.

$$C = \frac{C_V \rho}{100} \qquad (5.3)$$

In Equation 5.3, C is the mass concentration (g/L), C_V is the reported concentration by volume (%), and ρ is the gas density at atmospheric pressure and 25˚C (1.3080 g/L and 1.7989 g/L for O_2 and CO_2, respectively, Lide, 2008). This was converted to a mass of CO_2 gained and O_2 lost using Equation 4.8.

Based on this, the total mass of O_2 lost was 10.2 kg and the total mass of CO_2 gained was 21.5 kg over the course of treatment. The total treatment time for the CO_2 was 280 hours and for the O_2 data available was 235 hours. Since 45 hours of O_2 data were lost, the rate of O_2 mass loss was assumed to be consistent throughout treatment and the total mass of O_2 lost assumed to be 12.2 kg.

Kirtland et al. (2001) assumed that 25% of the carbon in the system was converted into biomass, and 80% of the CO_2 in the off-gas was from mineralization and 20% from plant respiration, based on radiocarbon measurements. The treatment area was covered prior to the start of plant growth, and removal of the treatment box showed minimal plant survival. However, removal of the outer walls found a large number of ant colonies between the vinyl and the plywood, so the CO_2 rates in this study are assumed to be 90% from mineralization, with no contribution from plant respiration and some additional biological component. Therefore, the total mass of CO_2 gained was adjusted to 19.4 kg.

Kirtland et al. (2001) also assumed that hexane could be used as an approximation of the bulk biodegraded gasoline mass. In this case, the oxidation of the gasoline mass would be represented by Equation 5.4.

$$C_6H_{14} + 9.5O_2 \rightarrow 6CO_2 + 7H_2O \quad (5.4)$$

CO_2 has a molecular weight of 44 g/mol, so the total mass of CO_2 gained would be 439.8 mol. Equation 5.4 suggests a 6:1 CO_2 to gasoline ratio, so 73 mol (6.3 kg) of gasoline would be mineralized. If 25% of the carbon from the gasoline were converted to biomass, as suggested by Kirtland et al., then 8.4 kg gasoline was removed as a result of biodegradation. O_2 has a molecular weight of 32 g/mol, so the total mass of O_2 lost would be 381 mol. Equation 5.4 suggests a 9.5:1 O_2: gasoline ratio, so 40.1 mol (1.3 kg) of gasoline would react with O_2. The CO_2 biodegradation rate is therefore 6.6 times that of the O_2 biodegradation rate.

The difference between O_2 and CO_2-derived biodegradation rates may be due to several factors. Aelion and Kirtland (2000) suggest that differences in biodegradation rates may be due to errors in the amount of carbon that is converted to biomass (i.e. less than 25% of carbon was converted to biomass), mineralization of native organic carbon, or carbon precipitation from carbonate soils. In this experiment, errors in biomass conversion are not sufficient to explain the difference in biodegradation rates, and the aquifer contains minimal non-hydrocarbon organic material. In addition, aquifers tend to resist changing redox states because the aquifer material acts as an oxygen sink for anaerobic aquifers (Barcelona, 1991). Therefore, the oxygen in the off-gas may give a lower biodegradation estimate.

Another source of error is in Equation 5.4 itself. Hexane has been suggested as the closest analogue for weathered gasoline, as discussed, but if the residual gasoline has a different C:H ratio, if this ratio varies depending on where the contamination is, or if the gasoline is not completely mineralized, the gasoline mass derived from the O_2 and CO_2 measurements may be off.

An average of the O_2 and CO_2 biodegradation rates suggest that 22% of the mass removed was through biodegradation. This is higher than the 15% suggested by Johnson et al. (1998), but within the 15-25% range suggested by Hinchee (1991), and the 23% suggested by Kirtland et al. (2001). Yang et al. (2005) found biodegradation rates up to 78% during active pulsed sparging.

Yang et al. (2005) and Johnson et al. (1998) suggest that biodegradation should proportionally remove more of the mass as the system continues to operate. This appears to be the case for this system. Figure 5-13 shows that the O_2 and CO_2 concentrations (and therefore mass removal calculated based on those concentrations) were relatively consistent throughout the experiment while the mass removal rates from volatilization decreased over time.

5.3.3 Individual compound biodegradation

Aerobic biodegradation rates from air sparging can be considered analogous to in-situ soil vapor biodegradation rates, which have been studied previously. Compounds with a faster vapor biodegradation rate should make up a larger proportion of the biodegraded mass. Hohener et al. (2003) examined biodegradation rates of a number of common gasoline components. Using column experiment results, which were considered to be more representative than batch experiment results and better-constrained than field data results from lysimeters, they determined the following biodegradation rates for compounds in the source area (based on Raoult's law): <0.01/day for pentane, 0.26/day for hexane, 1.31/day for toluene, 3.28/day for m-xylene, and 4.94/day for 1,2,4-TMB.

The overall mass of individual compounds biodegraded depends on a large number of factors that are difficult to quantify, including the mass retained after volatilization at a given time and the interaction of the air with various pockets of gasoline residual. This is likely the reason why most air sparging studies examining biodegradation, such as those by Johnson et al. (1998) Aelion and Kirtland (2000), Baker et al. (2000), and Yang et al. (2005), report biodegradation rates only for the hydrocarbon mass and not for individual compounds. The biodegradation rates do indicate that more of the TMB and xylene are likely to have been removed through biodegradation and that pentane and hexane are less likely to be removed.

5.4 Total Contaminant Mass Loss

The total mass removed via volatilization was calculated as 4.6 kg, 21% of the total mass estimated in the residual source, as described in Section 5.1.4. The total mass removal via biodegradation was estimated at 4.9 kg, or 22% of the total estimated mass. The total contaminant mass lost is about 9.5 kg or 43%.

The mass estimate removed depends on the initial source mass, as discussed in Section 2.6. The total percent removed could vary between 20 and 60 percent of the residual source mass. The percent loss via leakage outside of the box is much smaller than this variation and is not anticipated to significantly impact calculations of the mass volatilized.

Chapter 6: Plume Impacts

6.1 Hydraulic Conductivity

In June 2007, additional slug tests were performed from the row 2 open-screen wells to determine the hydraulic conductivity for each and thus determine discharge through each well. See Section 3.4.2 for slug test methods and Figure 3.2 for well locations. The discharge data were compared to the results from the multi-level wells to get a better understanding of concentrations downgradient of the source areas.

The Bouwer and Rice method (1976) was used to measure conductivity in wells GMT-R2-A through E and E10-R2-A through E. It uses the following equation:

$$K = \frac{r_c^{\,2} \ln\left(R_e / r_w\right)}{2L} \cdot \frac{1}{t} \cdot \ln \frac{Y_0}{Y_t} \qquad (6.1)$$

where r_c = casing radius, L = intake length, r_w = radial distance between the undisturbed aquifer and the well center, R_e = effective well radius, Y_0 = initial drawdown, and Y_t = vertical distance between the water level in the well at time t and equilibrium. The effective radius is not determined empirically; instead, the following equation is used to complete Equation 6.1:

$$\ln R_e / r_w = \left[\frac{1.1}{\ln\left(H / r_w\right)} + \frac{A + B \ln\left[\left(D - H\right) / r_w\right]}{L / r_w} \right] \qquad (6.2)$$

where H = the distance from the water table to the bottom of the intake, A and B are dimensionless coefficients that are a function of L/rw (taken from a graph), and D = the saturated aquifer thickness. Y_0, Y_t, and t are determined from a graph of the logarithmic change in head (H-h) with respect to time.

For these wells, the total aquifer thickness is 7 m; r_w = 1.5 in or 0.0381 m; r_c = 1.25 in or 0.03175 m; L = 5.03 m; L/ r_w = 132 (so A = 5.4 and B = 0.9) and the total well depth = 5.41 m.

Hydraulic conductivities for each well are presented in Table 6.1. The GMT wells are located in a cell that was not used for this work, so they are not discussed further. Slug test figures and data are presented in appendix D.2.

Well ID	K (m/s)		notes:
	falling head	rising head	
E10-A	--	9.54E-06	
E10-B	--	1.60E-05	
E10-B*	1.63E-05	1.51E-05	falling head: poor line fit
E10-C	--	1.14E-05	
E10-D	--	9.54E-06	
E10-E	1.36E-05	1.51E-05	falling head: best fit line 0 above actual 0
GMT-A	--	1.05E-05	
GMT-A*	--	1.15E-05	
GMT-B	--	1.09E-05	
GMT-C	1.02E-05	1.49E-05	rising head: poor line fit
GMT-D	1.85E-05	1.75E-05	falling and rising head: poor line fit
GMT-E	--	1.18E-05	

-- indicates that line fit was not possible with the data
*repeat of initial test

Table 6.1 Hydraulic conductivities for open-screened row 2 wells

Falling head tests were not performed on wells screened across the water table during testing, and the two wells in which the tests were performed had inferior results. Therefore, only rising head tests were considered.

6.2 Discharge Comparison

Contaminant discharge was measured using the open-screen wells and multi-level wells in row 2. See Appendix D.5 for discharge calculations.

6.2.1 Multi-level well mass discharge

The multi-level wells have been used to monitor the E10 plume since source emplacement. The mass of contaminants migrating through row 2 per unit of time was calculated using Equation 6.3 below (Augustine, 2007).

$$M_D = \sum_{i=1}^{n} q_i \cdot C_i \cdot A_i \qquad (6.3)$$

In Equation 6.3, M_D is the mass discharge (mg/day), q_i is the darcy discharge at sampling point I (0.03 m/day assumed for all points), C_i is the concentration at sampling point I (mg/L), and A_i is the cross sectional area of sampling point I perpendicular to flow. The sample intervals are the same except for the

bottom interval, which is significantly larger than the others. Therefore, the cross-sectional area has been calculated as 0.216 m^2 for all points except for the two deepest points, which were calculated to be 0.864 m^2.

6.2.2 Open screened sampling comparison

The open-screened wells were added to characterize mass discharge over the entire section of aquifer. The open screened wells were added because slug tests can be performed. Hydraulic conductivity data from the slug tests give a more accurate picture of the mass discharge over the entire screened interval.

Investigators do not agree which method is the most representative for sampling an open-screened well. A common method is to simply purge the well before sampling. EPA technical guidance suggests monitoring the purge water for stabilization and collecting samples using low-flow methods (EPA, 1992). Ontario Ministry of the Environment (MOE) regulations suggest that any methods that assure a representative sample are acceptable, as long as the sampling is carried out consistently (MOE, 1996).

In order to determine which open-screen sampling method was most appropriate for the Borden aquifer, samples were collected using the methods described in Section 3.4.1. See Table 6.2 for groundwater BTEX results.

	Benzene	Toluene	Ethylbenzene	P,M-xylene	O-xylene
multilevel	53.1	1613.6	1065.9	2122.1	800.2
method 1	54.4	883.7	1227.2	2452.4	830.6
method 2	12.8	256.5	185.0	369.0	143.1
method 3	10.1	133.3	114.9	215.8	74.5
method 4	9.9	167.6	133.8	270.0	92.1

Table 6.2 BTEX concentrations (µg/L) from well E

The first method produced significantly higher concentrations than the others. Methods 2 and 4 most likely had lower concentrations because of volatilization from filling and transferring water from larger containers. Method 3 minimized volatilization but is less likely to be representative of the aquifer as a whole because of the much smaller section of aquifer sampled and may have inadvertently targeted a section of relatively uncontaminated groundwater. Based on these results, Method 1 was used for post-treatment groundwater sampling of the open-screened wells.

6.2.3 Open screened mass discharge

The mass discharge from the open-screened wells is determined using Equation 6.3. In this case, the wells were screened below the water table so the cross-sectional area, A_i, is based on the entire screened interval (4.8 m^2 for wells A and D, 3.6 m^2 for wells B and C, and 2.4 m^2 for well E). Note that for these calculations, well E is considered to be within row 2, as it is 0.5 m directly behind well 3. The darcy discharge, q_i, is calculated from Equation 6.4 (Freeze and Cherry, 1979).

$$q_i = -K\frac{dh}{dl} \qquad (6.4)$$

In Equation 6.4, q_i has units of m/day, K is the hydraulic conductivity (m/day) from the slug test results, and dh/dl is the hydraulic gradient ($4.3x10^{-3}$ [unitless] from Sudicky, 1986).

6.3 Immediate Plume Impacts

The average groundwater velocity is estimated at 0.09 m/day, so it would take approximately 39 days for groundwater in the center of the source zone to reach row 2. June 23 was the final day of sparging and the day that the SF_6 was injected, so groundwater samples were collected on July 31 (38 days after SF_6 sparging) for the multi-level wells and August 1 for the open-screened wells in order to intercept the expected SF_6 plume. Results from this time would also be expected to yield the lowest hydrocarbon values prior to any potential rebound, because this groundwater would be from a fully-sparged source.

6.3.1 SF_6 concentrations

SF_6 data for row 2 is shown on Figure 6.1. Note that this cross section is shown facing downgradient with well IDs from left to right to be consistent with previous work at this site.

	Depth (m)	well ID									
		6	5	D	4	C	3/E	B	2	A	1
multi-level wells	1.5	0.2	2.6		0.4		<DL		11.9		0.5
	1.68	ND	<DL		0.2		5.5		1.7		0.2
	1.86	<DL	<DL		0.3		52.6		2.8		<DL
	2.04	<DL	1.0		18.9		43.9		25.0		5.3
	2.22	0.3	0.3		22.0		17.4		43.8		16.1
	2.4	ND	ND		5.9		<DL		2.0		17.1
	2.58	ND	0.3		8.6		4.8		34.6		0.7
	2.76	<DL	<DL		33.6		<DL		5.3		<DL
	2.94	ND	ND		55.1		20.8		7.7		40.3
	3.12	ND	0.2		31.8		5.5		156.1		99.1
	3.3	ND	3.6		33.1		176.1		--		53.4
	3.48	ND	8.5		5.4		50.8		120.5		9.6
	3.66	0.4	<DL		<DL		23.1		9.4		1.4
	3.84	--	0.2		10.8		42.3		21.7		<DL
	4.84	--	1.5		1.1		400.4		1707		505.5
open screened wells				229.2		11.3	29.8	13.0		249.3	

>1000 = 100-1000 = 10-100 = 1-10 = < 1 =

not sampled =

Figure 6.1 Cross section of SF_6 concentrations in groundwater (µg/L)

The method detection limit (DL on Figure 6.1) is 1µg/L. Three intervals were not sampled because the tubing was missing. Also note that open-screened well E is approximately 0.5 m downgradient of the rest of row 2, as it is directly behind multilevel well 3. Therefore, the SF_6 concentration may be lower than expected because the bulk of the SF_6 plume has not reached the well yet.

Firgure 6.1 shows that most of the dissolved SF_6 from sparging is in the lower portion of the treatment area. The multi-level wells on the left facing downgradient have the lowest SF_6 concentrations, which is consistent with previous hydrocarbon results (Mocanu, 2007) and show that the plume is not perfectly centered in the cell. The highest concentrations of SF_6 are generally at the bottom of wells 1 through 3, with the peak concentration in well 2. The lack of SF_6 coverage on the left side of the well network is not surprising because the plume is not centered within the cell; but rather, the center of the plume is closer to well 3, as discussed by Mocanu and shown in the pre-treatment data in Figure 6.2. Therefore, the groundwater flow would carry the SF_6 slightly to the right. However, the maximum concentration of SF_6 is to the right of the plume core, suggesting that more SF_6 was added via the injection wells on the right side. This supports evidence presented in Chapter 4 that relatively little air was injected using I-2, either because of well construction problems or relatively low-permeability aquifer material.

6.3.2 Total hydrocarbon plume morphology changes

Figure 6.2 on the following page compares total hydrocarbon (BTEX, TMB, and naphthalene) concentrations in groundwater before and after treatment.

July 2008 total VOC concentrations

	Depth (m)	well ID									
		6	5	D	4	C	3/E	B	2	A	1
multi-level wells	1.5	8.9	8.0		1.2		0.0		0.0		16.1
	1.68	3.2	7.0		0.9		0.0		0.0		19.6
	1.86	0.0	5.9		1.6		6.6		2.6		27.5
	2.04	2.1	3.9		0.0		25.4		3.7		26.2
	2.22	0.0	12.9		2.6		53.7		6.2		0.0
	2.4	0.0	31.5		12.4		46.2		12.4		12.6
	2.58	0.0	1.9		19.6		42.6		12.9		15.5
	2.76	0.0	1.8		82.5		16.7		15.9		16.1
	2.94	0.0	15.0		12.5		51.3		59.9		15.1
	3.12	0.9	5.1		25.1		142		37.2		4.2
	3.3	0.0	3.6		28.4		221		--		25.4
	3.48	0.0	0.0		31.8		3841		321		67.0
	3.66	0.0	1.4		70.2		20775		5158		97.8
	3.84	0.0	1.4		3.8		19096		13117		54.2
	4.84	0.0	1.6		43.6		14.7		11.3		0.0
open screened wells				2.98		8.84	652	169		24.7	

June, August 2007 total VOC concentrations

	Depth	6	5	D	4	C	3/E	B	2	A	1
multi-level wells	1.5	39.5	0.4		1.5		4.8		0.0		44.5
	1.68	--	1.9		1.5		4.2		0.3		12.1
	1.86	31.5	2.3		0.4		2.4		0.1		9.0
	2.04	20.7	0.3		0.0		1.7		0.3		8.7
	2.22	16.5	4.1		0.3		2.2		0.2		9.8
	2.4	11.7	1.7		0.2		2.5		0.3		3.4
	2.58	9.0	2.8		0.0		3790		0.0		5.7
	2.76	8.5	0.3		0.1		4.6		3.9		2.7
	2.94	9.1	2.2		0.1		20583		2.3		9.2
	3.12	4.1	3.7		1.0		39916		1.2		2.4
	3.3	7.1	1.2		0.3		30769		25.1		9.0
	3.48	3.2	1.1		314		21872		95.4		0.4
	3.66	3.0	1.3		335		4056		7590		1.9
	3.84	4.3	1.2		346		24131		3170		--
	4.84	3.2	4.5		2.5		12.2		6.3		17.3
open screened wells				368		7440	4441	5711		177	

>10,000 = 1000-10,000 = 100-1000 =

10-100 = 1-10 = <1 = no sample=

Figure 6.2 Cross sections of total VOCs in groundwater (µg/L) before and after sparging

Figure 6.2 shows that the plume core remains in place after treatment. However, the area of maximum concentrations is considerably smaller, with only three samples above 10 mg/L. The maximum total VOC concentration after treatment is only 52% of the maximum concentration prior to treatment. However, the treatment appears to have spread out the contamination so that the edges of the plume have higher concentrations than the concentrations before treatment.

The spreading-out of the plume core can be considered a negative consequence if the treatment criterion is the lateral extent of concentrations above a relatively low standard, such as the benzene EPA maximum contaminant level, or MCL, of 5 µg/L (EPA, 2008). However, the average total VOC concentration across the fence dropped from 1789 to 718 µg/L, a 60% decrease.

6.3.2 BTEX plume morphology changes

Plume morphology changes are broken out by compound below. Only values for multilevel wells are shown. Benzene plume morphology changes are provided in Figure 6.3. Note that the color scheme is the same as that used for Figure 6.2.

2007 Benzene concentrations (µg/L)					
6	5	4	3	2	1
0.0	0.0	0.0	0.0	0.0	0.0
--	0.0	0.0	0.0	0.0	0.0
0.0	0.0	0.0	0.0	0.0	0.0
0.0	0.0	0.0	0.0	0.0	0.0
0.0	1.2	0.0	0.0	0.0	0.0
0.0	1.3	0.0	0.0	0.7	0.0
0.0	1.2	0.0	0.0	0.0	0.0
0.0	0.0	0.0	0.0	0.5	0.0
0.0	1.1	0.0	51	0.0	0.0
0.0	1.2	0.0	147	0.6	0.0
0.0	1.2	0.0	175	1.0	0.0
0.0	1.1	7.0	170	1.2	0.0
0.0	1.1	9.1	59	63	0.0
0.0	1.2	8.1	168	49	1.3
1.4	1.3	0.0	1.4	1.3	0.0

2008 Benzene concentrations (µg/L)					
6	5	4	3	2	1
0.8	0.0	0.0	0.0	0.0	0.0
0.0	0.0	0.0	0.0	0.0	1.9
0.0	0.0	0.0	0.0	2.6	1.4
0.0	0.0	0.0	0.0	3.7	1.9
0.0	0.0	1.2	0.0	6.2	0.0
0.0	0.0	3.1	3.3	7.8	0.0
0.0	0.0	2.2	9.9	8.0	0.0
0.0	0.0	6.5	5.7	10	0.0
0.0	0.0	0.0	3.3	22	0.0
0.0	0.0	1.7	8.4	10	2.1
0.0	0.0	19	15	--	7.4
0.0	0.0	9.4	88	30	25
0.0	0.0	46	127	56	52
0.0	0.0	2.5	68	62	22
0.0	0.0	0.0	0.0	0.0	0.0

Figure 6.3 Benzene plume concentrations before and after sparging

The benzene plume appears to have a much smaller core. Concentrations to the left of the plume core facing downgradient have increased, and concentrations to the right facing downgradient have increased as well. The increased plume concentrations in the center and right of the monitoring well network may be due to increased mobilization of the source zone from the sparging.

2007 Toluene concentrations (µg/L)					
6	5	4	3	2	1
8.0	0.4	0.4	0.6	0.0	16
--	0.4	0.2	0.6	0.3	2.3
7.4	0.4	0.4	0.5	0.1	1.7
4.0	0.3	0.0	0.1	0.3	1.2
3.6	0.9	0.2	0.4	0.2	1.7
2.2	0.4	0.2	0.3	0.6	0.8
1.8	0.3	0.0	0.0	0.0	1.3
1.6	0.3	0.1	2.8	0.5	0.5
1.8	0.3	0.1	9705	0.5	1.6
1.1	0.5	0.0	15727	0.1	0.6
1.2	0.0	0.3	10668	2.1	1.3
0.8	0.0	21	5364	7.6	0.4
0.2	0.1	9.2	500	815	0.0
0.9	0.0	11	3236	245	3.1
0.2	0.9	0.5	2.1	0.5	0.0

2008 Toluene concentrations (µg/L)					
6	5	4	3	2	1
0.0	0.0	0.0	0.0	0.0	0.0
0.0	0.0	0.0	0.0	0.0	0.0
0.0	0.0	0.0	0.0	0.0	0.0
0.0	0.0	0.0	0.0	0.0	0.0
0.0	0.0	0.0	1.0	0.0	0.0
0.0	0.0	0.0	2.7	0.0	0.0
0.0	0.0	0.0	1.6	0.0	0.0
0.0	0.0	4.3	1.1	0.0	0.0
0.0	0.0	0.0	5.0	1.0	0.0
0.0	0.0	0.4	13	1.1	0.0
0.0	0.0	0.0	68	--	1.5
0.0	0.0	3.1	1736	12	8.2
0.0	0.0	3.4	1120	245	9.1
0.0	0.0	0.0	275	84	7.6
0.0	0.0	3.0	0.0	0.0	0.0

Figure 6.4 Toluene plume concentrations before and after sparging

Toluene concentrations do not show much evidence of plume migration other than a slight increase in concentration on the right side of the fence facing downgradient. The toluene concentrations dropped the most of all of the BTEX compounds, and this is reflected in the significant drop in peak concentration and core plume area.

2007 Ethylbenzene concentrations (µg/L)					
6	5	4	3	2	1
8.0	0.4	0.4	0.6	0.0	16
--	0.4	0.2	0.6	0.3	2.3
7.4	0.4	0.4	0.5	0.1	1.7
4.0	0.3	0.0	0.1	0.3	1.2
3.6	0.9	0.2	0.4	0.2	1.7
2.2	0.4	0.2	0.3	0.6	0.8
1.8	0.3	0.0	0.0	0.0	1.3
1.6	0.3	0.1	2.8	0.5	0.5
1.8	0.3	0.1	9705	0.5	1.6
1.1	0.5	0.0	15727	0.1	0.6
1.2	0.0	0.3	10668	2.1	1.3
0.8	0.0	21	5364	7.6	0.4
0.2	0.1	9.2	500	815	0.0
0.9	0.0	11	3236	245	3.1
0.2	0.9	0.5	2.1	0.5	0.0

2008 Ethylbenzene concentrations (µg/L)					
6	5	4	3	2	1
0.0	0.0	0.0	0.0	0.0	0.0
0.0	0.0	0.0	0.0	0.0	9.3
0.0	0.0	0.0	0.0	0.0	7.5
0.0	0.0	0.0	0.0	0.0	2.1
0.0	0.0	0.0	0.0	0.0	0.0
0.0	0.0	0.0	0.0	0.0	0.0
0.0	0.0	0.0	1.2	0.0	0.0
0.0	0.0	0.0	0.0	0.0	0.0
0.0	1.6	0.0	7.3	4.6	0.0
0.0	0.0	2.2	22	5.2	0.0
0.0	0.0	2.0	23	--	2.3
0.0	0.0	3.2	244	25	6.1
0.0	0.0	3.5	2529	500	6.9
0.0	0.0	0.0	2180	308	4.0
0.0	0.0	15	1.8	0.0	0.0

Figure 6.5 Ethylbenzene plume concentrations before and after sparging

Ethylbenzene concentrations have a similar trend to the toluene concentrations shown in Figure 6.4. In this case, the plume appears to have decreased in concentration, but not moved.

2007 m,p,x-xylene conc. (µg/L)					
6	5	4	3	2	1
21	0.0	1.1	3.1	0.0	38
--	1.5	1.3	2.7	0.0	7.7
18	1.9	0.0	1.8	0.0	5.8
12	0.0	0.0	1.7	0.0	6.0
9.2	2.0	0.0	1.8	0.0	6.5
7.3	0.0	0.0	1.6	3.0	2.7
5.4	1.3	0.0	3790	0.0	3.3
4.0	0.0	0.0	1.8	1.1	2.2
5.8	2.1	0.0	7391	1.6	6.0
3.0	0.8	1.0	15871	0.0	1.8
4.7	0.0	0.0	12785	13	6.2
2.4	0.0	126	10426	47	0.0
2.8	0.0	129	1973	3848	1.9
2.5	0.0	122	13411	1511	8.8
1.6	2.3	2.0	6.1	11	0.0

2008 m,p,x-xylene conc.(µg/L)					
6	5	4	3	2	1
5.1	7.0	1.2	0.0	0.0	14
1.8	5.5	0.9	0.0	0.0	1.5
0.0	4.3	1.6	3.8	0.0	5.5
2.1	3.9	0.0	20	0.0	13
0.0	11	1.5	45	0.0	0.0
0.0	29	7.7	33	4.7	7.6
0.0	1.9	15	25	4.9	12
0.0	1.8	66	8.9	5.7	15
0.0	13	11	23	26	13
0.9	5.1	18	64	19	2.1
0.0	3.6	7.1	85	--	14
0.0	0.0	11	1680	178	28
0.0	1.4	11	13596	3188	29
0.0	1.4	1.3	13453	9122	21
0.0	1.6	22	12	11	0.0

Figure 6.6 Total xylene plume concentrations before and after sparging

The total m/p/o-xylene plume concentrations changes were similar to those of benzene, with a smaller central core but more spreading away from the core, especially in well 4.

Additional post-treatment sampling is recommended to see if the plume morphology changes shown in Figures 6.3 through Figure 6.6 represent a significant departure or if they are a continuation of gradual changes over time. If the later is true, the long-term impact of sparging would be indeterminate.

6.3.3 BTEX mass discharge

BTEX mass discharge from 2007 (before treatment) and 2008 (after treatment) was calculated as described in Section 6.2. See Table 6.3 for BTEX concentrations and calculated mass discharges.

pre-treatment (2007)					
	Benzene	Toluene	Ethylbenzene	P,M-xylene	O-xylene
maximum concentration (µg/L)	175	15727	5310	11301	4570
average concentration (µg/L)	12.5	627	311	706	202
multilevel discharge (mg/day)	10.4	365	248	544	205
open-screen discharge (mg/day)	1.93	88.7	53.8	113	45.3
post-treatment (2008)					
	Benzene	Toluene	Ethylbenzene	P,M-xylene	O-xylene
maximum concentration (µg/L)	127	1736	2529	9830	3766
average concentration (µg/L)	10.2	48.8	80.0	405	163
Multilevel discharge (mg/day)	7.80	30.3	86.2	511	195
open-screen discharge (mg/day)	0.121	0.504	1.78	6.05	2.82
% loss from 2007 to 2008					
	Benzene	Toluene	Ethylbenzene	P,M-xylene	O-xylene
maximum concentration (µg/L)	27	89	52	13	18
average concentration (µg/L)	19	92	74	43	38
multilevel discharge (mg/day)	25	92	65	6	5
open-screen discharge (mg/day)	94	99	97	95	94

Table 6.3 BTEX concentrations and mass discharges before and after treatment

In Table 6.3, the maximum and average concentrations were taken from the multilevel wells. Data from well 6 were not included because historically the plume has bypassed the well and samples were not collected.

The maximum and average concentrations dropped significantly for all compounds except for benzene, which had a much smaller difference in concentrations between 2007 and 2008. However, benzene concentrations were significantly lower than those of the other BTEX compounds to begin with. Toluene had the highest initial concentrations and the largest percentage loss. This can be explained by toluene's higher vapor pressure, which is significantly higher than that of ethylbenzene and the xylenes. Figure 5.4 shows that the toluene would peak in the off-gas slightly before the other compounds.

The mass discharge for open-screened wells was significantly lower than that of the multi-level wells. The open-screened mass discharge is also significantly lower than the multilevel mass discharge post-treatment. One reason for this difference might be that the water level was significantly higher in 2008. The open-screened wells are screened from 1 to 5 m bgs, so the top of the screened interval is 1.5 m higher than the highest multilevel interval. The plume core for all analytes is toward the bottom of the monitored zone, so it is reasonable to expect that the higher water level would cause dilution at the top of the well screen.

6.3.4 Non-BTEX mass discharge

The groundwater analysis method discussed in section 3.2.2 was selected for consistency with previous groundwater data. It was originally selected because the lighter hydrocarbons of interest (pentane, hexane, and butane) have solubilities one to two orders of magnitude smaller than BTEX compounds and would not be expected to migrate downgradient in significant concentrations. However, as the air sparging preferentially removed the lighter hydrocarbons, it would be expected that the mass discharge of lighter hydrocarbons would decrease significantly.

However, the analytical method does not quantify the lighter hydrocarbons because of interference. Therefore, the TPH mass between the methylene chloride (used as a solvent) and toluene on the chromatograph was quantified for selected intervals to determine how much of the lower hydrocarbon mass had been removed. TPH was calculated based on toluene. Many of the lower-concentration samples did not have sufficient mass to quantify, so the samples with the highest concentrations were used. Air sparging preferentially removes the lighter hydrocarbons through volatilization, so the lighter hydrocarbons would be preferentially removed from the source. However, these undefined lighter hydrocarbons may not be as soluble and therefore may not be present in significant quantities in the plume. Table 6.4 shows the calculated light hydrocarbon concentrations.

	original values - light TPH (µg/L)									
	2-13	2-14	3-10	3-11	3-12	3-13	3-14	4-12	4-13	average
2007	764.5	480.0	2221	2032	1944	536.8	2030	136.5	139.3	1143
2008	656.1	835.0	75.1	135.8	1037	1299	713.5	86.9	471.5	590
	original values - total GC concentrations (µg/L)									
	2-13	2-14	3-10	3-11	3-12	3-13	3-14	4-12	4-13	average
2007	7230	3134	39,916	30,769	21,872	4056	24,131	314.5	35.1	14606
2008	5158	13,117	1429	221.9	3841	20,775	14.7	31.8	70.2	4962
	light hydrocarbons as a % of total									
	2-13	2-14	3-10	3-11	3-12	3-13	3-14	4-12	4-13	average
2007	10.6	15.3	5.6	6.6	8.9	13.2	8.4	43.4	396.9	7.82
2008	12.7	6.4	5.3	61.2	27.0	6.3	4853	273.3	671.7	11.9

Table 6.4 Light hydrocarbon concentrations in groundwater

The lighter hydrocarbon concentrations were approximately ½ the pre-treatment concentrations. However, the proportion of lighter hydrocarbons increased after treatment. This could be due to the relatively low solubility of the lighter hydrocarbons, or it could be a function of a relatively small sample size. Therefore, the total light hydrocarbon analysis is inconclusive.

As discussed above, the heavier compounds would be expected to make up a larger percentage of the source zone material after treatment and may dissolve into groundwater at a higher rate. TMB and naphthalene were analyzed in groundwater in addition to BTEX compounds; see Table 6.5 for results.

pre-treatment (2007)				
	1,3,5-TMB	1,2,4-TMB	1,2,3-TMB	Naphthalene
maximum concentration (µg/L)	467	1567	379	504
average concentration (µg/L)	31.8	113	25.1	31.7
multilevel discharge (mg/day)	26.9	92.6	21.1	24.9
open-screen discharge (mg/day)	6.35	21.0	5.05	6.28
post-treatment (2008)				
	1,3,5-TMB	1,2,4-TMB	1,2,3-TMB	Naphthalene
maximum concentration (µg/L)	708	2093	496	360
average concentration (µg/L)	31.1	90.0	23.0	12.6
multilevel discharge (mg/day)	40.15	118	29.4	14.8
open-screen discharge (mg/day)	0.383	0.982	0.30	0.11
% change from 2007 to 2008				
	1,3,5-TMB	1,2,4-TMB	1,2,3-TMB	Naphthalene
maximum concentration (µg/L)	52	34	31	-29
average concentration (µg/L)	-2	-20	-8	-60
multilevel discharge (mg/day)	49	28	39	-41
open-screen discharge (mg/day)	-94	-95	-94	-98

Table 6.5 TMB and naphthalene concentrations and mass discharges

Maximum concentrations and mass discharges generally increased for all TMB compounds and decreased for naphthalene. According to Montgomery (2000), naphthalene (0.012 mm Hg) has a lower vapor pressure than the TMB compounds (1-2 mm Hg), so it would be expected to remain in the source zone preferentially during air sparging and have an increased mass discharge compared to TMB. The lower post-treatment values for naphthalene are most likely due to its higher biodegradability, as the three TMB isomers are considered to be recalcitrant and have very low degradation rates in Borden materials (Chen et al., 2008).

As discussed in Section 6.3.3, the mass discharge determined from the open-screened wells in 2008 seems anomalously low, most likely due to dilution effects from a higher water table.

6.4 Long-Term Plume Impacts

The concentration and mass discharge changes noted in Section 6.3.3 and 6.3.4 may also result from long-term changes in plume composition.

6.4.1 Contaminant discharge

Mass discharge from five contaminants (benzene, toluene, 1,2,3-TMB, o-xylene, and ethanol) in the E10 gate have been determined in row 2 (Mocanu, 2007 and Augustine, 2007) since source emplacement. See Figure 6.3 for the benzene, toluene, TMB, and xylene trends. Note that ethanol is not included because it was not detected in any row 2 well starting in April 2005.

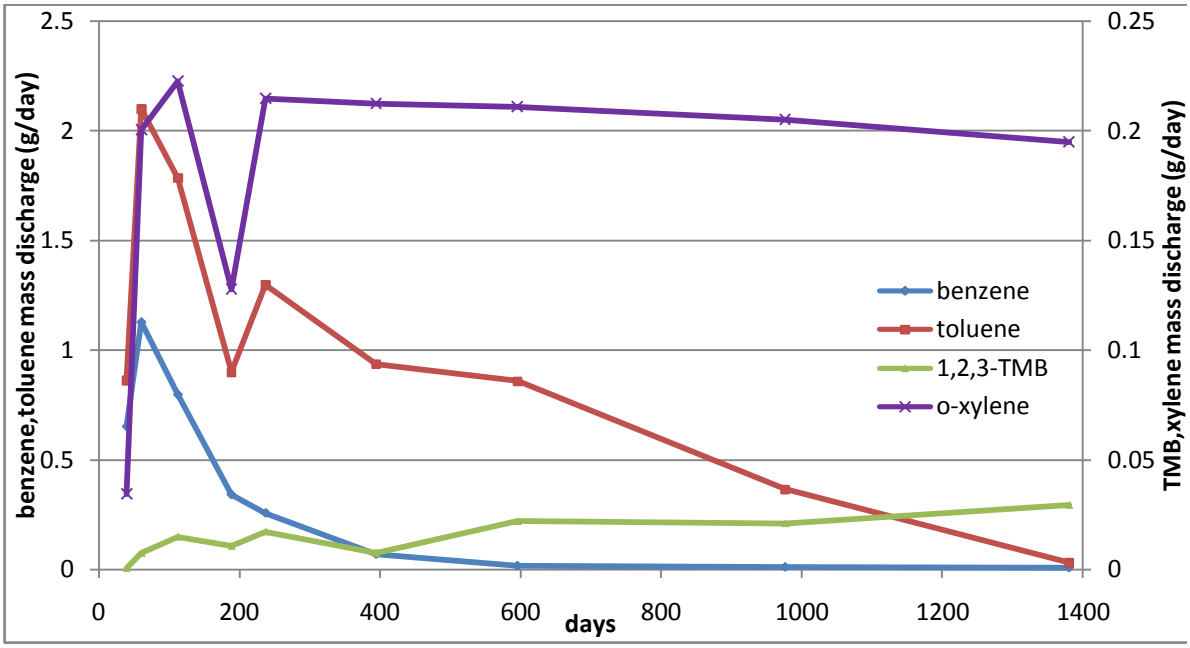

Figure 6.7 Long-term mass discharge of selected compounds

For Figure 6.7, note that the 2007 pre-treatment sampling round is approximately 980 days from source emplacement and the 2008 post-treatment sampling round is approximately 1400 days from source emplacement. The long-term trends for each compound help explain some of the differences between the pre- and post-treatment sampling discussed in Section 6.3.3 and 6.3.4.

The benzene data shows minimal change between the last two sampling rounds because most of the mass has already passed row 2. Raoult's law suggests that only minimal amounts of benzene remain in the source zone, as discussed in Section 2.6.1. Toluene concentrations also appear to be declining at the same rate as prior to 2007.

Treatment appears to have slightly decreased the o-xylene mass discharge at row 2, as the trend from 2007 is slightly steeper than that of the last several data points. O-xylene would require additional monitoring to determine if this decrease is statistically significant. Likewise, the 1,2,3-TMB mass discharge appears to have increased at a higher rate than would be otherwise expected.

6.4.2 Hydrocarbon ratios

The comparison of mass discharges in the previous section was inconclusive, so the ratios of the various compounds were compared as well to determine how the sparging may have affected the source zone. The multilevel mass discharge was used because it provides a single representative value for the plume for each hydrocarbon. The compounds analyzed in groundwater were the same as those used in Section 6.4.1. Benzene has the lowest mass discharge in the most recent sampling rounds, so the other compounds were compared to benzene. Results are shown in Figure 6.8.

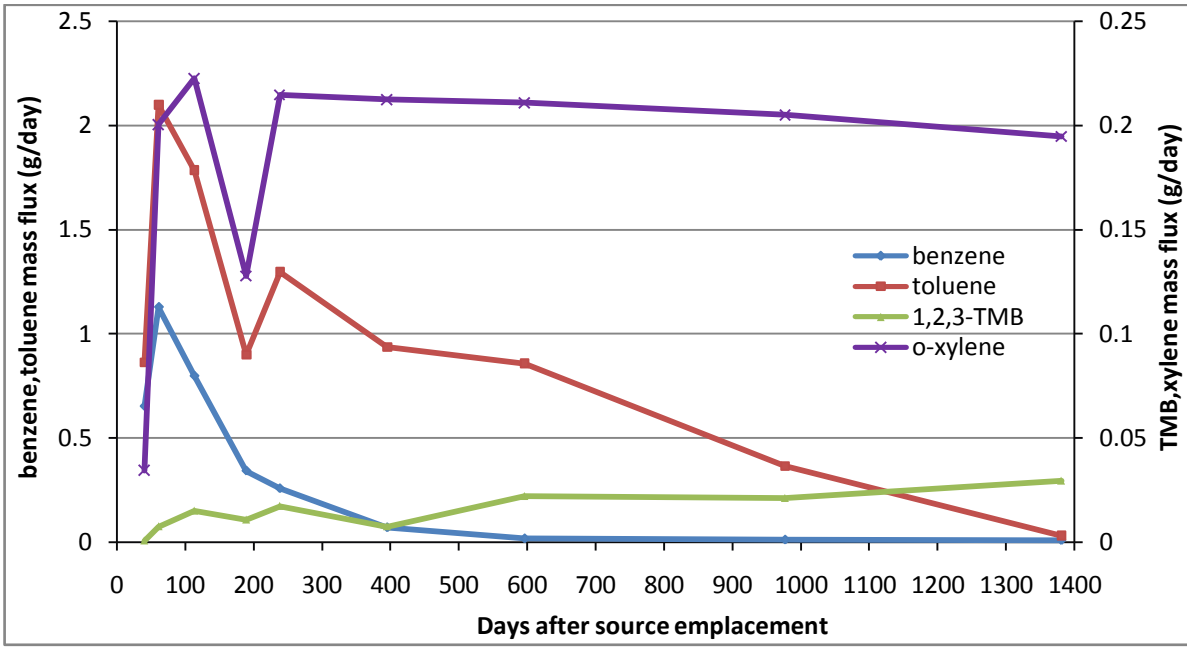

Figure 6.8 Long-term mass discharge ratios compared to benzene

Benzene is included (a 1:1 ratio for each time period) for comparison to the others. In this case, a comparison of the mass ratios doesn't appear to show any real difference between the post-treatment mass discharges and the earlier ones.

Chapter 7: Conclusions and Recommendations

The E10 source in the API gates at CFB Borden was remediated using air sparging coupled with an off-gas collection system. This project built on the results and used techniques developed from several studies in the Borden aquifer, especially those of Tomlinson et al. (2003), Nelson (2007), Fraser (2007), Mocanu (2007), and Yang (2008).

7.1 Conclusions

The air sparging system caused some perturbation of the groundwater in the immediate vicinity of the sparging points, as seen by groundwater mounding, water level changes recorded inside and outside the gas collection box, and groundwater temperature changes at the bottom of the piezometers within the box.

The most hydrocarbon mass was removed when sparging the central injection point (I-1). Both of the outer injection points became blocked; although I-2 was pumped and cleared of obstructions, the other point (I-3) never allowed sufficient air to remove much of the contaminant mass in that side of the source.

The hydrocarbon concentrations in the off-gas generally behaved as predicted by Raoult's law, with pentane concentrations peaking earlier than hexane concentrations. However, the BTEX concentrations in the off-gas remained much lower than both throughout treatment. Hydrocarbon removal rates were slower than initially predicted, and so the system was run for 98 hours of active sparging, three times longer than expected. However, the mass accumulation curves showed that sparging had reached the point of diminishing returns, with less than 10% more mass removal after sparging for twice as long.

Biodegradation rates were determined from off-gas CO_2 and O_2 concentrations. Off-gas CO_2 concentrations increased and O_2 concentrations decreased as expected for biodegradation, but did not follow a simple decay curve. The mass estimate of source removal using CO_2 was approximately 7 times the mass estimate using O_2.

The total mass removed via volatilization was 74 % (410 g) for pentane, 50 % (310 g) for hexane, 0.6 % (1.5 g) for toluene, 6.3 % (17 g) for ethylbenzene, 5.5 % (35 g) for p,m-xylene, 3.4 % (6.6 g) for o-xylene, and 21 % (4.6 kg) overall. The total mass removed via biodegradation was 22% (4.9 kg). Visual observations and measurements of the bubbles outside the box indicated that less than 0.2% of the off-gas was not collected. Tracer tests to corroborate this were inconclusive. The total mass removed via air sparging was estimated to be 45%.

Groundwater samples were taken when the most-aerated water would have passed through the monitoring fence. The average BTEX concentration after sparging was 40% of the pre-sparging concentration, with a 27% decrease in the benzene mass discharge, a 92% decrease in the toluene mass discharge, a 65% decrease in the ethylbenzene mass discharge, a 6% decrease in the p/m-xylene mass discharge, and a 5% decrease in the o-xylene mass discharge. The mass discharge for the less-volatile hydrocarbons increased 19% overall, as expected. However, the hydrocarbon mass discharge changes in groundwater before and after treatment did not vary enough from long-term rates to determine how much of a long-term effect the sparging had.

7.2 Recommendations

- Groundwater sampling should be continued at row 2 to determine if the post-treatment concentration trends continue. This should include SF_6 for at least one more round. Groundwater samples should be considered in high- and low-water table conditions to see if dilution impacts hydrocarbon concentrations more in the fully-screened wells.

- Source zone cores should be considered to determine how much of the source mass has been removed. If cores are collected, respiration tests are suggested to help constrain biodegradation rates.

- The sealed-box method of collecting soil gas appears to be an effective way to collect off-gas from relatively small sources with saturated soils. However, there was no way to differentiate flow rates or hydrocarbon concentrations from different areas using this method. If the support walls were to be sealed and extended below ground surface like the outer walls, the mass discharge from different areas could be quantified.

- The cumulative mass removal showed that the system was removing less and less of the source mass as treatment continued, yet slightly less than half of the mass was removed. Suggested ways to increase mass removal include increasing the flow rate, either by using a larger blower or putting the blower closer to the source zone; running multiple wells at the same time; and installing an additional well in the area of I-2, which added a relatively small amount of air to the subsurface.

References

Aelion, C. M. and Kirtland, B. C. 2000. Physical versus biological hydrocarbon removal during air sparging and soil vapor extraction. Environ. Sci. Technol. 34 (15): 3167-3173.

Aelion, C. M., Kirtland, B. C., and Stone, P. A. 1997. Radiocarbon assessment of aerobic petroleum bioremediation in the vadose zone and groundwater at an AS/SVE site. Environ. Sci. Technol. 31 (12): 3363-3370.

Ahlfeld, D. P., Dahmani, A., and Ji, W. 1994. A conceptual model of field behavior of air sparging and its implications for applications. Ground Water Mon. Remed. 14: 132–139.

Aronson, D. and Howard, P. H., 1997. Anaerobic biodegradation of organic chemicals in groundwater: a summary of field and laboratory studies: Final Report. Environmental Science Center Syracuse Research Corporation, North Syracuse, NY. November 12.

Augustine, D. 2007. Evidence for the impact of ethanol on BTEX persistence in a controlled field experiment at CFB Borden. B Sc thesis, University of Waterloo.

Baker, R. J., Baehr, A.L, and Lahvis, M. A. 2000. Estimation of hydrocarbon biodegradation rates in gasoline-contaminated sediment from measured respiration rates. J. Contam. Hydrol. 41: 175-192.

Barcelona, M. J. and Holm, T. R. 1991. Oxidation-reduction capacities of aquifer solids. Environ. Sci. Technol. 25, (9): 1565-1572.

Bass, D. H., Hastings, N. A., and Brown, R. A. 2000. Performance of air sparging systems: a review of case studies. J. Hazard. Mat. 72: 101–119.

Benner, M. L., Mohtar, R. H., and Lee, L. S. 2002. Factors affecting air sparging remediation systems using field data and numerical simulations. J. Hazard. Mat. 95 (3): 305-329.

Blackmer, a Dover Company. 1971. Vacuum limitations on Blackmer pumps. February. From http://www.blackmer.com/myapp/pdf/bul50.pdf

Bouwer, H. and Rice, R. C. 1976. A slug test for determining hydraulic conductivity of unconfined aquifers with completely or partially penetrating wells. Water Resour. Res. 12 (3): 423-428.

Brassington, K. J., Hough, R. L., Paton, G. I., Semple, K. T., Risdon, G. C., Crossley, J., Hay, I., Askari, K. and Pollard, S. J. T. 2007. Weathered hydrocarbon wastes: a risk management primer. Crit. Rev. Environ. Sci. Technol. 37 (3): 199-232

Brown, R. A., Hicks, R. J., and Hicks, P. M. 1994. Use of air sparging for in situ bioremediation. In: Hinchee, R. E., ed, Air Sparging for Site Remediation. CRC Press, Boca Raton, Florida. p. 38-55.

Bruce, C. L., Amerson, I. L., Johnson, R. L. and Johnson, P.C. 2001. Use of an SF_6-based diagnostic tool for assessing air distributions and oxygen transfer rates during IAS operation. Biorem. J. 5 (4): 337-347.

Bullister, J. L., Wisegarver, D. P., Menzia, F. A. 2002. The solubility of sulfur hexafluoride in water and seawater. Deep-Sea Research. Part I, Oceanographic research papers. 49 (1): 175–187.

Chapman, S. W., Bryerley, B. T., Smyth, D. J. A., and Mackay, D. M. 1997. A pilot test of passive oxygen release for enhancement of in situ bioremediation of BTEX-contaminated ground water. Ground Water Mon. Remed. 17, (2): 93-105.

Chatten, S. 2008. Personal communication. schatten@sciborg.uwaterloo.ca

Chen, Y. D., Barker, J. F., and Gui, L. 2008. A strategy for aromatic hydrocarbon bioremediation under anaerobic conditions and the impacts of ethanol: A microcosm study. J. Contam. Hydrol. 96: 17-31.

Cho, J. S., GiGiulio, D. C., Wilson, J. T., and Vardy, J. A. 1997. In situ air injection, soil vacuum extraction and enhanced biodegradation: a case study in a JP-4 jet fuel contaminated site. Envir. Progress. 16: 35–42

Devlin, J. F. and Barbaro, J. R. 2001. A method of estimating multicomponent nonaqueous-phase liquid mass in porous media using aqueous concentration ratios. Environ. Toxicol. Chem. 20 (11): 2443-2449.

Feenstra, S., Mackay, D. M. and Cherry, J. A. 1991. A method for assessing residual NAPL based on organic chemical concentrations in soil samples. Ground Water Mon. Remed. (11): 128-136.

Flynn, D. J. 1994. Soil vacuum extraction to remove residual and pools of perchloroethylene from a heterogeneous sand aquifer: a field trial. MASc Thesis, Department of Civil Engineering, University of Waterloo, Ontario, Canada.

Fraser, M. J. 2007. Long-term fate of an emplaced coal tar creosote source. MSc Thesis, Department of Earth Sciences, University of Waterloo, Ontario, Canada.

Freeze, R. A and Cherry, J. A. 1979. Groundwater. Prentice Hall, Englewood Cliffs, New Jersey.

Frind, E. O., Molson, J. W., Schirmer, M., and Guiguer, N. 1999. Dissolution and mass transfer of multiple organics under field conditions: the Borden emplaced source. Water Resour. Res. 35: 683-694.

Gallant, R. W. and Railey, J. M. 1984. Physical Properties of Hydrocarbons. 2nd ed. Gulf Publishing Co., Houston, Texas.

Greenwood, R., Mills, G., and Vrana, B. 2007. Passive Sampling Techniques in Environmental Monitoring. Elsevier, p 285.

Heath, J. S., Koblis, K., Sager, S. L., and Day, C. 1993. Risk assessment for total petroleum hydrocarbons. In Calabrese, E. J., and Kostecki, P. T. (eds.). Hydrocarbon Contaminated Soils - Volume III.. CRC Press, Boca Raton, FL. p. 267-301.

Hinchee, R. E., Downey, D. C., Dupont, R. R., Aggarwal, P. K., and Miller, R. N. 1991. Enhancing biodegradation of petroleum hydrocarbons through soil venting. J. Hazard. Mat. 27: 315-325.

Hohener, P., Duwig, C., Pasteris, G., Kaufmann, K., Dakhel, N., and Harms, H. 2003. Biodegradation of petroleum hydrocarbon vapors: laboratory studies on rates and kinetics in unsaturated alluvial sand. J. Contam. Hydrol. 66: 93–115.

Jellali, S., Benremita, H., Muntzer, P, Razakarisoa, O., and Shäfer, G. 2003. A large-scale experiment on mass transfer of trichloroethylene from the unsaturated zone of a sandy aquifer to its interfaces. J. Contam. Hydrol. 60: 31-53.

Ji, W., Dahmani, A., Ahlfeld, D., Lin, J.D. and Hill, E. 1993. Laboratory study of air sparging: air flow visualization. Ground Water Mon. Remed. 23(4): 115-126.

Johnson, C.D., Rayner, J. L., Patterson, B. M., and Davis, G. B. 1998. Volatilisation and biodegradation during air sparging of dissolved BTEX-contaminated groundwater J. Contam. Hydrol. 33: 377-404.

Johnson, P. C. 1998. Assessment of the contributions of volatilization and biodegradation to in situ air sparging performance. Environ. Sci. Technol. 32, (2): 276-281.

Johnson, R. L., Johnson, P. C., Amerson, I. L., Johnson, T. L., Bruce, C. L., Leeson, A., and Vogel, C. M. 2001A. Diagnostic tools for integrated in situ air sparging pilot tests. Biorem. J. 5 (4): 283-298.

Johnson, R. L., Johnson, P. C., Johnson, T. L., Thomson, N. R., and Leeson, A. 2001B. Diagnosis of in situ air sparging performance using transient groundwater pressure changes during startup and shutdown. Biorem. J. 5 (4): 299-320.

Johnson, R. L., Johnson, P. C., Johnson, T. L. and Leeson, A. 2001C. Helium tracer tests for assessing contaminant vapor recovery and air distribution during in situ air sparging. Biorem. J. 5 (4): 321-336.

Johnson , P.C., Johnson R. L., Bruce C. L., and Leeson, A. 2001D. Advances in in situ air sparging/biosparging. Biorem. J. 5 (4): 251-256.

King, M. W. G. and Barker, J. F. 1999. Migration and natural fate of a coal tar creosote plume. J. Contam. Hydrol. 39 (3-4): 249-279.

Kirtland, B. C. and Aelion, C. M. 2000. Petroleum mass removal from low permeability sediment using air sparging/soil vapor extraction: impact of continuous or pulsed operation. J. Contam. Hydrol. 41: 367-383.

Kirtland, B. C., Aelion, C. M., and Widdowson, M. A. 2001. Long-term AS/SVE for petroleum removal in low-permeability Piedmont saprolite. J. Environ. Engineering. 127 (2): 134-144.

Lide, D. R., ed. 2008. CRC Handbook of Chemistry and Physics, 88th ed. CRC Press/Taylor and Francis, Boca Raton, Florida.

Mackay, D., Freyberg, D. L, Roberts, P. V., and Cherry, J. A. 1986. A natural gradient experiment on solute transport in a sand aquifer. Approach and overview of plume movement. Water Resour. Res. 26, 13:2017-2029.

Martin, H., Patterson, B. M., Davis, G. B., and Grathwohl, P. 2003. Field trial of contaminant groundwater monitoring: comparing time-integrating ceramic dosimeters and conventional water sampling. Environ. Sci. Technol. 37: 1360-1364.

Mocanu, M. T. 2007. Behaviour of oxygenates and aromatic hydrocarbons in groundwater from gasoline residuals. MSc Thesis, Department of Earth Sciences, University of Waterloo, Ontario, Canada.

Montgomery, J. H. 2000. Groundwater Chemicals Desk Reference, 3rd ed. CRC Press, Boca Raton, Florida.

National Research Council (NRC), 2004. Committee on Source Removal of Contaminants in the Subsurface. Contaminants in the Subsurface: Source Zone Assessment and Remediation. National Academies Press, Washington, DC.

Nelson, N. C. 2007. Field trial of residual LNAPL recovery using CO_2-supersaturated water injection in the Borden aquifer. MSc Thesis, Department of Earth Sciences, University of Waterloo, Ontario, Canada.

Ontario Ministry of Environment and Energy Standards Development Branch (MOE). 1996. Guidance on Sampling and Analytical Methods for Use at Contaminated Sites in Ontario, version 1.1. December.

Rae Systems, 2008A. Application Note AN-100: RAE Systems Training Outline. Revision 2. from http://www.raesystems.com/~raedocs/App_Tech_Notes/App_Notes/AP-000_PID_Training_Outline.pdf

Rae Systems, 2008B. Technical Note TN-106: Correction Factors, Ionization Energies, and Calibration Characteristics. Revision 15. from http://www.raesystems.com/AppTech_Notes/TN

Rogers, S. W. Ong, S. K., Stenback, G. A., Golchin, J., and Kjartanson, B. H. 2007. Assessment of intrinsic bioremediation of a coal-tar-affected aquifer using two-dimensional reactive transport and biogeochemical mass balance approaches. Water Environ. Research. 79 (13): 13-28.

Ruzicka, V., Zabransky, M., Ruzicka, K., and Majer, V. 1994. Vapor pressures for a group of high-boiling alkylbenzenes under environmental conditions. Thermochimica Acta. 245:121-144.

Spargo, B. 1999. Naval Research Laboratory (NRL), Washington, D.C. Groundwater Circulating Well Technology Assessment. Document no. NRL/PU/6115-99-384. May.

Sudicky, E. A., Cherry, J. A., and Frind, E. O. 1983. Migration of contaminants in groundwater at a landfill: a case study. A natural-gradient dispersion test. J. Hydrol. 63: 81-108.

Tillman, F. D., Choi, J. W., and Smith, J. A. 2003. A comparison of direct measurement and model simulation of total discharge of volatile organic compounds from the subsurface to the atmosphere under natural field conditions. Water Resour. Res. 39 (10): 1284-1295.

Tomlinson, D. W., Thomson, N. R., Johnson, R. L., and Redman, J. D. 2003. Air distribution in the Borden aquifer during in situ air sparging. J. Contam. Hydrol. 67: 113-132.

U.S. Army Corps of Engineers (ACOE). 1997. Engineering and Design: In-Situ Air Sparging. Document number EM 1110-1-4005. 15 September.

U. S. Army Corps of Engineers (ACOE). 2002. Engineering and Design: Soil Vapor Extraction and Bioventing. Document number EM 1110-1-4001, June 3.

U.S. Environmental Protection Agency (EPA). 1992. RCRA Ground-Water Monitoring: Draft Technical Guidance. November. http://www.epa.gov/reg3wcmd/ca/pdf/Rcra_gwm92.pdf

U.S. Environmental Protection Agency (EPA). 2007. Treatment Technologies for Site Cleanup: Annual Status Report (Twelfth Edition). Document no. EPA-542-R-07-012. September.

U.S. Environmental Protection Agency (EPA). 2008. National Primary Drinking Water Regulations; organic chemicals. From http://www.epa.gov/safewater/contaminants/index.html

VanderGriendt, M. R. 2008. Personal communication. mrvander@sciborg.uwaterloo.ca

Yalkowski, S. H. and He, Y., ed. 2003. Handbook for Aqueous Solubility. CRC Press, Boca Raton, Florida.

Yang, T. 2008. Investigation of residual gasoline in the GMT and E10 sources in Borden aquifer. MSc Thesis, Department of Earth Sciences, University of Waterloo, Ontario, Canada.

Yang, X., Beckmann, D., Fiorenza, S., and Niedermeier, C., 2005. Field study of pulsed air sparging for remediation of petroleum hydrocarbon contaminated soil and groundwater. Environ. Sci. Technol. 39: 7279-7286.

Yaws, C. L. 1984. Handbook on Vapor Pressure, vol. 2. 2nd ed. Gulf Publishing Co., Houston, Texas.

Appendices

Appendix A: Initial treatment system and upgrades

A.1 Initial treatment system

The treatment system used to remediate the source zone is described in detail in Section 3.3. The SVE design was changed substantially after the initial sparging test in January 2008. The first SVE system is described in detail here. Figure A.1 and Figure A.2 show the system configuration schematic in plan view; Figure A.3 shows the SVE system connections; and Figure A.4 and Figure A.5 are pictures of the system during and post-construction, respectively.

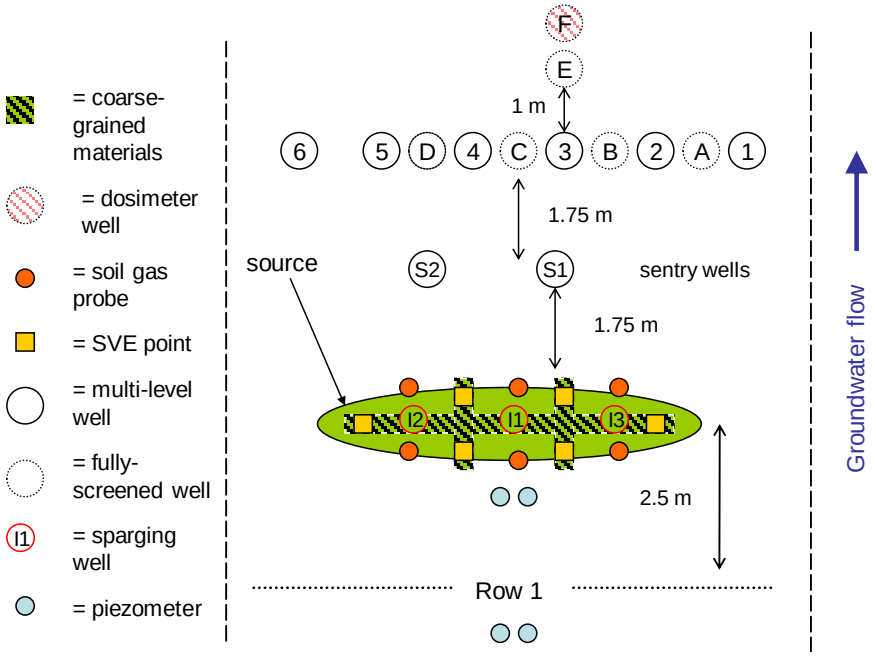

Figure A.1 Treatment system schematic with trench containing coarser material.

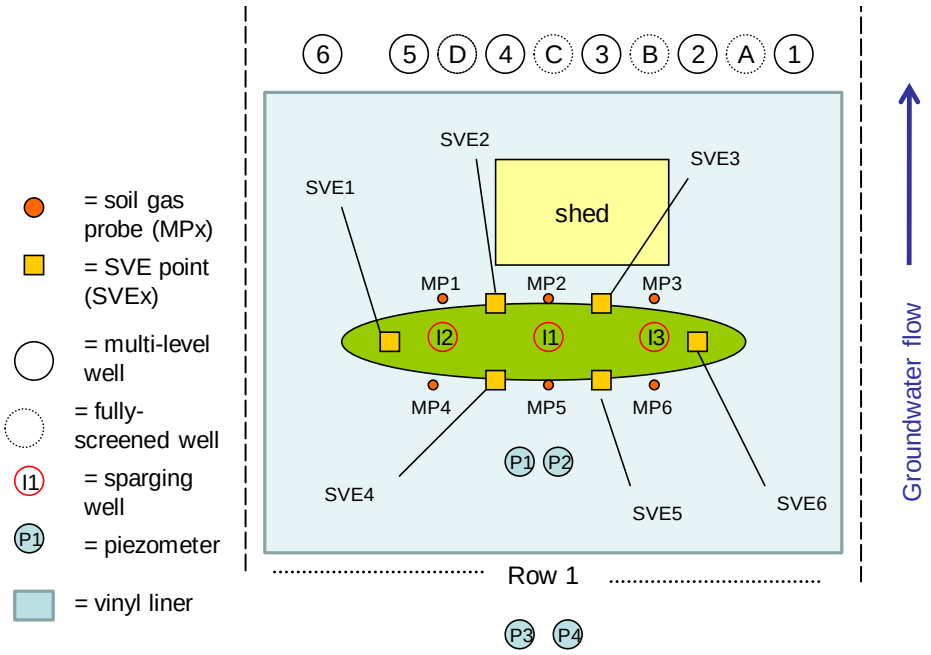

Figure A.2 Treatment system schematic for other remedial system components and location IDs

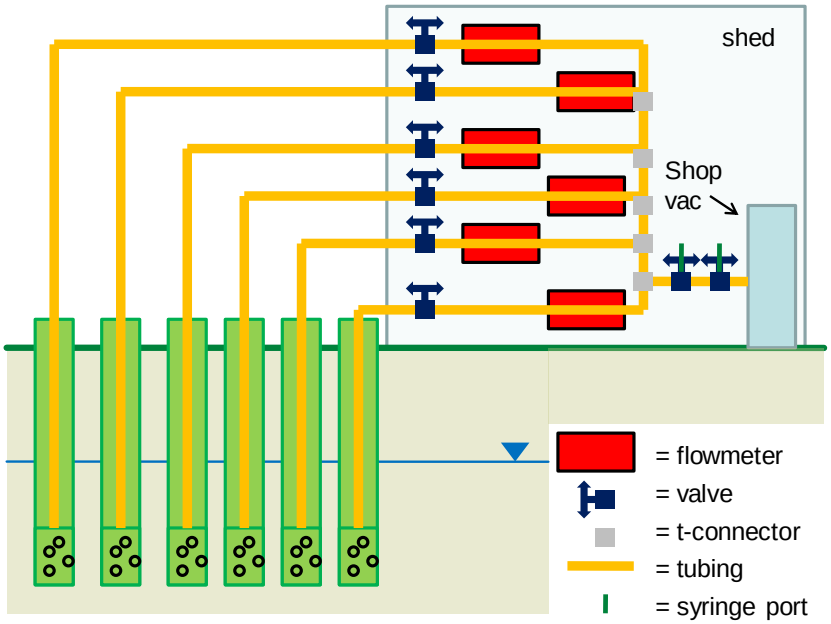

Figure A.3 Original SVE configuration

A pilot test was performed near the test cell to determine the SVE wells' radius of influence. The pilot test consisted of a number of soil gas probes located at varying distances from the extraction point. The soil gas probes were similar to those used by Flynn (1994), with 3 mm ID stainless steel tubing with a drive

point and soil gas sample inlets within the first 5 cm of the drive point. The extraction point had the same construction as the air sparging well (see Section 3.3 for details). The top of the soil probe had a rubber membrane that was pierced by a hand-held pressure transducer with a needle tip. A shop vac was used to exert a vacuum on the extraction point. The soil gas probes were placed at 0.2 m, 0.4 m, 0.8 m, and 1.2 m from the extraction point. In order to ensure that any pressure changes were due to the influence of the extraction point and not other pressure fluctuations, the target pressure change was 1 mbar instead of 0.25 mbar as suggested by the ACOE (2002).

The pilot test was inconclusive, with responses within the apparent range of atmospheric fluctuations. However, the pilot test was not conducted under a sealed surface as planned for the actual experiment. Therefore, the lack of pressure change in the observation wells was most likely due to air leakage (and therefore loss of pressure) around the tip of the soil probe.

Pilot test aside, the radius of influence is problematic as a measure of how far apart extraction wells should be. It indicates the existence of a pressure gradient toward the extraction well, or the potential for air to move in that direction. However, it does not indicate the speed of air flow. In addition, the standard measure of vacuum generally considered as an indicator of extraction well influence (0.25 mbar) can be easily overwhelmed by barometric or groundwater level changes greater than 1 mbar. The ACOE (2002) suggests using pore gas velocity to determine treatment time using SVE. However, for this study the SVE system is being used only as a soil gas containment method and not for soil remediation.

Based on this and the pilot test results, the maximum number of SVE points (6) considered was ultimately used for the treatment system. These points were placed around the source zone, with one on either side of the source and two points each upgradient and downgradient of the source. Refer to Figure 3.2 and Figure 3.3 for details. The SVE points were constrained vertically by the shallow depth to water; Brown et al. (1994) suggest that the desired depth to water should be at least 1.5 m (5 feet), while the depth to water at Borden varies seasonally from 1.5 m bgs to the ground surface. In order to minimize the capillary fringe and increase the effectiveness of the SVE system, a 20 cm trench was dug through the center of the source area and filled with gravel. “Arms” were added to the trench to reach all of the SVE points. Once installed, the SVE points were backfilled with clean coarse sand to keep them upright.

Six passive soil vapor monitoring probes were also installed to determine the lateral variation of soil vapors across the source zone. The passive monitoring probes were the same ones that were used in the radius of influence pilot test.

Figure A.4 Trench and piezometer setup prior to injection, SVE, and soil monitoring point installation.

Figure A.5 Treatment system setup with vinyl (snow-covered) on ground surface

A.2 Changes made after first sparging round

The first air sparging test was conducted on January 21, 2008, with an initial water level of 0.7 m bgs. After several minutes of SVE system operation began, water appeared in the SVE3 flowmeter, which was shut off for the rest of the test. The other SVE points were set at the flow rate established in the sampling plan. Approximately 5 minutes after starting air sparging, the water level was pushed up approximately 0.4 m, into the SVE intakes. Once water got into the flowmeters, flow estimates were impossible to determine. It was decided to pull up the SVE points so that the screens were moved from 0.5 m below ground surface (bgs) to 0.1 m bgs. The discrete air sampling points (MP1 through MP6) also had problems with water entering the screens and were also moved so that their sample ports were located at 0.15 m bgs, at the same depth as the midpoint of the SVE intake screens. However, groundwater levels increased during and after snowmelt, so the multiple SVE intake points were replaced with a single exhaust port in the center of the new off-gas collection box, which was positioned approximately 0.5 m from the central air sparging point. The discrete measuring points MP1-MP6 were expected to be underwater and were removed.

The PID sample port was originally placed between the vacuum source (a shop vac) and the manifold where all the SVE lines came together. It was added to this location so that it sampled the total mass of VOCs leaving the source and was next to the syringe sampling port for the lab samples. The lab samples

were taken from here because at this point, the air had only contacted the inside of the Teflon tubing and the flowmeters, minimizing cross-contamination. However, the PID was unable to draw in air because the internal pump for the instrument could not overcome the 8.5 ft^3/min force of the vacuum. The solution for this was to add a thin piece of tubing to the exhaust hose just after the vacuum, and run this tubing to the PID inlet. A potential problem is that the PID is no longer next to the sample port, and could be theoretically contaminated by the ordinary vacuum hose and the shop vac that the air flows through before reaching the tubing. Therefore, additional lab samples were planned to be collected from the PID sample port to compare with the "regular" sample port. The helium detector most likely would have the same problem as the PID, although the test was terminated prior to sampling the outlet for helium. As the helium detector is intended to take point samples, it was planned to use the same inlet port as the PID, recognizing that this would cause a temporary and very small loss in PID data (2 or 3 points at a time on a 10 second sample interval).

The other problem with the test setup was with the tracer delivery system. The helium and SF_6 gas lines were routed through separate flow meters, then combined into one delivery line that fed into the main air line from the compressor. The plan was to operate the flowmeters at as low a flow rate as possible so that they could be increased later. However, because these lines came together before the trunk line, pressure differences caused one to cut off the other. The flowmeters had been selected with the idea that only low flow rates would be used. However, these pressure differences caused excessive fluctuations of the balls in the flowmeters, causing them to get stuck in the top of the meters. The only way to knock the balls loose was to stop air flow and tap the meters with a hammer several times. Stopping air flow meant that the system had to be re-started again, and the end result was that the tracers were not added to the system before it was shut down by the water in the SVE points. Based on this experiment, the tracer gas delivery system was adjusted in two ways: the SF_6 was removed so that only one gas was bled in at a time; and a larger flowmeter was added. For the SF_6 tracer tests, the helium tank was replaced with a SF_6 tank, as these tests were not performed at the same time.

Once sparging began, air short-circuited to the closest open-screened wells (well C and to a lesser extent well D in row 2), causing aerated water to spill over the well casing at a rate estimated at several L/min for well C. This was addressed with a later iteration of the remediation plan whereby the wells in rows 1 and 2 were covered and included in the SVE area.

Appendix B: Daily Results

B.1 Water Level, Temperature, PID and GC Concentrations

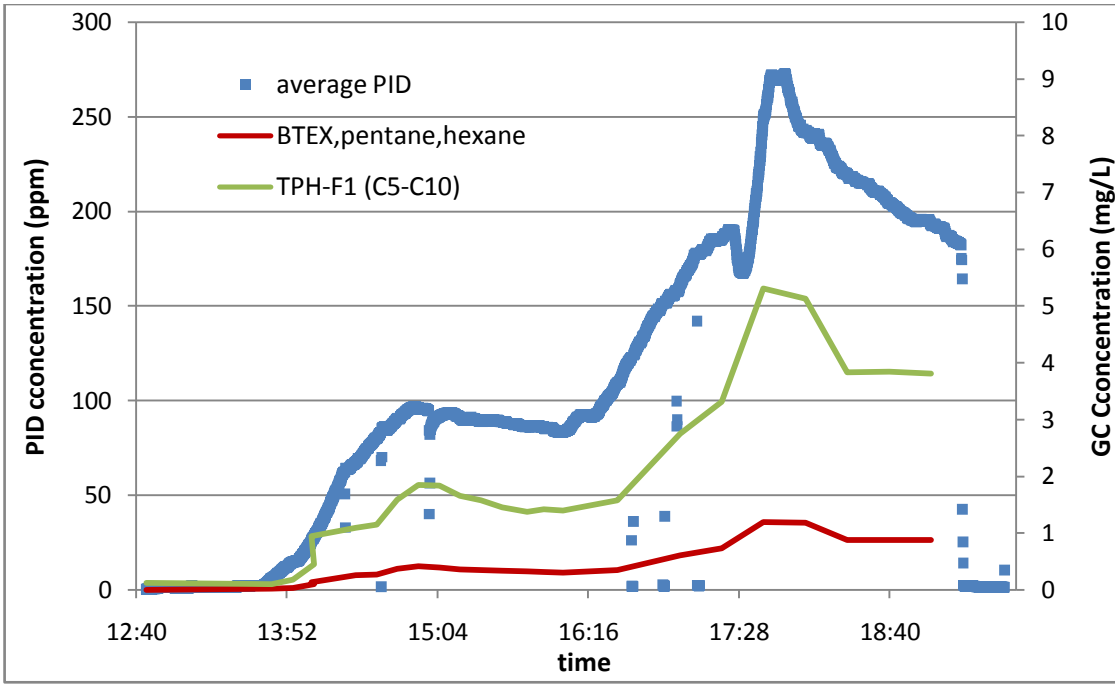

Figure B.1 April 28 PID/TPH

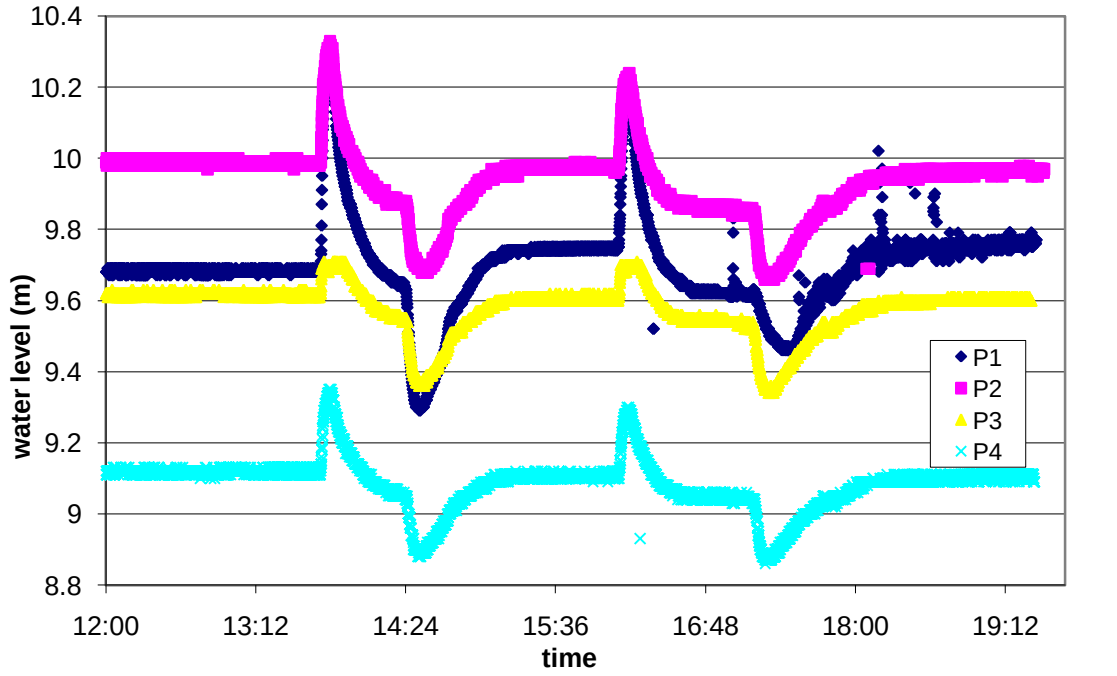

Figure B.2 April 28 water level

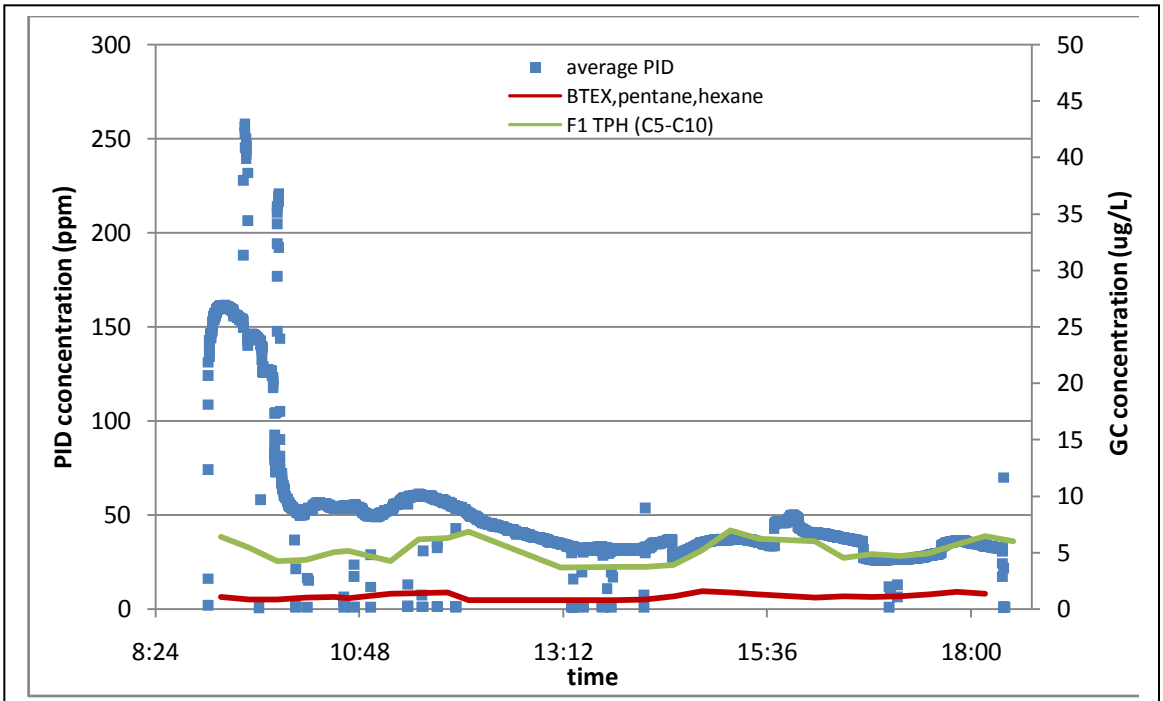

Figure B.3 April 29 PID/TPH

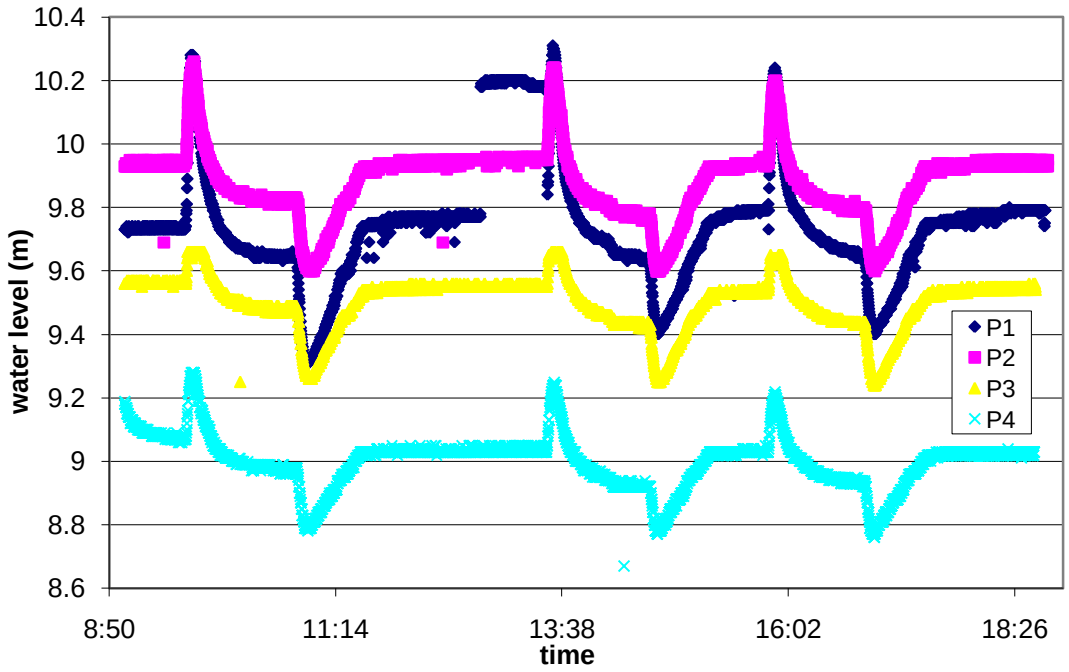

Figure B.4 April 29 water level

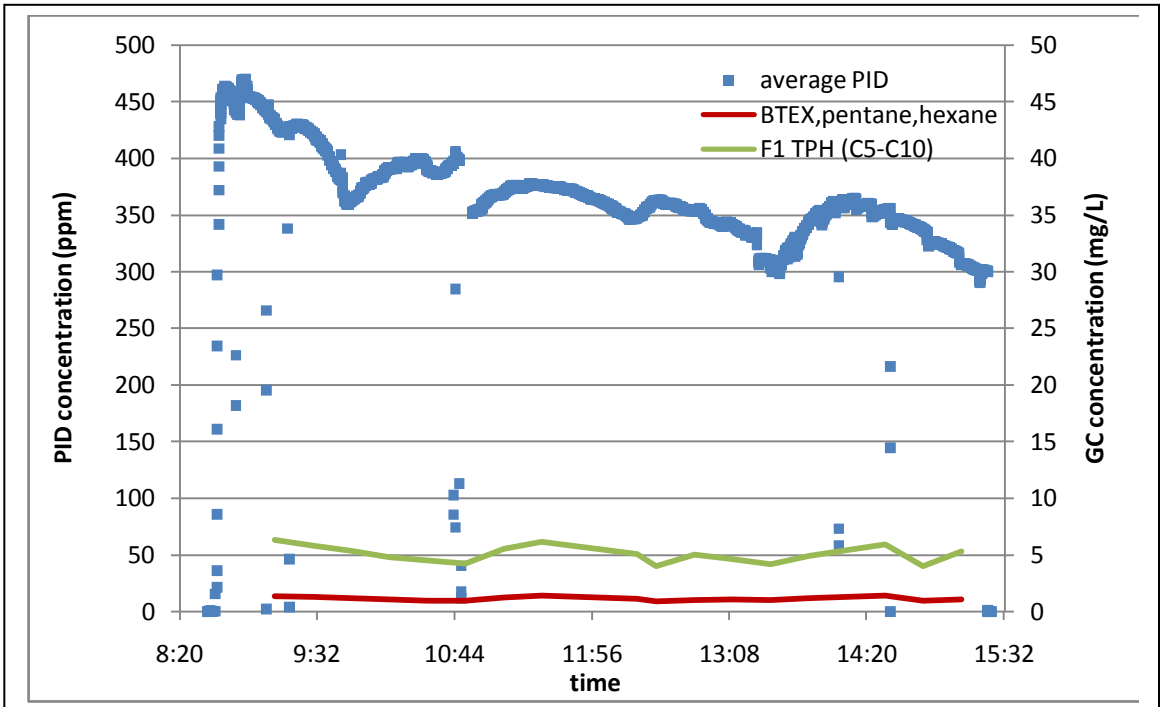

Figure B.5 April 30 PID/TPH

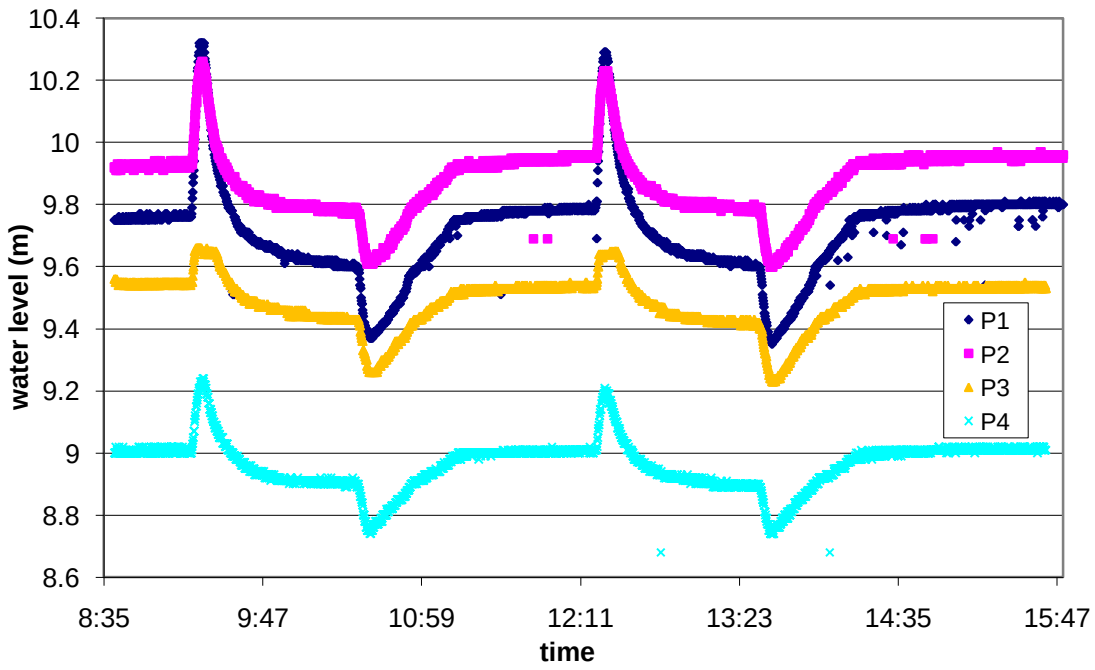

Figure B.6 April 30 water level

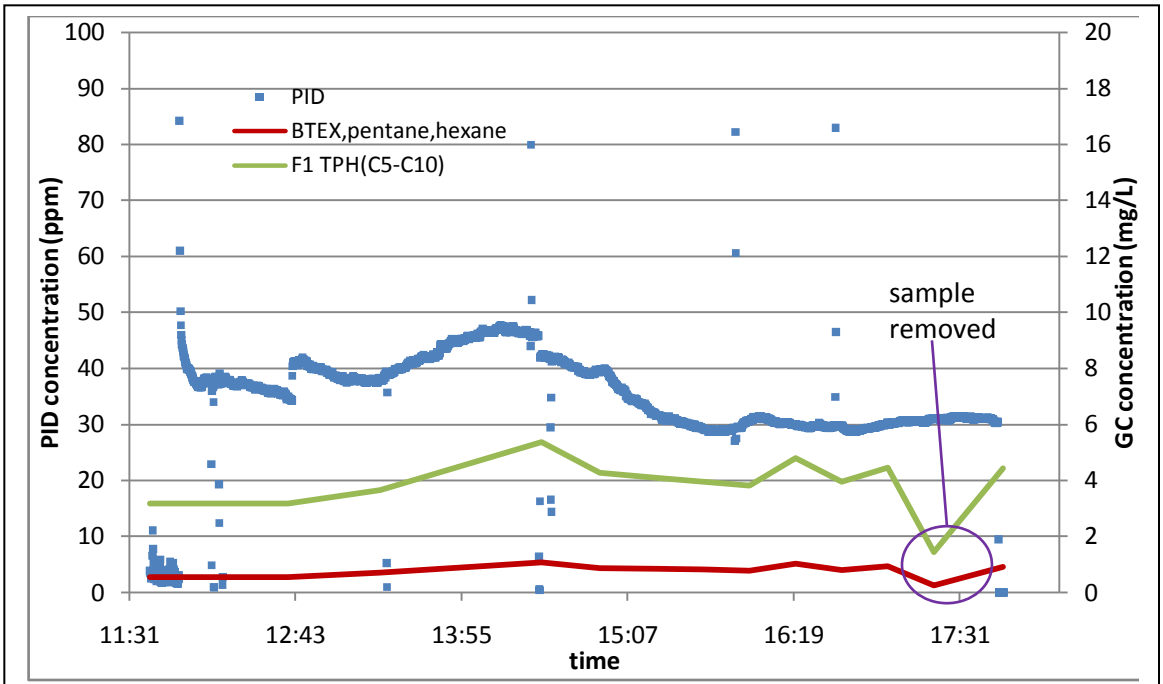

Figure B.7 May 4 PID/TPH

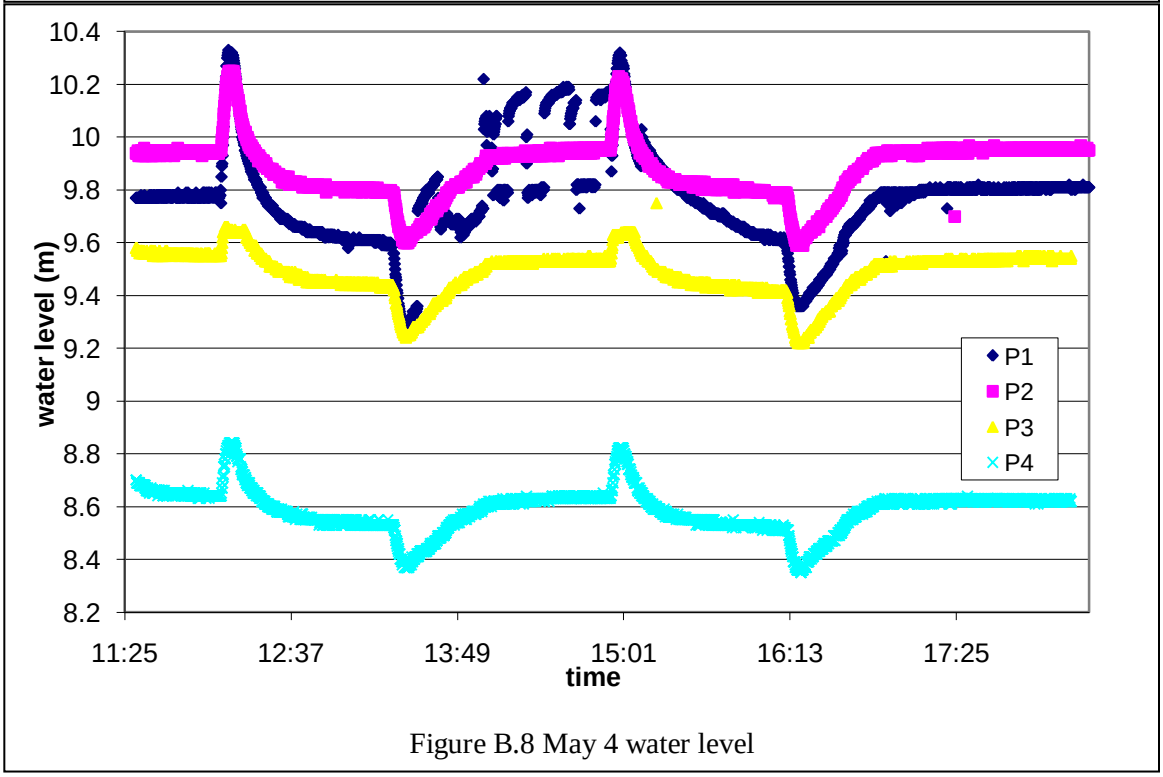

Figure B.8 May 4 water level

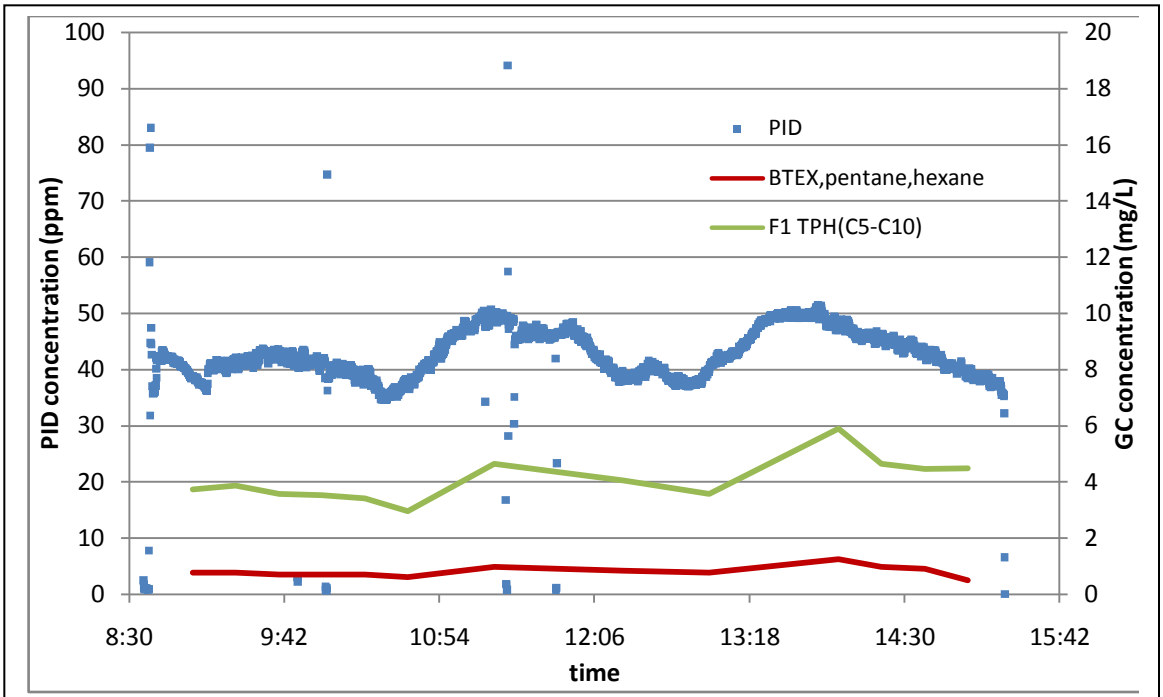

Figure B.9 May 5 PID/TPH

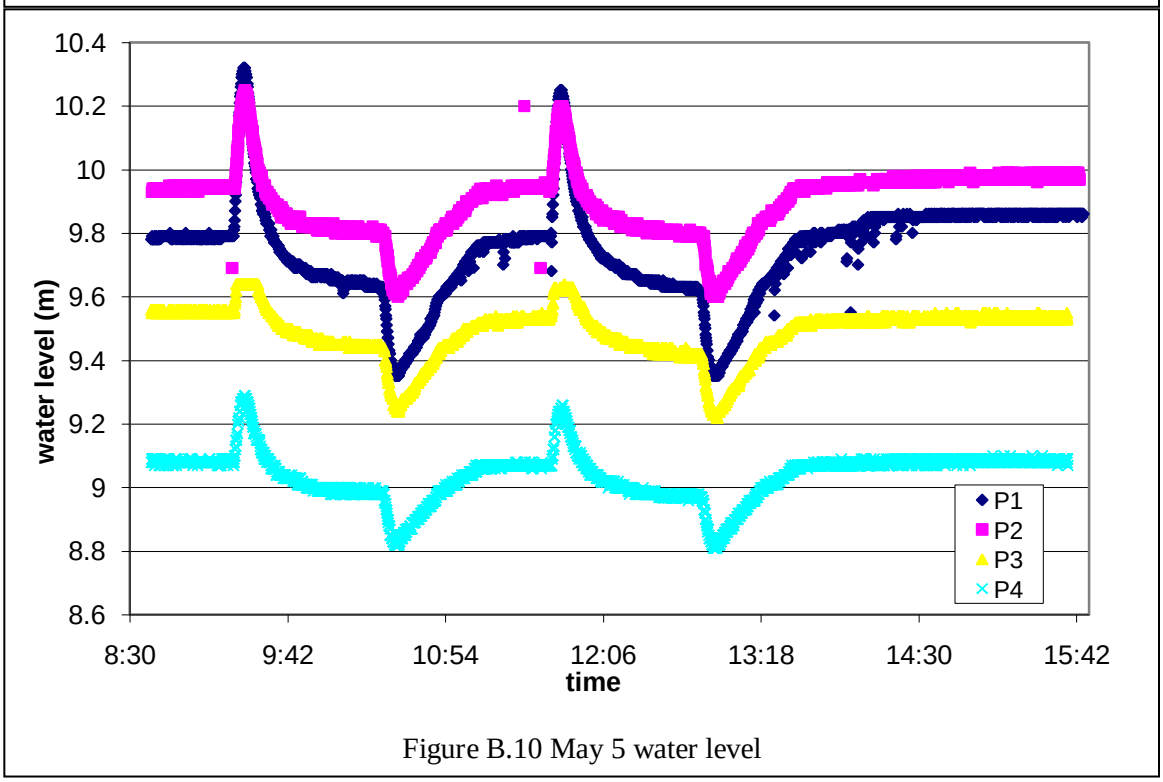

Figure B.10 May 5 water level

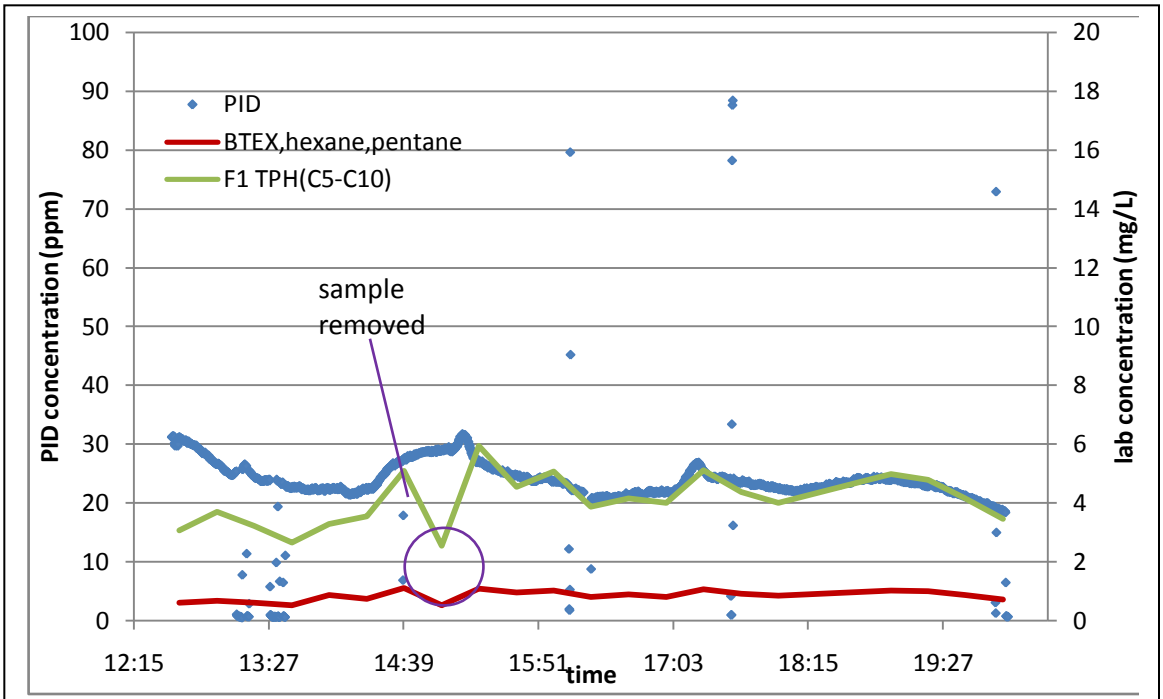

Figure B.11 May 8 PID/TPH

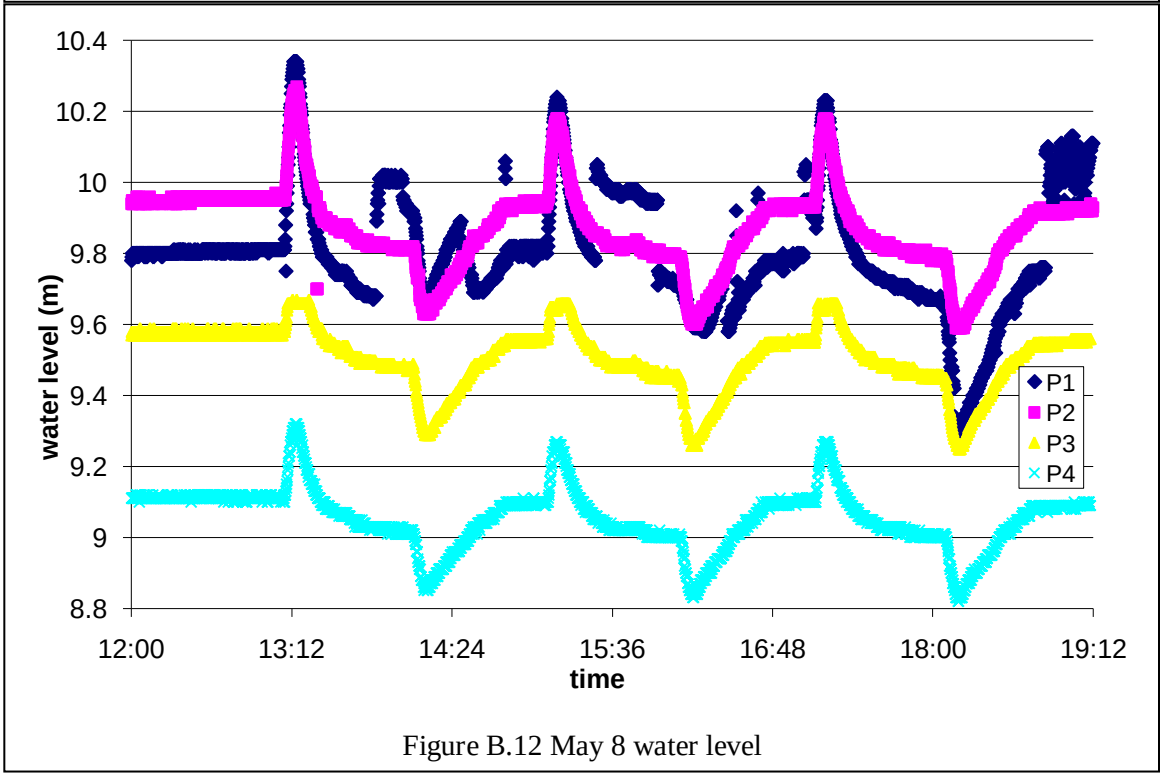

Figure B.12 May 8 water level

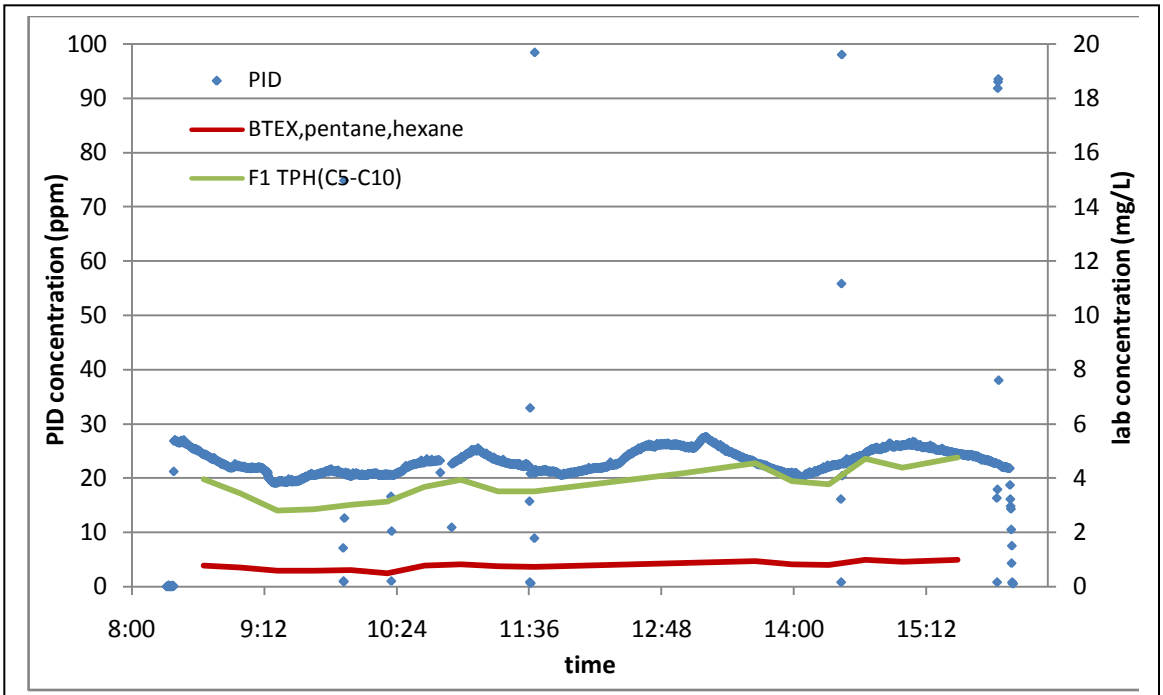

Figure B.13 May 9 PID/TPH

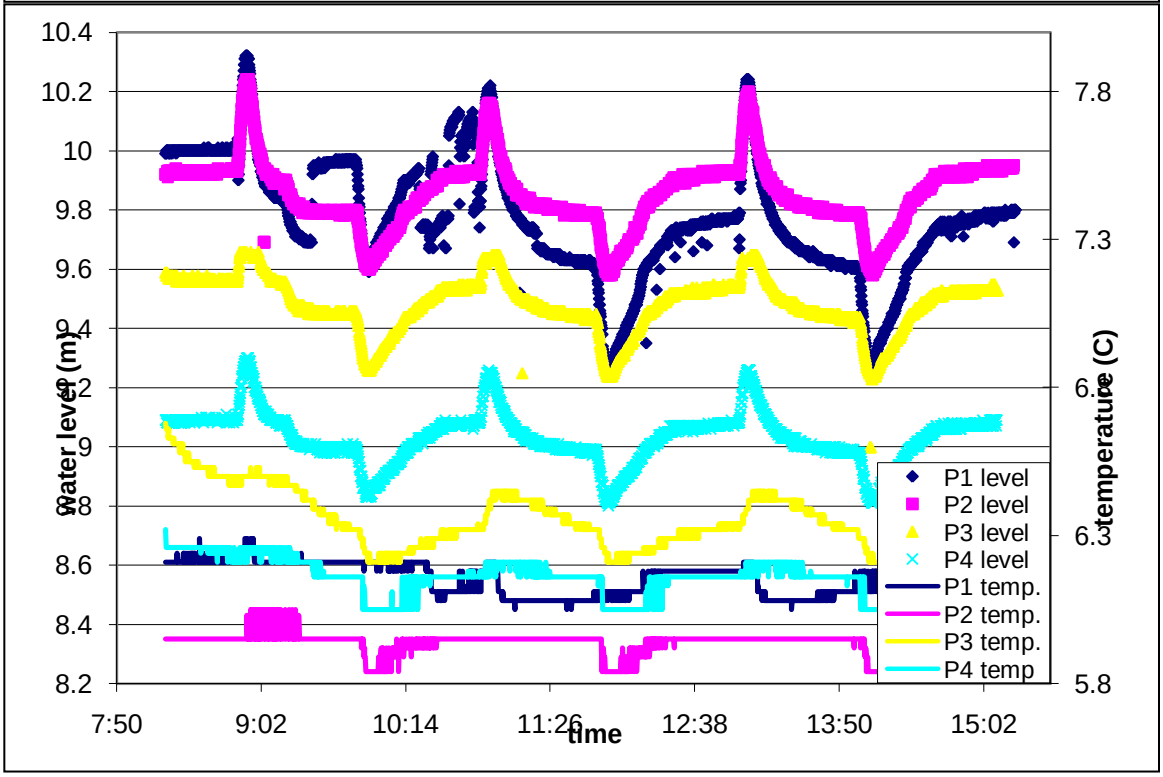

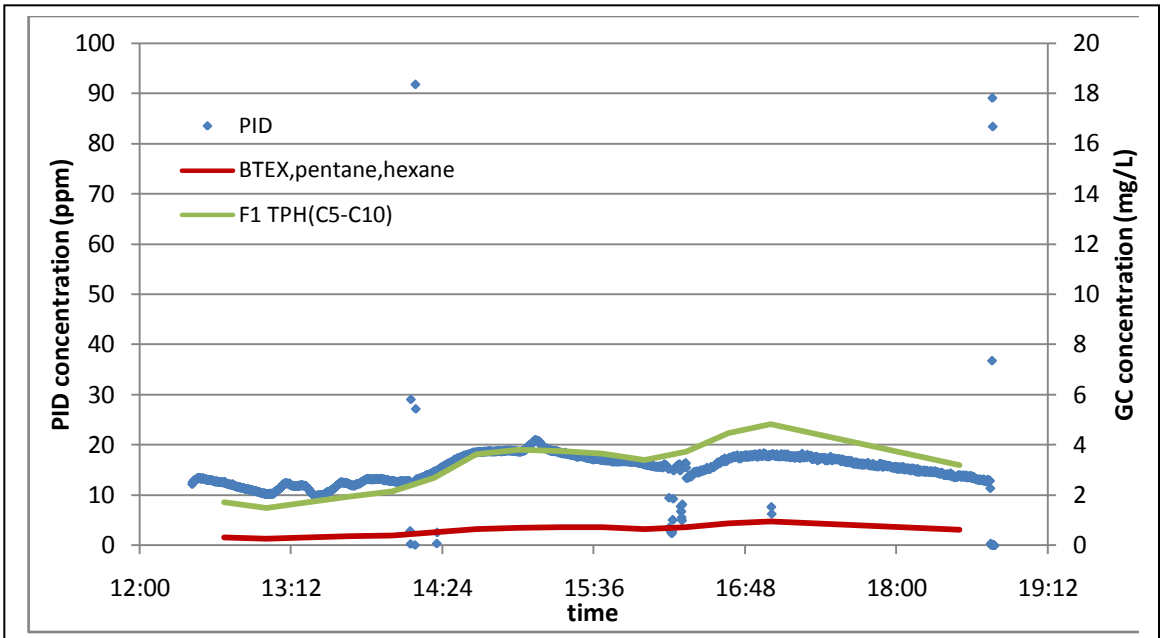

Figure B.15 May 12 PID/TPH

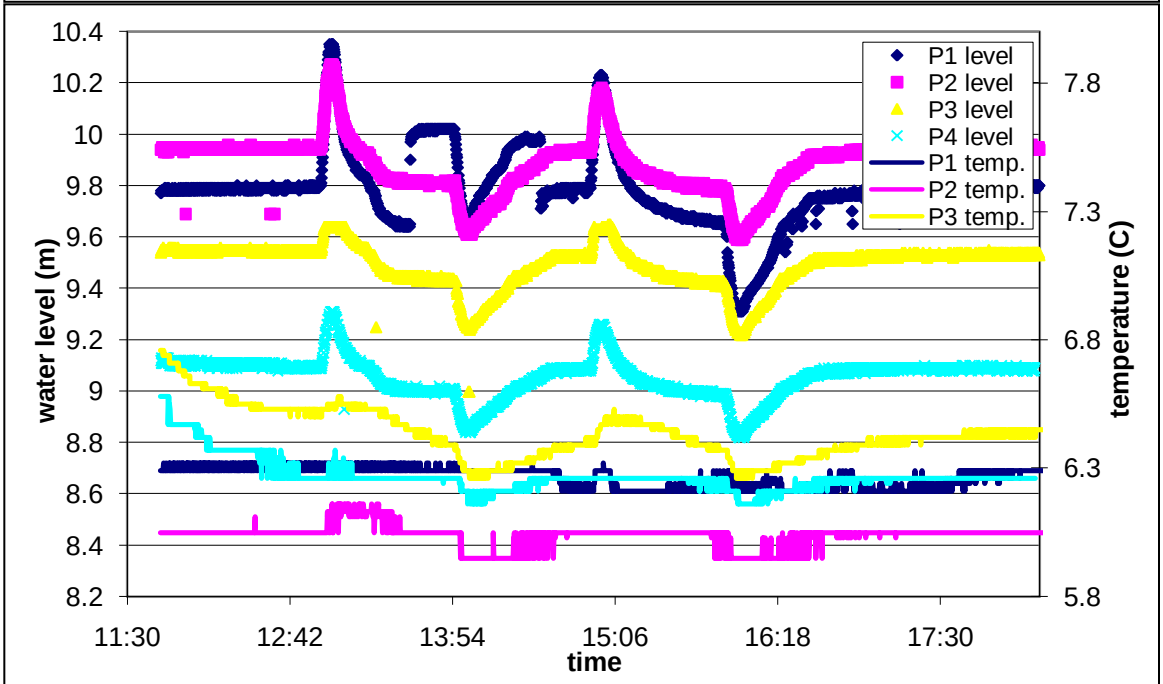

Figure B.16 May 12 water level and temperature

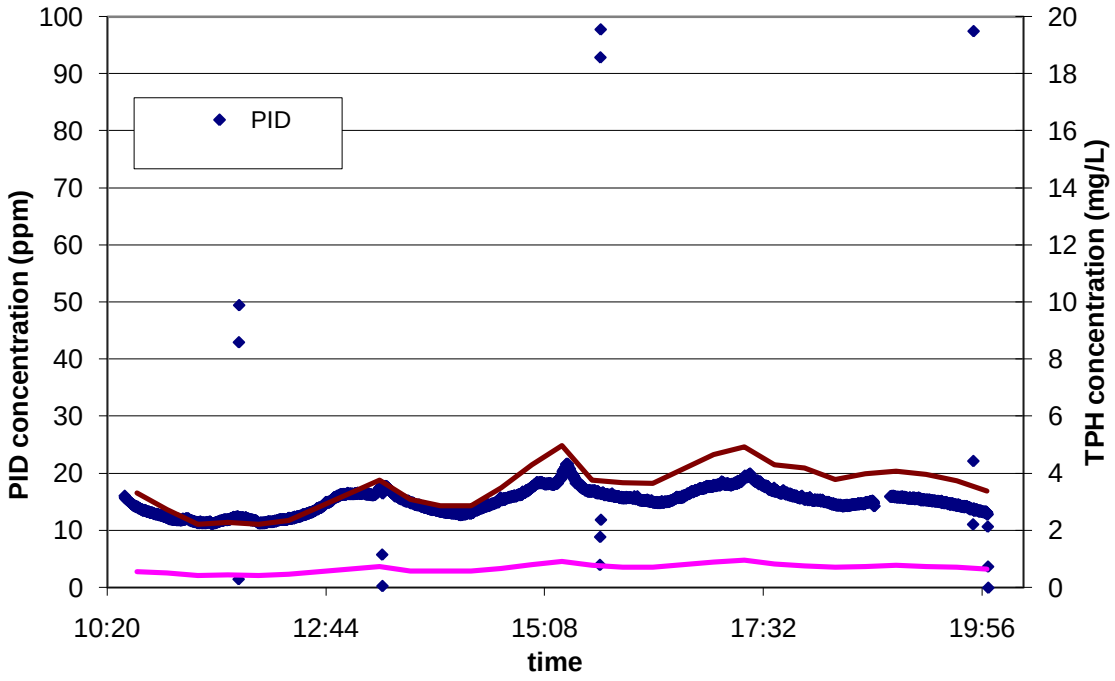

Figure B.17 May 13 PID/TPH

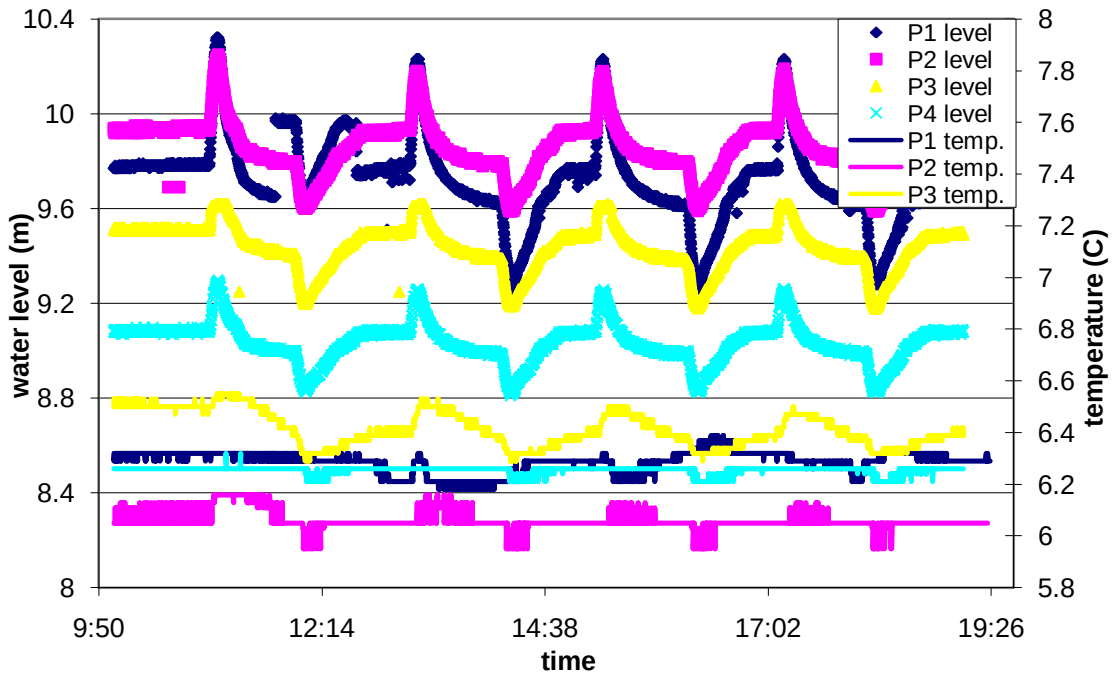

Figure B.18 May 13 water level and temperature

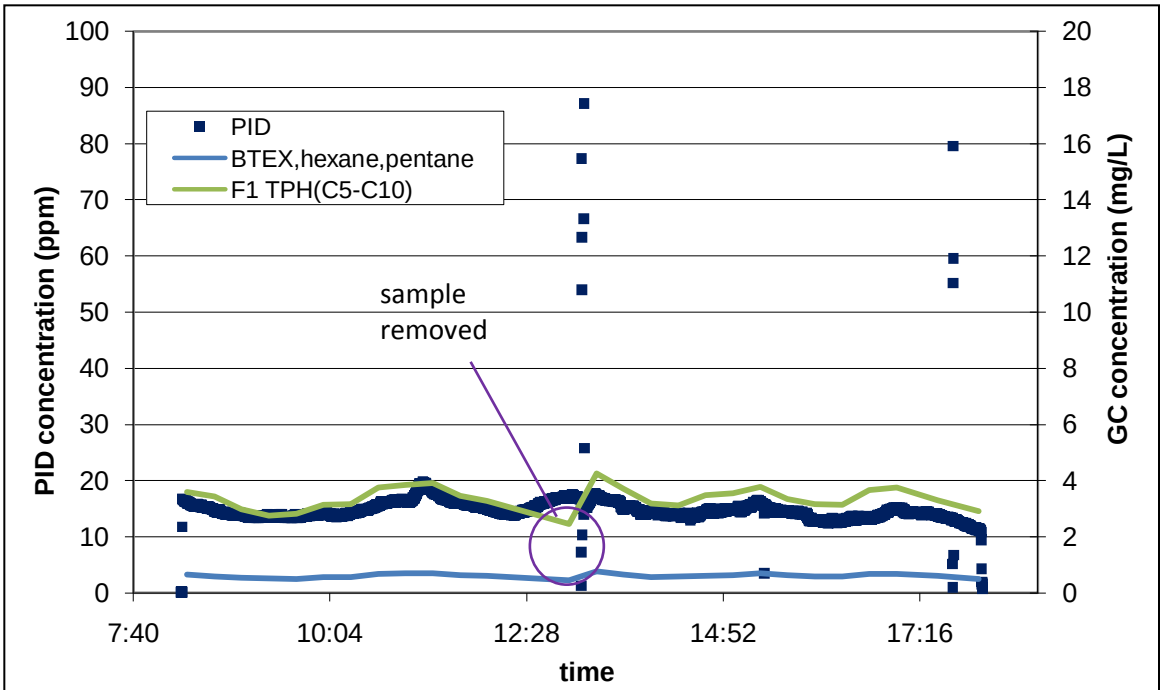

Figure B.19 May 14 PID/TPH

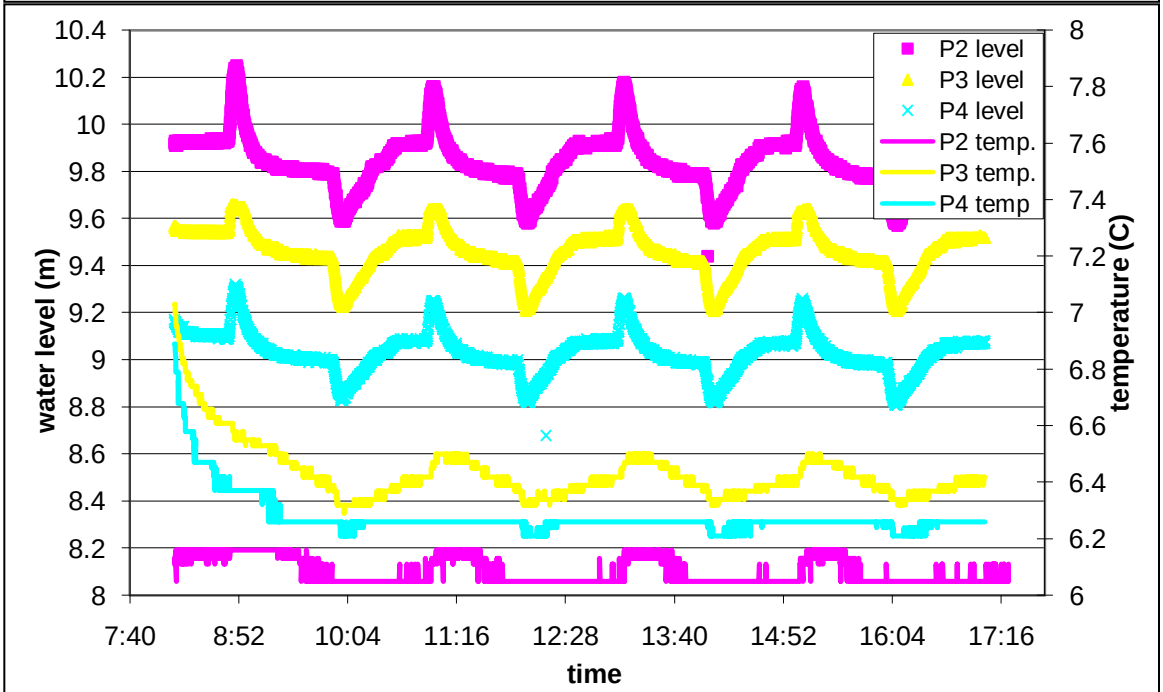

Figure B.20 May 14 water level and temperature

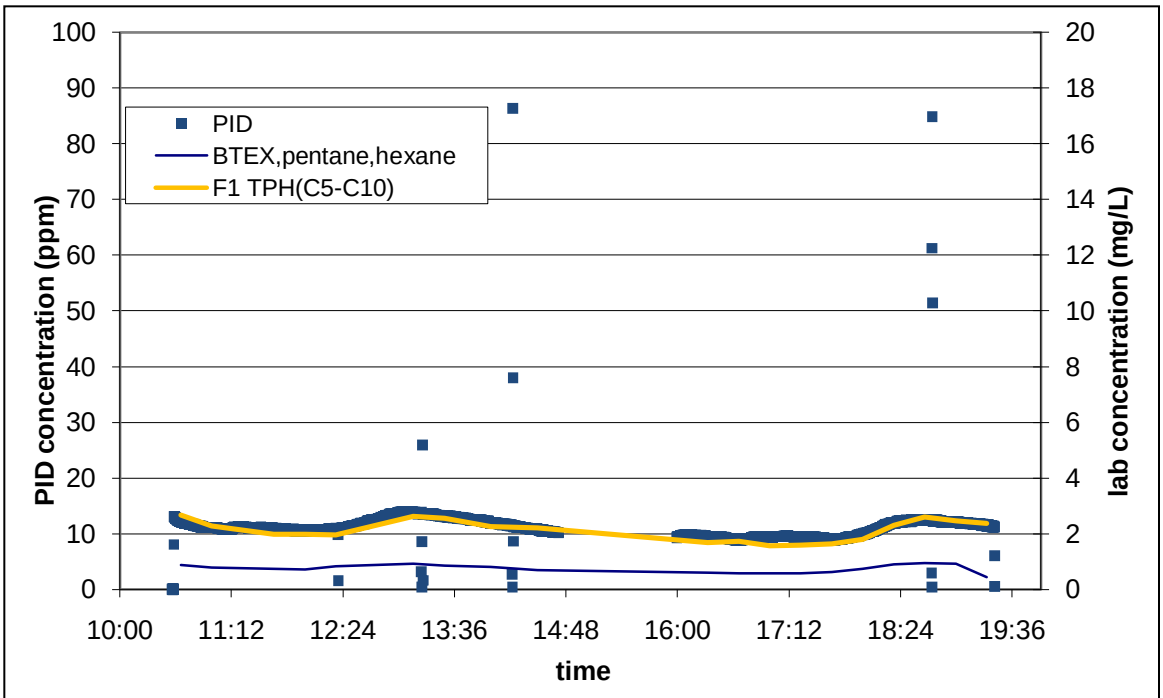

Figure B.21 May 15 PID/TPH

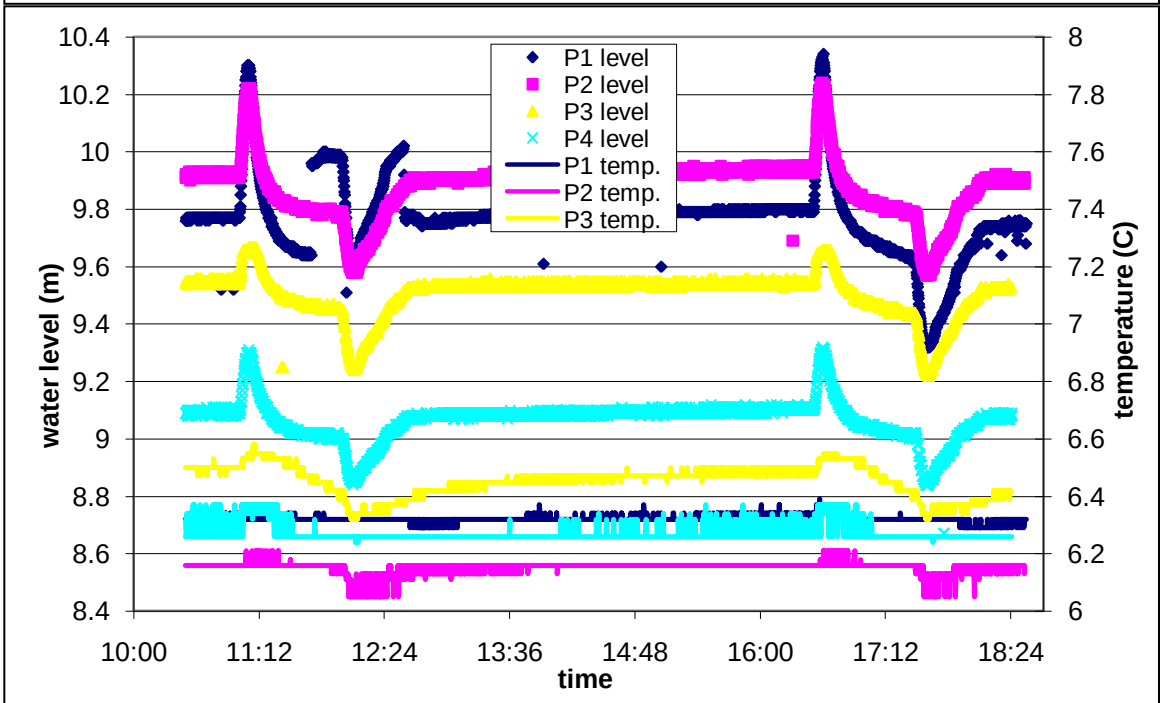

Figure B.22 May 15 water level and temperature

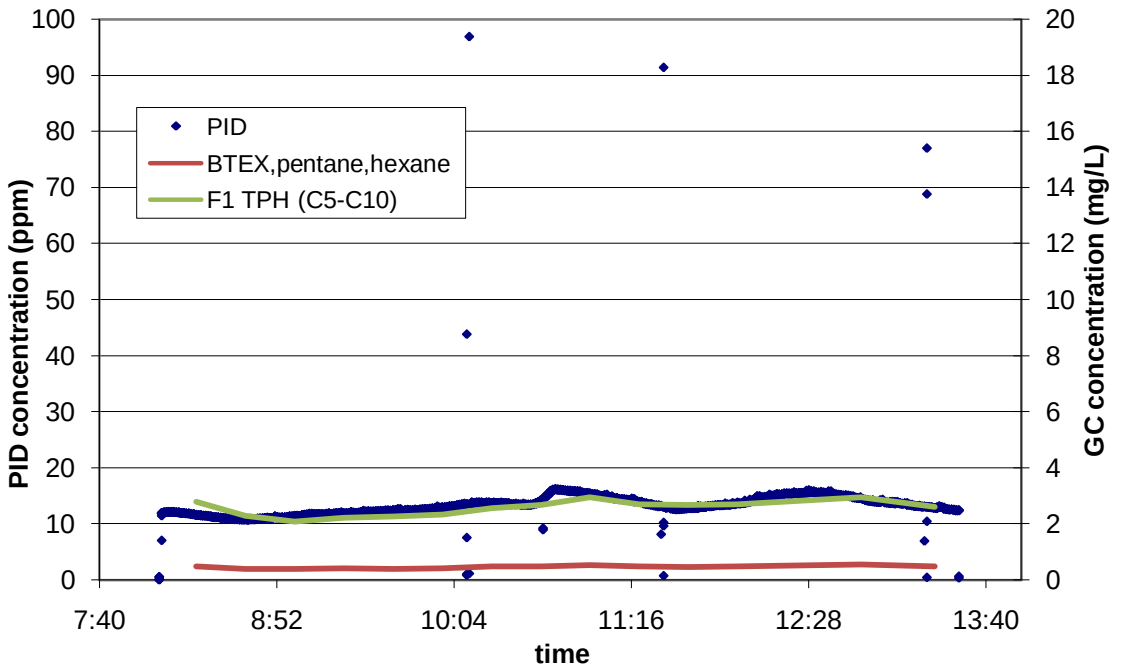

Figure B.23 May 16 PID/TPH

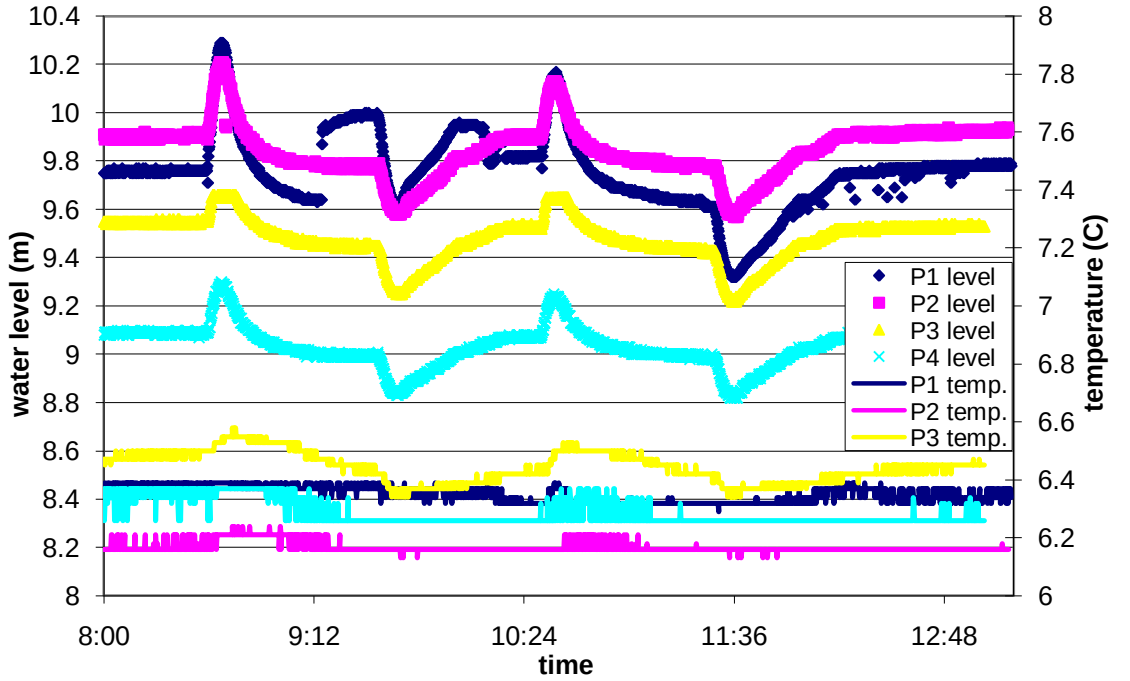

Figure B.23 May 16 water level and temperature

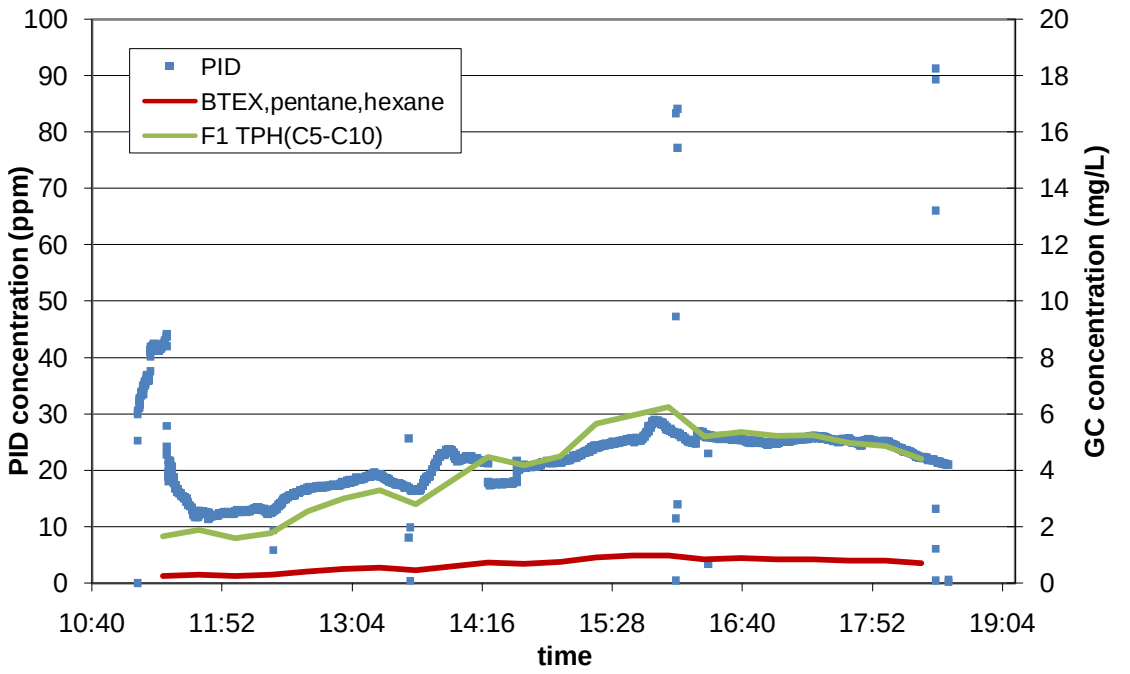

Figure B.25 May 18 PID/TPH

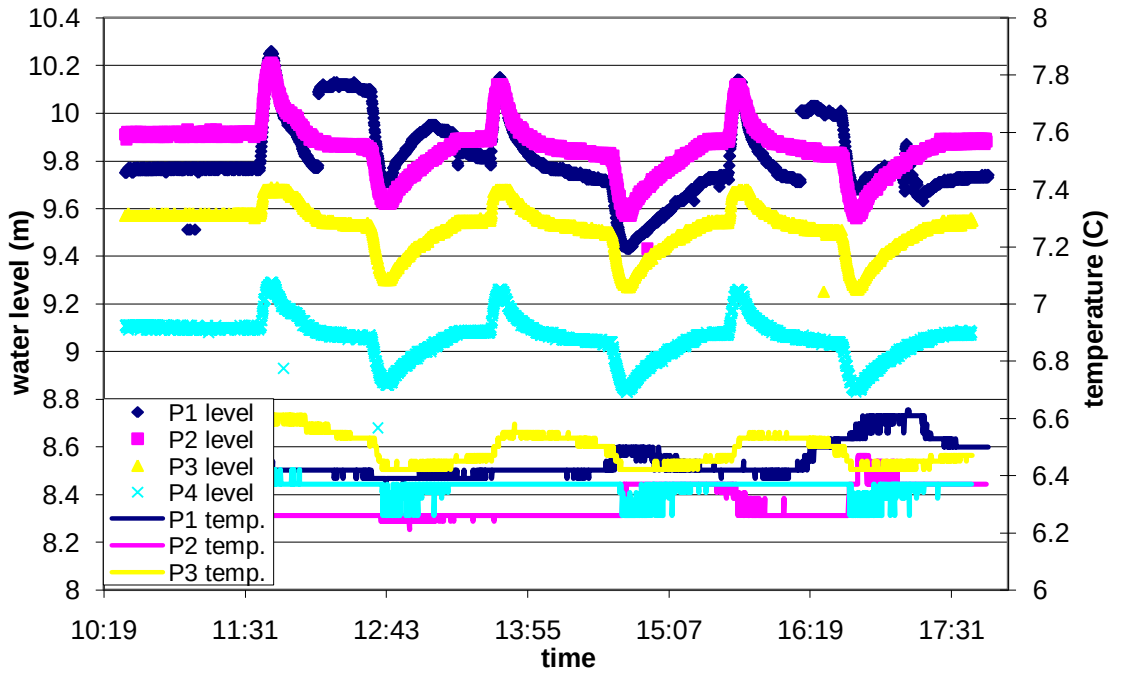

Figure B.26 May 18 water level and temperature

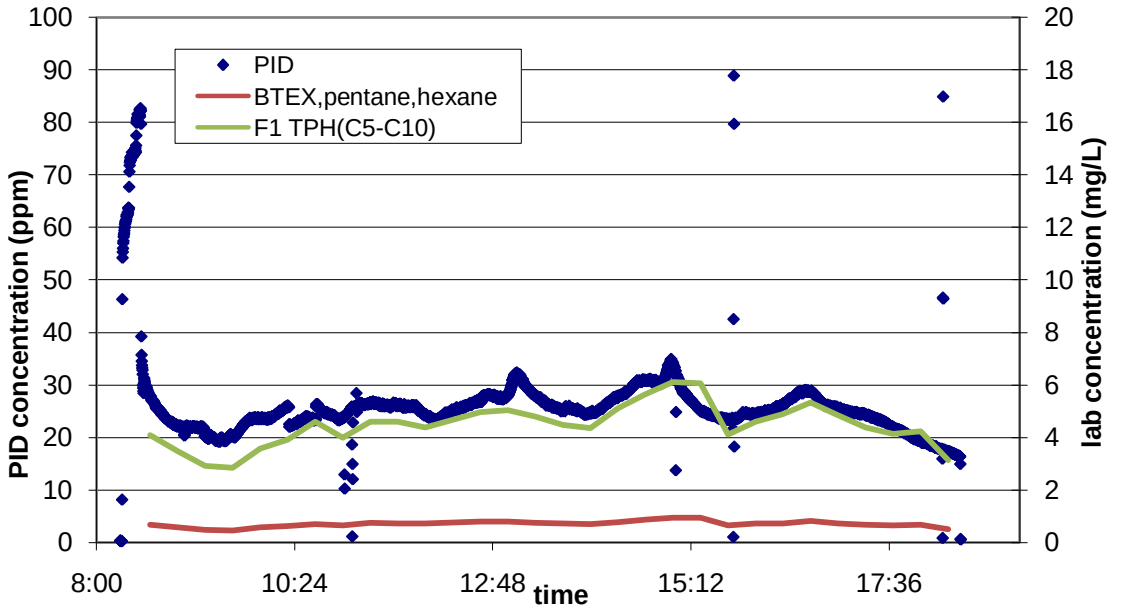

Figure B.27 May 19 PID/TPH

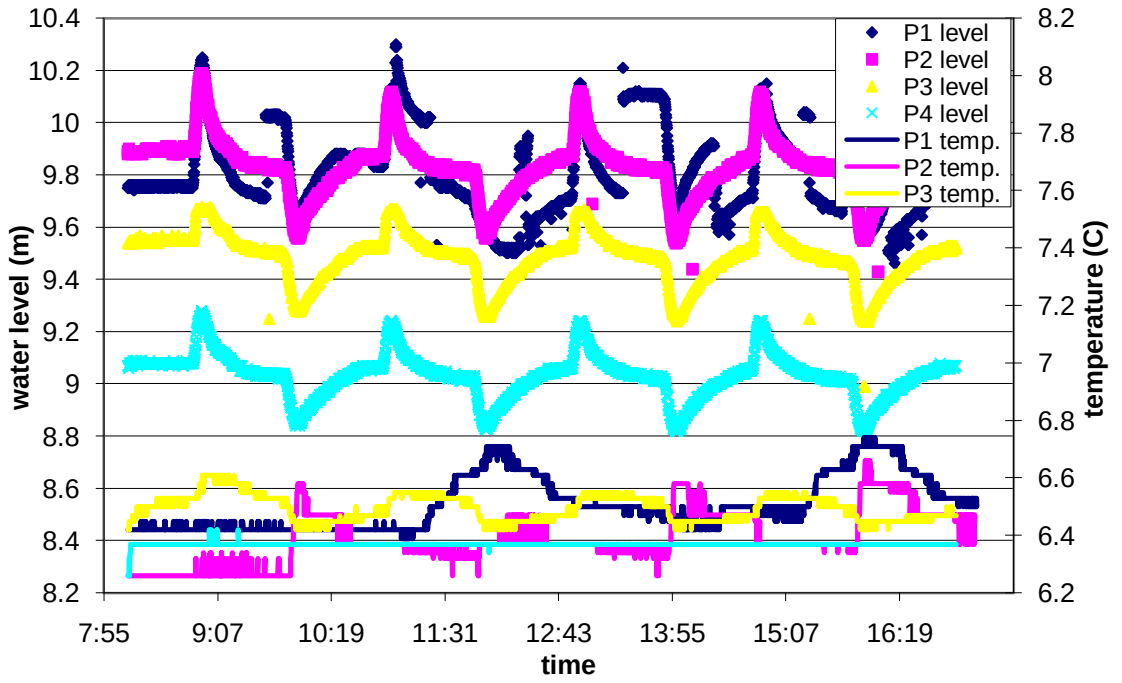

Figure B.28 May 19 water level and temperature

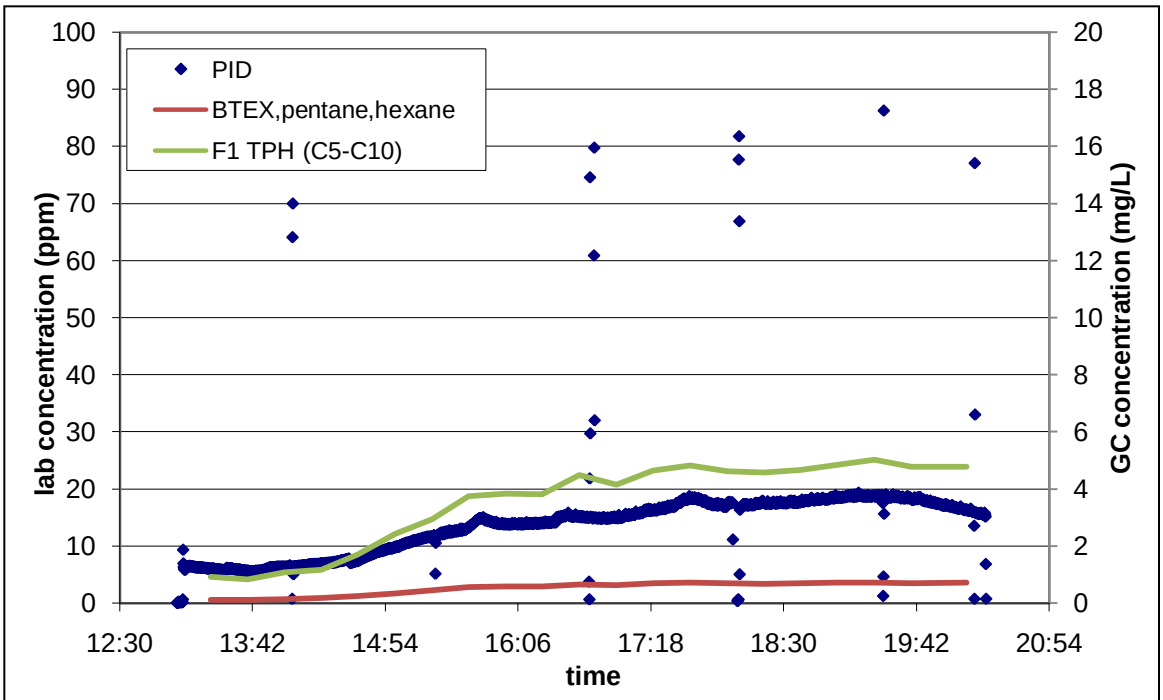

Figure B.29 May 25 PID/TPH

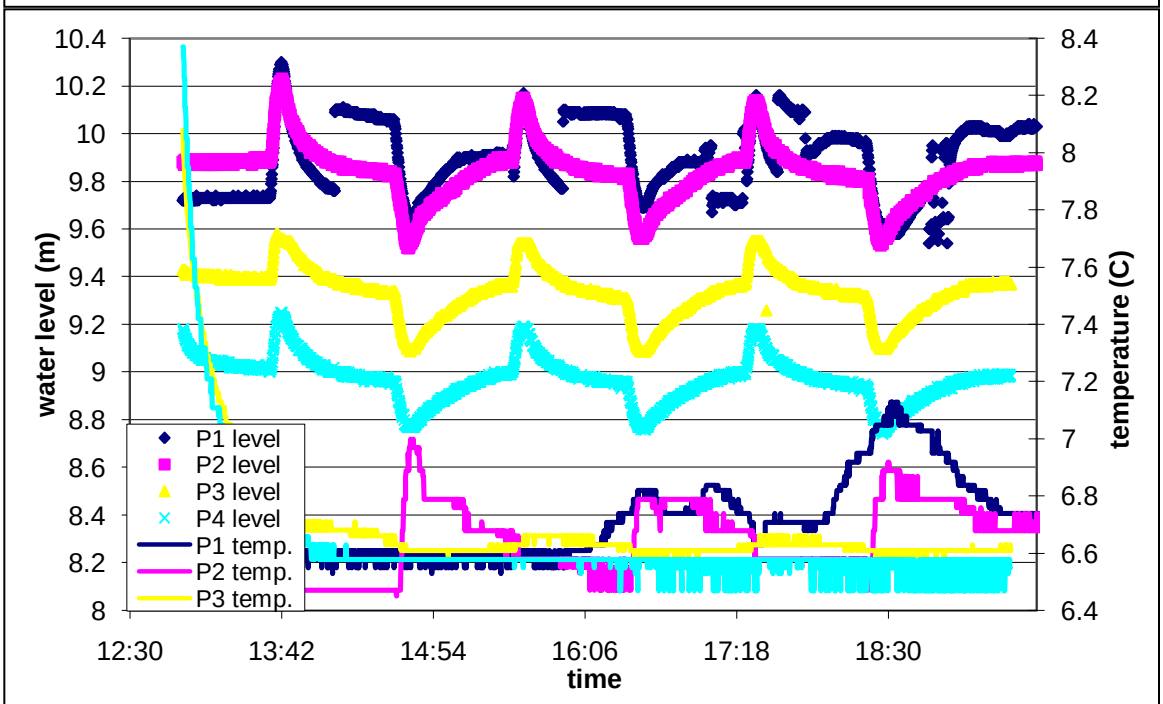

Figure B.30 May 25 water level and temperature

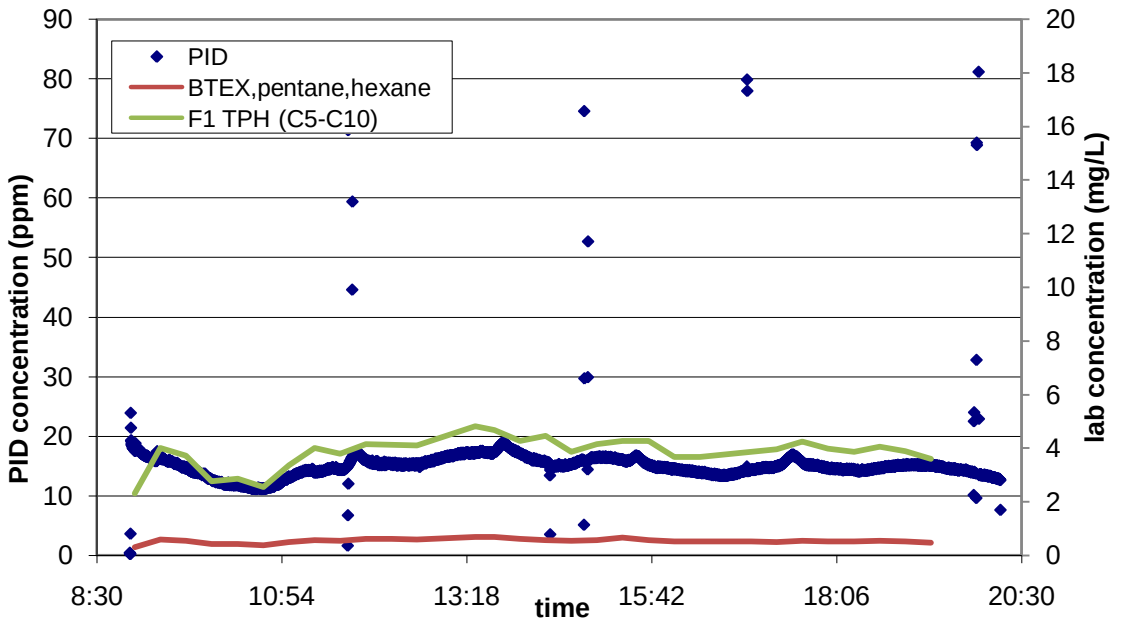

Figure B.31 May 26 PID/TPH

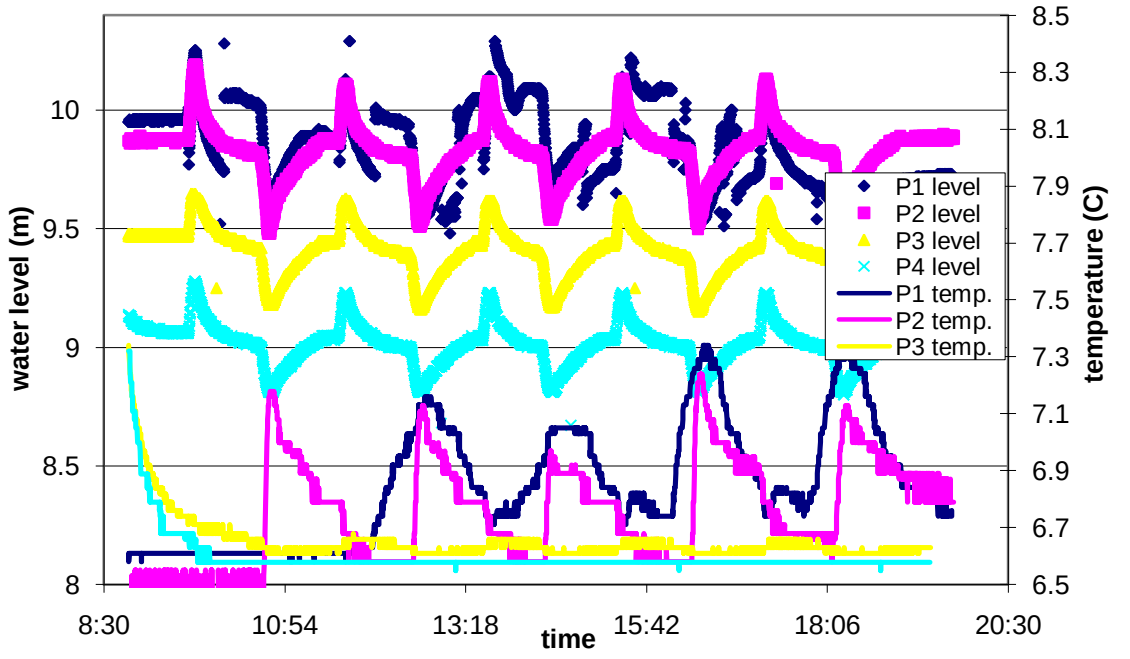

Figure B.32 May 26 water level and temperature

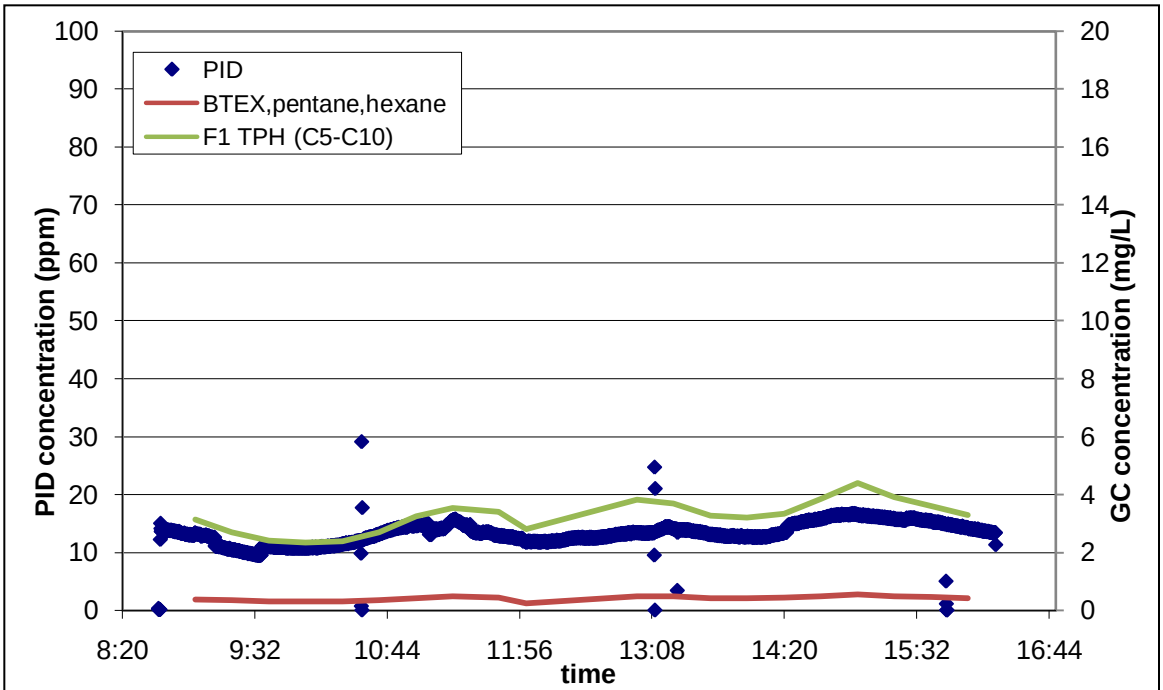

Figure B.33 May 27 PID/TPH

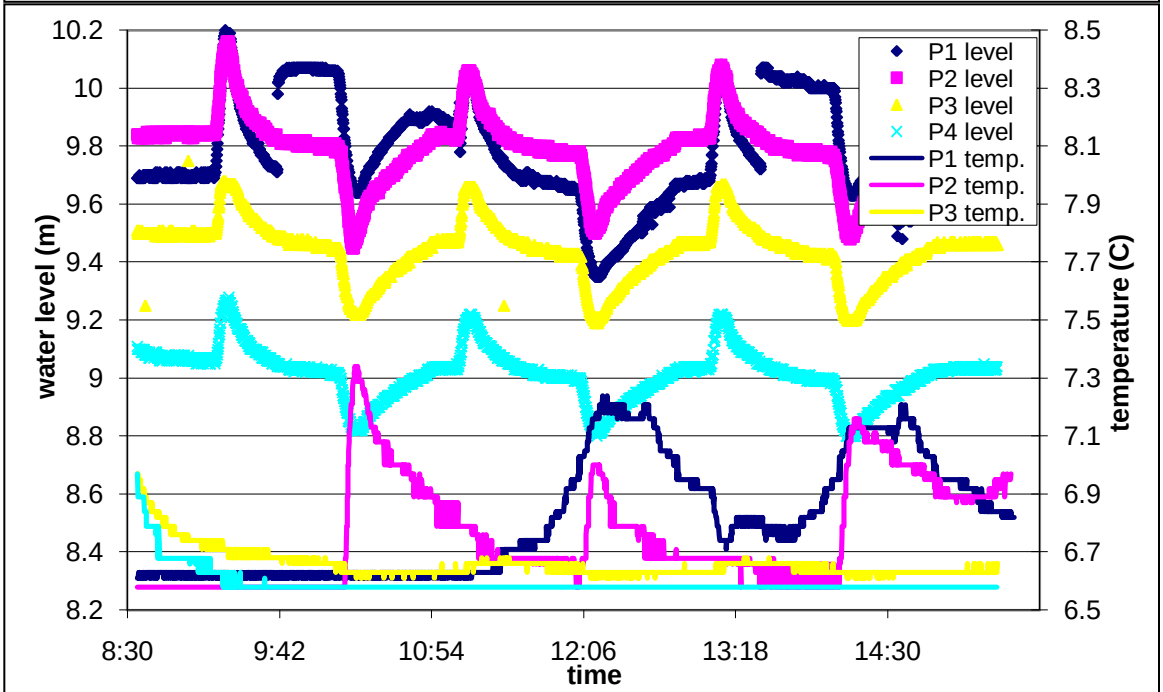

Figure B.34 May 27 water level and temperature

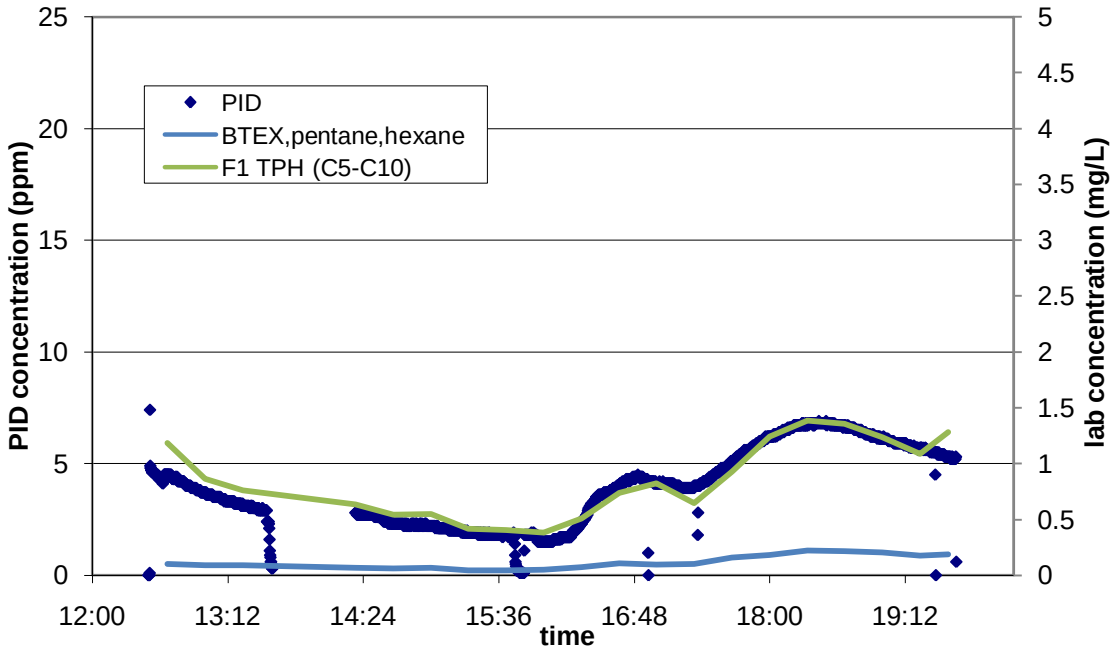

Figure B.35 June 1 PID/TPH

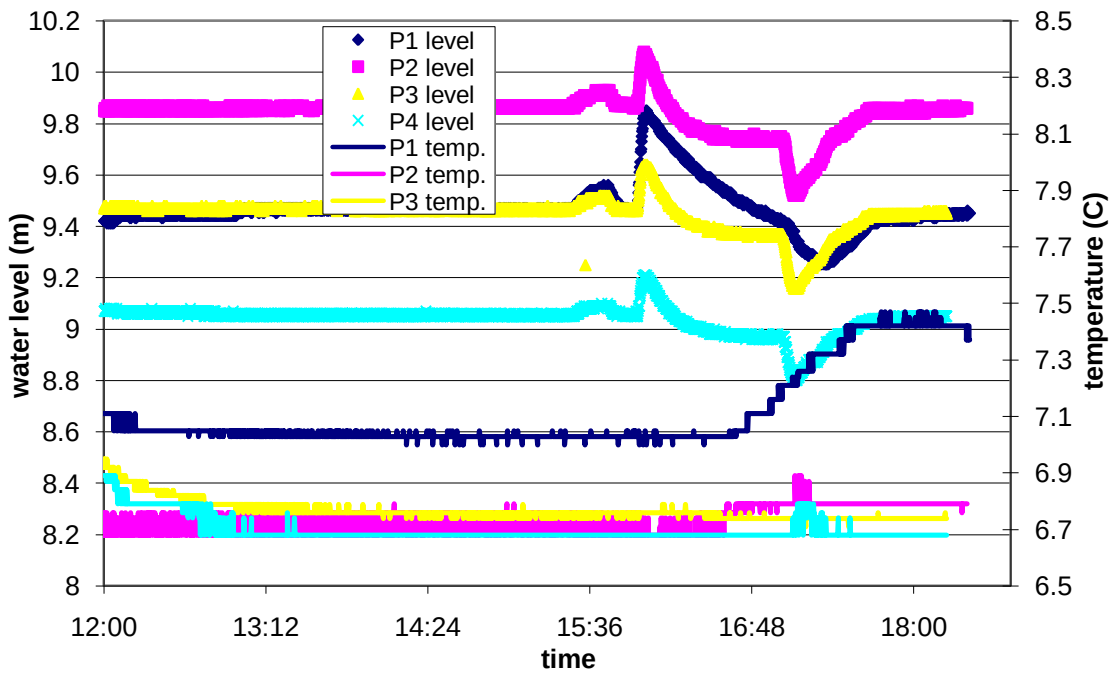

Figure B.36 June 1 water level and temperature

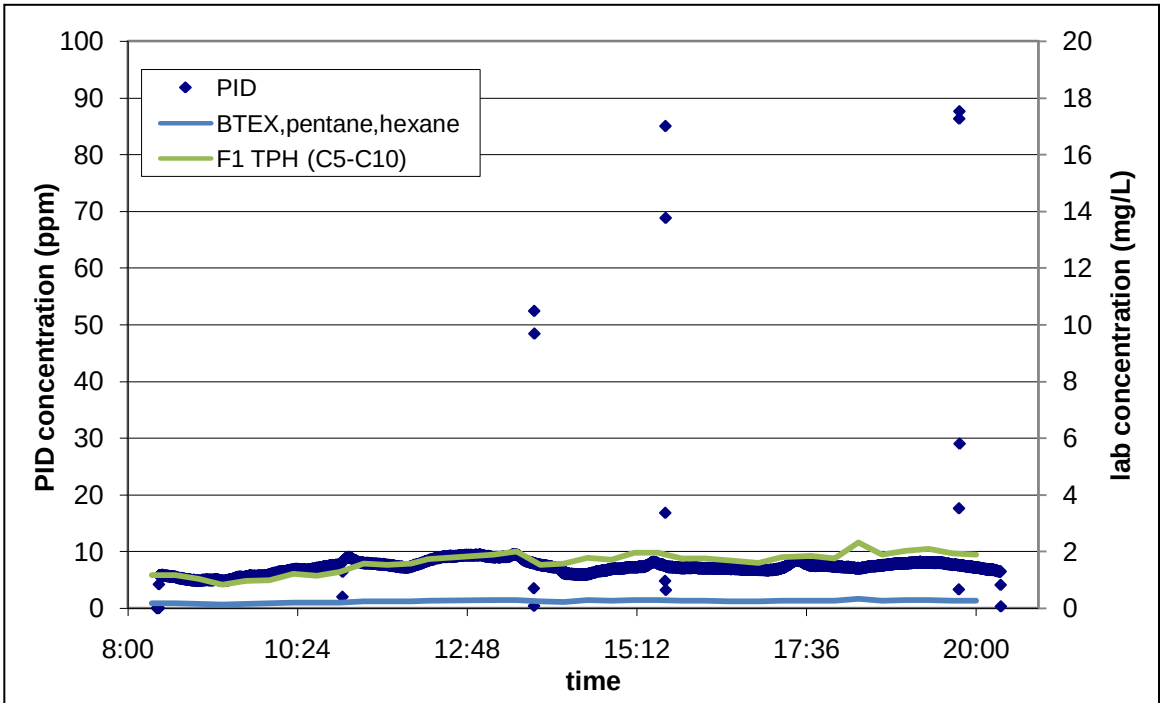

Figure B.37 June 2 PID/TPH

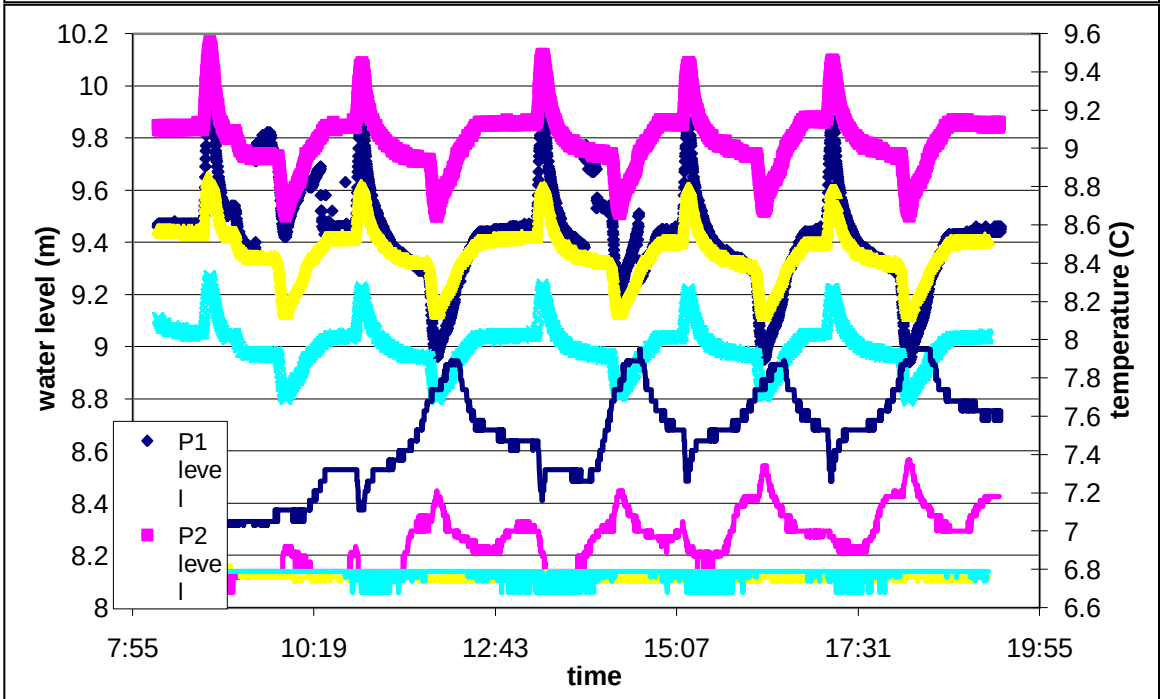

Figure B.36 June 2 water level and temperature

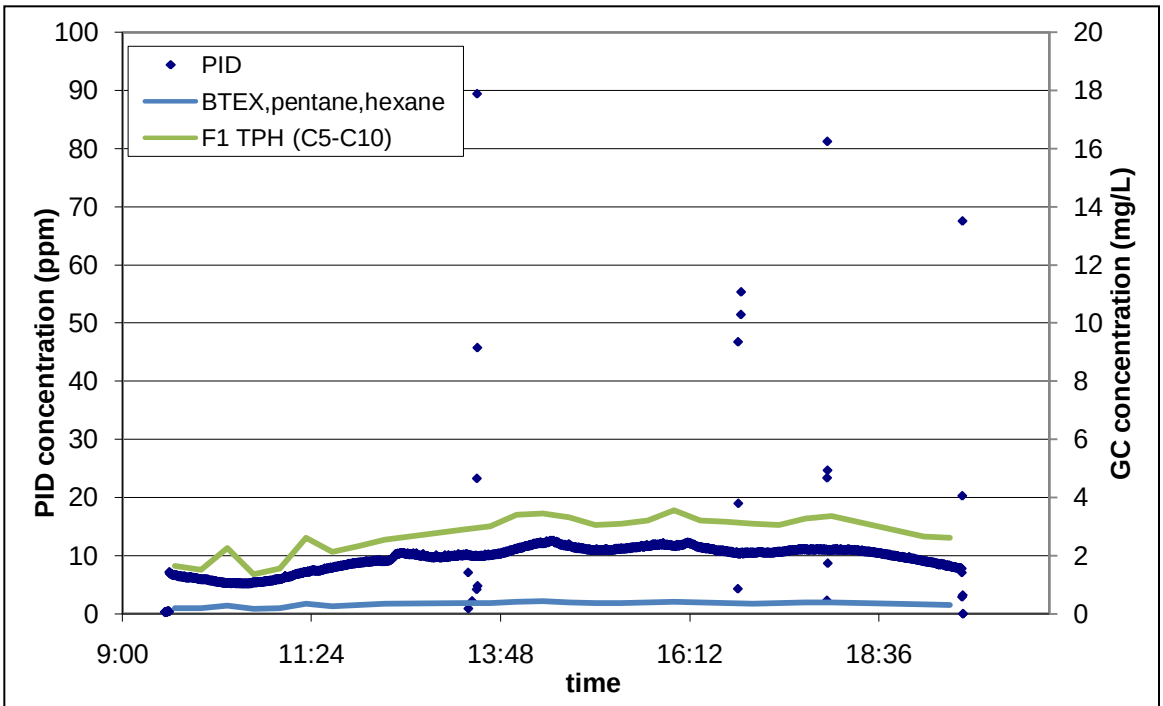

Figure B.39 June 3 PID/TPH

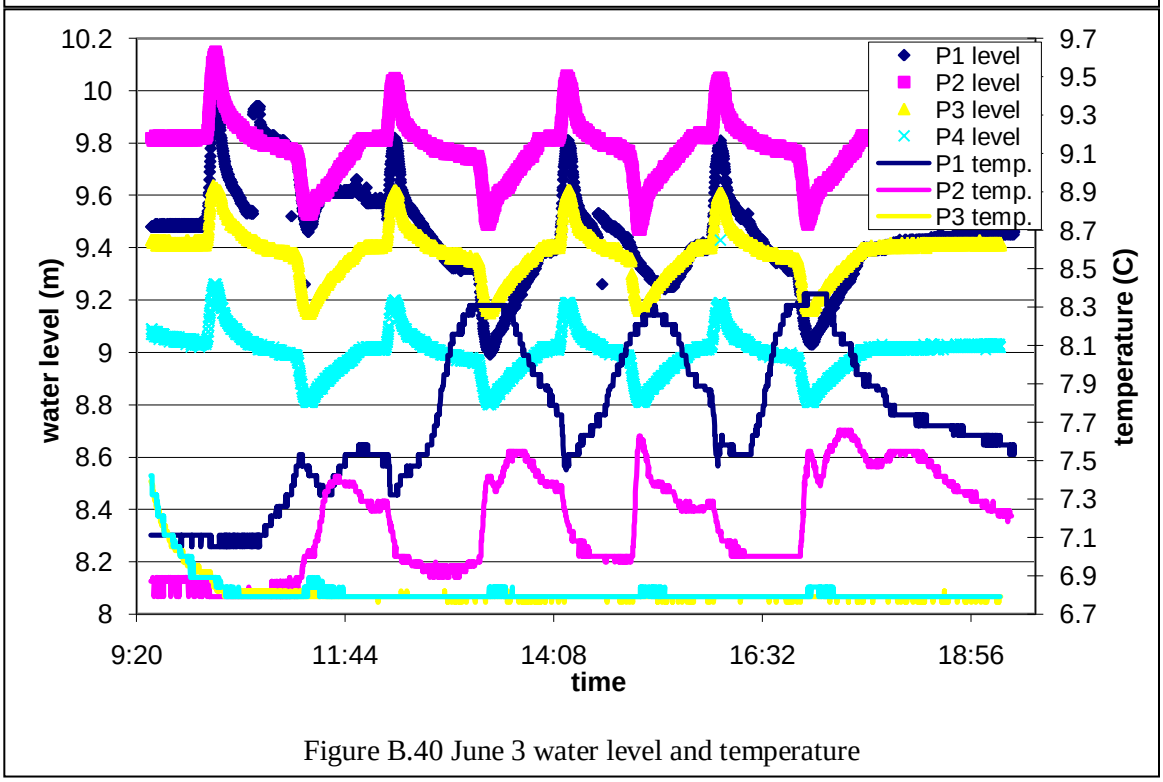

Figure B.40 June 3 water level and temperature

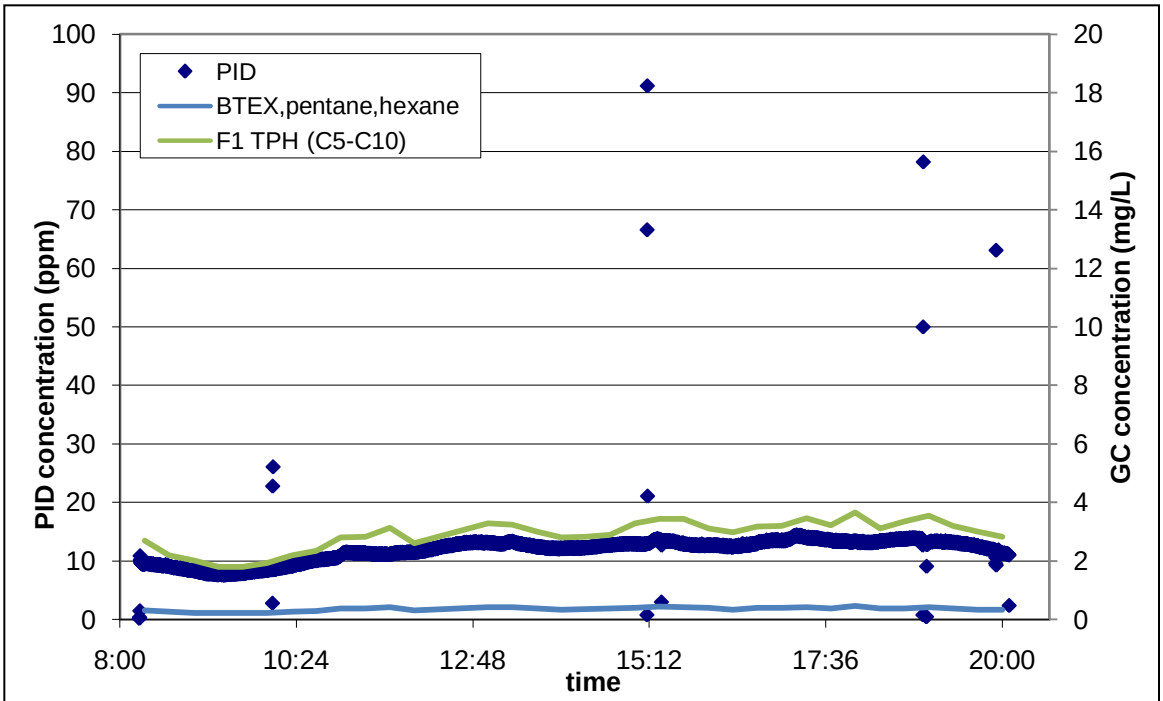

Figure B.41 June 4 PID/TPH

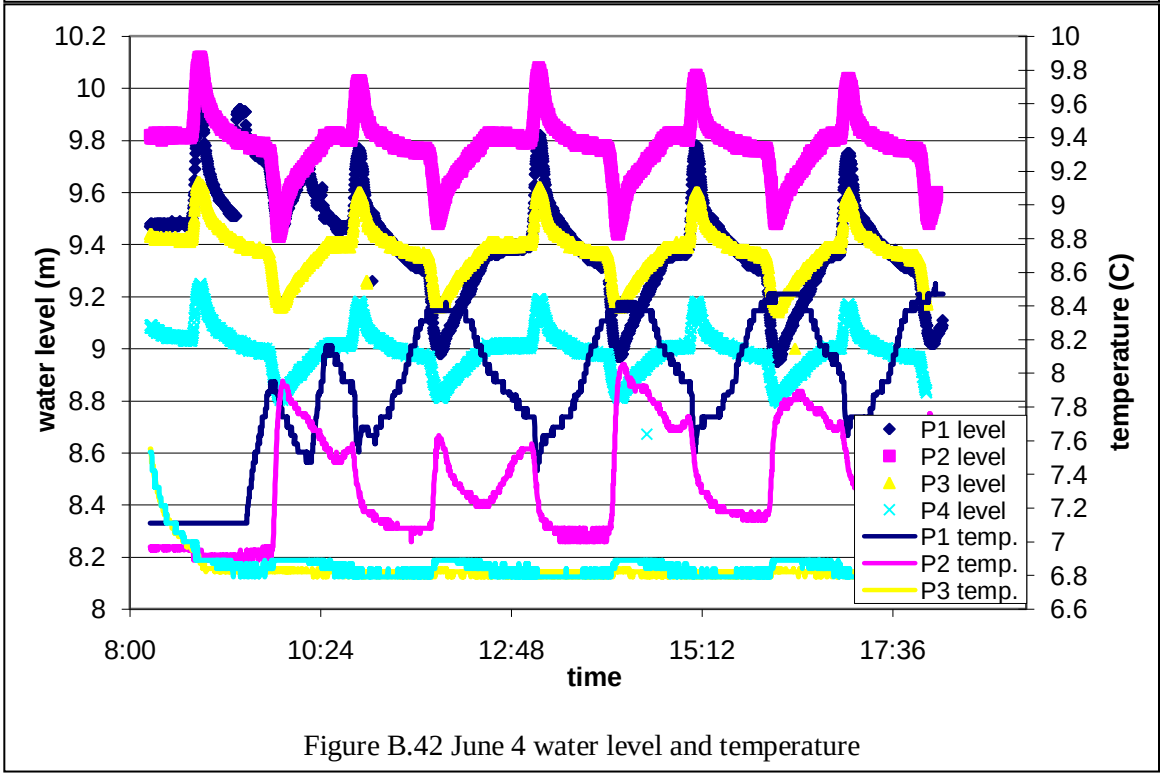

Figure B.42 June 4 water level and temperature

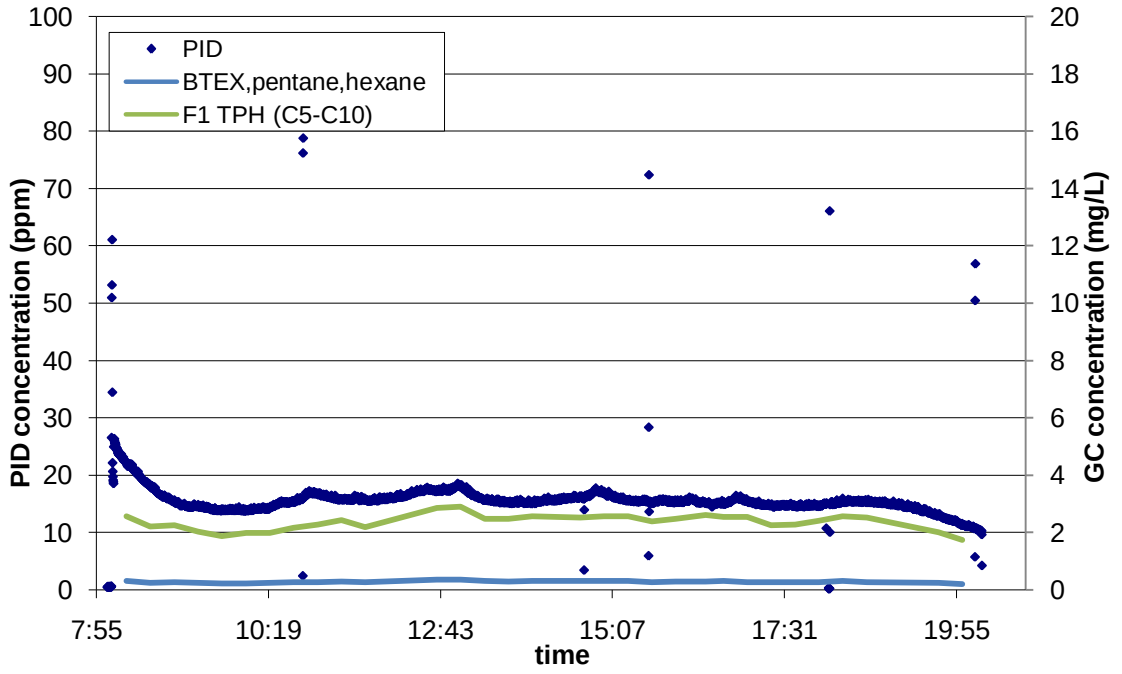

Figure B.43 June 5 PID/TPH

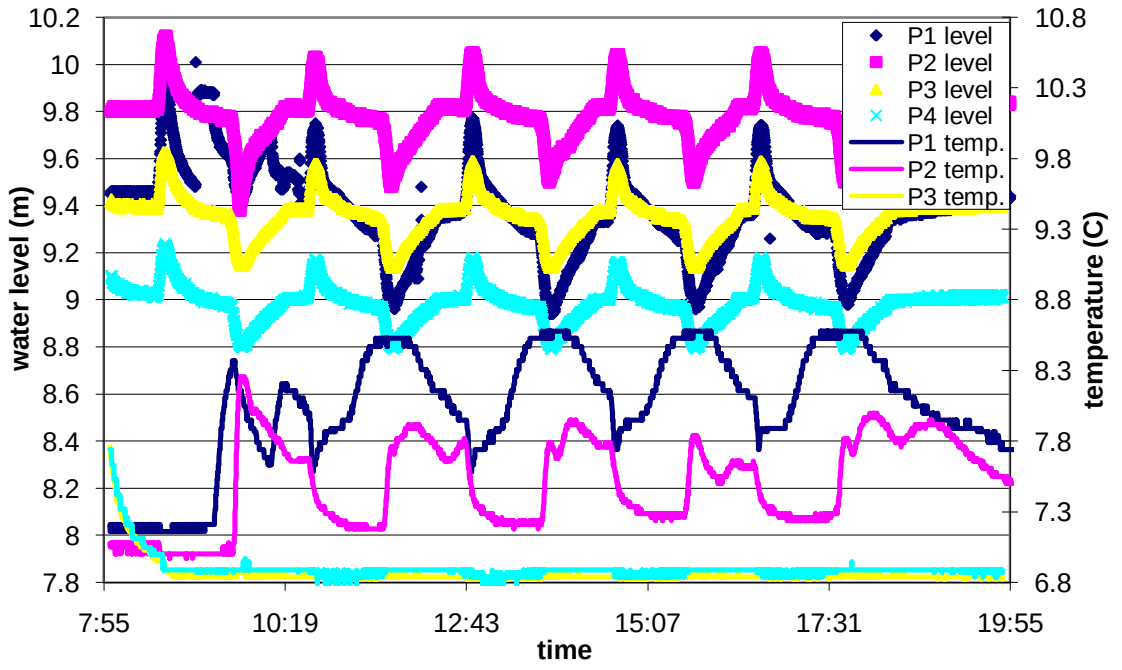

Figure B.44 June 5 water level and temperature

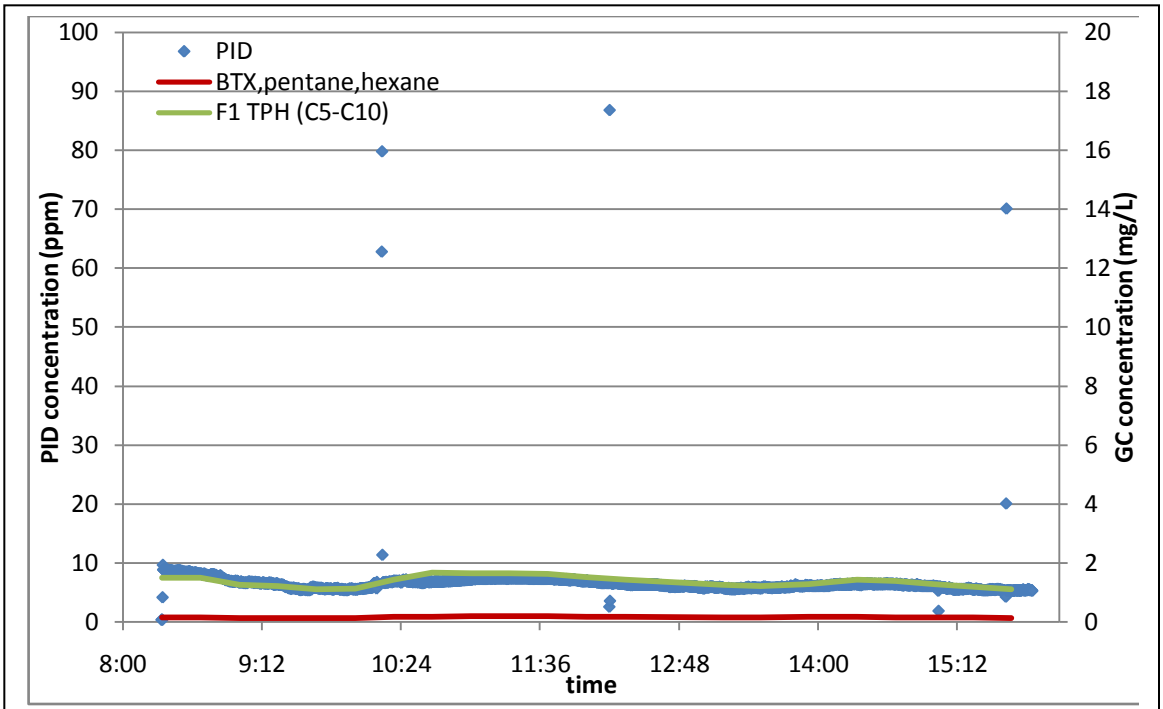

Figure B.45 June 6 PID/TPH

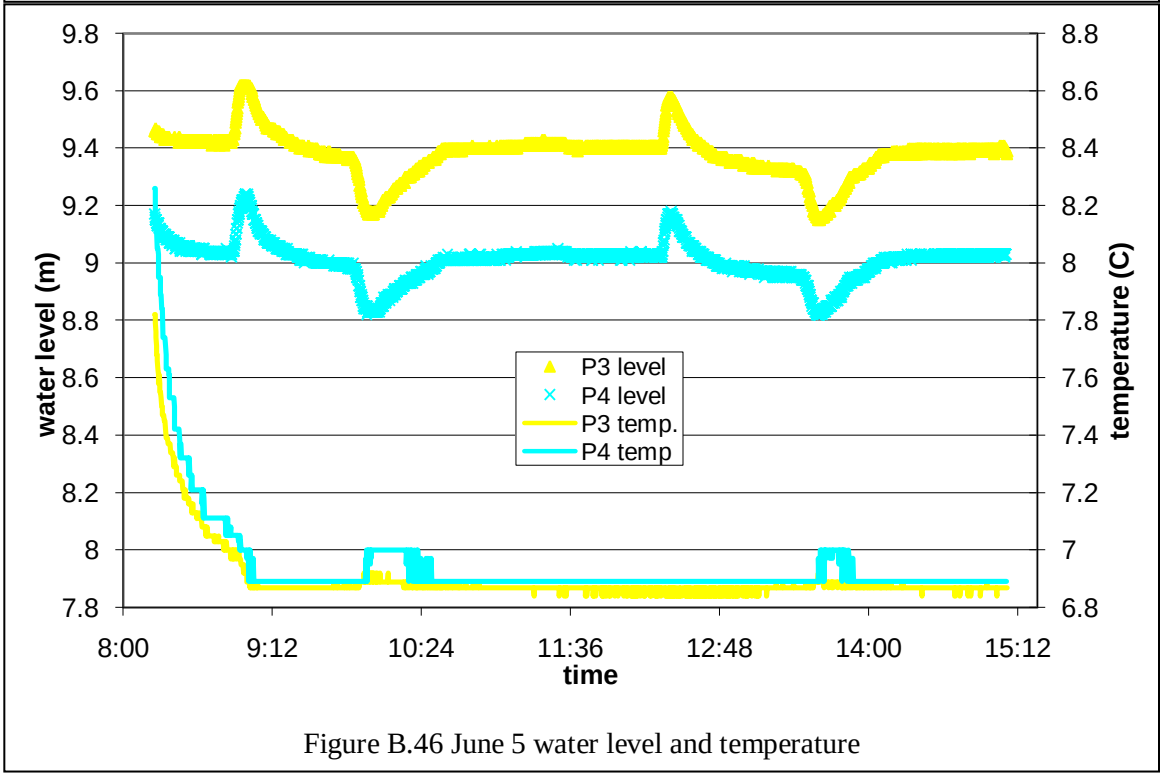

Figure B.46 June 5 water level and temperature

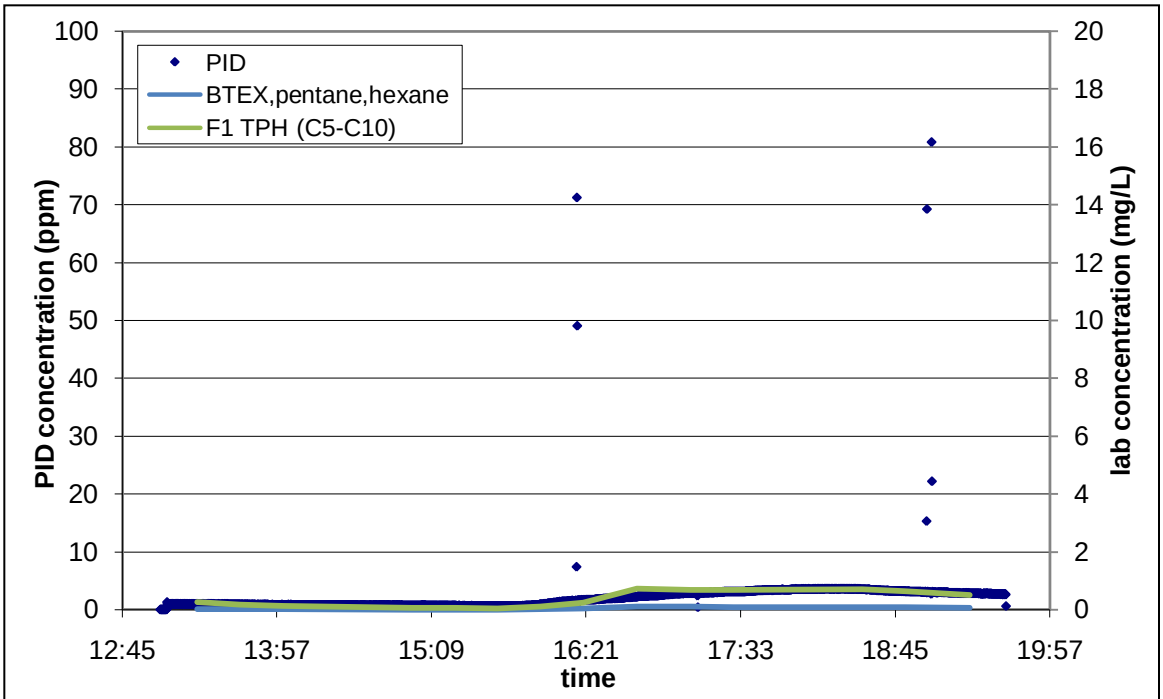

Figure B.47 June 10 PID/TPH

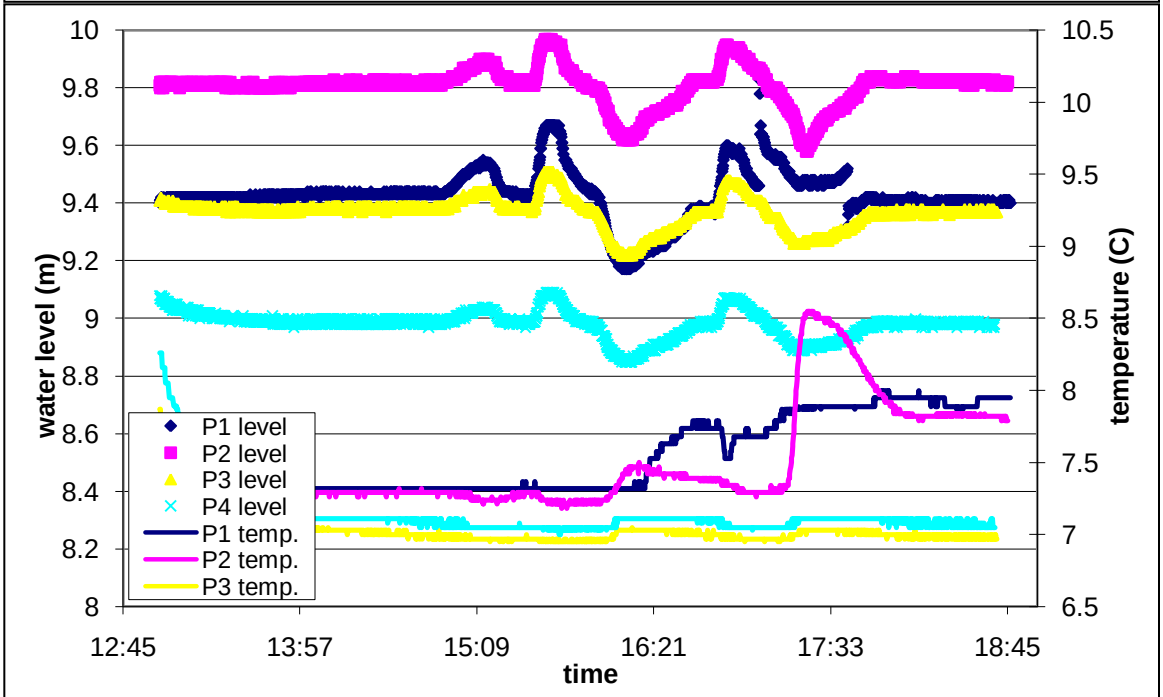

Figure B.48 June 10 water level and temperature

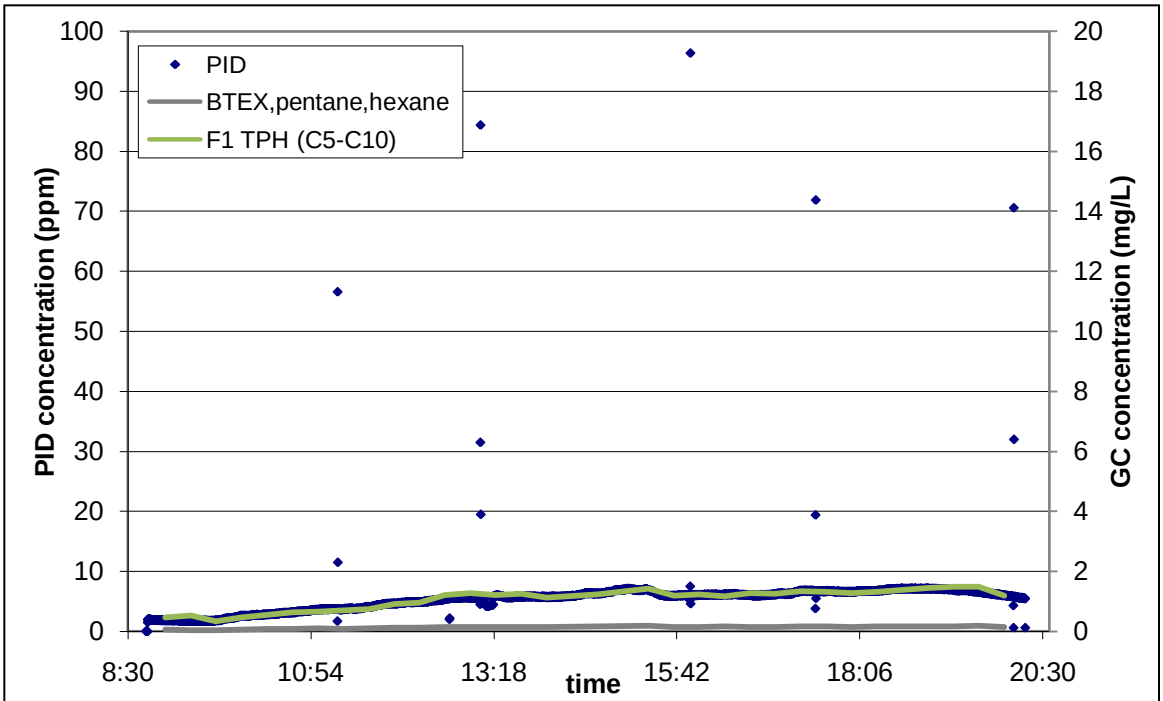

Figure B.49 June 11 PID/TPH

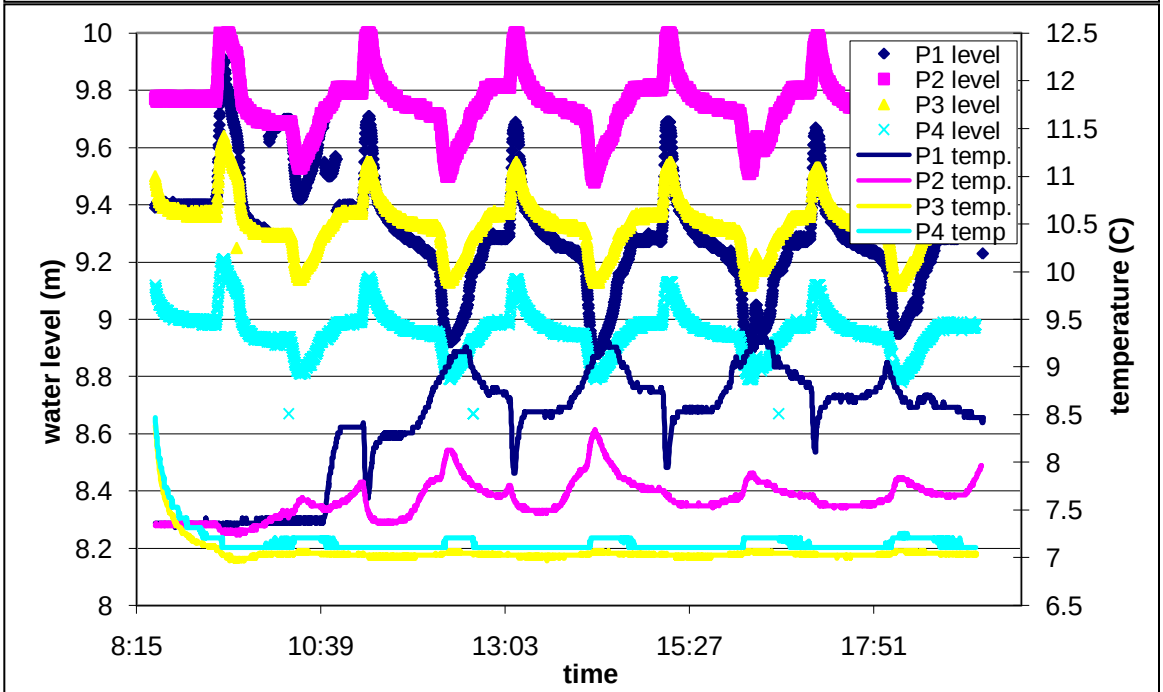

Figure B.50 June 11 water level and temperature

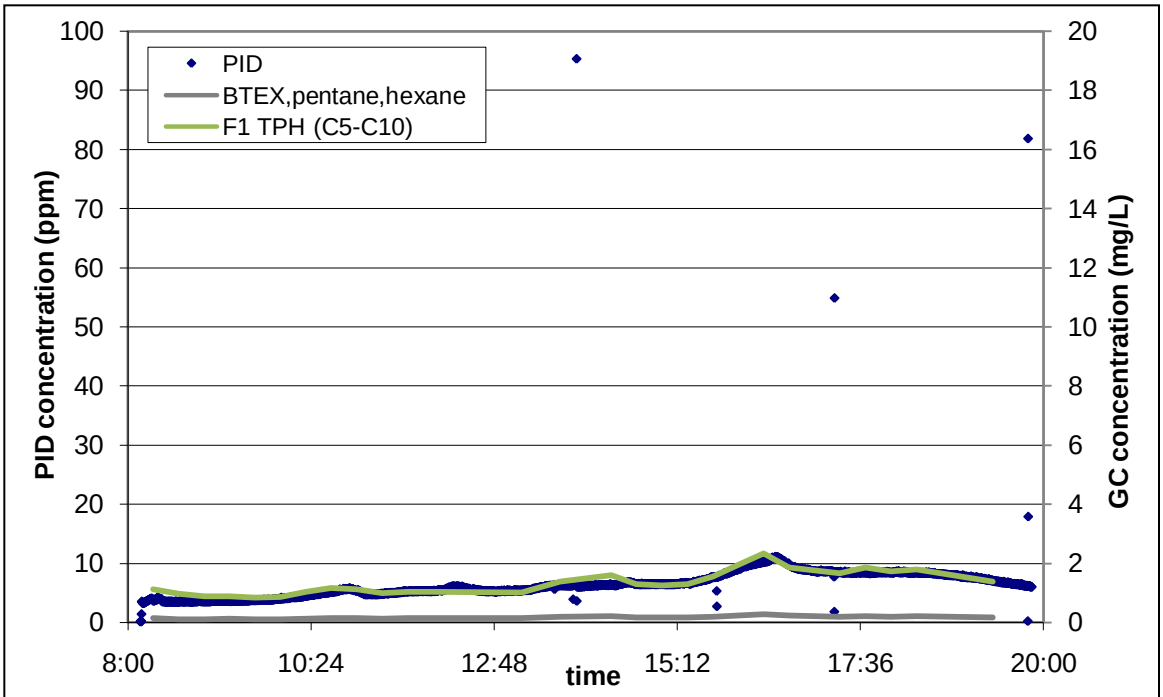

Figure B.51 June 12 PID/TPH

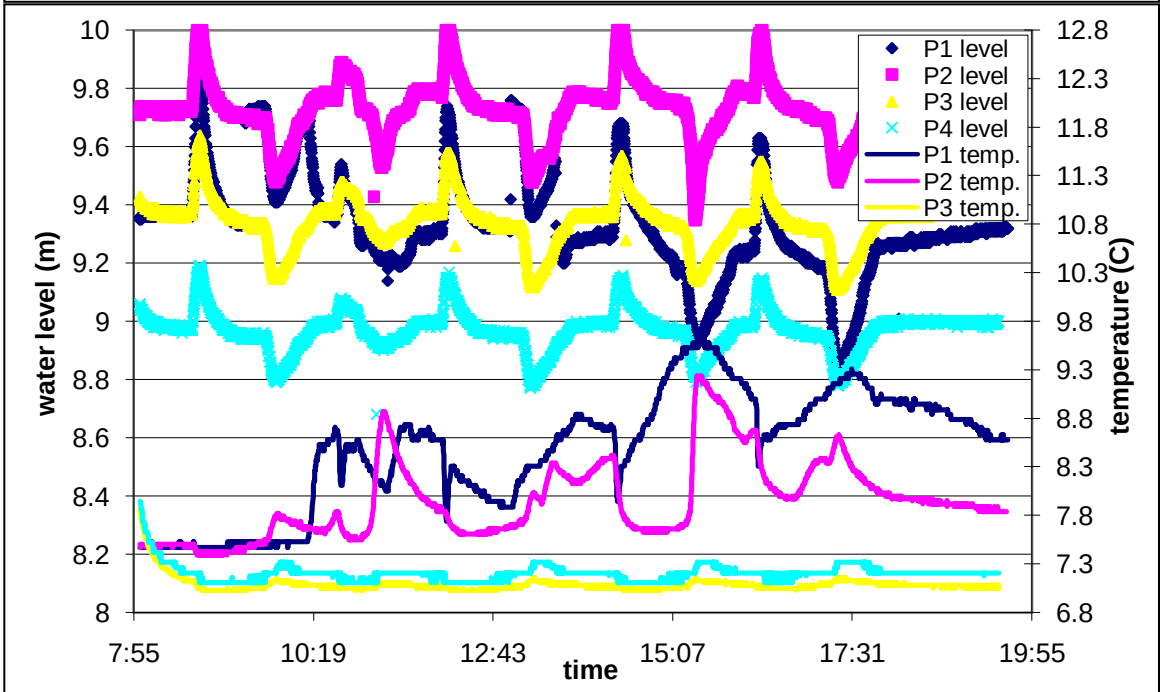

Figure B.52 June 12 water level and temperature

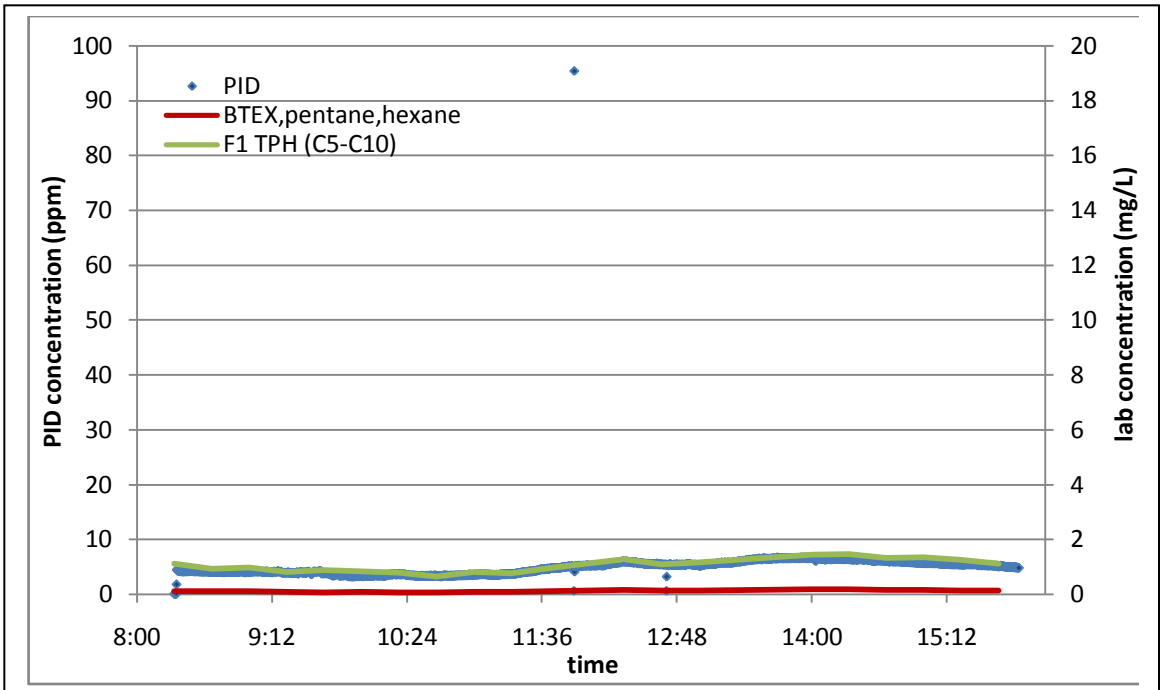

Figure B.53 June 13 PID/TPH

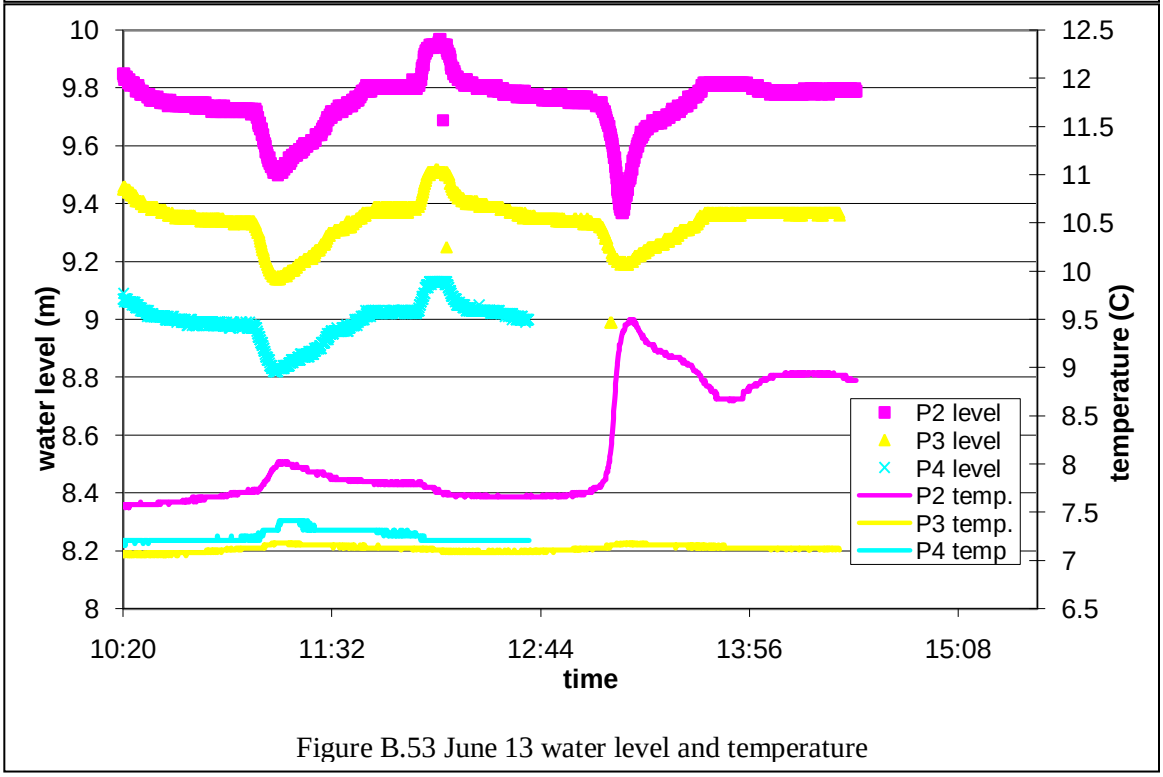

Figure B.53 June 13 water level and temperature

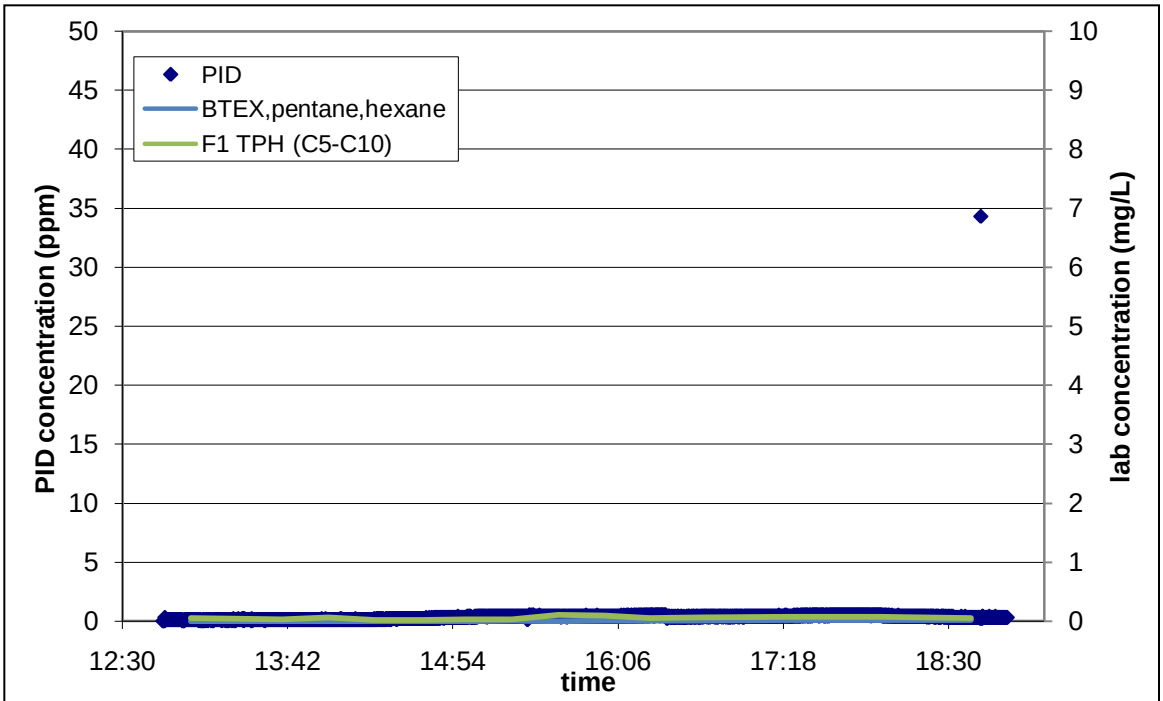

Figure B.55 June 17 PID/TPH

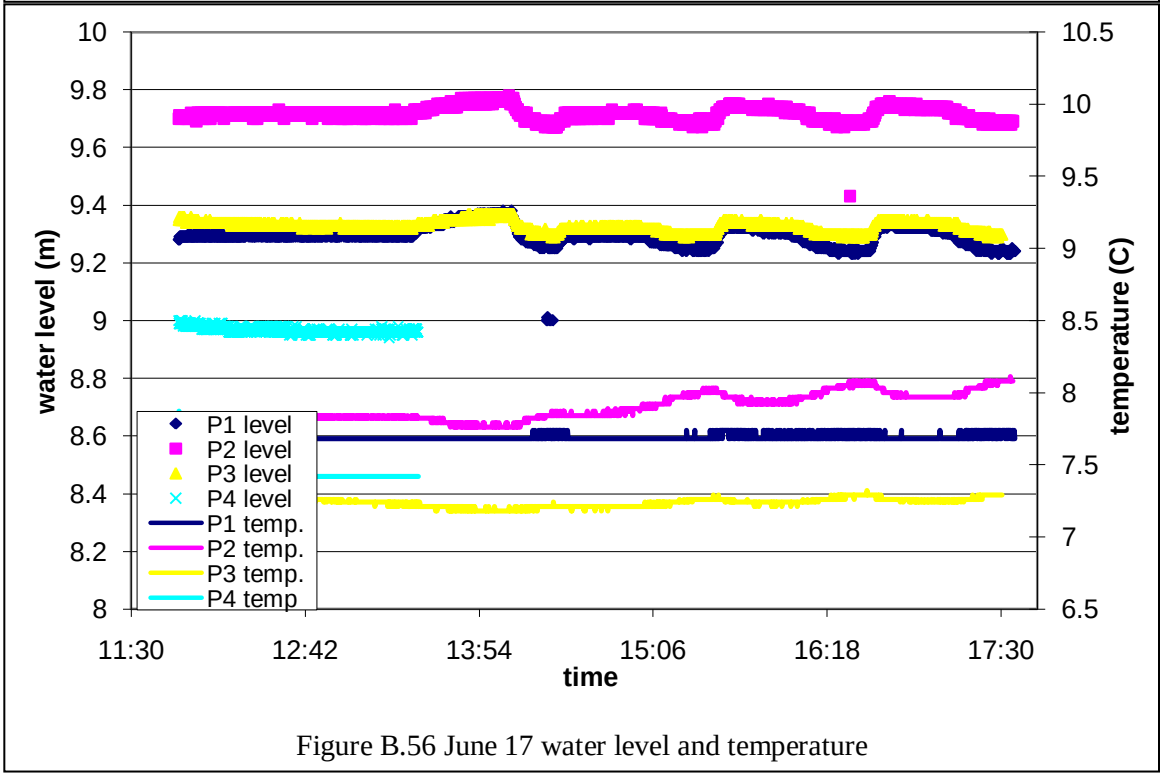

Figure B.56 June 17 water level and temperature

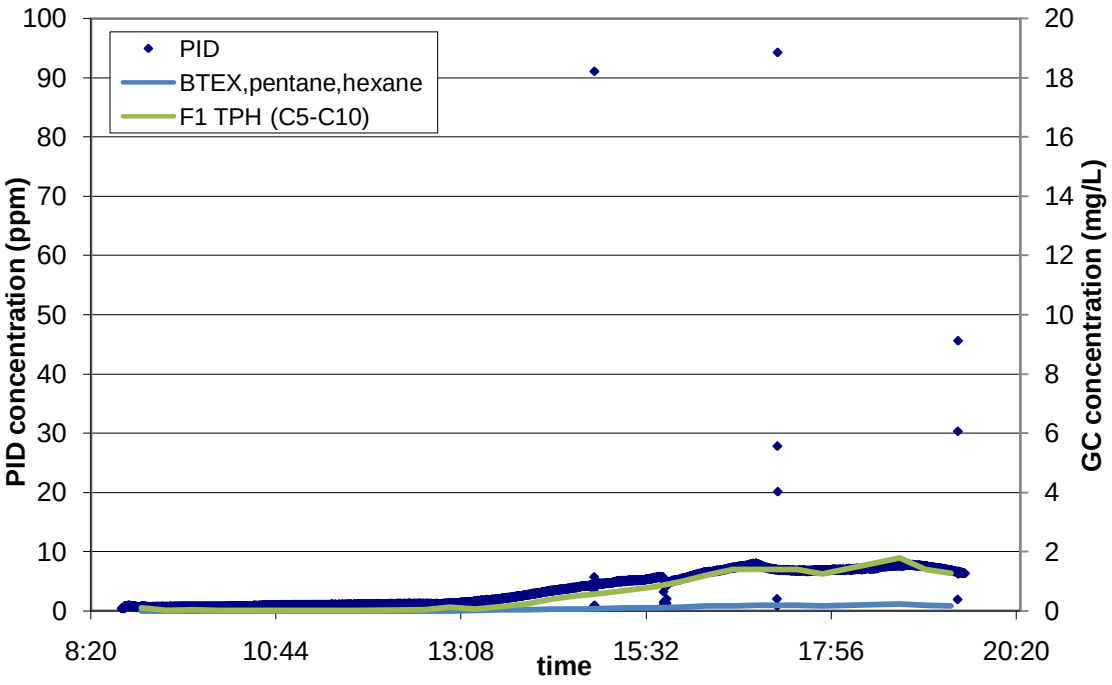

Figure B.57 June 18 PID/TPH

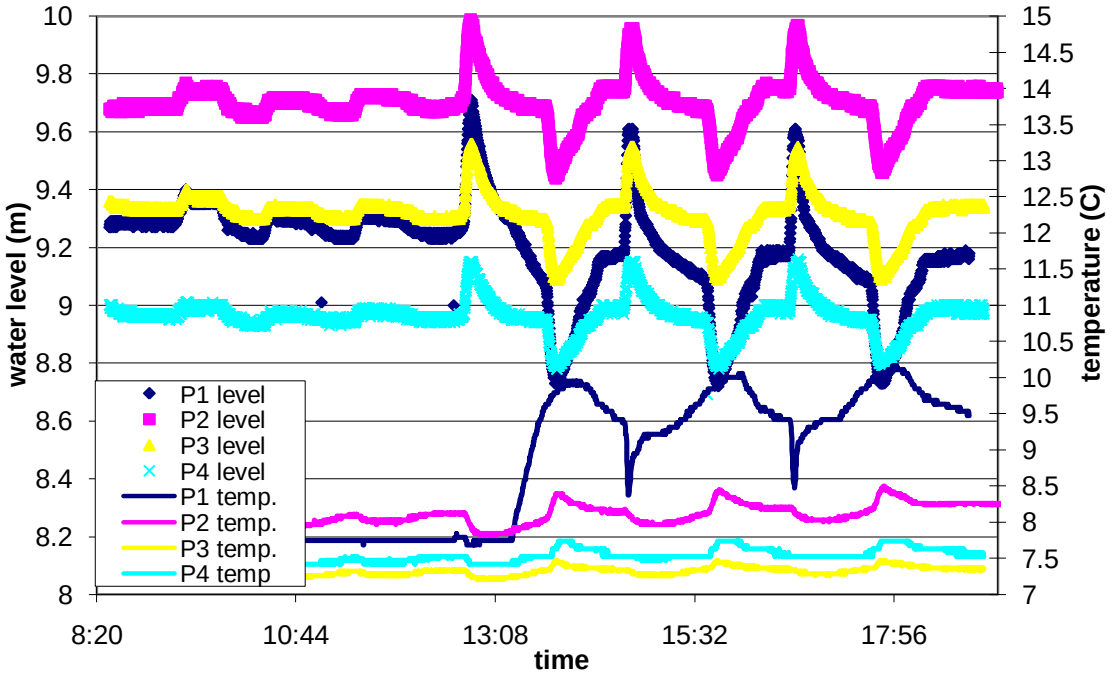

Figure B.58 June 18 water level and temperature

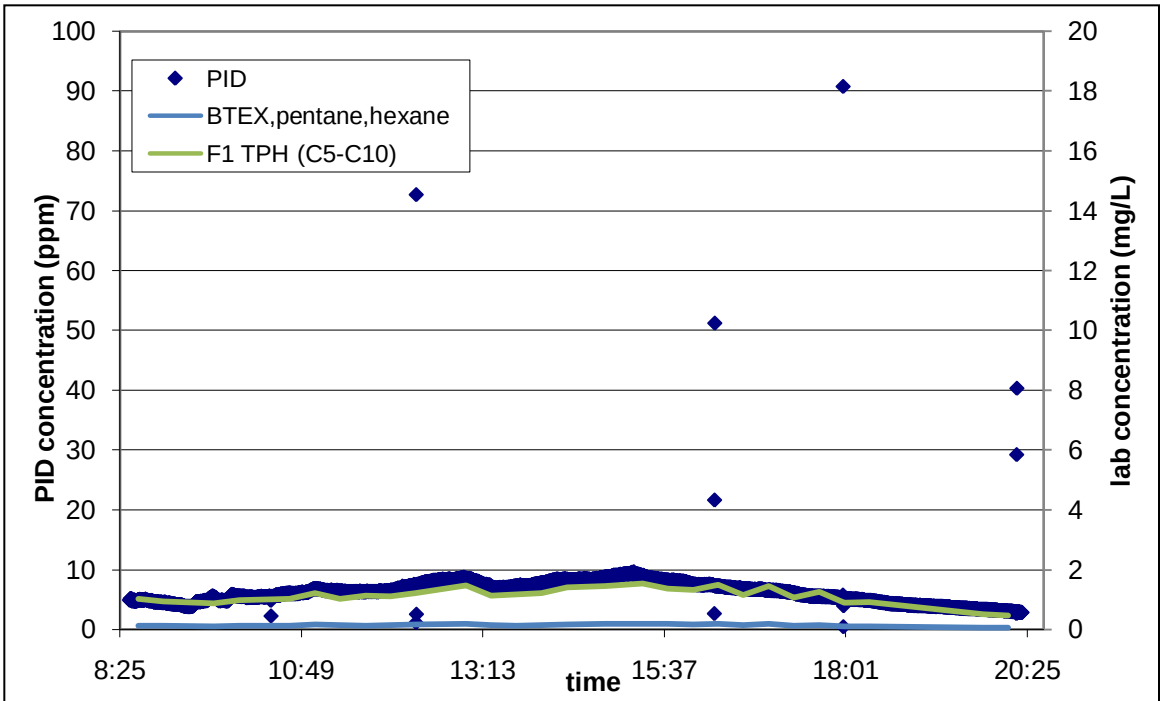

Figure B.59 June 19 PID/TPH

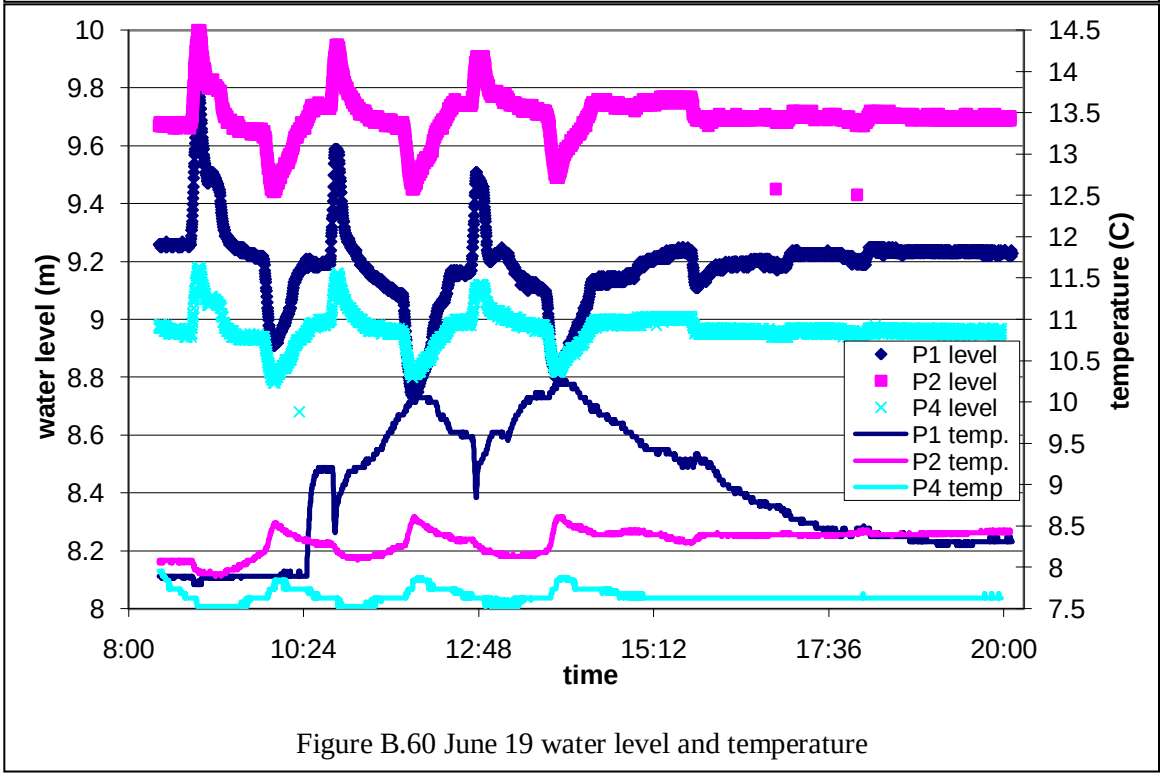

Figure B.60 June 19 water level and temperature

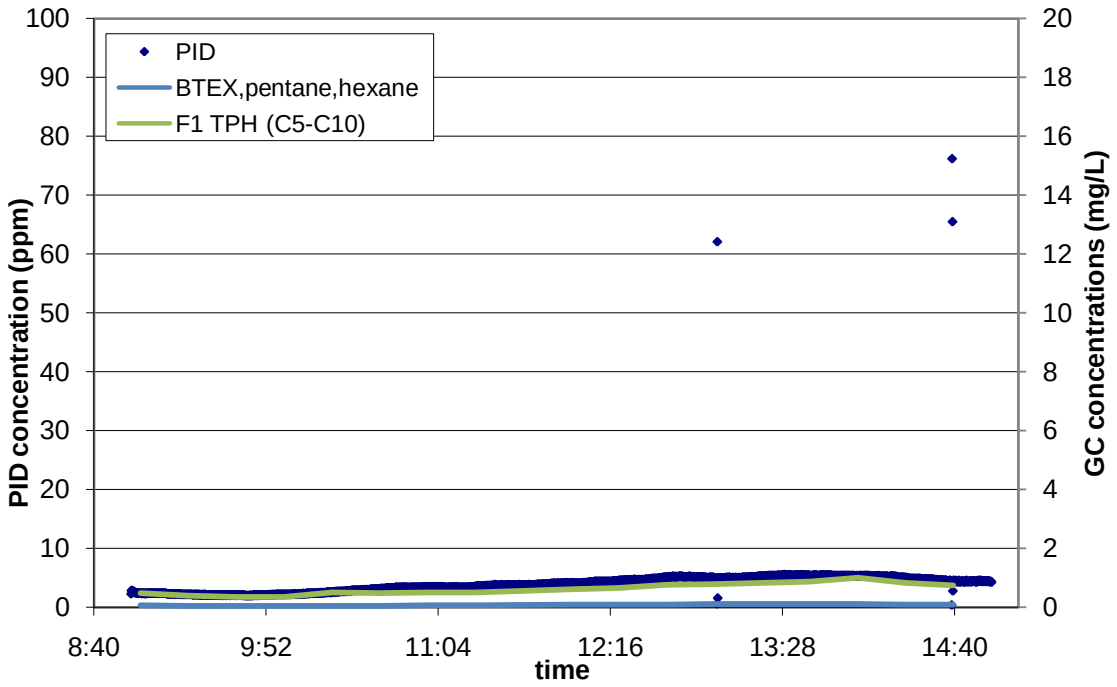

Figure B.61 June 20 PID/TPH

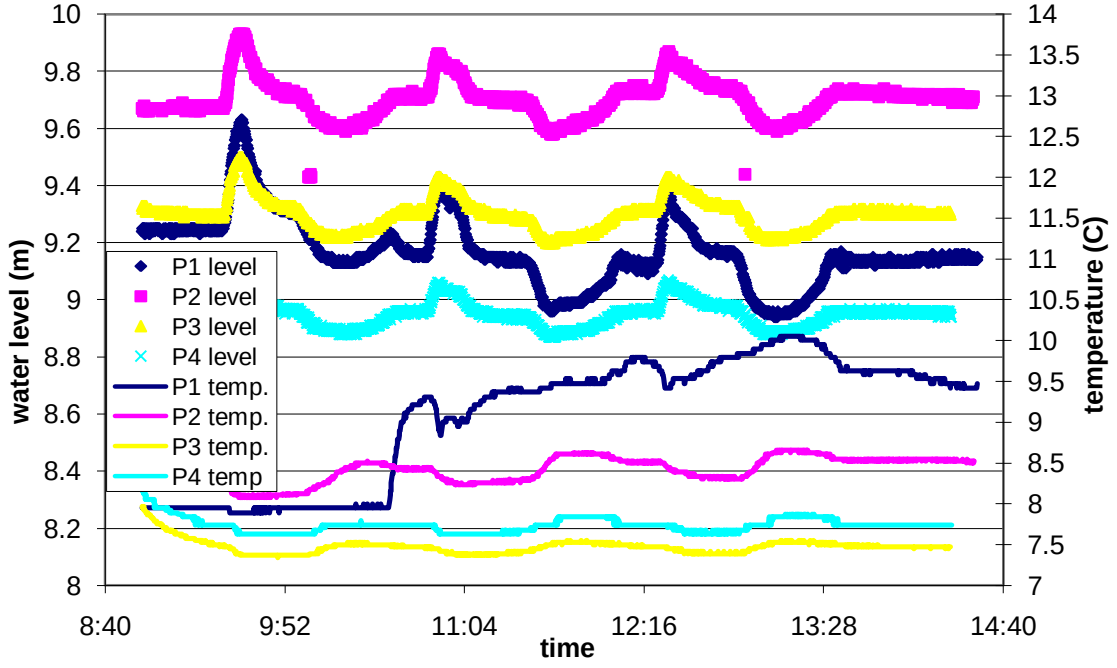

Figure B.61 June 20 water level and temperature

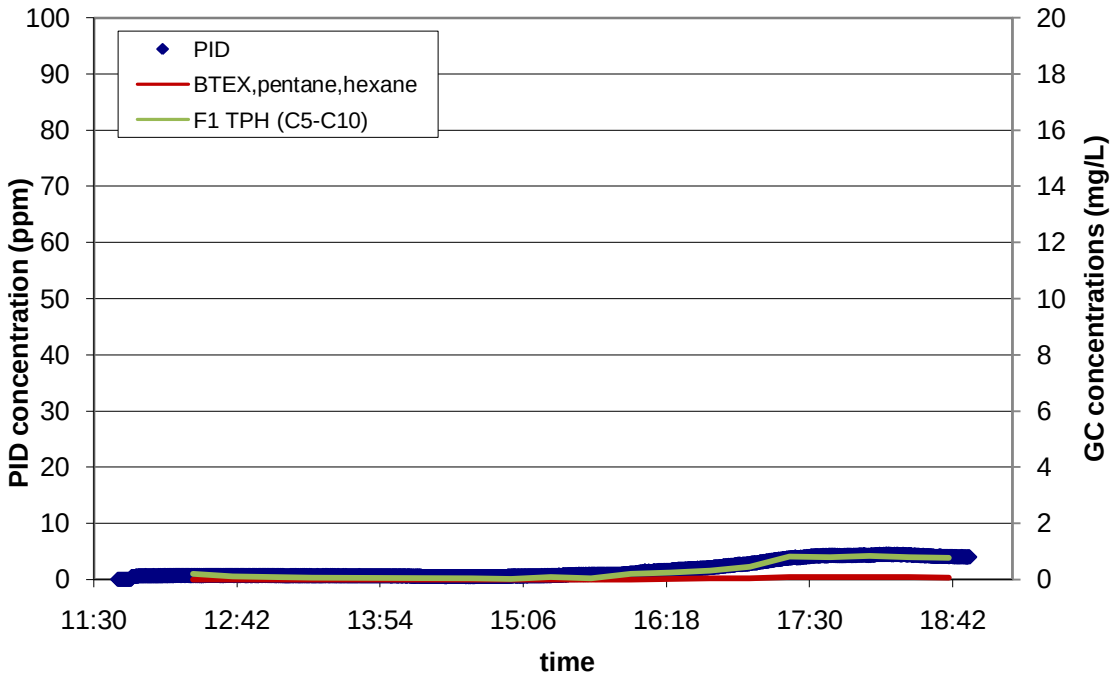

Figure B.63 June 22 PID/TPH

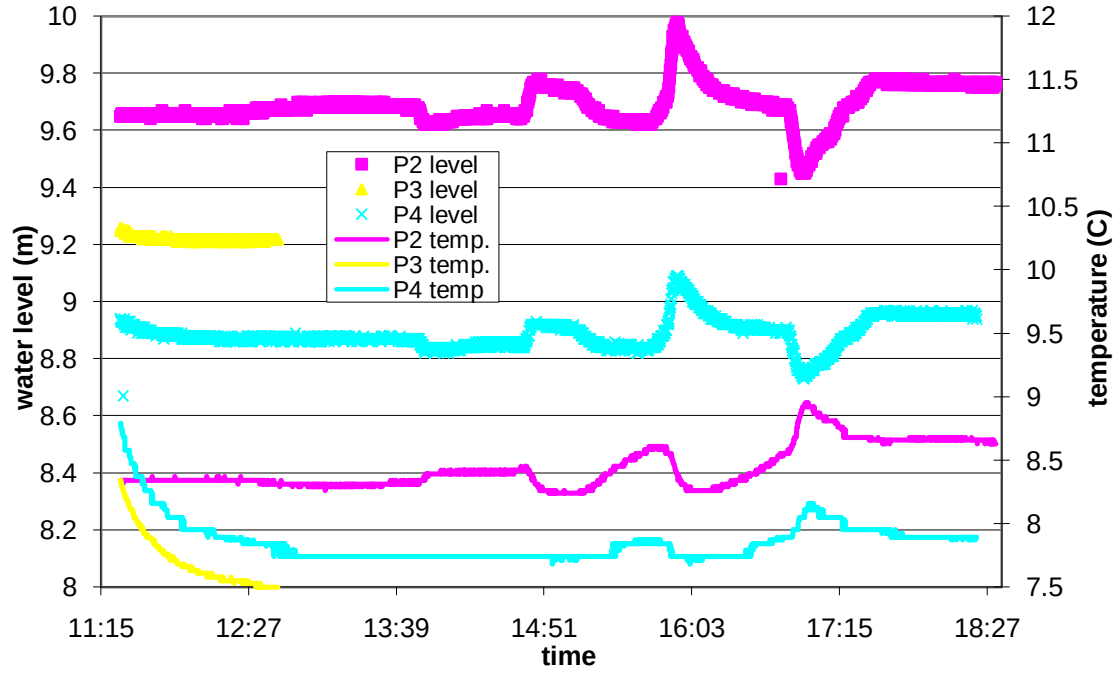

Figure B.64 June 22 water level and temperature

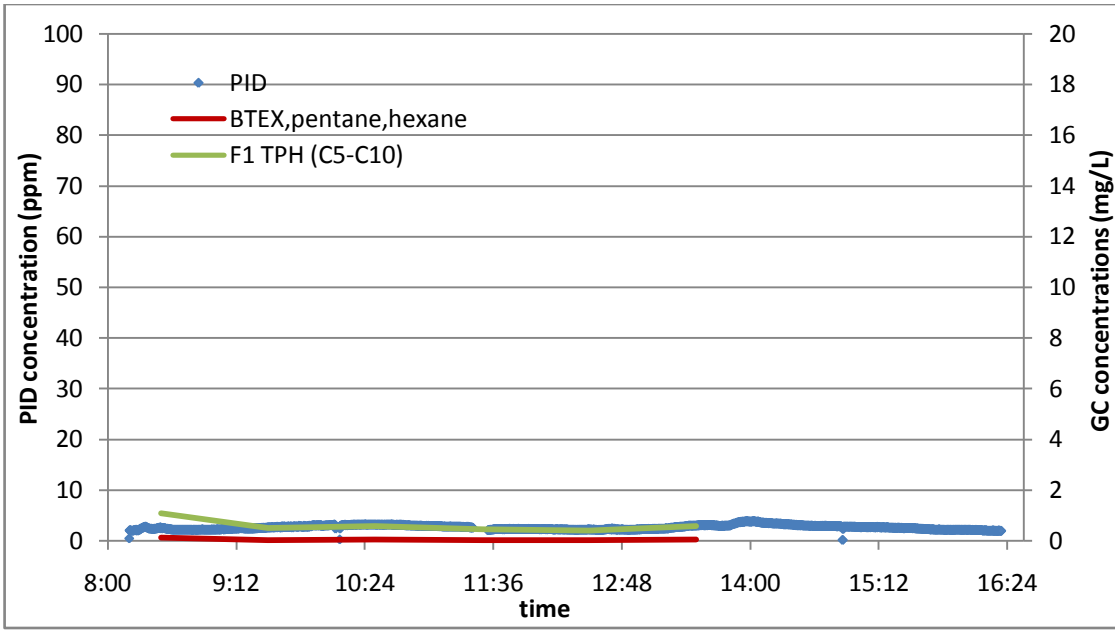

Figure B.65 June 23 PID/TPH

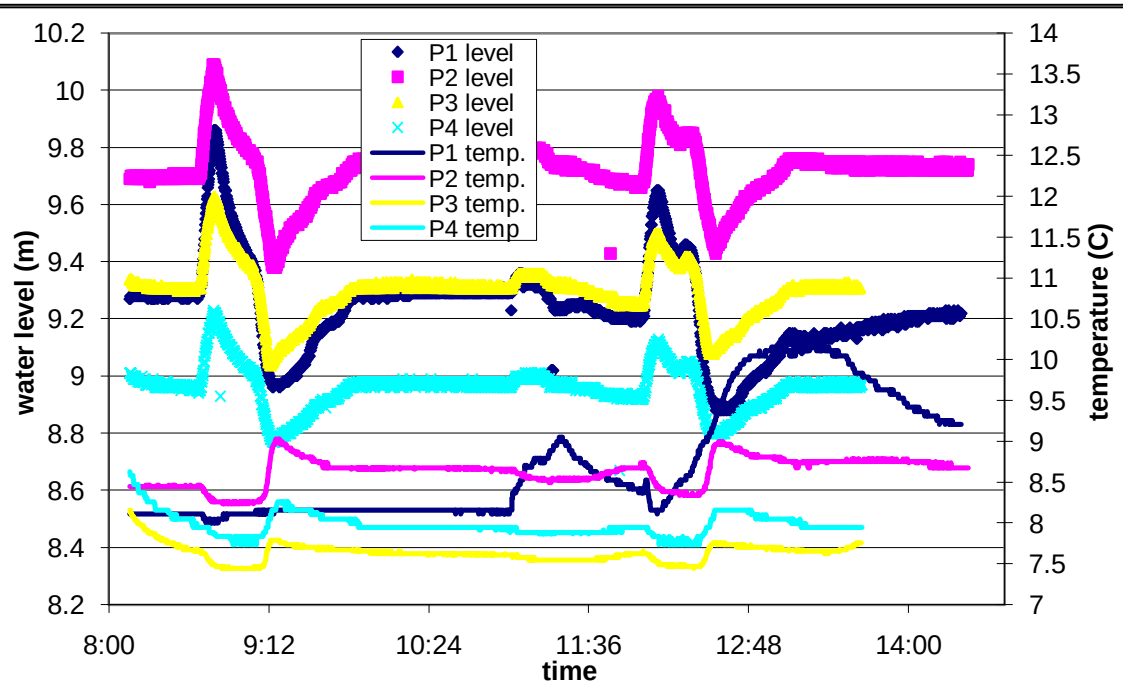

Figure B.66 June 23 water level and temperature

B.2 O_2/CO_2 Concentrations

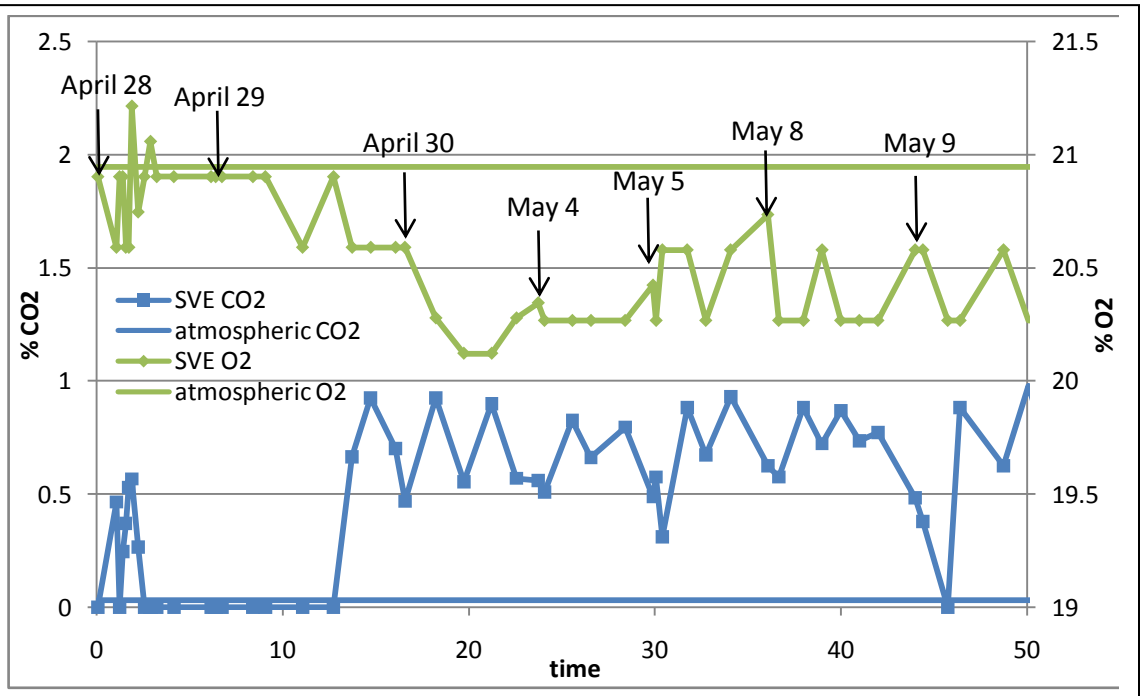

Figure B.67 April 28 – May 9 O_2/CO_2 data

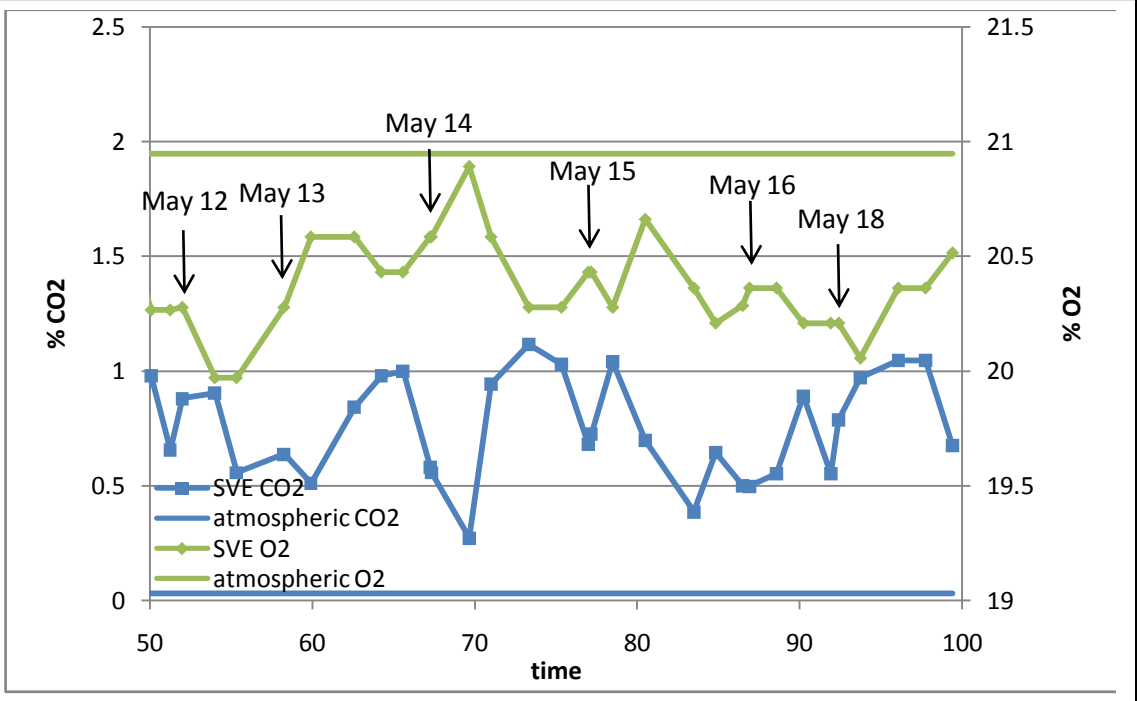

Figure B.68 May 12 – May 18 O_2/CO_2 data

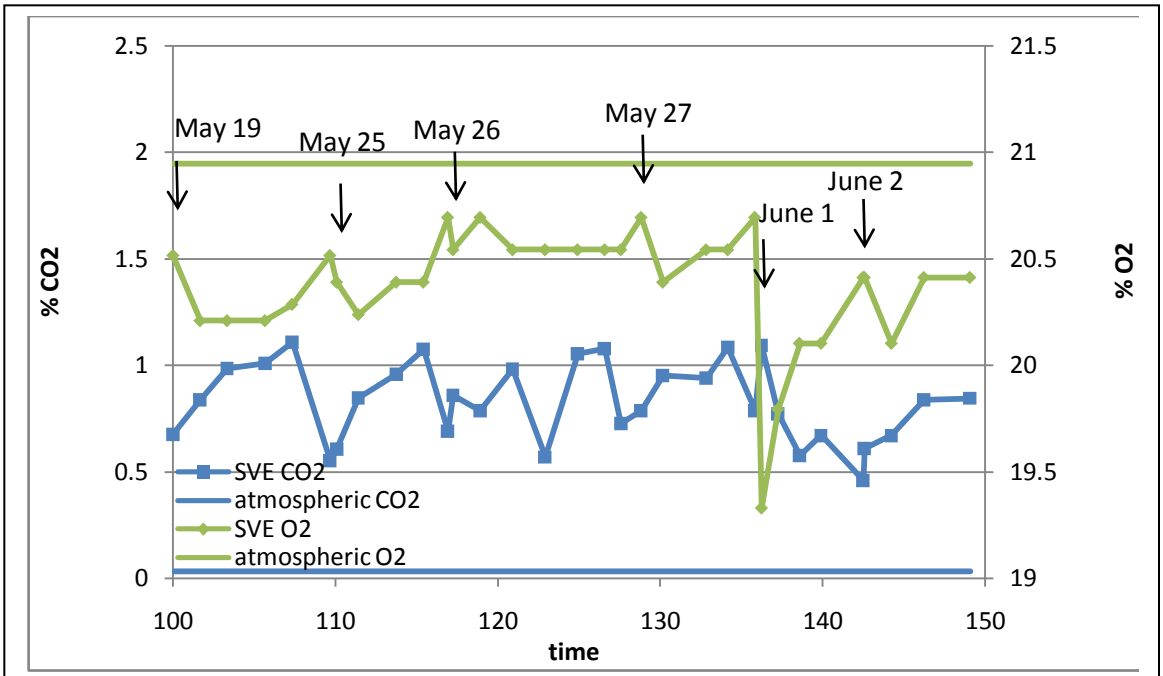

Figure B.69 May 19 – June 2 O_2/CO_2 data

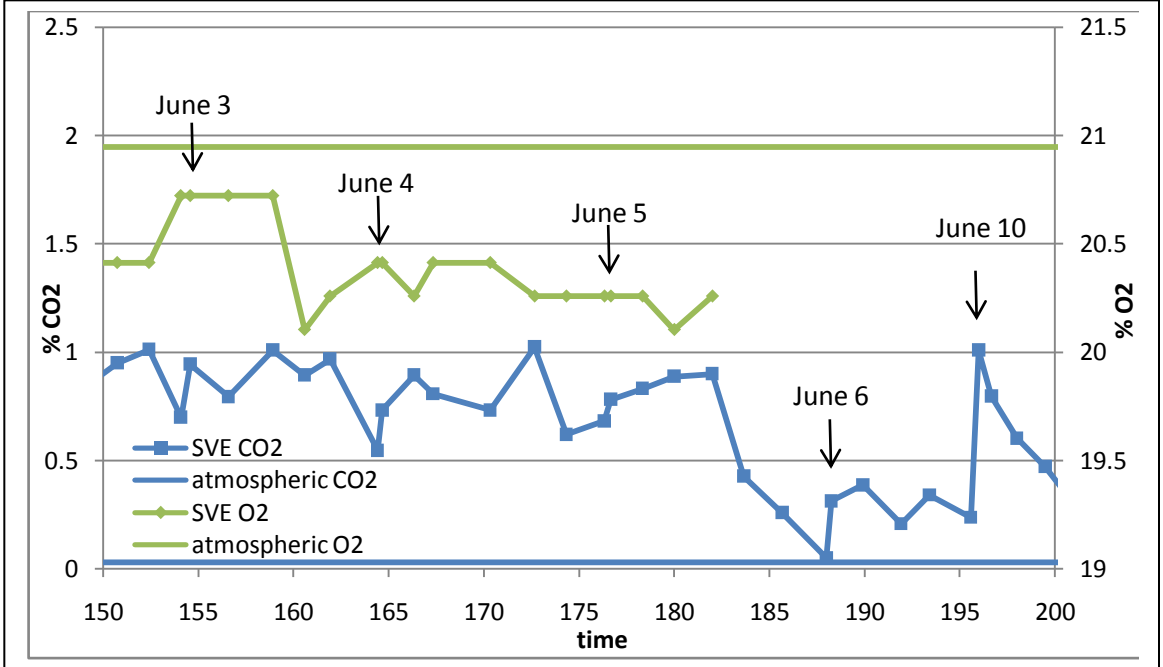

Figure B.70 June 3 – June 10 O_2/CO_2 data

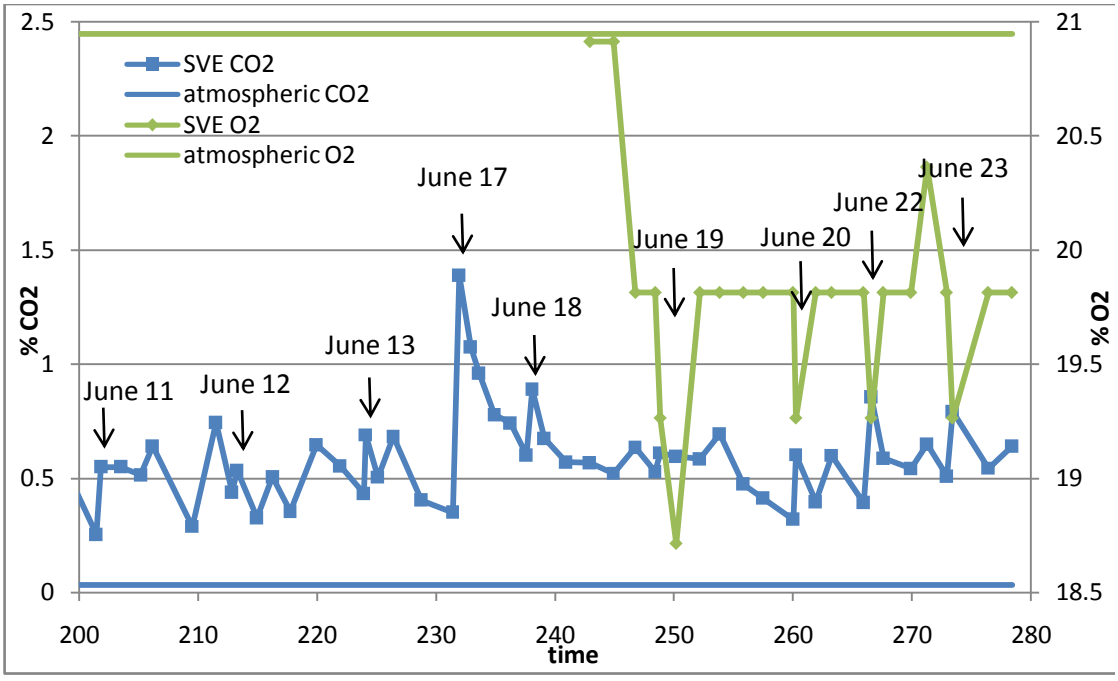

Figure B.71 June 11 – June 23 O_2/CO_2 data

B.3 Average Air Temperatures

	first		max temp		last	
date	time	temp	time	temp	time	temp
28-April	11:40	6.3	14:30	7.2	19:00	5.5
29-April	9:00	1.8	16:00	16.1	18:30	8.9
30-April	9:00	7.0	15:30	14.8	15:30	14.8
4-May	11:30	10.0	16:30	22.3	18:00	16.6
5-May	9:00	7.2	15:30	25.9	15:30	25.9
8-May	12:00	12.9	16:30	18.9	19:00	16.0
9-May	8:30	5.7	15:00	19.6	15:00	19.6
12-May	12:00	15.3	14:30	22.0	18:30	18.5
13-May	10:00	13.7	16:00	28.3	19:00	23.0
14-May	8:30	12.9	13:00	20.0	17:00	15.2
15-May	10:30	13.6	16:30	22.0	18:00	17.4
16-May	8:00	5.1	13:00	19.6	13:00	19.6
18-May	10:30	9.8	10:30	9.8	17:30	9.1
19-May	8:30	5.0	16:30	17.2	16:30	17.2
25-May	13:00	21.2	16:30	33.5	19:30	23.1
26-May	9:00	14.6	16:30	32.5	19:30	26.6
27-May	9:00	10.4	12:00	15.3	15:00	16.5
1-June	12:00	14.2	17:00	20.7	18:00	20.8
2-June	8:30	15.2	16:30	34.5	19:00	26.5
3-June	9:30	14.6	16:30	20.3	19:00	17.5
4-June	8:30	15.1	17:30	18.0	19:00	17.5
5-June	8:00	16.2	15:00	22.7	19:30	18.9
6-June	8:30	19.6	15:00	33.8	15:00	33.8
10-June	13:00	23.1	17:30	24.7	18:30	23.0
11-June	8:30	17.9	15:30	25.0	19:00	20.3
12-June	8:00	12.3	17:00	25.3	19:00	21.7
13-June	8:30	16.1	14:30	26.8	14:30	26.8
17-June	12:00	17.5	15:30	21.8	17:30	19.2
18-June	8:30	10.8	17:00	23.0	18:30	21.1
19-June	8:30	11.4	14:30	21.2	20:00	16.1
20-June	9:00	16.1	12:30	23.2	14:00	22.1
22-June	11:30	21.7	14:00	24.7	18:00	17.5
23-June	8:30	17.5	12:00	20.3	14:00	19.6

Table B.1 Air temperatures (˚C)

Appendix C: Treatment Timeline

date	sparge round	Sparge point	run time (min)	end ET (hr)	Notes
4/28					1140: transducer start time
					1240: SVE start time
					1250: SVE system stopped due to blown fuse
					1255: system restarted
					1320: Air sparging started
					1420: air sparging stopped
					1422: PID removed from exhaust to check He
					1440: PID check; 0 = 1.6, 100 = 100.1
	2	1	60	3	1502: PID tubing changed
4/28					1600: start sparging
					1610: PID off-line for He readings
					1620: PID off-line for He readings
					1640: PID off-line for He readings
					1655: PID off-line for He readings
					1700: PID check; 100 = 89.1, air sparging stopped
					1705: PID off-line for He readings
	3	1	60	7	1915: SVE stopped
4/29					0900: transducer, PID, SVE start time
					0930: air sparging start time
					0940: PID off-line for He reading
					1005: PID off-line for He readings
					1015: PID off-line for He readings
					1035: appear to have a helium leak; turn off tracer source
					1040: air sparging stopped; PID off-line for He readings
					1045: PID off-line for He readings
					1100: PID off-line for He readings
					1125: PID off-line for He readings
					1135: PID off-line for He readings
					1145: PID off-line for He readings
	4	1	60	11	1155: PID off-line for He readings
4/29					1320: air sparging started
					1345: changed PID tubing
					1410: PID check; 0 = 1.2, 100 = 101
	5	1	70	14	1425: air sparging off
4/29					1545: start air sparging
					1650: stop air sparging
					1710: PID check; 0 = 1.0, 100 = 101
	6	1	65	16	1830: SVE, PID shut off
4/30	7	1	75	20	0840: transducer, PID start time

					0845: SVE start time
					0855: having problems with power; blowers sounding more labored
					0950: PID check; 100 = 90.9 (actual value higher; ran out of cal gas)
					0915: start air sparging
					1030: stop air sparging
					1045: recalibrated PID
4/30					1215: start air sparging
					1330: stop air sparging
					1410: PID check; 100 = 90.9
	8	1	75	23	1530: PID, SVE stopped
5/4					1130 - start transducers
					1140 - start SVE (only have one shop vac until 1203)
					1210 - start A/S
					1215 - Start He tracer test
					1223 - End He injection (out of He)
					1325 - Stop A/S
	9	1	75	27	1435 - Re-calibrate PID
5/4					1500 - Start A/S; bubbles at well
					1610 - PID check: 100 = 84.2, 0 = 0.0
					1615 - Stop A/S
					1630 - Bubbles ~ every 6 s at well
					1645 - Bubbles every 5 s at well
					1650 - PID check: 100 = 83.2, 0 = 0.0
					1710 - Bubbles not appearing at well
	10	1	75	30	1800 - PID, SVE off
5/5					0840 - transducers started
					0845 - Start PID
					0850 - start SVE. Shop vac 1 letting in excessive air; SVE flow rate only 3.5. Will change at the end of the day
					0915 - Shop vac 1 fell over; SVE still has low flow (3.5)
					0920 – Start A/S
					1010 - PID check: 100 = 97.5, 0 = 0.5
					1020 - Still no bubbles at well
					1030 - end A/S
	11	1	70	33	1135 - PID check: 100 = 94.8, 0 = 0.5
5/5					1145 - Start A/S
					1215 - Bubbles appearing at well
					1255 - Bubbles appear to have stopped
	12	1	70	37	1530 - SVE, PID off
5/8					1200 - Start transducers
					1235 - Start SVE/PID
					1300 - Start A/S
					1310 - Start He tracer test
					1319 - End He injection
					1325 - Start he tracer test 2; PID off for this period
					1330 - End he injection
	13	1	60	39	1400 - A/S off

5/8					1500 – Start A/S
					1525 – Start He injection for tracer test
					1540 – End He injection
					1600 – End A/S
					1610 – PID check: 100 = 85.9, 0 = 1.8; PID saying “pump”
	14	1	60	41	1620 – PID had debris in inlet. Cleaned out and replaced silicone tubing; now seems to be ok.
5/8					1700 - Start A/S
					1725 - well bubbling ~every 2 s
					1735 - PID check: 100 = 88.6, 0 = 1.0
					1800 - Stop A/S
					1955 - PID check: 100 = 91.3, 0 = 1.0
	15	1	60	44	2005 - Stop SVE/PID
5/9					0815 – Transducers started
					0820 – PID/SVE start time
					0850 – Start A/S
					0903 – Start He tracer test injection
					0915 – End He tracer test injection
					0925 – No bubbles at well
					0950 – End A/S
	16	1	60	47	0955 - PID check: 100 = 101, 0 = 0.9
5/9					1050 – Start A/S; PID reading “pump”; clear and replace tubing
					1140 – PID check: 100 = 99.8, 0 = 0.5; have same pump problem; cleared, restarted PID
	17	1	60	49	1150 – Well bubbling about every 2s; A/S off
5/9					1300 – Start A/S
					1325 – Bubbles about every 2s at well
					1400 – Occasional (1/min) bubbles; A/S off
					1425 - PID check: 100 = 98.6, 0 = 0.8; Well bubbling about every 4s
					1500 - Well bubbling every minute
					1530 – Well has stopped bubbling
					1555 – PID check: 100 = 93.8, 0 = 0.8
	18	1	60	52	1600 – PID, SVE off
5/12					1145 - Start transducers
					1225 - Start SVE, PID
					1255 - Start A/S
					1257 - well bubbling near-continuously
					1305 - Start He tracer test injection
					1320 - End he injection
					1328 - Well not bubbling
					1355 - Stop A/S
	19	1	60	54	1410 - PID check: 100 = 104, 0 = 0.4; had to re-start PID due to pump issues
5/12					1455 - Start A/S
					1500 - No bubbles in well
	20	1	60	58	1510 - Another small leak; water coming out of box ~1 cm above

					water table
					1535 - air bubbles near-continuous in well (~2/s)
					1543 - He detector turned off from He test prev. sparge
					1555 – End A/S
					1555 - air bubbles at ~2/s at well; stop A/S
					1600 - air bubbles at ~1/s at well
					1607 - shop vac 2 sounds labored - will replace
					1610 - shop vac 2 motor burning - stop using
					1620 - No other shop vacs on site works; max flow rate is 3 cfm
					1645 - well not bubbling
					1845 - SVE, PID off
5/13					1000 - transducers started
					1030 - SVE/PID started
					1100 - start A/S
					1103 - bubbles every s in short-circuiting well
					1106 - start He tracer for test
					1115 - no bubbles at well
					1120 - end He tracer injection
					1148 - PID check: 100 = 98.3, 0 = 0.0
					1200 - Stop A/S
	21	1	60	61	1230 - stop He monitoring
5/13					1310 - Start A/S
					1335 - well not bubbling (few stray bubbles only)
					1405 - Bubbles at rate of ~1/s at well
					1410 - Stop A/S
					1420 - bubbles at rate of ~2/s at well
					1445 - Well bubbling ~ every s
	22	1	60	63	1450 - Well bubbling ~ every 10 s
5/13					1510 - Start A/S
					1545 - Well bubbling ~1/s; PID check: 100 = 98.3, 0 = 0.2
					1610 - End A/S
					1615 - bubbles~ every 2s in well
	23	1	60	64	1655 - no bubbles at well
5/13					1705 - Start A/S
					1725 - bubbles near-continuous at well
					1745 - bubbles near-continuous at well
					1805 - end A/S
					1835 - Well bubbling ~ every 5 s
					1855 - Battery ran down on PID; re-started and plugged in
					1950 - PID check: 100 = 98.3, 0 = 0.0
	24	1	60	67	2000 - PID, SVE off
5/14	25	1	70	70	0810 - Start transducers

					0815 - Start SVE/PID
					0845 - start A/S
					0850 - Bubbles every 20 s in short-circuiting well; well beyond has a constant stream of water ~1 cm above the water surface
					0910 - water flow and air bubbles have stopped
					0955 - Stop A/S; no bubbles in well
5/14					1055 - Start A/S
					1120 - Bubbles ~1/s in well
	26	1	60	72	1155 - Stop A/S; bubbles ~1/s in well
5/14					1300 - Start A/S
					1305 – No bubbles at well; PID check: 100 = 87.5, 0 = 0.9
					1325 - Bubbles near-continuous (twice/s) at well
	27	1	60	74	1400 - Stop A/S
5/14					1500 - Start A/S
					1530 - Can't see potential short-circuiting to well due to heavy rain
					1600 - Stop A/S
					1730 - P1 had corrupted data file - re-tried setup and data collection (lost day's data in order to do so) and it did ok. Will replace.
					1745 - PID check: 100 = 80.6, 0 = 1.0
	28	1	60	77	1800 - SVE, PID stopped
5/15					1030 - transducers start; SVE and PID start
					1100 - start A/S
					1140 - Well not bubbling
					1200 - Stop A/S
					1225 - Well not bubbling
					1315 - PID check: 100 = 85.4, 0 = 0.5
					1415 - PID check: 100 = 90.4, 0 = 0.5
	29	1	60	83	1445 - PID, SVE off
5/15					1600 - Start SVE/PID
					1610 - No bubbling in well
					1630 - Start A/S. Note slightly higher air flow and more water intake after re-sealing injection well 2
					1645 - No bubbles at well
					1725 - No bubbles at well
					1730 - Stop A/S; well bubbling ~ every 2 s
					1755 - Well bubbling near-continuously
					1845 - PID check: 100 = 85.5, 0 = 0.5; no bubbles at well
	30	1	60	87	1925 - PID, SVE off
5/16					0800 - Transducers started
					0805 - PID/SVE start
					0835 - Start A/S
					0900 - No bubbles at well
	31	1	60	89	0935 - A/S off; no bubbles at well

					1010 - PID check: 100 = 104, 0 = 0.8 (somewhat erratic readings)
5/16					1030 - Start A/S
					1105 - No bubbles at well
					1130 - A/S off; PID check: 100 = 100, 0 = 0.6 (not erratic)
					1315- PID check: 100 = 98.3, 0 = 0.3 (not erratic)
	32	1	60	92	1335 - SVE, PID off
5/18					1030 - transducers on
					1105 - Start SVE
					1135 - Start A/S
					1146 - Start He injection for tracer test
					1159 - End He injection
					1235 - End A/S
	33	3	60	95	1332 - End He monitoring for tracer test
5/18					1335 - Start A/S; PID check: 100 = 92.8, 0 = 0.3
					1425 - Well bubbling at rate of 1/s
					1435 - End A/S
	34	3	60	97	1515 - Well bubbling about every 2s
5/18					1535 - Start A/S
					1555 - Near-continuous bubbles at well
					1605 - PID check: 100 = 84.4, 0 = 0.5
					1610 - Near-continuous bubbles at well
					1635 - End A/S
					1645 - Well bubbling about every 2 s
					1715 - Well bubbling about every 5 s
					1735 - Well bubbling about every 10 s
					1805 - Well bubbling about every 15 s
					1830 - PID check: 100 = 91.1, 0 = 0.4
	35	3	60	100	1835 - PID, SVE off
5/19					0810 - Transducers started
					0820 - Start SVE/PID
					0850 - Start A/S
					0905 - Start helium tracer test injection
					0915 - End helium injection
					0925 - No bubbles from well
					0935 - No bubbles from well
					0950 - Stop A/S
	36	3	60	102	1019 - End helium test
5/19					1050 - Start A/S
					1105 - PID check: 100 = 100, 0 = 1.1
					1120 - Well bubbling almost continuously
	37	3	60	104	1150 - End A/S

					1155 - No bubbles at well
5/19					1250 - Start A/S
					1255 - No bubbles at well
					1345 - Bubbles appearing about every s
	38	3	60	106	1350 - End A/S
5/19					1445 - Start A/S; bubbles ~ every 8 s at well
					1545 - End A/S; PID check: 100 = 89.9, 0 = 1.0
					1645 - Bubbles every 7 s at well
					1655 - Transducers removed/stopped
					1815 - PID check: 100 = 86.1, 0 = 0.9
	39	3	60	110	1830 - Stop PID/SVE
5/25					1255 - Start transducers
					1305 - Start SVE/PID
					1335 - Start A/S
					1405 - PID check: 100 = 88.4, 0 = 0.7
					1425 - No bubbles at well
					1435 - Stop A/S
	40	3	60	112	1510 - No bubbles at well
5/25					1530 - Start A/S
					1625 - Bubbles appearing ~ every 2s; AS off (overheated)
	41	3	55	114	1645 - PID check: 100 = 80.7, 0 = 0.6
5/25					1720 - Start A/S
					1805 - PID check: 100 = 82.4, 0 = 0.6
					1820 - End A/S
					1925 - PID check: 100 = 87.3, 0 = 1.2
					2015 - PID check: 100 = 86.6, 0 = 0.7
	42	3	60	117	2020 - SVE/PID off
5/26					0850 - Start transducers
					0855 - Start SVE/PID
					0925 - Note that ground is starting to dry up; only have puddles in a few places and at right downgradient corner of box
					0935 - Start A/S
					0955 - No bubbles at well
					1020 - Well bubbling about every 4s
	43	3	60	120	1035 - End A/s
5/26					1135 - Start A/S
					1145 - PID check: 100 = 95.7, 0 = 0.0
	44	3	60	122	1235 - End A/S
5/26					1330 - Start A/S
					1340 - no bubbles at well
					1420 - A/S stopped - blower overheated
	45	3	50	124	1450 - PID check: 100 = 96.8, 0 = 0.0
5/26					1515 - Start A/S
					1545 - Bubbles about every 3s at well
	46	3	60	125	1605 - Bubbles about every 3s at well

					1615 - End A/S
					1630 - Bubbles about every 15s at well
					1655 - PID check: 100 = 82.4, 0 = 0.0 (old bag of isobutylene used)
5/26					1710 - Start A/S
					1735 - Well bubbling about every 2s
					1755 - Well bubbling about every 3s
					1810 - A/S off; well bubbling ~ every 10 s
					1925 - Well bubbling about every min
					1930 - Noticed a series of small leaks/bubbles from puddles (1/2 size of those at well)
					1955 - PID check: 100 = 85.7, 0 = 0.0 (started reading "pump" so cleaned and re-started)
					2000 - Still have minor bubbling outside of well
					2010 - largest non-well leak fills 20 mL vial in about 5 min
	47	3	60	129	2015 - SVE, PID off
5/27					0835 - Start transducers
					0840 - Start SVE/PID
					0910 - Start A/S
					0915 - Bubbles every 2s at well; water trickling from further well. Note - only have puddles around box
					1010 - A/S off; bubbles every 10s at well
					1015 - bubbles mostly stopped
	48	3	60	131	1030 - PID check: 100 = 89.6, 0 = 0.7
5/27					1105 - Start A/S
					1110 - Start He tracer test
					1122 - End He tracer injection
					1130 - End He tracer test - no He detected (note - probably didn't wait long enough)
	49	3	60	133	1205 - End A/S
5/27					1305 - Start A/S
					1310 - PID check: 100 = 89.3, 0 = 0.6
					1355 - Found and patched a small (5mm) hole in top downgradient left corner of cover - inspection didn't find additional holes
					1405 - End A/S
					1510 - Well bubbling about every 30 s
					1550 - PID check: 100 = 90.6, 0 = 0.7
	50	3	60	136	1615 - PID/SVE off
6/1					1155 - Transducers started
					1230 - Start PID/SVE
					1300 - Start A/S at I-2
					1305 - Tubing popped off injection point; stop A/S and re-tighten
					1315 - Re-start sparging
					1325 - A/S stopped
					1335 - Turned off SVE/PID. Everything looks ok, but blower won't start. Will wait 15 minutes and try again.
	51	2	25	138	1420 - Re-starting SVE/PID
6/1	52	2	5	139	1450 - Start A/S

					1455 - A/S off - appears that point is clogged, so no air getting through (reason for compressor shutoff).
					1545 - SVE off
6/1					1550 - Start SVE
					1555 - Start A/S
					1630 - Few water leaks out (previous location and far left corner facing d-gradient) and occasional air bubble between box and well
					1645 - PID check: 100 = 95.3, 0 = 0.0
					1700 - A/S off
					1930 - PID check: 100 = 89.9, 0 = 0.0
	53	1	65	143	1940 - SVE, PID off
6/2					0815 - Start transducers
					0820 - Start SVE/PID
					0825 - Realized that PID was not hooked up - lost first 5 min of data
					0850 - Start A/S
					0910 - Start He injection for tracer test
					0916 - End He injection
					0950 - End A/S
	54	1	60	145	1039 - Turn off He detector
6/2					1050 - Start A/S
					1130 - Bubbles every 2 s at well; occasional small bubbles at 4-5 locations around area with puddles. Hearing bubbling noise from under downgradient side of box.
					1150 - End A/S
	55	1	60	148	1210 - Well bubbling about once/s
6/2					1315 - Start A/S
					1345 - PID check: 100 = 92.5, 0 = 0.3
					1415 - A/S off
	56	1	60	149	1425 - Have lots of tape coming lose where it was exposed to water and sun. Will patch.
6/2					1510 - Start A/S
					1535 - PID check: 100 = 86.9, 0 = 0.4
	57	1	60	151	1610 - A/S off
6/2					1705 - Start A/S
					1735 - Near-constant stream of small bubbles between box and well (previous “out” sample today); no bubbles at well; no other bubbles
					1805 - A/S off
					1950 - Well bubbling ~ every 3s; bubbles between well and box about every second. Small spot near footstools (sampled last week) bubbling every few s
					2005 - Well bubbling ~ every 6 s; spot next to it bubbling once/s
					2015 - Still have bubbles every 8s at well
	58	1	60	154	2020 - PID/SVE off
6/3					0930 - Start transducers
	59	3	60	157	0935 - Start SVE/PID; pools dried up except for right side (downgradient end) between box and sheetpiling

					1030 - A/S pushed water table to ground surface; from footstools to 1 ft to the left of well (facing downgradient) now covered with water
					1035 - No bubbles at well
					1110 - End A/S
6/3					1210 - Start A/S
					1315 - End A/S
					1320 - No bubbles at well
	60	3	65	159	1330 - PID check: 100 = 91.1, 0 = 0.3
6/3					1410 - Start A/S
					1443 - Start He injection for tracer test
					1453 - End He injection
					1500 - End A/S (blower overheated)
	61	3	50	161	1510 - Location between well and box bubbling about every 2s
6/3					1555 - Start A/S
					1650 - PID check: 100 = 90.9, 0 = 0.0
					1655 - End A/S
					1701 - He detector off
					1755 - PID check: 100 = 82.1, 0 = 0.0 (probably higher; was using an old bag of cal gas)
					1910 – Water level down significantly; have a few small puddles
	62	3	60	165	1940 - Accidentally lost suction for pump while attempting to check calibration; end PID/SVE for the night here
6/4					0815 - Start transducers; start PID/SVE
					0845 - Start A/S
					0910 - Area started out dry; puddles have been re-filling since starting A/S - now at maximum extent
					0925 - Flowmeter for A/S leaking at top and bottom; have little bubbles coming up over puddle area - bubbles not appearing at well
					0945 - A/S off
	63	3	60	167	1005 - PID check: 100 = 104, 0 = 0.7
6/4					1045 - Start A/S
	64	3	60	169	1145 - End A/S
6/4					1255 - Start A/S
	65	3	60	171	1355 - End A/S
6/4					1500 - Start A/S
					1510 - PID check: 100 = 104, 0 = 0.7
					1535 - Well bubbling ~ every 15s; 3-4 spots of bubbles elsewhere
	66	3	60	173	1600 - End A/S
6/4					1655 - Start A/S
					1735 - Well bubbling about every 20s
					1745 - Found a large hole (~8" along right side of box facing downgradient), 1m from downgradient edge. Looks like a large rodent chewed on it. Damage did not extend to lower vinyl under edge of plywood, so may not have as much leakage as originally feared. Taped to seal – will get vinyl for a more permanent patch.
	67	3	60	176	1755 - A/S off

					1855 - PID check: 100 = 87.4, 0 = 0.7 - PID read “pump” so turned off to re-set and replaced tubing
					1900 - Shop vac making strange hissing noises (loud) - will try to keep going until scheduled shutdown, then replace tomorrow AM.
					1955 - PID check: 100 = 103, 0 = 0.5
					2005 - PID/SVE off
6/5					0800 - Start transducers
					0805 - Start SVE/PID; PID initial concentration quite high until new shop vac starts to leak (buckles)
					0835 - Start A/S
					0844 - Start He injection for tracer test
					0851 - End He injection for tracer test
					0855 - puddle spreading rapidly from footstools toward well
					0935 - End A/S
	68	3	60	179	1010 - Well bubbling about every 10s
6/5					1035 - Start A/S
					1110 - PID check: 100 = 112, 0 = 0.7
	69	3	60	181	1135 - End A/S
6/5					1240 - Start A/S
					1322 - End He monitoring for tracer test (from earlier this morning)
	70	3	60	183	1340 - End A/S
6/5					1435 - Start A/S
					1535 - End A/S; PID check: 100 = 91.0, 0 = 0.2
					1605 - P thunder; may need to stop sampling/taking readings
					1610 - Thunder; turned off computer and detached power cord (raining heavily and very dark)
	71	3	60	185	1615 - Torrential rain; lightning - will not sample until storm passes
6/5					1630 - Start A/S
					1635 - Storm has mostly passed
					1735 - A/S off
					1805 - PID check: 100 = 115, 0 = 0.5 - read “pump” when checking; had to stop and re-start PID
					2010 - PID check: 100 = 90.0, 0 = 0.7
	72	3	65	188	2015 - Stop PID/SVE
6/6					0815 - Start transducers
					0820 - Start PID/SVE
					0850 - Start A/S
					0950 - End A/S
					1010 - PID check: 100 = 80.2, 0 = 0.5 - read “pump”; re-started PID
	73	3	60	191	1030 - Moved to I-2; had slight pressure loss from removing port from I3 inlet and removing rubber stopper from I2
6/6					1045 - Start A/S
					1050 - I2 doesn’t appear to have any flow - will run anyway to see if the pressure has an impact on water levels
					1053 - End A/S - compressor shut off
					1115 - Still have built-up pressure; will release by moving to point I1
	74	2	60	192	1135 - Move point to I1; may have small transducer peak from attaching airline to I1

					1210 - PID check: 100 = 100, 0 = 0.0
6/6					1220 - Start A/S
					1325 - End A/S
					1400 - Extremely hot weather; may have problems losing VOCs
					1430 - Well bubbling about every 6s (several bubbles each time)
					1525 - Unable to download P1, P2 data, likely from high box temp.
					1535 - PID check: 100 = 100, 0 = 0.0
	75	1	65	196	1550 - PID/SVE off
6/10					1300 - Start transducers
					1305 - Start SVE/PID
					1335 - Start A/S
	76	2	12	198	1345 - End A/S; compressor stopped (no air in)
6/10					1530 - Start A/S
					1552 - End A/S (compressor stopped - overheated?)
	77	3	22	199	1615 - PID check: 100 = 90.8, 0 = 0.3
6/10					1645 - Start A/S
					1650 - No bubbles visible, although water table has risen to surface
					1705 - End A/S. Not sure why it's shutting down early; haven't had problems with this point before
					1900 - PID check: 100 = 89.2, 0 = 0.3
	78	3	20	202	1935 - PID, SVE off
6/11					0830 - Start transducers
					0835 - Re-tightened I1 ferrels
					0845 - Start SVE
					0915 - Start A/S
					0925 - Start He injection for tracer test
					0935 - End He injection
					1010 - Significant bubbling in several areas around well
	79	1	60	204	1015 - End A/S
6/11					1110 - Start A/S
					1115 - PID check: 100 = 95.0, 0 = 0.4
	80	1	60	206	1210 - End A/S
6/11					1305 - Start A/S
					1355 - PID check: 100 = 85.0, 0 = 0.5
	81	1	60	208	1405 - A/S off
6/11					1505 - Start A/S
					1550 - PID check: 100 = 96.9, 0 = 0.5
					1605 - A/S off
	82	1	60	210	1620 - Accidentally re-started A/S, which ran for ~ 2 min
6/11					1700 - Start A/S
					1730 - PID check: 100 = 98.3, 0 = 0.7
					1745 - Turned He detector off. It went over 15 min without any detections; previous detections (1718-1725) seem erroneous
					1800 - A/S off
					2005 - PID check: 100 = 99.4, 0 = 0.6
	83	1	60	213	2015 - PID, SVE off
6/12					0800 - Start transducers
	84	1	60	216	0810 - Start SVE/PID

					0935 - Significant bubbling around well; filled 2 “out” vials in about 8 min. No bubbles near footstools
					0940 - A/S off
					1015 - Switch air inlet to I3
6/12					1035 - Start A/S
					1055 - A/S off. Injection port must be partially clogged. Last time this was used, had aquifer response, will continue to try and fix
	85	3	20	217	1150 - Able to flush water through using a peri pump with no trouble; not sure where blockage is
6/12					1200 - Start A/S
					1305 - A/S off
					1330 - Move back to I-1
	86	1	65	219	1350 - PID check: 100 = 108, 0 = 0.0
6/12					1415 - Start A/S
					1515 - A/S off
	87	3	60	221	1530 - Switch to inlet at I1
6/12					1610 - Start A/S
					1710 - A/S off
					1715 - PID check: 100 = 108, 0 = 0.0
					1810 - Remove inlet line from I1 and switch to I3
					1825 - Well bubbling about every 5s; not other bubbles seen (puddle starting to recede)
	88	1	20	224	1950 - PID check: 100 = 99.5, 0 = 0.1; SVE/PID off
6/13					0815 - Start transducers
					0820 - Start SVE/PID; have distant rumbling of thunder
					0825 – T-storm moving through; thunder, lightning, and heavy rain
					0910 - A/S stopped despite flushing out yesterday.
	89	3	60	226	0945 - Moved to I1; will flush out I3 again.
6/13					1005 - Start A/S
					1045 - Start pumping water out of I3; not getting much water out (a few L). Will let the peri pump run a while, then pump water back in.
					1105 - A/S off
					1110 - Water couldn’t be pumped back in I3 (overflowed up tubing)
					1145 - Changed intake over to I3
	90	1	60	228	1150 - PID check: 100 = 97.3, 0 = 0.2
6/13					1200 - Start A/S
					1300 - End A/S
					1400 – Got a bug into the SVE flowmeter; not sure how. Must have a leak somewhere (everything looks good going from the box).
	91	3	60	233	1550 - SVE/PID off
6/17					1140 - Start transducers
					1248 – Start SVE
					1320 - Start A/S
					1330 - A/S off - blower stopped; blower previously stopped at 10 minutes with no change in water level. Have minimal VOCs (0.2 ppm max). Will try 1 more round after 1 hour, then end for the day.
	92	2	10	233	1420 - Have a small puddle forming in area just short of outer footstools and halfway under middle footstool; must have air going in. Will do 1 more round, then do helium test next field day of this

					point, then I1 He test, then done unless we can think of other options.
6/17					1425 - Start A/S
	93	2	10	234	1435 - End A/S
6/17					1525 - PID check: 100 = 89.4, 0 = 0.0
					1530 - Start A/S
					1541 - End A/S
					1545 - Took picture of puddle - appears to be at maximum size
	94	2	11	236	1620 - Another picture (puddle increased)
					1635 - Start A/S
					1645 - End A/S
					1710 - Take picture of puddle extent. No bubbles seen in area.
					1830 - Released pressure on I2
					1845 - PID check: 100 = 84.5, 0 = 0.0
6/17	95	2	10	238	1855 - SVE, PID off
6/18					0830 - Start transducers
					0840 - Trying to get bug out of flowmeter - unsuccessful (but able to move to the side)
					0845 - Start SVE/PID
					0915 - Start A/S; start He injection for tracer test
					0925 - End A/S, end He injection
					0937 - Compressor turned on (automatically); quickly turned off
	96	2	10	239	0940 - Moisture at lower corner of box (downgradient right)
6/18					1020 - Start A/S
	97	2	10	241	1030 - End A/S; have not had a detection over 25 ppm in 25 min; stop He detector
6/18					1125 - Start A/S
	98	2	5	242	1130 - End A/S; pump off
6/18					1245 - Start A/S
					1312 - He detector off
	99	1	60	244	1345 - A/S off
6/18					1440 - Start A/S
					1450 - PID check: 100 = 101, 0 = 0.7
					1455 - Have another bug in the SVE flowmeter
					1505 - Bug may throw off flow measurements, so He test not done. Will disconnect everything and try to remove bug after sparging.
					1540 - A/S off
					1545 - Turn off SVE system and remove bug
	100	1	60	246	1547 - Re-start SVE system. Flow now reading 3.5 (expected value, not previous value of 5+)
6/18					1640 - Start A/S
					1715 - PID check: 100 = 94.7, 0 = 0.7
					1740 - A/S off
					1900 - Area 2” downgradient of and to left of well is bubbling regularly (several bubbles every 5s)
					1935 - PID check: 100 = 103, 0 = 0.7
	101	1	60	249	1940 - SVE, PID off
6/19	102	1	60	251	0825 - Start transducers; replace P1 battery

					0830 - Start SVE/PID
					0850 - Start A/S
					0855 - Upon startup, blower sounded rough; sounds ok now
					0905 - Start He injection for tracer test
					0915 - End He injection
					0950 - End A/S
6/19					1045 - Start A/S
					1145 - End A/S
					1210 - Pumped out I-3 in preparation for sparging and He test
	103	1	60	253	1220 - PID check: 100 = 105, 0 = 0.5
6/19					1240 - Start A/S
	104	3	60	255	1340 - End A/S
6/19					1450 - Start A/S
	105	2	10	256	1500 - A/S off
6/19					1555 - Start A/S
				257	1605 - A/S off
	106	2	10	0	1615 - PID check: 100 = 102, 0 = 0.3
6/19					1700 – Start A/S
					1709 – A/S off
	107	2	9	258	1755 - PID check: 100 = 100, 0 = 0.3
6/19					1805 – Start A/S
					1815 – A/S off
					2015 - PID check: 100 = 99.6, 0 = 0.3
	108	2	10	260	2020 – SVE, PID off
6/20					0855 – Start transducers, SVE/PID
					0925 – Start A/S
					0928 – Start He injection for tracer test
					0934 – End He injection
	109	3	22	262	0947 – End A/S
6/20					1048 – Start A/S
					1114 – He detector battery died; put on charge
					1122 – A/S off
	110	3	34	264	1205 – He detector re-started
6/20					1220 – Start A/S
					1230 – He detector may have overheated (desiccant almost used up) – results may be unreliable
					1245 – End A/S
					1300 – PID check: 100 = 102, 0 = 0.7 – OUT OF CAL GAS
					1325 – Bug in flowmeter – will be unable to determine flow. Will make this the last round of the day and try to remove bug afterward.
					1435 - PID check: 100 = 93.7, 0 = 0.3
	111	3	25	266	1455 – End PID/SVE
6/22					1125 – Start transducers; remove bug from flowmeter
					1145 – Start SVE/PID
					1215 – Start A/S
					1217 – Start He injection for tracer test
	112	2	10	268	1224 – End injection (out of He)

					1225 - End A/S
6/22					1325 – Start A/S
	113	2	5	269	1330 – End A/S; compressor shut down early, assuming that no air got into formation
6/22					1440 – Start A/S
					1455 – End A/S
					1515 – Turn off He detector
	114	2	15	270	1530 – Heavy rain, some thunder and lightning
6/22					1550 – Start A/S
					1650 – End A/S
					1830 – P3 had a short log again; will replace battery
					1835 – P1 not working; file is huge and crashed program repeatedly
	115	1	60	273	1850 – SVE, PID off
6/23					0810 – Start transducers, SVE/PID
					0840 – Start A/S
					0845 – Start SF_6 injection
					0905 – End SF_6 injection; A/S off
					1005 – Stepped on PID tubing; reads “pump”, restarting
	116	1	25	276	1010 – Pumped out I3 in preparation for sparging
6/23					1025 – Other SF_6 tank is empty.
					1040 – Other tank on site has gas; will switch tanks
					1100 – Start A/S and SF_6 injection
					1110 – End A/S and SF_6 injection
	117	2	10	277	1125 – PID reading “pump” again; fixed
6/23					1200 – Start A/S
					1215 – Start SF_6 injection
					1223 – Out of gas; end A/S
	118	3	23	282	1650 – End PID, SVE

Appendix D: Additional Calculations (see disk)

Note that all files are in excel 2007.

D.1 Raoult's Law Calculations

D.1.1 Source zone (solubility-based)

D.1.2 Off-gas collection (vapor pressure-based)

D.2 Slug Test Calculations

D.3 Tracer Test Calculations

D.3.1 Helium test results

D.3.2 SF_6 test results

D.4 Off-Gas Mass Removal Calculations

D.4.1 Hydrocarbon results

D.4.2 O_2 and CO_2 results

D.5 Groundwater Mass Discharge Calculations

Appendix E: Analytical Data (see disk)

E.1 Groundwater Data

E.2 Off-Gas Data